Évolution des pathogènes en réponse à l'hétérogénéité spatio-temporelle des traitements

Alicia Walter

THÈSE POUR OBTENIR LE GRADE DE DOCTEUR DE L'UNIVERSITÉ DE MONTPELLIER

En Sciences de l'évolution

École doctorale GAIA

Unité de recherche UMR 5175 CEFE

Evolution des pathogènes en réponse à l'hétérogénéité spatio-temporelle des traitements

Présentée par Alicia WALTER
Le 22 novembre 2021

Sous la direction de Sébastien LION

Devant le jury composé de

Ophélie RONCE, DR, CNRS	Présidente du jury
Mike BOOTS, PR, UC Berkeley	Rapporteur
Pauline EZANNO, DR, INRAE	Rapportrice
Samuel ALIZON, DR, CNRS	Examinateur
Jean-Baptiste FERDY, PR, Université Toulouse 3	Examinateur
Sébastien LION, DR, CNRS	Directeur de thèse

UNIVERSITÉ DE MONTPELLIER

Remerciements

Merci à Sébastien, mon directeur de thèse, d'avoir permis à ce travail de voir le jour. Merci pour les discussions enrichissantes, ta bienveillance, ta bonne humeur et tes conseils. Merci de m'avoir toujours encouragée, de t'être rendu disponible quand j'en avais besoin et d'avoir été à l'écoute. Le Covid ne nous a pas simplifié la tâche mais on y est arrivés,

Merci à Pauline Ezanno, Mike Boots, Samuel Alizon, Ophélie Ronce et Jean-Baptiste Ferdy, d'avoir accepté d'évaluer mon travail et de faire parti de mon jury de thèse,

Merci à Thierry Boulinier, Mircea Sofonea, Gaël Thebaud et Minus van Baalen d'avoir participé à mon comité de thèse. Merci pour vos conseils, votre soutien et les discussions qui ont permis d'enrichir ce travail,

Merci à Sylvain de m'avoir accueillie dans l'équipe, pour les précieux échanges scientifiques lors de cette dernière année, et merci pour ta bonne humeur quotidienne,

Merci à Philippe de m'avoir accueillie quelques semaines dans ton équipe à Nantes, et merci pour l'apport mathématique que tu as apporté à ce travail (et de ne pas m'avoir spoilé Game of Thrones),

Merci à Sébastien, Sylvain et Philippe pour les parties de babyfoot et de ping-pong endiablées, ce fût bref mais intense,

Merci à Valentin, Martin, Juliet, David, Hélène, Rémi, pour les discussions, scientifique ou non, qui m'ont permis de m'évader ainsi que la bonne humeur que vous apportez au quotidien. Valentin et Martin, y a un petit virus qui nous met des bâtons dans les roues mais je ne désespère pas de cette soirée jeu.

Merci, au hockey, hockeyeurs et hockeyeuses qui se reconnaîtrons, d'avoir été ma soupape pendant ces 3 années,

Merci, à mes amis, famille et belle famille, je ne vous citerai pas de peur d'en oublier mais merci d'être d'un soutien sans faille, quoique j'entreprenne.

Merci à Rumba et Plume d'avoir apporté un peu de douceur à ces derniers mois et de me rappeler que rien n'est plus important que nos besoins fondamentaux,

et Merci Mathilde, pour ton soutien quotidien et ton humour sans faille qui embellit mes journées.

Table des matières

1 Introduction **1**

1.1 Épidémiologie et évolution : l'épidémiologie évolutive 5

1.1.1 Une brève histoire des maladies infectieuses 5

1.1.2 Des hôtes et des pathogènes 6

1.1.3 L'arrivée des traitements 7

1.1.4 Traitements oui, mais imparfaits 9

1.1.5 Processus d'évolution 11

1.1.5.1 De nouveaux allèles à sélectionner 11

1.1.5.2 Évolution des pathogènes 12

1.1.5.2.1 Différentes résistances 12

1.1.5.2.2 Évolution de la virulence 13

1.1.6 Hétérogénéité d'hôtes 15

1.2 L'approche par la modélisation 16

1.2.1 Intérêts de la modélisation 16

1.2.2 Modéliser l'épidémiologie 17

1.2.2.1 Modèle SIR 17
1.2.2.2 Force d'infection 18
1.2.2.3 Modèle structuré 19
1.2.2.4 Nombre de reproduction de base (R_0) 20
1.2.2.4.1 En environnement constant 21
1.2.2.4.2 En environnement périodique 22
1.2.3 Modéliser l'évolution 22
1.2.3.1 Sur le long terme 23
1.2.3.1.1 Compromis virulence transmission 23
1.2.3.1.2 Fitness d'invasion 25
1.2.3.1.3 Dynamique adaptative 26
1.2.3.2 Sur le court terme : phases transitoires 29
1.2.3.2.1 Génétique quantitative 29
1.2.3.3 Les valeurs reproductives, une mesure de qualité 31
1.3 Objectif de la thèse 34
1.4 Stratégie de la thèse 34

2 Epidemiological and evolutionary consequences of periodicity in treatment coverage 39

2.1 Introduction 43
2.2 Model 45
2.3 Epidemiology 49

2.3.1 Constant treatment coverage 50
2.3.2 Periodic treatment coverage 50
2.3.2.1 Anti-infection and anti-transmission treatments 51
2.3.2.2 Anti-growth and anti-toxin treatments 52
2.4 Evolution 53
2.4.1 Anti-infection and anti-transmission treatments 54
2.4.2 Anti-growth and anti-toxin treatments 55
2.5 Discussion 60

3 Evolutionary implications of spatial heterogeneity in treatment distribution 67

3.1 Introduction 71
3.2 Model 72
3.3 Long-term virulence evolution using adaptive dynamics 76
3.3.1 Mutant invasion fitness 76
3.3.2 Selection gradient 77
3.3.3 Second-order derivative 77
3.4 Numerical applications 78
3.4.1 Habitats quality according to treatments 78
3.4.2 Treatments alone 79
3.4.2.1 Anti-growth 79
3.4.2.2 Anti-toxin treatments 81
3.4.3 Combination of treatments 81

3.4.3.1 Combination with anti-growth treatment 83

3.4.3.2 Combination with anti-toxin treatments 83

3.5 Discussion 84

4 Vaccine escape in metapopulations, the example of SARS-CoV-2 pandemic 91

4.1 Introduction 95

4.2 Model 96

4.2.1 Vaccine escape mutant dynamics in each class of the metapopulation . . . 98

4.2.2 Vaccine escape mutant dynamic in each population 100

4.2.3 Vaccine escape mutant dynamic in the metapopulation 101

4.3 Application 103

4.4 Discussion and perspectives 105

5 Discussion générale 113

5.1 Synthèse des résultats 115

5.1.1 Hétérogénéité d'hôtes 115

5.1.2 Des habitats de bonne ou de mauvaise qualité 117

5.1.3 Évolution à court et long-terme 119

5.2 Applications des résultats 120

5.2.1 Un champs de maïs 120

5.2.2 Deux champs de maïs 122

5.2.3 n champs de maïs 123

5.3 Limites et perspectives 124

5.3.1 Une vaccination plus tardive 124

5.3.2 Mutant d'échappement et fluctuation temporelle 125

5.3.3 Application expérimentales 125

Annexes **127**

Annexe A : Version du Chapitre 2 publiée dans *Proceedings of The Royal Society B* . . 129

Annexe B : Annexes du Chapitre 2 **141**

B.1 Typical behaviour of the heterogeneous model for various types of treatments 143

B.2 Basic reproduction number R_0 144

2.1 Basic reproduction number in a constant environment 144

2.2 Basic reproduction number in a periodic environment for anti-infection (r_1) and anti-transmission (r_3) treatments 145

2.3 Basic reproduction number in a periodic environment for anti-growth (r_2) and anti-toxin (r_4) treatments 146

2.4 Invasion threshold as a function of r and p 149

B.3 Disease-free dynamics 149

B.4 Evolutionary dynamics 151

4.5 Resident-mutant dynamics 151

4.6 Analytical derivation for the selection gradient using time-dependent reproductive values 151

4.7 Numerical calculation of invasion fitness using Floquet's theory . 155

B.5 Impact of recovery 157

B.6 Impact of the shape of the coverage functions 159

Annexe C : Annexes du Chapitre 3 **159**

C.1 Epidemiology 161

1.1 Equilibrium 161

1.2 Basic reproduction number 161

1.3 Prevalence 162

C.2 Evolution 164

2.4 Mutant invasion fitness 164

2.5 Selection gradient expression 164

2.6 Second order derivative calculation 165

C.3 R_A and R_B and their derivatives 167

C.4 Anti-infection and anti-transmission treatments 168

C.5 Evolution in a monomorphic population 169

C.6 Combination of treatments 172

C.7 Numerical exploration of all combinations of ν_A and ν_B, with different migration rates or efficacy, for anti-growth and anti-toxin treatments . . . 174

Annexe D : Annexes du Chapitre 4 **176**

D.1 Full ODE system 177

D.2 Rate of change of the vaccine escape mutant in each class 178

D.3 Vaccine escape mutant dynamics in each subpopulation 181

D.4 Vaccine escape mutant dynamics in the global population 184

D.5 Vaccine escape frequency with the V_τ vaccine 186

Tableau des paramètres utilisés dans la thèse

Définition	Notation chapitre 1	Notation chapitre 2	Notation chapitre 3	Notation chapitre 4
		Hôtes		
Sensibles naïfs	S_N	S_N	S_A^N, S_B^N	S^A, S^B
Sensibles traités	S_T	S_T	S_A^T, S_B^T	$\widehat{S}^A$, $\widehat{S}^B$
Infectés naïfs	I_N	I_N	I_A^N, I_B^N	I^A, I^B
Infectés traités	I_T	I_T	I_A^T, I_B^T	$\widehat{I}^A$, $\widehat{I}^B$
Infectés naïfs mutant	I'	I'_N	$I_A^{N'}$, $I_B^{N'}$	$I^{A'}$, $I^{B'}$
Infectés traités mutant	NA	I'_T	$I_A^{T'}$, $I_B^{T'}$	$\widehat{I}^{A'}$, $\widehat{I}^{B'}$
		Paramètres écologiques		
Natalité / immigration	b	b	b	b
Mortalité	d	d	d	d
		Paramètres épidémiologiques		
Couverture des traitements	ν	$\nu(t)$	ν_A, ν_B	ν_A, ν_B
Transmission des naïfs	β_N	β_N	β_A^N, β_B^N	β_A^N, β_B^N
Transmission des traités	β_T	β_T	β_A^T, β_B^T	β_A^T, β_B^T
Virulence des naïfs	α_N	α_N	α_A^N, α_B^N	$\delta_i^A c_i^A$, $\delta_i^B c_i^B$
Virulence des traités	α_T	α_T	α_A^T, α_B^T	$\widehat{\delta}_i^A \widehat{c}_i^A$, $\widehat{\delta}_i^B \widehat{c}_i^B$
Rétablissement des naïfs	γ_N	γ	NA	$\delta_i^A(1 - c_i^A)$, $\delta_i^B(1 - c_i^B)$
Rétablissement des traités	γ_T	γ	NA	$\widehat{\delta}_i^A(1 - \widehat{c}_i^A)$, $\widehat{\delta}_i^B(1 - \widehat{c}_i^B)$

Chapitre 1

Introduction

Avant-propos

Ce manuscrit est le résultat des trois années de thèse que j'ai réalisées au Centre d'Écologie Fonctionnelle et Évolutive de Montpellier, sous la direction de Sébastien Lion, de septembre 2018 à novembre 2021. Cette thèse porte sur des thématiques d'épidémiologie évolutive, où nous étudions les impacts de l'utilisation de traitements sur l'épidémiologie et l'évolution des pathogènes responsables de maladies infectieuses.

1.1 Épidémiologie et évolution : l'épidémiologie évolutive

1.1.1 Une brève histoire des maladies infectieuses

Les maladies infectieuses ont façonné l'histoire et les populations humaines, animales et végétales. Avec l'arrivée de l'agriculture, les populations humaines ont commencé à s'organiser et à croitre (Bollet and Jay, 2004). Les populations humaines se sont densifiées, favorisant ainsi la circulation des maladies. De plus, le développement contemporain de l'élevage a rapproché les humains des animaux, permettant l'apparition et la circulation de zoonoses.

Les premières traces d'épidémies pourraient trouver leurs origines dans l'Égypte ancienne. Elle aurait été frappée par une épidémie de peste en 1325 B.C. (*Before Christ*), et des momies recouvertes de lésions caractéristiques de la variole témoignent qu'elle pouvait déjà sévir de 1200 à 1100 B.C. (Fenner et al., 1988). Les retranscriptions d'épidémies sont plus nombreuses à l'Antiquité. En l'an 1930 B.C., les morsures de chiens étaient déjà craintes et connues pour avoir entrainé la mort. C'est en Chine ($\sim$ 56 B.C.) qu'est mentionnée pour la première fois la rage du chien. La rouille du blé consumait les champs ($\sim$ 700 B.C.) et a entrainé de nombreuses famines. Les romains priaient Robigus, le dieu de cultures, et lui sacrifiaient des animaux rouges, à cause des traces rouges sur les feuilles causées par la rouille, en retour de la protection de leurs champs de blé (Saunders et al., 2019). Plus tard, de 430 à 427 B.C., une épidémie de peste à Athènes causée par le virus de la variole (*smallpox*) ou de la rougeole (*measles*), a certainement causé la défaite des Athéniens contre Sparte lors de la Guerre du Péloponnèse, à cause du grand nombre de pertes humaines dans les troupes (Hays, 2005). Puis une succession d'épidémies (peste Antonines (165), de Cyprien (249-262) et de Justinien (541 - 749)) pourraient être à l'origine du déclin de l'empire Romain (Harper, 2019). La pandémie de peste noire en Europe de 1346 à 1353 a été l'une des plus meurtrière (Hays, 2005), probablement transmise à l'homme par la puce du rat. Cette pandémie a

eu pour conséquence le déclin de la seigneurie. Le mildiou de la pomme de terre a ravagé l'Irlande en 1843 et entrainé la plus grande famine qu'ait connue le pays. Les élevages ont été frappés par la peste bovine dès la fin du XIX^{ieme} siècle (Pastoret et al., 2006). Plus récemment, depuis 2019, la pandémie de SARS-CoV-2 témoigne des impacts économiques, sanitaires et sociétaux que peuvent causer les maladies infectieuses.

1.1.2 Des hôtes et des pathogènes

Les maladies infectieuses sont causées par des agents pathogènes qui utilisent un hôte pour effectuer leur cycle de vie et se reproduire. Ce sont souvent des organismes de taille microscopique (bactéries, virus, champignons, protozoaires) mais parfois macroscopique (helminthes). Du point de vue écologique, le pathogène est un parasite pour son hôte. En effet, son interaction avec l'hôte lui est bénéfique, alors qu'elle est néfaste pour l'hôte. Le pathogène est un parasite particulier qui induit une maladie chez son hôte. Comme le dit Schmidt-Hempel (2011), *all living organism are parasitized by one species at least*, tout organisme vivant, de l'animal au végétal jusqu'à la bactérie, est l'hôte d'un parasite potentiellement pathogène.

Les agents pathogènes peuvent se transmettre d'un hôte à un autre, soit verticalement (i.e. à la naissance), soit horizontalement (i.e. d'un individu à un autre indépendamment des liens de parenté) par voie directe ou indirecte. La transmission par voie directe requière un contact entre les hôtes au cours duquel le pathogène est transmis d'un hôte infecté à un hôte sensible, par exemple par morsure. La transmission par voie indirecte requière la libération du pathogène dans l'environnement où il va entrer en contact avec un hôte sensible, qui deviendra alors infecté. Dans ce cas, la transmission de l'agent pathogène d'un hôte à un autre peut se faire via des vecteurs biologiques ou mécaniques. Dans le cas d'une transmission par vecteur mécanique, le pathogène peut être aéroporté, comme c'est le cas avec la sporulation des champignons, ou pour l'éternuement. Il peut aussi être libéré dans l'eau ou encore déposé sur une surface. Dans le

cas d'une transmission par vecteur biologique, le pathogène est transmis à l'hôte final par un autre organisme dans lequel le pathogène réalise une partie de son cycle de vie. Les moustiques sont vecteurs de nombreux pathogènes, par exemple l'anophèle femelle est vecteur de l'agent du paludisme, du genre *Plasmodium*.

Les maladies infectieuses peuvent être plus ou moins dangereuses pour l'hôte. Cette dangerosité est quantifiée par la virulence. Cependant, en fonction des domaines d'étude, sa définition varie. En biologie théorique, la virulence est définie comme la mortalité de l'hôte due à la maladie. En biologie expérimentale, la virulence caractérise les effets néfastes du parasite sur l'hôte autres que sa mortalité. En phytopathologie et en génétique des populations, la virulence caractérise la capacité du pathogène à infecter (Read, 1994; Frank, 1996; Day, 2002; Alizon et al., 2009).

La virulence et la transmission d'un pathogène sont des traits biologiques d'intérêt en épidémiologie évolutive. Ces traits, agissant directement sur leur cycle de vie, et affectant ainsi leur survie et leur reproduction, sont des traits d'histoire de vie des pathogènes (Galvani, 2003; Michalakis et al., 2009).

Dans cette thèse nous utilisons les termes de pathogène ou de parasite de manière interchangeable pour caractériser des micro-pathogènes. De plus, nous considérons essentiellement les maladies à transmission directe ou indirecte par vecteur mécaniques. La prise en compte des maladies à vecteur biologique nécessite la considération du cycle biologique du vecteur. Enfin, la virulence d'un pathogène sera définie comme la mortalité additionnelle de l'hôte induite par la maladie, et nous nous intéresserons à son évolution.

1.1.3 L'arrivée des traitements

Avant l'apparition des vaccins et des antibiotiques, la mortalité liée aux maladies infectieuses était très élevée et les moyens de luttes peu efficaces. Les maladies ont été longtemps considérées comme une malédiction des Dieux et les incantations, sacrifices ou rituels magiques n'étaient pas

rares (Habicht et al., 2020). La théorie des miasmes a longtemps imputé au mauvais air l'apparition des maladies infectieuses, et pendant la pandémie de peste noire, les gens sortaient avec des petits bouquets de fleurs à respirer pour éviter l'infection (Kokayeff, 2012).

La théorie microbienne, initiée en 1546 par Girolamo Fracastoro, proposant que les maladies soient causées par des organismes invisibles, ouvre ainsi la voie de la compréhension (Kokayeff, 2012). Finalement, suite aux épidémies de variole qui sévissaient aux quatre coins du globe, il a été observé que les survivants étaient immunisés contre la maladie. C'est ainsi qu'a débuté la variolisation, dont le principe était d'inoculer du virus de la variole prélevé sur des individus infectés, à des individus non immunisés (Riedel, 2005). Cependant l'opération était risquée car le virus de la variole reste très virulent avec un taux de mortalité de 2% à 3%. C'est en 1796 qu'Edward Jenner observe que les patients ayant contracté une maladie proche de la variole, la vaccine (*cowpox*) dont la virulence est moindre, étaient immunisés contre la variole. C'est ainsi qu'Edward Jenner débute des inoculations du virus de la vaccine pour immuniser les individus contre la variole, et qu'il crée le premier vaccin.

C'est près d'un siècle plus tard que l'immunologie connait une avancée fulgurante, lorsque Louis Pasteur s'intéresse aux formes atténuées des virus. Il découvre qu'au fur et à mesure des générations, les virus perdaient en virulence. Grâce à cette technique de cultures successives, il met au point en 1879 un vaccin contre le choléra aviaire (*fowl cholera*), puis en 1881 un vaccin contre la maladie du charbon (*antrax*), en 1883 un vaccin contre le rouget de porc (*swine erysipela*) et en 1885, le vaccin contre la rage (Berche, 2012).

Enfin, les antibiotiques ont fait leur apparition en 1928, avec la découverte de la pénicilline par Alexander Flemming. Cependant, les antibiotiques ne sont efficaces que contre une seule classe de pathogènes, les bactéries.

Les vaccins représentent l'une des armes les plus efficaces contre les maladies infectieuses (Roush Sandra and Murphy Trudy, 2007). A ce jour, la vaccination a permis d'éradiquer deux

maladies infectieuses. D'abord la variole (*smallpox*), qui est à l'origine d'au moins 500 000 morts au cours des cent dernières années, est mondialement éradiquée depuis 1980 grâce à des campagnes de vaccination de grande envergure (Breman and Arita, 1980; Henderson, 2009). Ensuite, la peste bovine (*Rinderpest*), qui touchait principalement les élevages de bovins, est éradiquée depuis 2010 (Roeder, 2011). Une troisième maladie, la poliomyélite, est en voie d'éradication grâce à la vaccination (WHO, 2019).

Au-delà de l'éradication, la vaccination permet aussi d'instaurer une immunité collective dans les populations. Cette immunité est atteinte lorsqu'une proportion suffisante de la population est immunisée, ce qui ralentit la circulation du pathogène et diminue sa prévalence jusqu'à une possible extinction (Fine, 1993). De cette manière, la grande proportion d'hôtes immunisés protège la petite proportion d'hôtes qui ne peuvent pas être immunisés (à cause de maladies auto-immunes par exemple).

Dans la suite de ce manuscrit nous utiliserons le terme traitement pour caractériser toute mesure prophylactique utilisée visant à limiter la propagation de maladies infectieuses, telle que les vaccins, les antibiotiques utilisés en prévention, et les fongicides.

1.1.4 Traitements oui, mais imparfaits

Le rôle des traitements est de prévenir la propagation des pathogènes dans les populations pour limiter les pertes. La transmission et la virulence des pathogènes sont deux traits d'histoire de vie clés en épidémiologie. Dans cette thèse, nous considérons plusieurs types de traitements qui vont limiter la transmission et/ou la virulence des pathogènes. Cependant, les traitements n'agissent pas sur tous les traits biologiques en même temps (Read et al., 2015), et leurs efficacité est relative et variable d'un traitement à un autre, mais rarement efficace à 100%, ce qui en font des traitements imparfaits.

Comme dans Gandon et al. (2001*b*), nous considérons quatre types de traitements. Ils sont

récapitulés dans le tableau 1.1, et sont représentés graphiquement en figure 1.1.

Le traitement **anti-infection** (noté r_1 ou r_σ) vise à réduire la susceptibilité des hôtes à l'infection. Un hôte sensible traité a moins de chance d'être infecté s'il entre en contact avec un pathogène qu'un hôte sensible non traité.

Le traitement **anti-croissance** (noté r_2), vise à réduire la croissance intra-hôte du pathogène, ce qui va affecter sa transmission et sa virulence. Un hôte infecté traité émettra moins de pathogènes et il est moins probable qu'il meure des suites de la maladie.

Le traitement **anti-transmission** (noté r_3 ou r_τ), vise à réduire la transmission des pathogènes. Un hôte infecté traité émettra moins de pathogènes qu'un hôte non traité.

Le traitement **anti-toxine** (noté r_4), vise à réduire les conséquences négatives de la maladie. Un hôte infecté traité a une probabilité plus faible de mourir des suites de la maladies qu'un hôte non traité qui aurait été infecté.

TABLE 1.1 – Types et actions des traitements considérés dans cette thèse.

Type de traitement	**Mode d'action**	**Exemple**	**Notation dans la thèse**
anti-infection	réduit la susceptibilité des hôtes sensibles	Bouillie Bordelaise (Barker and Gimingham, 1911)	r_1 (chapitre 2, 3), r_σ (chapitre 4)
anti-croissance	réduit la reproduction intra-hôte du pathogène	ABT-538 contre le VIH (Ho et al., 1995)	r_2 (chapitre 2, 3)
anti-transmission	réduit la transmission des hôtes infectés	Vaccin contre le calcivirus félin (Lappin et al., 2006)	r_3 (chapitre 2, 3), r_τ (chapitre 4)
anti-toxine	réduit la mortalité des hôtes infectés	Vaccin contre la diphtérie (Gandon and Day, 2008)	r_4 (chapitre 2, 3)

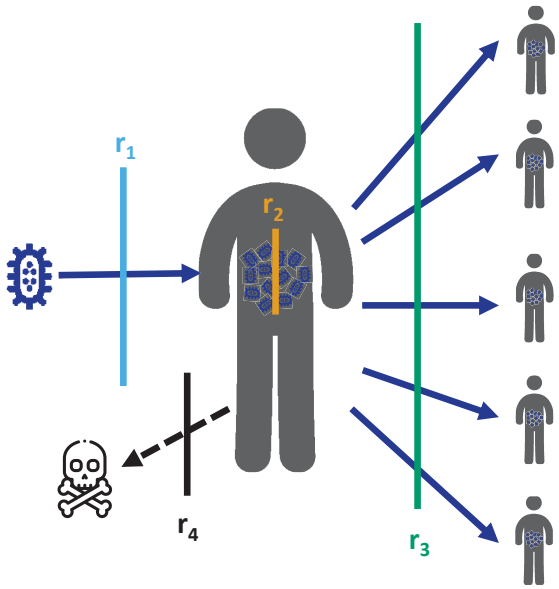

FIGURE 1.1 – Processus d'infection et mode d'action des différents types de traitements, anti-infection (r_1, bleu), anti-croissance (r_2, orange), anti-transmission (r_3, vert) and anti-toxin (r_4, noir), avec un humain pour illustrer l'hôte.

1.1.5 Processus d'évolution

L'évolution est un changement de la fréquence des allèles dans une population. L'apparition d'un nouvel allèle peut être causée par des facteurs démographiques (mouvements de populations) ou par des facteurs génétiques (mutations), qui sont ensuite maintenus par la sélection naturelle. Une souche est définie comme une variante allélique intraspécifique.

1.1.5.1 De nouveaux allèles à sélectionner

Du fait de leur cycle de vie rapide, les mutations génétiques sont fréquentes chez les pathogènes. Les mutations sont des erreurs aléatoires de réplication du matériel génétique qui subsistent malgré le système de relecture. Les mutations sont généralement neutres, c'est à dire qu'elles n'auront pas de conséquences sur le cycle de vie de l'organisme. Cependant, certaines mutations peuvent être délétères et vont diminuer le succès reproducteur de cette souche de pathogène. A l'inverse,

certaines mutations peuvent être bénéfiques et conférer un avantage à la souche nouvellement apparue par rapport à la souche originelle.

Une deuxième source d'allèles est la migration. En effet, lorsqu'un organisme immigre dans une population, il représente un apport de matériel génétique nouveau. Bien qu'il puisse ne pas y avoir de différence phénotypique, son génotype peut être légèrement différent de celui de la population dans laquelle il a immigré. Si son génotype différent lui confère un avantage, il va potentiellement être maintenu et envahir la population.

Initiée à l'antiquité par Lucrèce, formulée au XIX^{ieme} par Lamarck puis adoptée à partir de 1859 avec Darwin, la théorie de l'évolution fournit une explication à l'apparition de nouvelle espèces et à la disparition d'autres. Dans son livre, "L'Origine des espèces" (Darwin, 1964), Charles Darwin introduit la notion de sélection naturelle et la définit comme *the survival of the fittest*, la survie du mieux adapté. Ainsi, lors d'une compétition entre deux génotypes différents, la sélection naturelle favorise celui qui a le meilleur succès reproducteur (i.e. fitness).

1.1.5.2 Évolution des pathogènes

Face à la pression exercée sur les pathogènes, par les hôtes ou par les traitements par exemple, différents traits des pathogènes peuvent être sélectionnés. Ils peuvent développer une résistance face à certains traitements, contourner l'immunité conférée par les vaccins ou encore changer leur exploitation des hôtes par une modification de leurs traits d'histoire de vie.

1.1.5.2.1 Différentes résistances Lorsqu'une souche résistante à un traitement apparaît, ce dernier diminue en efficacité et de nouvelles méthodes sont requises, ce qui fait de la résistance un problème majeur en santé publique et animale, ainsi qu'en agriculture. En effet, des souches résistantes peuvent émerger suite à l'utilisation massive de traitements pour lutter contre les maladies infectieuses, qui exercent une forte pression de sélection sur les pathogènes. Nous observons

aussi bien de la résistance aux fongicides (Brent and Hollomon, 1998), qu'aux antibiotiques (Witte, 2000).

L'évolution de la résistance est majoritairement observée en réponse à l'utilisation de médicaments et moins observée en réponses aux vaccins (Kennedy and Read, 2017), qui agissent de manière différentes sur les pathogènes. En effet, les vaccins sont généralement utilisés en prophylaxie pour stimuler la réponse immunitaire de l'hôte alors que les médicaments sont plutôt utilisés en thérapeutique (bien que certains antibiotiques soient utilisés en prophylaxie). Dans Kennedy and Read (2017) les auteurs soutiennent que cette différence du moment d'administration et les cibles multiples des vaccins sont la principale raison qui expliquent l'apparition de résistances. L'utilisation précoce de vaccins diminue la diversité génétique des pathogènes et ainsi la potentielle émergence de résistance. De plus, les vaccins ont de multiples cibles à la surface des pathogènes, ce qui diminue les probabilités d'apparition et les avantages d'une éventuelle résistance.

Cependant, des mutants d'échappement aux vaccins peuvent malgré tout apparaître. Ce type de mutant a été observé par exemple, pour les vaccins contre l'hépatite B (Carman et al., 1990) et la fièvre aphteuse (Domingo et al., 2003). Dans le cas du Covid-19, l'apparition d'un mutant d'échappement menace et est surveillé. Thompson et al. (2021) ont montré que la probabilité d'émergence d'un mutant d'échappement au vaccin était lié à l'incidence (figure 1.2).

1.1.5.2.2 Évolution de la virulence La virulence caractérise la dangerosité d'un pathogène vis à vis de son hôte, ce qui en fait un trait biologique d'intérêt. Étudier l'évolution de la virulence à long-terme a un intérêt particulier dans la gestion des maladies infectieuses, dans le but de favoriser des traitements qui sont bénéfiques à court- et à long- terme. Le pathogène peut augmenter en virulence en réponse à la pression de sélection causée par les traitements, ou par l'augmentation de résistance de son hôte.

Dans Gimeno (2008), l'auteure examine les origines de l'évolution du virus responsable de

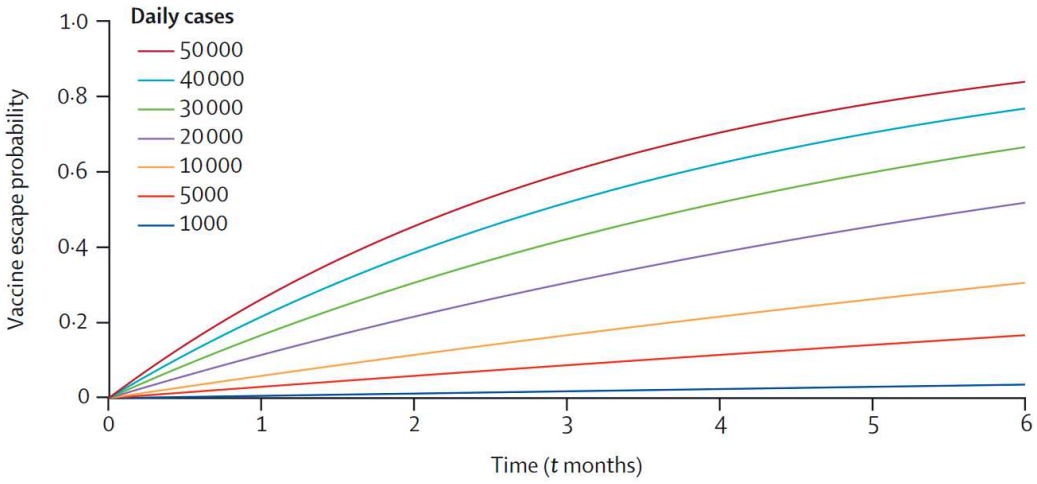

FIGURE 1.2 – Probabilité d'apparition d'un mutant d'échappement au vaccin au terme d'un temps t, en fonction de l'incidence et avec une probabilité d'échappement de 2.10^{-7} par infection (Thompson et al., 2021).

la maladie de Marek dans les élevages de poules (figure 1.3). Cette maladie, très contagieuse et très virulente a de grandes conséquences sanitaires et économiques. A la fin de la seconde guerre mondiale, l'élevage s'est intensifié et les densités d'animaux dans les fermes sont accrues. Cette densité importante d'animaux sensibles a augmenté la prévalence du virus, ce qui a probablement favorisé l'augmentation de la virulence du virus. Read et al. (2015) ont montré que l'utilisation de vaccins anti-toxine, qui diminuent la virulence du pathogène mais qui ne limitent pas sa transmission, est à l'origine de l'augmentation de la virulence du virus de la maladie de Marek, ce qui accroît le risque pour les hôtes non-vaccinés. Gandon et al. (2001*b*, 2003) ont également montré que les traitements qui visent à réduire la dangerosité de la maladie entraînaient une augmentation de la virulence sur le long terme. Ces traitements qui réduisent la mortalité de l'hôte, favorisent le maintien du pathogène dans la population et ainsi son évolution.

L'augmentation de la virulence des pathogènes peut être une conséquence d'une coévolution avec son hôte. Un exemple de coévolution est celui du virus causant la myxomatose (*Myxoma virus*) chez le lapin Européen. En 1950 le virus a été introduit en Australie pour réguler les populations envahissantes de lapins. L'épizootie s'est répandue dans le pays et la population de

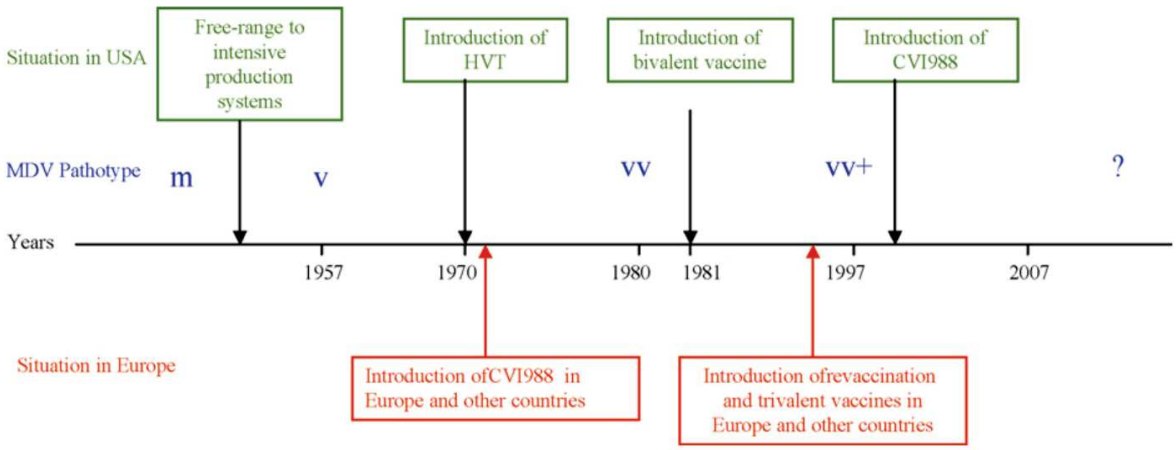

FIGURE 1.3 – Évolution du virus de la maladie de Marek. Quatre pathogénéicités ont été décrites : moyenne (m), virulente (v), très virulente (vv), très virulente + (vv+) (Gimeno, 2008).

lapins à drastiquement chuté, avec un taux de mortalité allant jusqu'à 99.8%. Au fil des saisons et des générations, de nouvelles souches sont apparues de moins en moins virulentes, et les lapins ont commencé à présenter des résistances génétiques au virus (Dwyer et al., 1990; Kerr, 2012).

Dans une étude expérimentale où des Carpodaque du Mexique sont infectés par une bactérie (*Mycoplasma gallisepticum*), Fleming-Davies et al. (2018) ont montré que des hôtes infectés par une souche très virulente développaient une immunité contre des souches moins virulentes. Ainsi, seules les souches les plus virulentes parviennent à se maintenir dans la population.

De ce fait, les pathogènes peuvent évoluer en réponse à un changement dans leurs habitat. Nous allons étudier dans cette thèse, un modification de l'habitat des pathogènes causé par le traitement des hôtes, et nous allons nous intéresser à l'évolution de la virulence sur le long-terme, et à la vitesse d'apparition d'un mutant d'échappement aux vaccins sur le court-terme.

1.1.6 Hétérogénéité d'hôtes

Les populations sont composées d'hôtes tous différents. Les hôtes varient les uns des autres à cause de facteurs génétiques ou de facteurs acquis, et cette hétérogénéité peut affecter la pression

de sélection.

Premièrement, l'hétérogénéité des hôtes peut varier dans le temps. Dans beaucoup d'espèces animales, des changements physiologiques cycliques apparaissent, notamment liés aux périodes de reproduction, période où les organismes sont affaiblis et plus sensibles aux agents infectieux (Dowell, 2001). De plus, les stratégies de protection peuvent elles aussi varier dans le temps, comme l'épandage de fongicides qui suit le cycle biologique des plants, la vaccination ponctuelle de populations isolées ou en fonction du cycle de vie des pathogènes par exemple.

Deuxièmement, l'hétérogénéité peut varier dans l'espace. Les populations sont implantées dans des zones géographiques différentes. Dans ces zones, les maladies infectieuses ne circulent pas de la même manière en raison des différences climatiques ou de politiques locales. Cependant, les maladies aéroportées ou véhiculées par l'eau par exemple, peuvent se répandre sur de grandes distances et infecter des populations sensibles qui auraient été traitées de manière différentes. De plus, la mondialisation favorise le déplacement des hôtes et des pathogènes et donc favorise la propagation de maladies infectieuses.

Ainsi, l'hétérogénéité des hôtes dans une population est un facteur clé à prendre en compte en épidémiologie évolutive. Dans cette étude, nous considérons que l'hétérogénéité des hôtes varie dans le temps dans le chapitre 2, et dans l'espace dans les chapitres 3 et 4.

1.2 L'approche par la modélisation

1.2.1 Intérêts de la modélisation

Les résultats théoriques ne sont pas toujours considérés comme de vrais résultats, en comparaison des résultats empiriques (Goldstein, 2018). En réalité, l'intérêt des modèles mathématiques est intrinsèquement lié à la question biologique qui a motivé leur élaboration. Par exemple, alors que

la variole sévit, Bernoulli à montré en 1766 dans un modèle mathématique que la variolisation pouvait augmenter l'espérance de vie de 3 ans (Bacaër, 2011). La modélisation a permis de grandes avancées dans la recherche sur le virus de l'immunodéficience humaine (VIH) (Otto and Day, 2011). Les mathématiques permettent non seulement de comprendre des données biologiques, mais aussi de fournir des prédictions et hypothèses à tester expérimentalement. Finalement, la modélisation ne peut pas exister sans la biologie, mais la biologie ne peut pas avancer seule.

1.2.2 Modéliser l'épidémiologie

Les systèmes biologiques sont très complexes, et leur analyse nécessite de passer par des simplifications. En dynamique des populations, nous cherchons à étudier les interactions biologiques entre organismes, et nous émettons des hypothèses basées sur des observations ou sur des prédictions. Définir ces hypothèses permet de simplifier des phénomènes biologiques complexes, et est la première étape de développement d'un modèle. Les interactions biologiques sont ensuite traduites analytiquement et numériquement. Appliquée à l'épidémiologie, la modélisation permet de mieux comprendre l'origine ainsi que la dynamique des épidémies et de mettre en exergue les paramètres intervenant dans leur émergence, leur maintien et leur déclin.

1.2.2.1 Modèle SIR

Un modèle classique en épidémiologie est le modèle à compartiment SIR pour *Susceptible* - *Infected* - *Recovered*, Sensibles - Infectés - Rétablis. Les hôtes sont répartis dans des compartiment en fonction de leur statut vis-à-vis de l'infection, non infectés (sensibles, notés S), infectés (notés I) ou rétablis (notés R). Le changement de statut d'un hôte est modélisé par les flux reliant les différents compartiments, traduisant la transmission et la guérison par exemple. Dans le modèle présenté en figure 1.4, les hôtes infectés transmettent le pathogène aux hôtes sensibles à un taux β, et les hôtes infectés guérissent de la maladie à un taux γ. Les hôtes arrivent dans la population

non-infectés à taux b, et tous les hôtes meurent à taux d, avec une mortalité additionnelle pour les hôtes infectés, α (virulence). Ces interactions peuvent être exprimées en un système d'équations différentielles ordinaires (ODE) permettant de suivre les dynamiques de chaque classe d'hôtes, tel que

$$\begin{aligned} \frac{\mathrm{d}S}{\mathrm{d}t} &= b - (d + \beta I)S\,, \\ \frac{\mathrm{d}I}{\mathrm{d}t} &= \beta IS - (d + \alpha + \gamma)I\,, \\ \frac{\mathrm{d}R}{\mathrm{d}t} &= \gamma I - dR\,. \end{aligned} \tag{1.1}$$

Ce modèle est présenté graphiquement en figure 1.4.

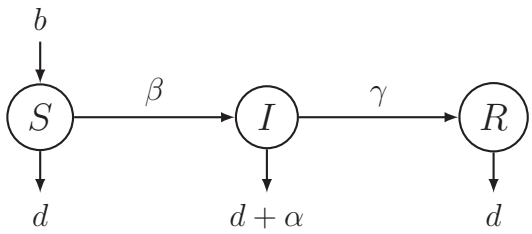

FIGURE 1.4 – Diagramme de flux d'un modèle SIR (*Susceptible-Infected-Recovered*).

1.2.2.2 Force d'infection

La force d'infection caractérise la probabilité qu'un hôte infecté entre en contact avec un hôte sensible et que le contact soit infectieux. La force d'infection est notée h et dépend de trois paramètres, la densité d'hôte infectés dans la population, I, le taux de contact, c, et la probabilité que le pathogène soit transmis lors du contact, i. Dans notre étude nous regroupons le taux de contact et la probabilité que le contact soit infectieux dans $\beta = ci$. Ainsi, $h = \beta I$, la transmission est donc densité-dépendante. Cependant, il existe des modèle où la transmission est fréquence-dépendante ($h = \beta I/N$, où N est la population totale). Le type de transmission est un paramètre important à considérer lors de l'établissement d'un modèle car il doit être adapté aux

spécificités de la maladie infectieuse considérée et influe grandement les résultats évolutifs (Day, 2001; Roche et al., 2011; Cortez and Weitz, 2013).

1.2.2.3 Modèle structuré

Afin de prendre en compte l'hétérogénéité des hôtes, nous nous sommes intéressés à des populations d'hôtes dites structurées. En effet, les hôtes diffèrent les uns des autres, que ce soit au niveau de leur génotype ou de leur emplacement géographique par exemple. Les hôtes sont alors classés dans différentes classes. Dans cette thèse, nous nous intéressons plus spécifiquement à la variabilité des statuts immunitaires des hôtes, classés selon qu'ils aient été traités ou non. Deux classes s'ajoutent alors à notre précédent modèle (1.1), les hôtes dits naïfs (N) et les hôtes dits traités (T). Une proportion ν des hôtes arrivant dans la population sont traités et rejoignent la classe des hôtes non-infectés traités (S_T), le reste est non traité et rejoint la classe des non-infectés non-traités S_N, à taux $1-\nu$. Chaque hôte sensible, traité ou non, peut être infecté, à des taux respectifs β_T et β_N, puis guérir de l'infection à des taux respectifs de γ_T et γ_N. Nous définissons $\beta_T = (1-r)\beta_N$ où r est l'efficacité du traitement qui varie entre 0 (traitement inefficace) et 1 (traitement parfait). Enfin, les hôtes infectés, traité ou non, subissent une mortalité additionnelle notée α_T et α_N. Ainsi, nous avons cinq classes d'hôtes différentes, les non-infectés non traités (S_N), les non-infectés traités (S_T), les infectés non-traités (I_N), les infectés traités (I_T) et les rétablis (R), dont la dynamique représentée graphiquement en figure 1.5 et est décrite par le système d'ODE

$$\begin{aligned}
\frac{\mathrm{d}S_N}{\mathrm{d}t} &= b(1-\nu) - (\beta_N I_N + \beta_T I_T)S_N - dS_N\,,\\
\frac{\mathrm{d}S_T}{\mathrm{d}t} &= b\nu - (\beta_N I_N + \beta_T I_T)S_T - dS_T\,,\\
\frac{\mathrm{d}I_N}{\mathrm{d}t} &= (\beta_N I_N + \beta_T I_T)S_N - (d+\alpha_N+\gamma_N)I_N\,,\\
\frac{\mathrm{d}I_T}{\mathrm{d}t} &= (\beta_N I_N + \beta_T I_T)S_T - (d+\alpha_T+\gamma_T)I_T\,,\\
\frac{\mathrm{d}R}{\mathrm{d}t} &= \gamma_N I_N + \gamma_T I_T - dR\,.
\end{aligned} \tag{1.2}$$

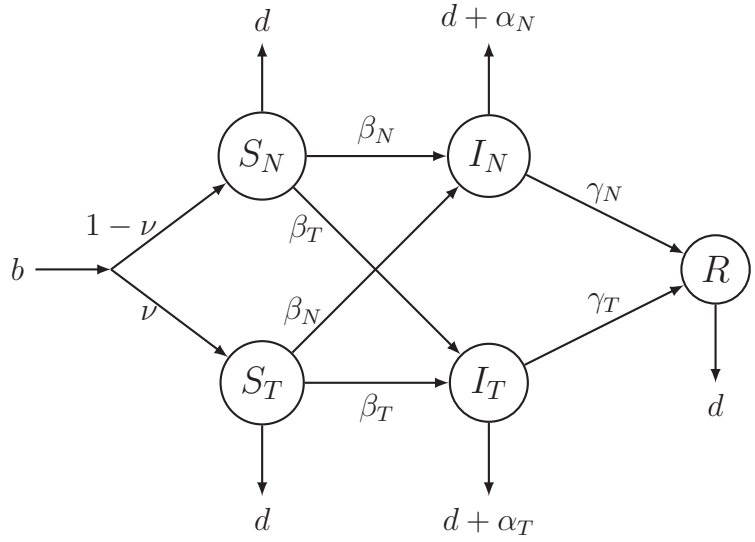

FIGURE 1.5 – Diagramme de flux d'un modèle SIR structuré.

1.2.2.4 Nombre de reproduction de base (R_0)

Quand un pathogène arrive dans une population d'hôtes sensibles, sa capacité à envahir la population est quantifiée par le nombre de reproduction de base, communément noté R_0. Le R_0 mesure le nombre moyen d'hôtes secondairement infectés par un seul hôte infecté (Anderson and May, 1986, 1991; Lion and Metz, 2018). Si le R_0 est supérieur à 1, c'est à dire qu'un hôte infecté infecte plus qu'un hôte sensible en moyenne, le pathogène va croître exponentiellement et envahir la population, causant une épidémie. Si le R_0 est inférieur à 1, un hôte infecté va infecter moins d'un hôte en moyenne, ne permettant pas au pathogène de se maintenir dans la population. Le R_0 caractérise donc la capacité d'un pathogène à envahir une population totalement sensible, et dépend de ses traits d'histoire de vie, notamment sa transmission β et sa virulence α. La valeur de ce R_0 est variable d'une maladie à une autre et d'une population à une autre. Cependant, l'environnement dans lequel se développent les pathogènes n'est pas toujours constant et peut varier dans le temps. Nous distinguons ainsi le calcul du R_0 en environnement constant ou périodique.

1.2.2.4.1 En environnement constant

En reprenant l'exemple d'un modèle non structuré montré en (1.1), le R_0 s'exprime

$$R_0 = \frac{\beta S}{d + \alpha + \gamma}. \tag{1.3}$$

En modèle structuré il faut passer par l'écriture matricielle du modèle et appliquer le théorème de génération suivante (*Next generation theorem*, encadré 1).

Encadré 1 : Théorème de génération suivante (*Next Generation Theorem*)

Le modèle présenté en (1.2) peut être écrit sous forme matricielle tel que $\dot{I} = \mathbf{A}I$ où $I = (I_N \quad I_T)^\top$ et

$$\mathbf{A} = \begin{pmatrix} \beta_N S_N - (d + \alpha_N + \gamma_N) & \beta_T S_N \\ \beta_N S_T & \beta_T S_T - (d + \alpha_T + \gamma_T) \end{pmatrix}$$

où les S_N et S_T sont évalués dans une population sans maladie. La matrice $\mathbf{A}$ peut être écrite sous la forme $\mathbf{F} - \mathbf{V}$ avec $\mathbf{F}$ la matrice de natalité et $\mathbf{V}$ la matrice de mortalité tels que

$$\mathbf{F} = \begin{pmatrix} \beta_N S_N & \beta_T S_N \\ \beta_N S_T & \beta_T S_T \end{pmatrix} \text{ et } \quad \mathbf{V} = \begin{pmatrix} (d + \alpha_N + \gamma_N) & 0 \\ 0 & (d + \alpha_T + \gamma_T) \end{pmatrix}$$

Comme tous les éléments de $\mathbf{V}^{-1}$ et de $\mathbf{F}$ sont positifs et que les valeurs propres de $-\mathbf{V}$ sont négatives, le théorème peut être appliqué (Diekmann et al., 1990; Hurford et al., 2009), et le R_0 est la valeur propre dominante de la matrice $\mathbf{F}.\mathbf{V}^{-1}$, ce qui donne

$$R_0 = \frac{\beta_N S_N}{d + \alpha_N + \gamma_N} + \frac{\beta_T S_T}{d + \alpha_T + \gamma_T}$$

1.2.2.4.2 En environnement périodique

La transmission des pathogènes peut varier dans le temps en fonction de son cycle de vie ou pour suivre celui de l'hôte par exemple. Ainsi, il est nécessaire d'avoir des outils pour étudier les variations temporelles des maladies infectieuses.

L'interprétation du R_0 en environnement fluctuant est plus complexe qu'en environnement constant. En effet, le nombre d'individus secondairement infectés varie au cours du temps en fonction de la périodicité de l'épidémie. Grassly and Fraser (2006) définissent le R_0 en environnement périodique comme le nombre moyen d'hôtes secondairement infectés après l'introduction d'un hôte infecté dans une population de sensibles, à n'importe quel moment de la période. D'après Bacaër and Guernaoui (2006), en modèle non structuré et en supposant que les traits d'histoire de vie du pathogènes (β et α) sont périodiques, le R_0 s'exprime

$$R_0 = \int_{t-T}^{t} \frac{\beta(t)S}{d + \alpha(t) + \gamma}\,, \tag{1.4}$$

où T est la période de la fluctuation.

En modèle structuré, son expression est plus complexe, et requière d'utiliser la théorie de Floquet (Bacaër (2011), encadré 2).

1.2.3 Modéliser l'évolution

Dans cette thèse, nous avons utilisé des techniques de dynamique adaptative (chapitre 2 et 3) et de génétique quantitative (chapitre 4) pour caractériser l'évolution, mais d'autres méthodes peuvent être utilisées (Otto and Day, 2011). La dynamique adaptative permet d'étudier l'évolution des pathogènes sur le long-terme, et la génétique quantitative permet de mesurer l'évolution des pathogènes à court-terme.

En considérant l'apparition d'un mutant dans une population non structurée, les équations du

modèle (1.1) deviennent

$$\begin{aligned}
\frac{\mathrm{d}S}{\mathrm{d}t} &= b - (\beta I + \beta' I')S - dS\,, \\
\frac{\mathrm{d}I}{\mathrm{d}t} &= \beta I S - (d + \alpha + \gamma)I\,, \\
\frac{\mathrm{d}I'}{\mathrm{d}t} &= \beta' I' S - (d + \alpha' + \gamma')I'\,, \\
\frac{\mathrm{d}R}{\mathrm{d}t} &= \gamma I + \gamma' I' - dR\,,
\end{aligned} \tag{1.5}$$

où l'apostrophe symbolise la souche mutante, le modèle est présenté graphiquement en figure 1.6.

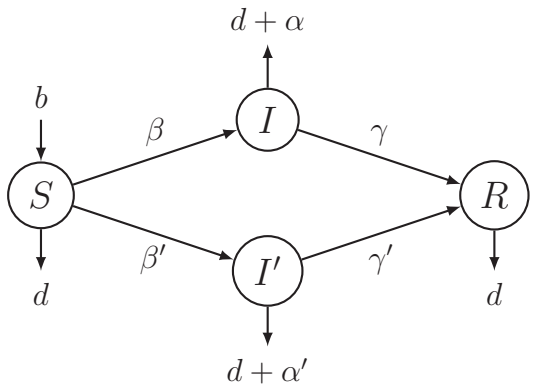

FIGURE 1.6 – Diagramme de flux d'un modèle SIR avec des hôtes infectés par la souche résidente (I) ou mutante (I').

1.2.3.1 Sur le long terme

1.2.3.1.1 Compromis virulence transmission La sélection naturelle favorise les souches qui ont la plus forte contribution au générations futures, ce qui dépend de la transmission et de la virulence de la souche. La théorie d'un compromis entre la transmission et la virulence a été introduite par Anderson and May (1982) et suggère une corrélation positive entre l'évolution de la transmission et de la virulence. En effet, un gain en transmission augmente la survie du pathogène en augmentant le nombre d'hôtes infectés et ainsi sa fitness d'invasion. En revanche, un gain en virulence va réduire la durée de l'infection en augmentant la mortalité de son hôte, ce qui diminue

ainsi la transmission du pathogène, et donc diminue sa fitness d'invasion (Galvani, 2003).

Nous pourrions supposer plusieurs formes de compromis entre la virulence et la transmission. Dans un compromis linéaire entre ces deux traits d'histoire de vie, les deux traits augmenteraient ensemble indéfiniment, ce qui parait peu probable avec les observations biologiques. Un compromis convexe impliquerait une transmission de plus en plus importante avec l'augmentation de la virulence, ce qui ne correspond pas non plus aux observations. Enfin, la forme de compromis communément admise et la plus probable biologiquement est une forme concave saturante. Elle correspond à une augmentation conjointe de la virulence et de la transmission, jusqu'à un certain seuil où la transmission n'augmente plus avec la virulence (Alizon et al., 2009). Intuitivement, nous comprenons que la transmission d'un pathogène ne peut pas augmenter indéfiniment sans entrainer un coût en terme d'augmentation de la virulence, sinon toutes les souches auraient évolué vers de l'avirulence. Cependant, la virulence d'un pathogène ne peut pas augmenter indéfiniment sans provoquer une diminution de la transmission à cause de l'augmentation de la mort de l'hôte qu'elle induit (Anderson and May, 1982; Ewald, 1983; Gandon et al., 2001*a*; Dieckmann, 2002; Galvani, 2003; Alizon et al., 2009). Ainsi, l'augmentation de la virulence est un effet pléiotrope à l'augmentation de la transmission (Miller and Metcalf, 2019).

Il existe quelques études empiriques qui appuient cette théorie, réalisées sur le parasite responsable du paludisme (Mackinnon and Read, 1999), sur le bactériophage f1 infectant *Escherichia coli* et *Salmonella typhimurium* (Messenger et al., 1999), sur le virus de l'immunodéficience humaine (Fraser et al., 2007), sur le virus de la mosaïque du chou fleur (Doumayrou et al., 2013), sur *Ophryocystis elektroscirrha*, un parasite protozoaire des papillons monarque (De Roode et al., 2008), ou encore sur la bactérie *Pasteuria ramosa* qui infecte les Daphnies. Cependant, ces études restent peu nombreuses en comparaison du nombre d'agents pathogènes, du fait de la difficulté de quantifier expérimentalement la fitness des parasites.

Au cours de cette thèse nous considérons un compromis concave saturant entre la transmission

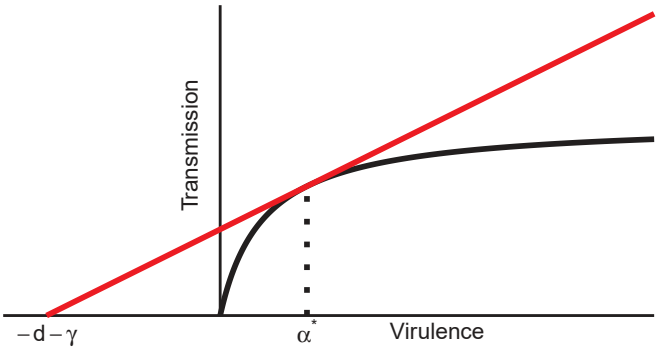

FIGURE 1.7 – Méthode graphique pour calculer l'ES virulence suivant le théorème de la valeur marginale (Charnov et al., 1976), avec un compromis concave saturant entre la transmission (β) et la virulence (α). La tangente (en rouge) passant par le point $(-d-\gamma,\, 0)$ coupe la courbe de compromis en α^*, l'ES virulence.

et la virulence, et nous discutons de l'évolution qualitative de la virulence, ses variations quantitatives sont très liées aux différentes valeurs de paramètres spécifiques à chaque interaction hôte-pathogène (Alizon and van Baalen, 2005).

1.2.3.1.2 Fitness d'invasion La fitness d'invasion caractérise le taux de croissance d'une souche mutante dans une population à l'équilibre endémique avec une souche résidente (Metz et al., 1992; Lion and Metz, 2018). La fitness d'invasion est notée $s(z, z')$, où z est le trait de la souche résidente et z' le trait de la souche mutante. Ainsi, la fitness d'invasion prend en compte l'environnement dans lequel se trouve la souche et prédit sa capacité à l'envahir ou non. En effet, si $s(z, z') > 0$, la souche mutante remplace la souche résidente et se maintient dans la population. Au contraire, si $s(z, z') < 0$, la souche mutante ne persiste pas dans la population. Une fois que la souche mutante a envahi la population et se trouve sur l'équilibre endémique, une nouvelle souche mutante peut éventuellement envahir si son aptitude d'invasion est positive. La fitness d'invasion

de la souche mutante dans le modèle (1.5) s'écrit

$$s(z, z') = \beta(z')\widehat{S} - (d + \alpha(z') + \gamma)\,, \tag{1.6}$$

avec $\widehat{S}$ la densité d'hôtes sensibles à l'équilibre endémique du résident, nous avons $\widehat{S} = \dfrac{d + \alpha(z) + \gamma}{\beta(z)}$. En le remplaçant dans la fitness d'invasion du mutant (équation (1.6)), nous avons

$$s(z, z') > 0 \Longleftrightarrow \frac{\beta(z')}{(d + \alpha(z') + \gamma)} > \frac{\beta(z)}{(d + \alpha(z) + \gamma)}$$

Ainsi, le mutant avec le plus grand R_0 envahi toujours. Ce principe de maximisation du R_0 a ses limites et n'est plus valable pour des modèles plus complexes (structuration ou infection multiples par exemple). Il est ainsi nécessaire de calculer la fitness d'invasion (Dieckmann, 2002; Lion and Metz, 2018).

1.2.3.1.3 Dynamique adaptative Le principe général de la dynamique adaptative est de prédire l'évolution d'une population sur le long terme, après des mutations de faible effet et fixations successives. En dynamique adaptative, il est communément considéré que les échelles de temps épidémiologiques et évolutive sont découplées. En effet, l'évolution est considérée comme plus lente que les dynamiques épidémiologiques, car nous supposons que les mutations sont rares, de telle sorte que les mutants apparaissent seulement quand l'équilibre épidémiologique est atteint (Metz et al., 1995; Geritz et al., 1998; Lion, 2018*c*) .

Gradient de sélection Le gradient de sélection permet de trouver les équilibres évolutifs (ou singularités). Il est représenté par la dérivée de la fitness d'invasion évaluée à $z' = z$ et s'exprime

$$\mathcal{S} = \left.\frac{\partial^2 s(z, z')}{\partial z'^2}\right|_{z'=z}\,. \tag{1.7}$$

Lorsque le gradient de sélection s'annule, $\mathcal{S} = 0$, le système a atteint un point d'équilibre, z^*, dont il conviendra de déterminer la stabilité. Dans notre exemple (1.5) le gradient de sélection s'exprime

$$\mathcal{S} = \frac{\mathrm{d}\beta(z')}{\mathrm{d}z'}\widehat{S} - \left.\frac{\mathrm{d}\alpha(z')}{\mathrm{d}z'}\right|_{z'=z} . \tag{1.8}$$

Ainsi, à partir de l'équation (1.8) évaluée à $z = z'$, une singularité est obtenue si $\mathcal{S} = 0$, soit

$$\begin{aligned} \frac{\mathrm{d}\beta(z')}{\mathrm{d}z'}\widehat{S} - \frac{\mathrm{d}\alpha(z')}{\mathrm{d}z'} = 0 &\iff \frac{1}{\widehat{S}} = \frac{\mathrm{d}\beta(z)/\mathrm{d}z}{\mathrm{d}\alpha(z)/\mathrm{d}z} \\ &\iff \frac{\beta(z)}{d+\alpha(z)+\gamma} = \frac{\mathrm{d}\beta(z)/\mathrm{d}z}{\mathrm{d}\alpha(z)/\mathrm{d}z} . \end{aligned} \tag{1.9}$$

L'équation (1.9) est une variante du théorème de valeur marginale (*Marginal Value Theorem*, Charnov et al. (1976)), qui permet de caractériser graphiquement la singularité. Ainsi, nous déduisons que l'ES virulence est le point tangent à la courbe de compromis, passant par le point $(-d-\gamma,\, 0)$ (figure 1.7).

Dérivée seconde La dérivée seconde permet de calculer la stabilité des équilibres calculés avec le gradient de sélection, et prédit ainsi la direction de la sélection. Notée $\mathcal{D}$, elle est la dérivée seconde de la fitness d'invasion exprimée au point d'équilibre $z' = z = z^*$, et s'exprime

$$\mathcal{D} = \left.\frac{\partial s(z,z')}{\partial z'}\right|_{z'=z=z^*} \tag{1.10}$$

Si la dérivée seconde est positive ($D > 0$) au point d'équilibre, le point est instable et la sélection est disruptive. A l'inverse si la dérivée seconde est négative ($\mathcal{D} < 0$), le point est stable et la sélection est stabilisante. Dans notre exemple, la dérivée seconde de la l'aptitude d'invasion equation (1.6), s'exprime

$$\mathcal{D} = \frac{\mathrm{d}^2\beta(z')}{\mathrm{d}z'^2}\widehat{S} - \left.\frac{\mathrm{d}^2\alpha(z')}{\mathrm{d}z'^2}\right|_{z'=z=z^*} \tag{1.11}$$

Ainsi, une pour qu'une stratégie soit évolutivement stable (*Evolutionarily Stable Strategy*, ESS), elle doit satisfaire $\mathcal{S} = 0$ et $\mathcal{D} < 0$ (Otto and Day, 2011). Ainsi, à partir de l'équation (1.11), évaluée à $z = z' = z^*$, l'ESS est obtenue si

$$\begin{aligned}\frac{\mathrm{d}^2\beta(z)}{\mathrm{d}z^2}\widehat{S} - \frac{\mathrm{d}^2\alpha(z)}{\mathrm{d}z^2} < 0 &\Longleftrightarrow \frac{1}{\widehat{S}} < \frac{\mathrm{d}^2\beta(z)/\mathrm{d}z^2}{\mathrm{d}^2\alpha(z)/\mathrm{d}z^2} \\ &\Longleftrightarrow \frac{\beta(z)}{d + \alpha(z) + \gamma} < \frac{\mathrm{d}^2\beta(z)/\mathrm{d}z^2}{\mathrm{d}^2\alpha(z)/\mathrm{d}z^2}\,. \end{aligned} \tag{1.12}$$

***Pairwise invasibility plots* (PIP)** Les PIP permettent de visualiser graphiquement les équilibres et leur stabilité. En effet, ces diagrammes montrent l'issue évolutive de mutations successives en représentant graphiquement le signe de $s(z, z')$ en fonction des valeurs du trait phénotypique du résident z et du mutant z'. Ces graphiques représentent le signe de la fitness d'invasion du mutant pour toutes les combinaisons (z, z') possibles. Dans les zones "+", le mutant réussi à envahir le résident ($s(z, z') > 0$) et, dans les zones "−", le mutant échoue à envahir le résident ($s(z, z') < 0$). Le long de la diagonale $z' = z$, où le trait du mutant et le trait du résident ont la même valeur, la fitness d'invasion s'annule $s(z, z') = 0$ (Dieckmann, 2002; Otto and Day, 2011). Les points où l'isocline croise la diagonale $z' = z$, sont les singularités et, en ces points, le gradient de sélection est nul ($\mathcal{S} = 0$). Il existe plusieurs types de singularités définies par leur stabilité :

- Stratégie continuellement stable, *Continuously Stable Strategy* : les mutations successives convergent vers la singularité qu'aucun nouveau mutant ne peut envahir. Le point est convergent stable et évolutivement stable (ESS),
- Jardin d'Eden, *Garden of Eden* : les mutations successives ne convergent pas vers la singularité, néanmoins aucun nouveau mutant ne peut l'envahir. La singularité est convergente instable mais évolutivement stable (ESS),
- Points de branchement évolutif, *Evolutionary Branching Point* : les mutations successives

convergent vers la singularité, qui peut néanmoins être envahie. La singularité est convergente stable mais évolutivement instable (pas une ESS),

- Répulsif, *Repellor* : les mutations successives ne convergent pas vers la singularité, qui peut être envahie. La singularité est convergente instable et évolutivement instable (pas une ESS),

Ainsi, les ESS ne peuvent pas être envahies et sont toujours du monomorphisme. Au contraire, les points de branchement évolutifs peuvent induire du polymorphisme dans la population. Notons qu'il existe deux types de stratégies évolutivement stables, la stratégie continuellement stable (CSS) et le Jardin d'Eden. Dans ce manuscrit, le terme ESS sera utilisé pour caractériser une CSS, le Jardin d'Eden étant, par définition, impossible à atteindre.

1.2.3.2 Sur le court terme : phases transitoires

1.2.3.2.1 Génétique quantitative La génétique quantitative permet de suivre les changements en fréquence de souches mutantes au cours du temps. Jusqu'à présent, nous nous sommes intéressés à l'évolution de la virulence sur le long terme, en séparant les échelles de temps épidémiologiques et évolutives. Cependant, des souches transitoires potentiellement virulentes peuvent apparaître et disparaître, et s'installer temporairement dans les populations, affectant la dynamique de l'épidémie. Ainsi, la génétique quantitative permet d'étudier les dynamiques épidémiologiques et évolutives sur la même échelle de temps, pour mettre en évidence ces phases transitoires. De plus, l'étude sur une même échelle de temps permet de prendre en compte la boucle de rétroaction entre l'épidémiologie et l'évolution générée par l'impact du pathogène sur son hôte (Day and Proulx, 2004; Day and Gandon, 2006, 2007).

Imaginons maintenant que notre modèle (1.5) n'est plus envahi par une seule souche mutante mais par n souches mutantes (figure 1.8). Nous pouvons écrire la dynamique totale des infectés $I_T = \sum_i I_i$, avec $i \in \{1, n\}$, qui dépend des transmissions totales des n souches $\overline{\beta} = \sum_i \beta_i f_i$, de la virulence totale $\overline{\alpha} = \sum_i \alpha_i f_i$ et du rétablissement total $\overline{\gamma} = \sum_i \gamma_i f_i$. La fréquence du mutant, notée

$f_i = I_i/I_T$, dépend de la différence entre la croissance *per capita* de la souche i, notée r_i, et de la croissance moyenne *per capita*, notée $\overline{r}$, avec $r_i = \beta_i S - (d + \alpha_i + \gamma_i)$ et $\overline{r} = \sum_i r_i f_i$. Les équations du modèle s'expriment alors

$$\text{Epidemiologie} \quad \begin{cases} \frac{\mathrm{d}S_T}{\mathrm{d}t} = b\nu - (d + \overline{\beta} I_T) S_T \,, \\ \frac{\mathrm{d}I_T}{\mathrm{d}t} = \overline{\beta} I_T S_T - (d + \overline{\alpha} + \overline{\gamma})\, I_T \,, \\ \frac{\mathrm{d}R}{\mathrm{d}t} = \overline{\gamma} I_T - dR \,, \end{cases}$$

$$\text{Evolution} \quad \begin{cases} \frac{\mathrm{d}f_i}{\mathrm{d}t} = f_i (r_i - \overline{r}) \,, \end{cases}$$

où la natalité est notée b, la mortalité naturelle, d, et la couverture en traitements, ν.

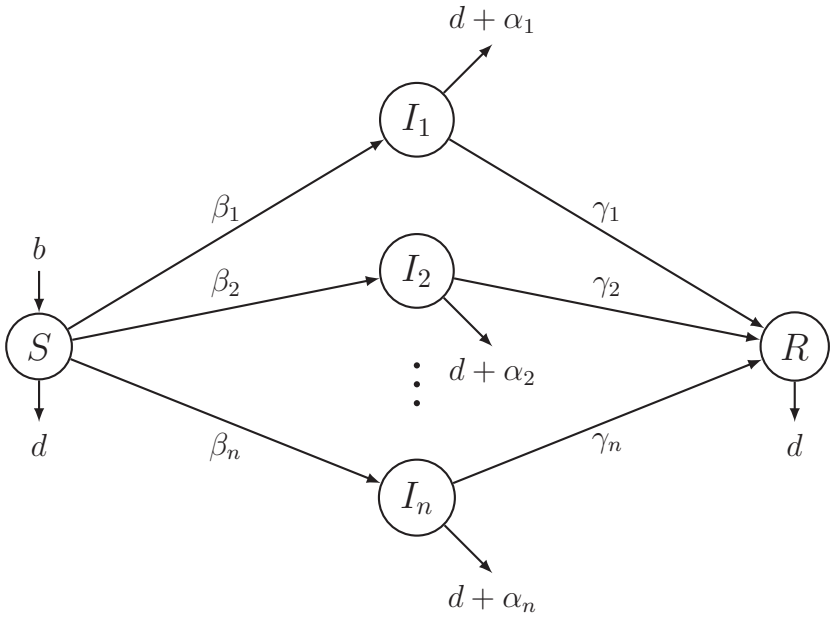

FIGURE 1.8 – Diagramme de flux d'un modèle SIR avec des hôtes infectés par n souches.

Ainsi, la fréquence d'une souche i va augmenter en fréquence dans la population si sa croissance *per capita* est supérieure à la croissance moyenne des n souches ($r_i > \overline{r}$). Les fréquences des différents mutants en phases transitoires permettent de mettre en évidence les traits biologiques

(virulence ou échappement) favorisés au cours d'épidémies, et la dynamique de ces fréquences permet l'étude de la vitesse d'adaptation des mutants.

1.2.3.3 Les valeurs reproductives, une mesure de qualité

Chaque individu contribue différemment au futur de la population. Par exemple, un plant très fertile va fortement contribuer aux futures générations en comparaison d'un plant stérile. De la même manière des jeunes adultes vont produire plus de descendants que des personnes âgées. Ainsi, les populations peuvent être structurées en classes d'individus, en fonction de leur contribution aux générations futures.

Introduites par Fisher en 1930, les valeurs reproductives de classes permettent de quantifier la contribution de chaque classe d'individus aux générations futures (Fisher, 1930). Elles représentent la somme des valeurs reproductives individuelles au sein d'une classe. D'un point de vue écologique, les valeurs reproductives permettent de classer les habitats en "bon" ou "mauvais". Un bon habitat est un habitat dans lequel les individus vont fortement contribuer aux générations futures, au contraire, dans un mauvais habitat les individus auront une faible contribution (Rousset, 1999; Lion, 2018*a*). Du point de vue du pathogène, l'hôte représente son habitat et sa ressource. De ce fait, les hôtes sont classés en fonction de la capacité des pathogènes qui les infectent, à contribuer aux futures générations de pathogènes.

Ces valeurs reproductives de classes peuvent permettre de réécrire le gradient de sélection en pondérant la fitness par les valeurs reproductives de classes. Ainsi, lorsque de nouveaux allèles arrivent dans une population, nous pouvons montrer si c'est à cause de facteurs démographiques (qualité des habitats) ou de sélection naturelle (fitness du mutant comparée à la fitness du résident).

Nous utilisons le concept de valeurs reproductives dans les chapitres 2 et 3, où les habitats sont différenciés en fonction du statut traité ou non-traité des hôtes (encadré 3).

Encadré 2 : Théorème de Floquet

Le modèle présenté en (1.2) peut être écrit sous forme matricielle tel que $\dot{I} = \mathbf{A}I$ où $I = (I_N \quad I_T)^\top$ et

$$\mathbf{A} = \begin{pmatrix} \beta_N S_N - (d + \alpha_N + \gamma_N) & \beta_T S_N \\ \beta_N S_T & \beta_T S_T - (d + \alpha_T + \gamma_T) \end{pmatrix},$$

où les S_N et S_T sont évalués dans une population dans maladie. La matrice $\mathbf{A}$ peut être écrite sous la forme $\mathbf{F} - \mathbf{V}$ avec $\mathbf{F}$ la matrice de natalité et $\mathbf{V}$ la matrice de mortalité tels que

$$\mathbf{F} = \begin{pmatrix} \beta_N S_N & \beta_T S_N \\ \beta_N S_T & \beta_T S_T \end{pmatrix} \text{ et } \quad \mathbf{V} = \begin{pmatrix} (d + \alpha_N + \gamma_N) & 0 \\ 0 & (d + \alpha_T + \gamma_T) \end{pmatrix}$$

D'après (Bacaër, 2011), le R_0 est obtenu par la résolution sur une période de

$$\dot{\mathbf{X}} = \frac{\mathbf{F}}{R}.\mathbf{X} - \mathbf{V}\mathbf{X}$$

avec la condition initiale $\mathbf{X}(0) = \begin{pmatrix} 1 & 0 \\ 0 & 1 \end{pmatrix}$. Nous pouvons faire varier la valeur de R par dichotomie jusqu'à ce que la valeur propre dominante de $\mathbf{X}(t)$ (multiplicateur de Floquet) soit 1. Alors, la valeur de R est le R_0.

Encadré 3 : Valeurs reproductives

Environnement constant Dans une population structurée envahie par un mutant, la dynamique des hôtes infectés par la souche mutante peut s'écrire sous forme matricielle $\dot{I}^* = \mathbf{A}^* I^*$ où $I = (I_N^* \quad I_T^*)^\top$ et

$$\mathbf{A}^* = \begin{pmatrix} \beta_N^* S_N - (d + \alpha_N^* + \gamma_N^*) & \beta_T^* S_N \\ \beta_N^* S_T & \beta_T S_T - (d + \alpha_T^* + \gamma_T^*) \end{pmatrix} .$$

Le gradient de sélection est proportionnel à

$$\left.\frac{\partial s(z,z')}{\partial z'}\right|_{z'=z} \propto \mathbf{v}^\top \left(\left.\frac{\partial \mathbf{A}^*}{\partial z'}\right|_{z'=z} \right) \mathbf{f} .$$

Associés à la valeur propre dominante de $\mathbf{A}^*$, le vecteur propre à gauche, $\mathbf{v}$, caractérise les valeurs reproductives de chaque classe d'hôtes et le vecteur propre à droite, $\mathbf{f}$, caractérise les fréquences des hôtes dans chaque classe(Otto and Day, 2011; Lion, 2018*a*).

Environnement périodique Dans une population structurée envahie par un mutant, la dynamique des hôtes infectés par la souche mutante peut s'écrire sous forme matricielle $\dot{I}^*(t) = \mathbf{A}^*(t) I^*(t)$ où $I = (I_N^*(t) \quad I_T^*(t))^\top$ et

$$\mathbf{A}^*(t) = \begin{pmatrix} \beta_N^* S_N(t) - (d + \alpha_N^* + \gamma_N^*) & \beta_T^* S_N(t) \\ \beta_N^* S_T(t) & \beta_T S_T(t) - (d + \alpha_T^* + \gamma_T^*) \end{pmatrix} .$$

Le gradient de sélection est proportionnel à

$$\left.\frac{\partial s(z,z')}{\partial z'}\right|_{z'=z} \propto \left\langle \mathbf{v}^\top \left(\left.\frac{\partial \mathbf{A}^*}{\partial z'}\right|_{z'=z} \right) \mathbf{f} \right\rangle ,$$

où les $\langle\,\rangle$ représentent l'intégration sur une période. Le vecteur à gauche, $\mathbf{v}(t)$, caractérise les valeurs reproductives de chaque classe d'hôtes à l'instant t et le vecteur à droite, $\mathbf{f}(t)$, caractérise les fréquences des hôtes dans chaque classe à l'instant t (Lion, 2018*a*).

1.3 Objectif de la thèse

Dans cette thèse, nous cherchons à comprendre l'effet des hétérogénéités spatio-temporelles des hôtes, qui induisent une variation de l'habitat des pathogènes, sur leur épidémiologie et évolution. La figure 1.9 présente schématiquement l'approche employée dans cette thèse.

1.4 Stratégie de la thèse

Dans le premier chapitre d'introduction générale, nous avons présenté le contexte dans lequel s'inscrivent ces travaux de thèse et les différents outils conceptuels utilisés.

Dans un second chapitre nous avons développé un modèle épidémiologique structuré en classes d'hôtes naïfs ou traités, dont les proportions dans la population varient dans le temps. En effet, la distribution des traitements dans la population varie périodiquement, entre une couverture de 100% et une couverture de 0%. L'hôte étant la ressource et l'habitat des pathogènes, ces derniers sont exposés successivement à une population entièrement naïve ou entièrement traitée. L'objectif de ce chapitre est d'analyser les effets d'une variation périodique de l'habitat des pathogènes sur la prévalence et l'évolution de la virulence sur le long terme. Ainsi, nous utilisons le cadre de la dynamique adaptative pour étudier l'évolution de la virulence, le concept du R_0 en environnement périodique, le multiplicateur de Floquet pour dériver le gradient de sélection, et le concept des valeurs reproductives de classe.

Dans un troisième chapitre, nous avons développé un modèle de métapopulation avec migration du parasite entre les sous-populations. Chaque sous-population est composée d'hôte naïfs et traités, dont les proportions varient en fonction de la couverture, qui est différente d'une sous-population à l'autre. L'objectif de ce chapitre est de mettre en évidence l'impact de la migration du pathogène entre deux populations sous différentes couvertures de traitement, sur l'évolution de la virulence

sur le long-terme. Nous utilisons dans ce chapitre le cadre de la dynamique adaptative pour étudier la stabilité à long-terme. De plus, le gradient de sélection est exprimé en fonction des valeurs reproductives de classes de chaque sous-population.

Enfin, dans un quatrième chapitre, nous avons étendu le modèle étudié dans le chapitre 3, afin d'étudier l'évolution des pathogènes à court terme. Ce chapitre s'inscrit dans le contexte de la pandémie de la Covid-19 et a pour but de construire un cadre théorique pour suivre la fréquence d'un mutant d'échappement au vaccin, dans les différentes classes de la métapopulation. L'objectif de ce chapitre est de mettre en évidence l'effet de la migration et de différentes couvertures vaccinales entre deux populations connectées, sur la vitesse d'apparition d'un mutant d'échappement. Nous utilisons ici le cadre de la génétique quantitative pour exprimer la dynamique de la fréquence d'une mutant d'échappement dans les hôtes naïfs ou traité de chaque classes, puis dans chaque sous-population, et enfin dans la métapopulation.

Enfin, dans une synthèse générale, nous discutons des résultats obtenus dans les différents chapitres, pour terminer sur des perspectives à donner à ce travail de thèse.

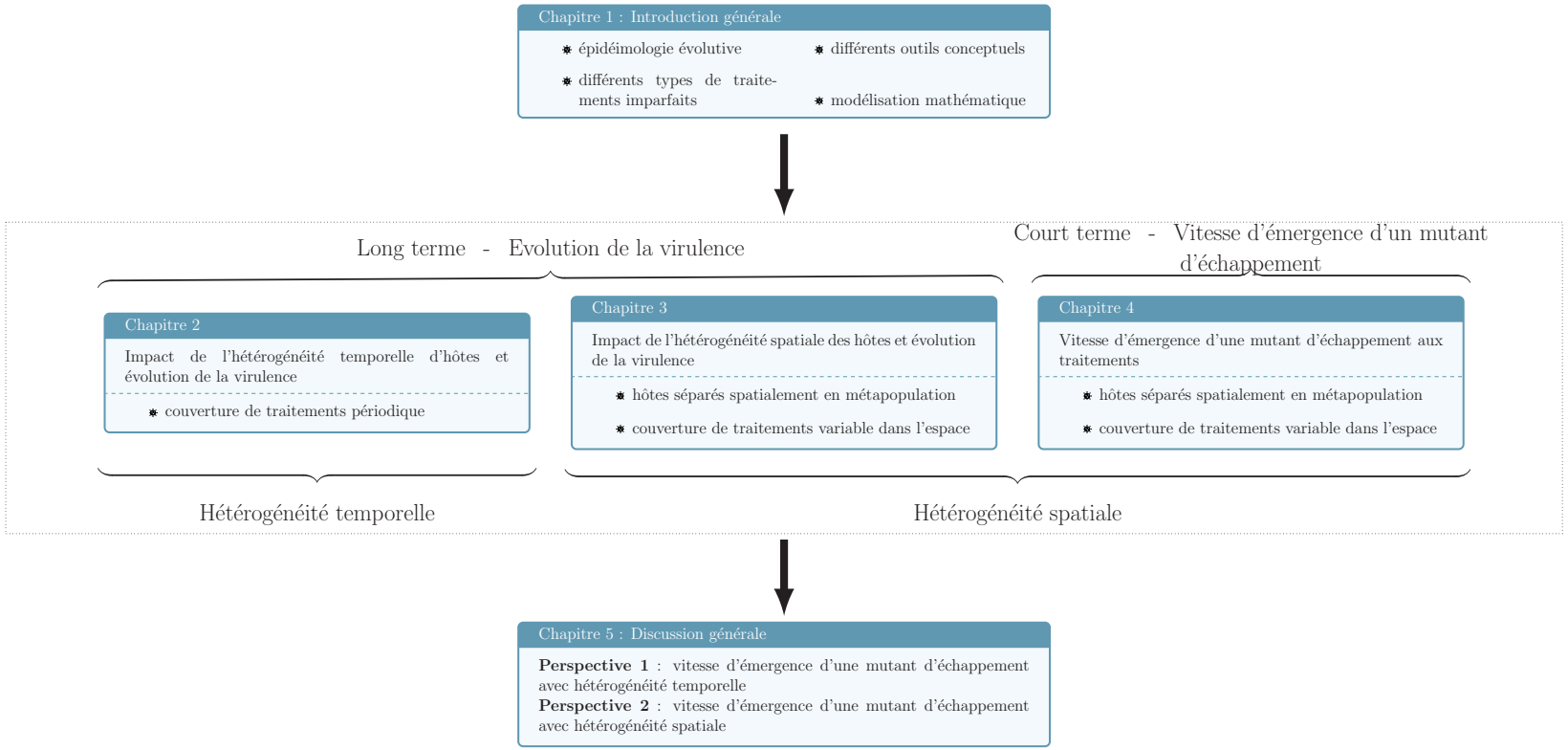

FIGURE 1.9 – Plan de la thèse

Chapitre 2

Epidemiological and evolutionary consequences of periodicity in treatment coverage

Alicia Walter & Sébastien Lion

As published in the Royal Society Proceedings B the 10 march 2021

Walter, A., and S. Lion. 2021. Epidemiological and evolutionary consequences of periodicity in treatment coverage. Proceedings of the Royal Society B 288 :20203007.

Abstract

Host heterogeneity is a key driver of host-pathogen dynamics. In particular, the use of treatments against infectious diseases creates variation in quality among hosts, which can have both epidemiological and evolutionary consequences. We present a general theoretical model to highlight the consequences of different imperfect treatments on pathogen prevalence and evolution. These treatments differ by their action on host and pathogen traits. In contrast with previous studies, we assume that treatment coverage can vary in time, as in seasonal or pulsed treatment strategies. We show that periodic treatment strategies can limit both disease spread and virulence evolution, depending on the type of treatment. We also introduce a new method to analytically calculate the selection gradient in periodic environments, which allows our predictions to be interpreted using the concept of reproductive value, and can be applied more generally to analyse eco-evolutionary dynamics in class-structured populations and fluctuating environments.

2.1 Introduction

Parasites are an ubiquitous threat to plant, animal and human populations. This has led to the development of numerous pre- and post-infection treatments, which play a central role in the fight against infectious diseases. At a fundamental level, this has also motivated a long line of research in epidemiology to devise control measures that can limit the potentially dramatic effects of epidemics for animal and plant species (Anderson and May, 1991; Keeling and Rohani, 2011). A key driver of this theoretical work is to find the optimal strategy to deploy treatments in order to maximise the short-term (epidemiological) benefits of treatments while mitigating their potential long-term (evolutionary) negative consequences.

Indeed, it is increasingly acknowledged that pathogens may evolve in response to treatments, as exemplified by the evolution of antibiotic resistance or vaccine escape. Pathogen evolution is fuelled by the high reproduction rate of pathogens and the increasing use of treatments. In particular, both empirical evidence (Gandon and Day, 2008; Read et al., 2015; WHO et al., 2014) and theoretical predictions (Dieckmann et al., 2005; Gandon et al., 2001*b*, 2003) support the idea that imperfect treatments may cause selection on pathogen life-history traits, such as transmission and virulence.

In practice, treatments are rarely perfect, either because of partial efficacy, or limited coverage. From an ecological perspective, this introduces heterogeneity in the host population. Indeed, naive and treated hosts can be viewed as two habitats with different qualities for the pathogen. We expect pathogens to have higher fitness in good habitats (e.g. untreated hosts), and lower fitness in bad habitats (e.g. treated hosts). However, if the pathogen adapts to the bad habitat (e.g. treated hosts) by increasing its virulence, this can negatively impact untreated hosts in the population. The potential negative effects of such imperfect treatments have been theoretically studied, showing in particular that some types of treatments (notably those reducing host susceptibility or pathogen

transmissibility) can be viewed as evolution-proof, while others (such as those that mainly increase the tolerance of hosts to the disease) can lead to the long-term evolution of virulence (Gandon et al., 2001*b*, 2003; Zurita-Gutiérrez and Lion, 2015).

A central assumption of these earlier studies is that treatment coverage is constant in time. In practice, however, treatment coverage fluctuates in time, either because of social or economical constraints (vaccine scares, shortage in drugs, vaccination campaigns linked to time-limited scientific or humanitarian missions), or because of specific treatment strategies. For instance, pulse vaccination has been the main strategy deployed to eradicate polio and significantly decreased its incidence (John et al., 1983). In addition, many crop diseases are seasonally treated, either directly in fields, or by pre-treatment at the seed stage. Periodic treatments may also be implemented through rotation between naive and treated plants, which has been shown to reduce pathogen prevalence (Nilusmas et al., 2020). In this context, it is of major interest to study the consequences of periodic treatment strategies through theoretical studies to guide future experimentations or applications. In particular, an important question is whether temporal variations in treatment may increase or decrease selection on pathogen virulence or transmission. At a conceptual level, fluctuations in treatment coverage will cause temporal variation in host quality for the pathogen, and it is not clear that the optimal strategy in a constant environment will also maximise pathogen fitness in this context.

Our purpose here is to analyse the epidemiological and evolutionary effects of periodic imperfect prophylactic treatments that create heterogeneity among hosts. Building on previous theoretical studies of imperfect treatments with constant coverage (Gandon et al., 2001*b*, 2003; Zurita-Gutiérrez and Lion, 2015), we first present the consequences of periodic treatment coverage on the prevalence of the disease and the pathogen's basic reproduction number. We then assume that a rare mutation occurs in the pathogen, modifying the life history traits, and we analyse how the selective pressures on the mutant pathogen depend on (i) the mode of action, and (ii) the temporal distribution of

treatments. Part of our analysis is based on a new approach to analyse selection in fluctuating environments, which allows us to measure host quality using a dynamical concept of reproductive value (Lion, 2018*a*). We discuss the practical and conceptual implications of our work.

2.2 Model

We consider a host-pathogen interaction with the life cycle depicted in figure 2.1a (see table 2.1 for notations). The host population is structured in two classes corresponding to the host's immune state, naive (N) or treated (T). Hosts can be either susceptible (S) or infected by a pathogen responsible of an infectious disease (I). This leads to four different types of hosts, S_N, S_T, I_N, and I_T. Host reproduction occurs at rate b. Upon birth, offspring have a probability ν of being treated, in which case they enter the S_T class, and a probability $(1-\nu)$ of remaining untreated, in which case they enter the S_N class. All hosts (susceptible and infected) have a background mortality rate, d, with an additional disease-induced mortality (i.e. virulence), which we note α_N and α_T respectively for naive or treated infected hosts. A susceptible naive (respectively treated) host can be infected by naive and treated infected hosts, I_N and I_T, at rate h_N (respectively h_T). The forces of infections, h_N and h_T, directly depend on the horizontal transmission of the pathogen, such that $h_N = \beta_N I_N + \beta_T I_T$ and $h_T = \sigma h_N$, where β_N and β_T are the transmissibilities of naive and treated hosts respectively, and σ represents the relative susceptibility of treated hosts. With these assumptions, the epidemiological dynamics can be described by the following ODE system :

$$\frac{\mathrm{d}S_N}{\mathrm{d}t} = (1-\nu(t))b - (d+h_N)S_N\,, \tag{2.1a}$$

$$\frac{\mathrm{d}S_T}{\mathrm{d}t} = \nu(t)b - (d+h_T)S_T\,, \tag{2.1b}$$

$$\frac{\mathrm{d}I_N}{\mathrm{d}t} = h_N S_N - (d+\alpha_N)I_N\,, \tag{2.1c}$$

$$\frac{\mathrm{d}I_T}{\mathrm{d}t} = h_T S_T - (d+\alpha_T)I_T\,, \tag{2.1d}$$

The model is based on a previously analysed model of imperfect vaccines Gandon et al. (2001*b*, 2003), but instead of a constant treatment coverage, we consider that ν is a function of time. In most simulations, we use a T-periodic square function (figure 2.2a) that varies between ν_{min} and ν_{max}. The treatment coverage takes the value ν_{max} during pT and ν_{min} during $(1-p)T$, with p the fraction of the period with a maximum coverage. The average coverage is thus $\bar{\nu} = p\,\nu_{max} + (1-p)\,\nu_{min}$. For the sake of simplicity, we choose $\nu_{max} = 1$ and $\nu_{min} = 0$ in our simulations, so that the average coverage is $\bar{\nu} = p$.

As typical in the literature, we assume a trade-off between transmission and virulence, so that a pathogen cannot see its transmission increase without paying a cost through an increase of the host's death (Anderson and May, 1982; Alizon et al., 2009). Following this hypothesis we assume an increasing saturating trade-off between transmission, β and virulence, α. In figures we typically use the function $\beta[\alpha] = 5\alpha/(1+\alpha)$.

As in Gandon et al. (2001*b*, 2003); Zurita-Gutiérrez and Lion (2015), we assume that treatments are imperfect : being treated does not guarantee a full and lifelong protection against pathogens. Several imperfect vaccines against cholera for instance have been reported, with various efficacies (Richie et al., 2000; Sur et al., 2009). Following Gandon et al. (2001*b*), we consider four different types of treatments showed in figure 2.1b. First, we consider an anti-infection treatment that prevents the primary infection of the host by the pathogen. Potential examples include the human papillomavirus (HPV) vaccine, which aims to reduce the penetration of the HP virus into cells (Giuliano et al., 2011), or the copper in Bordeaux mixture, which lowers the risk of infection by preventing the germination of fungal spores on leaves (Barker and Gimingham, 1911). Second, we consider an anti-growth treatment which aims to decrease the intra-host growth rate of the pathogen, and has an action on its life history traits (virulence α and transmission β). This is reminiscent of the mode of action of the ABT-538 drug, which reduces the within-host replication of HIV (Ho et al., 1995; Otto and Day, 2011). The third treatment acts by reducing the transmission

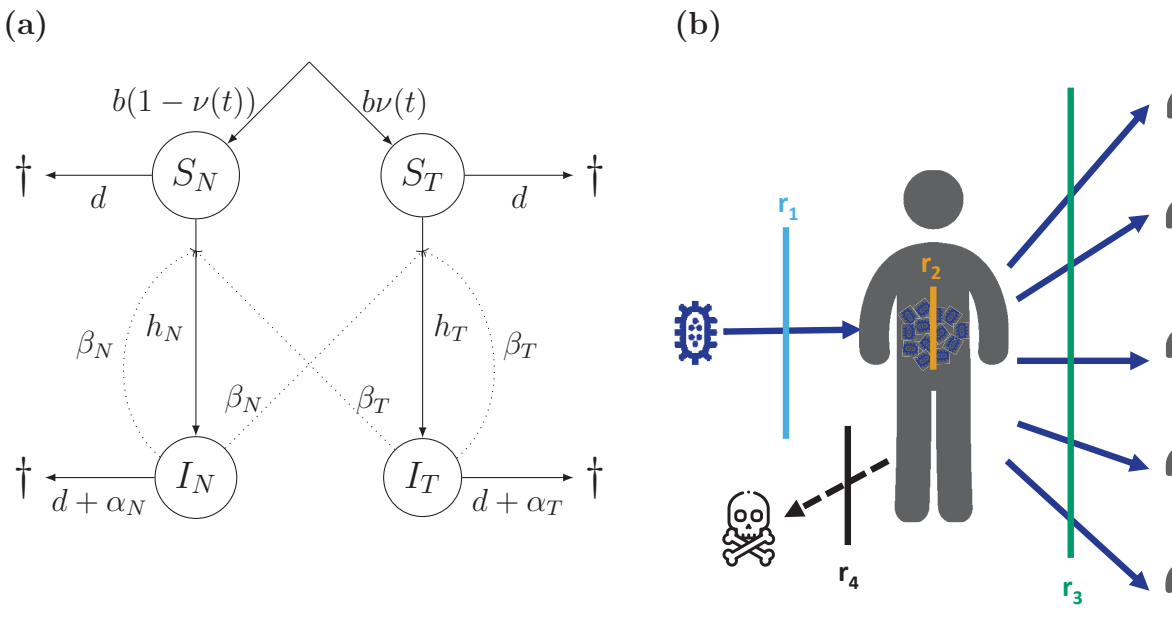

FIGURE 2.1 – (a) Life cycle of the host-pathogen interaction, showing transition rates between classes. (b) Infection process and the different treatment mechanisms : anti-infection (r_1, blue), anti-growth (r_2, orange), anti-transmission (r_3, green) and anti-toxin (r_4, black), with a human as illustration of hosts.

of pathogens to other hosts. For instance, it has been shown that an effect of the feline calcivirus vaccine is to reduce virus shedding (Lappin et al., 2006; Radford et al., 2007). Fourth, we consider a leaky anti-toxin treatment that only reduces pathogen's virulence, as documented for instance for the vaccine against Marek's disease (Read et al., 2015), or the toxoid vaccine against Diphteria (Gandon and Day, 2008).

In naive hosts, the virulence and transmission rates are simply $\alpha_N = \alpha$ and $\beta_N = \beta(\alpha)$, where α is the virulence trait. Treatments cause a reduction in virulence, transmission or susceptibility of hosts, depending on the treatment type i, with an efficacy r_i that takes values between 0 (no effect) and 1 (perfect treatment). With our definitions for the different types of treatments, we have :

$$\sigma = 1 - r_1 \qquad \alpha_T = (1-r_2)(1-r_4)\alpha \qquad \beta_T = (1-r_3)\beta[(1-r_2)\alpha] \tag{2.2}$$

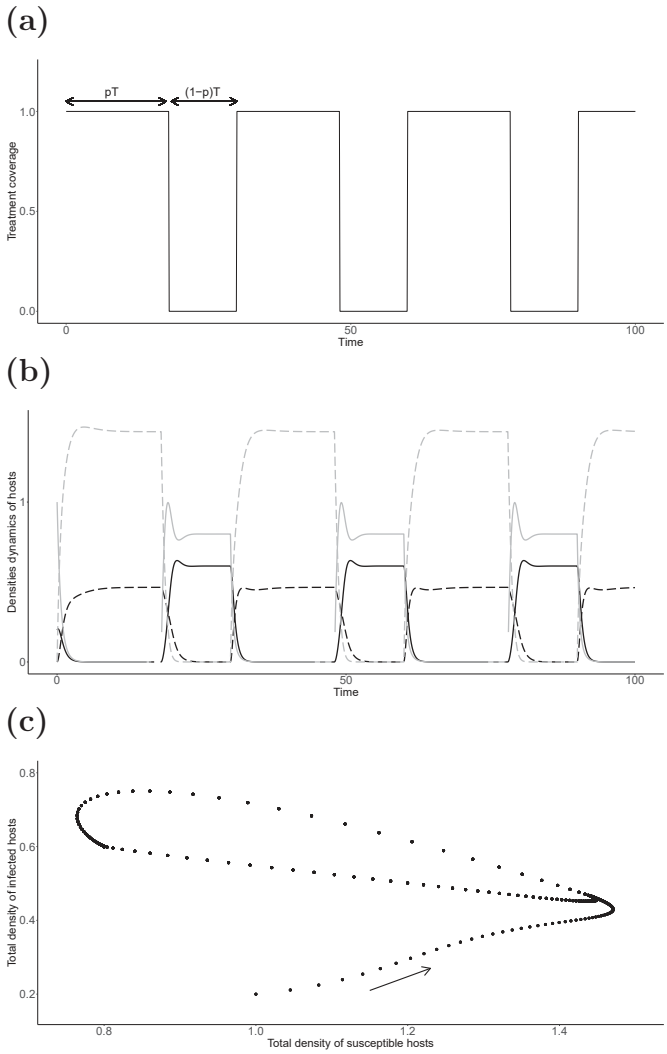

FIGURE 2.2 – Typical behavior of the model, for an anti-growth treatment. (a) Square function for treatment coverage : ν takes the value 1 during pT (all newborns are treated), and the value 0 during $(1-p)T$ (no newborn is treated). (b) Corresponding densities dynamics for susceptible naive (plain grey), susceptible treated (plain black), infected naive (dashed grey) and infected treated (dashed black). (c) Phase portrait for the total densities of susceptible ($S_N + S_T$) and infected ($I_N + I_T$) hosts, showing convergence to a periodic attractor. Parameter values : $r_2 = 0.8$, $p = 0.6$, $T = 30$, $\alpha = 1$, $b = 2$, $d = 1$. Typical behaviours of the model with anti-infection, anti-transmission and anti-toxin treatments are shown in appendix B.1

TABLE 2.1 – Table of parameters and variables

Parameter	Definition
Life history traits	
α_k	disease induced death rate (virulence) of the resident strain in class k
α'_k	disease induced death rate (virulence) of the mutant strain in class k
α^*	evolutionarily stable virulence
β_k	transmission of the disease of the resident strain in class k
β'_k	transmission of the disease of the mutant strain in class k
b	birth rate
d	natural death rate
h_k	force of infection in class k
σ	susceptibility of hosts
Treatments	
$\nu(t)$	periodic treatment coverage function
T	period of the treatment function
p	fraction of T with treatment
r_i	efficacy of the i treatment (see section 2)
Reproductive values	
c_k^e	pathogen class reproductive value in class k under a constant coverage
c_k	pathogen class reproductive value in class k under a periodic coverage
	k stands for naive (N) or treated (T) hosts

2.3 Epidemiology

In this section we investigate how the periodicity of treatment coverage affects the ability of a pathogen to spread in an uninfected host population and the endemic prevalence of the disease. The invasion success of a pathogen can be quantified by its basic reproduction number, R_0, which represents the average number of hosts to which a single infected host in a disease-free population can transmit the pathogen over its lifetime. In a deterministic model, the pathogen can create an epidemic if $R_0 > 1$, or die out if $R_0 < 1$ (Anderson and May, 1986; Diekmann et al., 1990; Lion and Metz, 2018). R_0 is calculated in the stable population in the absence of the disease, typically an equilibrium in most studies. In our model, however, the disease-free population settles on a periodic attractor, due to the periodic forcing $\nu(t)$.

2.3.1 Constant treatment coverage

When the treatment coverage is constant ($\nu(t) = \bar{\nu}$), the population settles on an equilibrium in the absence of the disease. We can therefore calculate R_0 using the Next Generation Theorem (see appendix B.2, Diekmann et al. (1990); Hurford et al. (2009)), which leads to :

$$R_0 = R_N S_N^0 + \sigma R_T S_T^0 \tag{2.3}$$

with

$$R_N = \frac{\beta_N}{d + \alpha_N} \qquad \text{and} \qquad R_T = \frac{\beta_T}{d + \alpha_T}\,, \tag{2.4}$$

the basic reproductive numbers in a fully naive ($\bar{\nu} = 0$) or fully treated ($\bar{\nu} = 1$) population respectively, and S_N^0 and S_T^0 the densities of susceptible hosts at the disease-free equilibrium, which are given by $S_N^0 = (1 - \bar{\nu})b/d$ and $S_T^0 = \bar{\nu}b/d$ (appendix B.3). Thus, the basic reproductive number in a heterogeneous population corresponds to the sum of R_0's in a fully naive and a fully treated population, weighted by the densities of susceptible hosts in each class.

2.3.2 Periodic treatment coverage

When host dynamics are periodic (figures 2.2a and 2.2b), the Next Generation Theorem cannot be applied to calculate the basic reproductive number. However, the concept of Floquet multipliers can be used to extend the definition of R_0 Diekmann et al. (1990) to periodic environments Bacaër and Guernaoui (2006); Bacaër (2011). Floquet theory allows for the study of the stability of continuous-time periodical systems (Drazin and Drazin (1992) ; see e.g. Klausmeier (2008) for an ecologically oriented treatment). In our study, we can distinguish two cases : anti-infection and anti-transmission treatments, for which an analytical study is possible, and anti-growth and anti-toxin treatments for which R_0 can only be calculated numerically.

2.3.2.1 Anti-infection and anti-transmission treatments

For these treatments, we show in appendix B.2 that, following Bacaër and Guernaoui (2006), we can calculate the basic reproduction number as :

$$R_0 = \frac{\beta}{d+\alpha}\left(\left\langle S_N^0\right\rangle + (1-r_1)(1-r_3)\left\langle S_T^0\right\rangle\right) \tag{2.5}$$

where $\langle S_k^0\rangle = \int_t^{t+T} S_k^0(\tau)\,\mathrm{d}\tau$ gives the average density of susceptible hosts in class k during one period. In particular, we show in appendix B.3 that, for our model

$$\left\langle S_N^0\right\rangle = \frac{(1-\bar{\nu})b}{d} \quad \text{and} \quad \left\langle S_T^0\right\rangle = \frac{\bar{\nu}b}{d}\,. \tag{2.6}$$

We can see that the average susceptible densities, $\langle S_N^0\rangle$ and $\langle S_T^0\rangle$ have the same expressions as the equilibrium densities in the constant case, and only depend on b, d, and the average treatment coverage, $\bar{\nu}$ (eq.2.6). As a result, the invasion threshold is independent of the period, and only depends on the average coverage $\bar{\nu}$. Hence, any periodic treatment with average coverage $\bar{\nu}$ leads to the same condition for pathogen invasion as a constant treatment with coverage $\bar{\nu}$.

After pathogen invasion, the population settles on a periodic endemic attractor (Figure 2.2c), and the average prevalence is then the fraction of infected hosts in the population integrated over one period. Increasing the average coverage ($\bar{\nu} = p$) decreases the average prevalence for these treatments (figure 2.3a, blue and green lines), until extinction above a critical value of p. Moreover, an increase of the period T also reduces the average prevalence (Figure 2.3b). Note that periodicity in treatment coverage always leads to a lower prevalence compared to the corresponding constant coverage.

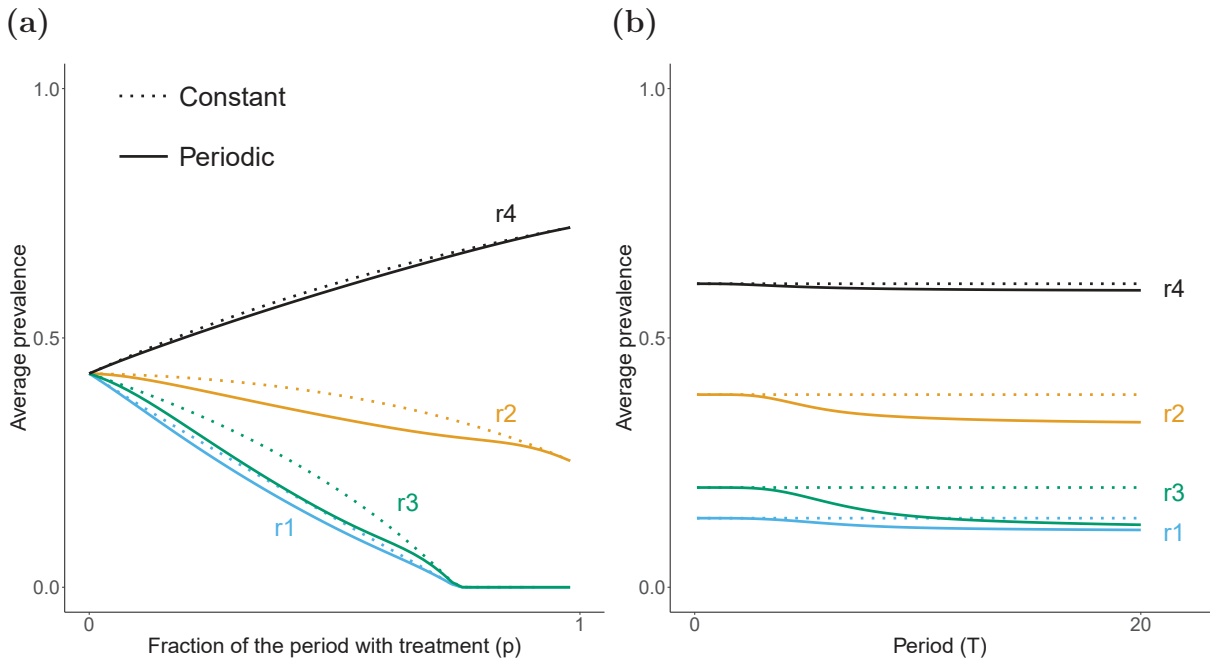

FIGURE 2.3 – Disease prevalence as a function of (a) the fraction of time at maximum treatment p ($T = 10$), or (b) the period T ($p = 0.5$), for anti-infection (blue), anti-growth (orange), anti-transmission (green) and anti-toxin (black) treatments, all with efficacy $r_i = 0.8$. In solid lines the prevalence under a periodic treatment coverage that corresponds to the average prevalence over a period. In dotted lines the respective constant average coverage. Other parameters as in figure 2.2.

2.3.2.2 Anti-growth and anti-toxin treatments

For these treatments, the basic reproduction number cannot be expressed in a closed analytical form, but can be calculated numerically using Floquet's theory (Bacaër, 2007; Klausmeier, 2008). We show in appendix B.2 that the effect of periodicity on R_0 is weak, but tends to slightly lower the extinction threshold for both types of treatments.

As the average coverage ($\bar{\nu} = p$) increases, the average prevalence decreases with an anti-growth treatment and increases with an anti-toxin. This can be intuitively explained by the fact that anti-toxin treatments merely reduce the survival cost of pathogens and cause infected hosts to transmit for a longer time. In contrast, anti-growth treatment directly impacts the transmission-virulence

trade-off. It causes a reduction of pathogen spread for treated hosts, counterbalanced by a reduction of host mortality. This explains the lower decrease of the prevalence compared to anti-infection or anti-transmission treatments (figure 2.3a). As for previous treatments, the average prevalence decreases when the period increases and the periodic treatment is beneficial compared to the constant coverage in terms of average prevalence reduction (figure 2.3b).

To understand why, note that the prevalence for short periods can be approximated by the prevalence with the corresponding constant average coverage. Indeed, the dynamics are characterised by small oscillations around the equilibrium solution. Hence, for short periods, pathogens are exposed, at any given time, to a heterogeneous population of naive and treated hosts. For large periods, however, the environment experienced by the pathogen alternates between temporary equilibria corresponding to either fully naive or fully treated populations. The average prevalence then tends to the arithmetic mean between the equilibrium prevalences in fully naive and fully treated poulations, which is always lower than the prevalence in a heterogeneous population at equilibrium (figure 2.3b). Note that, due to the epidemiological feedbacks, the endemic attractor is more sensitive to the forcing period than the disease-free state of the population, which explains why periodicity has a weaker impact on the invasion threshold compared to the average prevalence.

2.4 Evolution

Assuming the population has reached an endemic attractor, we now aim to understand how imperfect treatments and periodicity may jointly affect the evolution of pathogen life-history traits, such as virulence. In this section, we consider that a pathogen strain is characterised by a trait z (for instance the pathogen's within-host growth rate) and that the virulence and transmission traits are all functions of this trait. For simplicity, we assume $\alpha_N = z$, so that z represents virulence in naive hosts. Eventually, a host population infected by the resident strain settles on its endemic

attractor $(\hat{S}_N(t)\,,\hat{S}_T(t)\,,\hat{I}_N(t)\,,\hat{I}_T(t))$. Extensive numerical simulations show that the period of the attractor is always equal to the period of $\nu(t)$. Now let us assume that a mutant with a trait z' which is slightly different from the resident's appears (the full model including the infected hosts by the mutant strain is shown in appendix B.4). Whether the mutant can invade the population or not is determined by the sign of its invasion fitness (Metz et al., 1992, 1995; Geritz et al., 1998; Lion, 2018*c*). We use this conceptual tool to investigate the direction of selection on pathogen traits, and potential evolutionary endpoints.

2.4.1 Anti-infection and anti-transmission treatments

For these treatments, the invasion fitness of a rare mutant pathogen can be calculated analytically from the mutant pathogen's basic reproduction number $R(z',z)$, which acts as a proxy for invasion fitness (Lion and Metz, 2018). Using the same approach used to derive equation 2.5, we find that a rare mutant can invade the resident population on its periodic attractor if $R(z',z)>1$, where

$$R(z',z)=\frac{\beta(z')}{d+\alpha(z')}\left(\left\langle\hat{S}_N\right\rangle+(1-r_1)(1-r_3)\left\langle\hat{S}_T\right\rangle\right). \tag{2.7}$$

Because for the resident pathogen we have $\left\langle\hat{S}_N\right\rangle+(1-r_1)(1-r_3)\left\langle\hat{S}_T\right\rangle=(d+\alpha(z))/\beta(z)=1/R_0(z)$, it follows that

$$R(z',z) \;=\; \frac{R_0(z')}{R_0(z)}\,. \tag{2.8}$$

Equation (2.8) shows that selection favours the strain that maximises the epidemiological R_0, as in the case with constant coverage (Gandon et al., 2001*b*, 2003; Zurita-Gutiérrez and Lion, 2015). As a result, periodicity in treatment coverage does not impact the evolutionarily stable virulence for these two treatments. This can be numerically confirmed using Floquet's theory (figure S.5). For completeness, we note that, in the original models by Gandon et al (Gandon et al., 2001*b*,

2003), the prediction that higher efficacy selects for lower virulence was due to the possibility of superinfection, which we ignore here, as a full analysis of the interplay between multiple infections and environmental fluctuations is beyond the scope of this paper.

2.4.2 Anti-growth and anti-toxin treatments

For anti-growth and anti-toxin treatments, an analytical expression of the invasion fitness $s(z', z)$ (or its proxy $R(z', z)$) is beyond our reach. However, we use a new approach to derive an analytical expression of the selection gradient, $\mathcal{S}(z) = \partial s/\partial z'|_{z'=z}$. The zeros of the selection gradient give the evolutionarily singular points (Geritz et al., 1997).

As a useful baseline scenario, we first examine the case of a constant coverage analysed in (Gandon et al., 2001*b*, 2003). We then have

$$\mathcal{S}_e = c_N^e \left(\beta_N'(z) \frac{d + \alpha_N}{\beta_N} - \alpha_N'(z) \right) + c_T^e \left(\beta_T'(z) \frac{d + \alpha_T}{\beta_T} - \alpha_T'(z) \right) . \tag{2.9}$$

The selection gradient then takes the form of a weighted sum, where the weights c_N^e and $c_T^e = 1 - c_N^e$ are the pathogen's class reproductive values in naive and treated hosts, in a resident population at equilibrium (Taylor, 1990; Rousset, 2004; Zurita-Gutiérrez and Lion, 2015; Lion, 2018*a*). Thus, the ES virulence is intermediate between the value which maximises the basic reproduction number in a fully naive population (i.e. when $c_N^e = 1$) and that maximises the basic reproduction number in a fully treated population (i.e. when $c_T^e = 1$). The class reproductive value c_T^e is a measure of the quality of treated hosts from the point of view of the parasite.

With periodic treatment coverage, we show in appendix B.4 that the average change in mean trait over one period on the resident periodic attractor, is approximately proportional to

$$\mathcal{S} = \langle c_N \rangle \left(\beta_N'(z) \frac{d + \alpha_N}{\beta_N} - \alpha_N'(z) \right) + \langle c_T \rangle \left(\beta_T'(z) \frac{d + \alpha_T}{\beta_T} - \alpha_T'(z) \right) \tag{2.10}$$

where $c_T(t)$ is the class reproductive value of resident pathogens infecting treated hosts at time t, and $c_N(t) = 1 - c_T(t)$ is the class reproductive value on naive hosts. Note that equation (2.10) is directly comparable to equation (2.9), but, in contrast with the classical definition, reproductive values are here time-dependent quantities (Lion, 2018*a*). This reflects the fact that the relative qualities of the different classes of hosts for the pathogen change as the population moves along the periodic attractor.

Equation (2.10) shows that, as in the constant treatment model, the ES virulence in a heterogeneous host population is intermediate between the value which maximises the basic reproduction number in a fully naive population and that maximises the basic reproduction number in a fully treated population. Interestingly, the potentially complex effects of fluctuations on the exact value of the ESS are captured by a single variable, which is the average class reproductive value over one period, $\langle c_T \rangle$. In general, $\langle c_T \rangle$ will deviate from the class reproductive value c_T^e in the constant treatment model (figures 2.4a–2.4c), and as a result the ESS will be different in periodic vs. constant environments.

For anti-toxin treatments, where $\beta_N = \beta_T = \beta(\alpha)$ and $\alpha_T = \alpha(1 - r_4)$, a useful graphical representation can be obtained from equation (2.10) by noting that the ES virulence must satisfy

$$\beta'(\alpha) = \frac{\beta(\alpha)}{d + \alpha} \frac{1 - r_4 \langle c_T \rangle}{1 - r_4 \langle c_T \rangle \frac{\alpha}{d+\alpha}} \tag{2.11}$$

which is a form of Marginal Value Theorem (Charnov et al., 1976). As shown graphically in figure 2.4d, the ES virulence for periodic anti-toxin treatment is lower than in a constant treatment. This effect is mediated by the average class reproductive value which decreases as the period T increases (figure 2.4c). For large T, $\langle c_T \rangle$ converges towards $\bar{\nu} = p$ (appendix B.4), which provides a lower bound for the reduction in virulence that can be achieved by using periodic treatments.

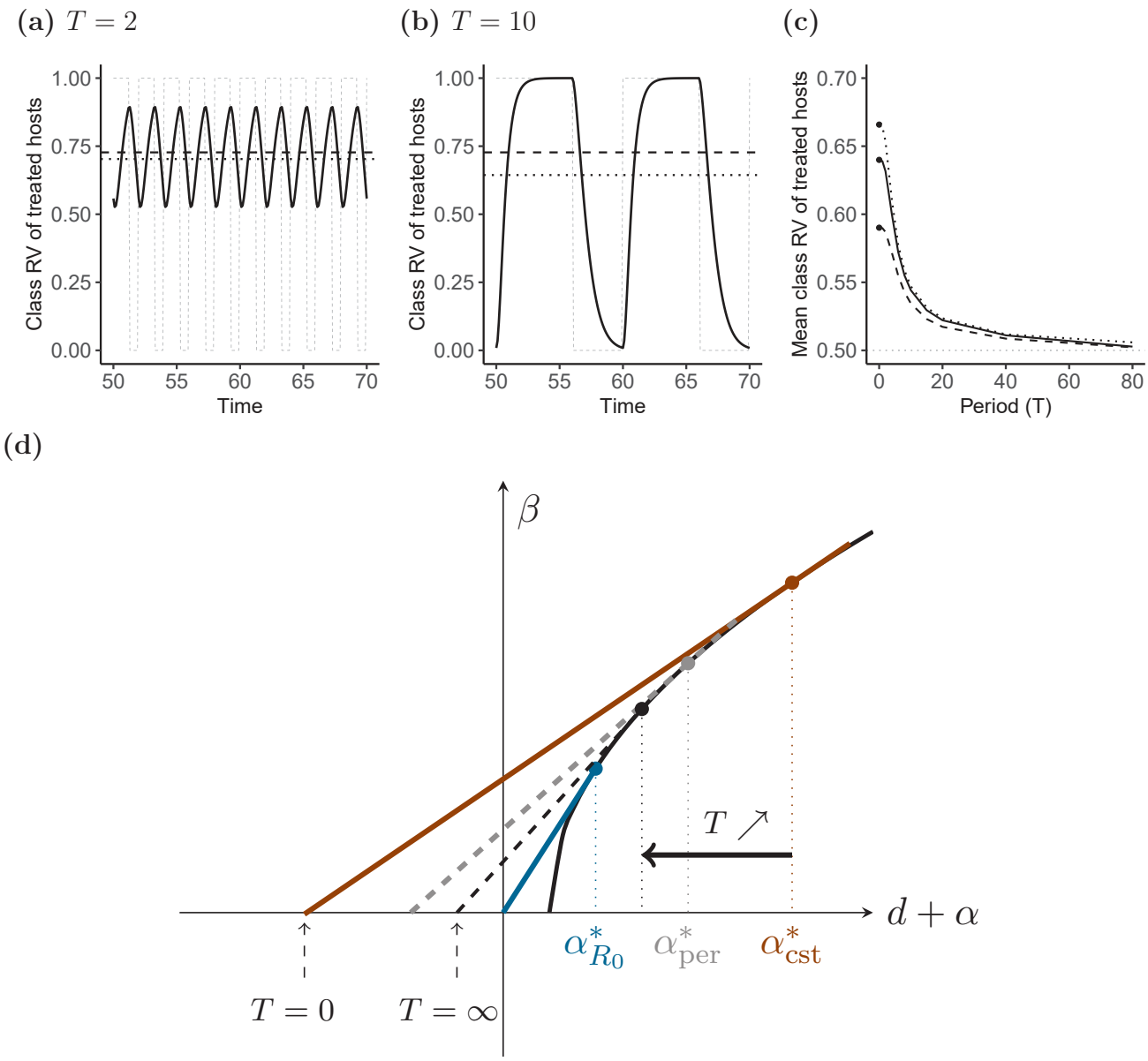

FIGURE 2.4 – (a,b) Dynamics of the class reproductive value of treated hosts, $c_T(t)$ for short (a, $T = 2$) and longer (b, $T = 10$) period of an anti-toxin treatment coverage. Also shown are the periodic treatment function $\nu(t)$ (dashed grey lines), the mean value $\langle c_T(t) \rangle$ (dotted lines) and the value in the constant model c_T^e (dashed line). Parameters : $r_4 = 0.5$, $p = 0.6$, $z = 1$. (c) Mean class reproductive value $\langle c_T(t) \rangle$ as a function of the period. Parameters : $r_4 = 0.5$, $\bar{\nu} = p = 0.5$, $z = 0.5$ (dashed), 1 (solid), 1.4 (dotted). Other parameters as in figure 2.2. (d) Graphical representation of the effect of periodicity on the ES virulence for an anti-toxin treatment. In a homogeneous population, the ES virulence $\alpha^*_{R_0}$ is obtained by maximising the epidemiological R_0. Graphically, this implies that the slope at the ESS goes through the origin (blue line). For a constant treatment ($T = 0$), the slope at the ESS is smaller (red line), resulting in a higher ES virulence α^*_{cst}. As the period increases, so does the slope at the ESS, given by equation (2.11), resulting in a lower ES virulence. The slope at the ES virulence (grey line) then goes through the point $(-dr_4 \langle c_T \rangle / (1 - r_4 \langle c_T \rangle, 0)$, where $\langle c_T \rangle$ is the average class reproductive value of treated hosts over one period. Because, as the period T goes to infinity, $\langle c_T \rangle$ converges to its lower bound p (figure 2.4c), the ES virulence under periodic anti-growth treatment coverage also has a lower bound, which is always greater than $\alpha^*_{R_0}$ (which would be the solution for $\langle c_T \rangle = 0$).

For our trade-off function $\beta(\alpha) = 5\alpha/(1+\alpha)$, this lower bound can be calculated as

$$\alpha^* = \frac{1}{\sqrt{1-pr_4}}, \tag{2.12}$$

which implies that, for a fixed efficacy r_4, the ES virulence should be lower for low values of p (e.g. short bouts of treatment).

While the average value $\langle c_T \rangle$ is sufficient to determine the ES virulence, the impact of periodicity on the full dynamics of $c_T(t)$ sheds light on the process by which higher periods select for lower virulence. Figure 2.4a shows that, for short periods, the class reproductive value rapidly fluctuates around its mean value, which is close to the equilibrium value c_T^e but overestimates the average state of the environment, $\bar{\nu}$. As the period increases, the environmental change becomes slower and easier to track by the pathogen, and the class reproductive value more closely matches the environmental signal $\nu(t)$ (figure 2.4b). Because the pathogen is now better able to perceive the true alternance of good and bad epochs, its optimal strategy is less biased towards treated hosts. Note that equation (2.10) also allows us to understand why anti-infection and anti-transmission treatments are insensitive to periodicity, since, for these treatments, the class-specific selection gradients (the terms between brackets) are equal, so that both classes have the same optimum.

These analytical predictions can be checked using a numerical calculation of the invasion fitness $s(z', z)$, which is the Floquet exponent associated to the mutant dynamics on the resident periodic attractor (see appendix B.4). Figure 2.5a shows that the predictions of equation (2.10) closely match the Floquet analysis and confirms that the ES virulence decreases as the period increases, with a stronger effect for anti-growth than for anti-toxin treatments. There is however a lower bound to the reduction in virulence that can be achieved using periodic treatments, as the ES virulence saturates as T becomes large. Nonetheless a tentative conclusion of our work is that selection for virulence is weaker with treatments with periodic coverage such as pulse vaccination, compared to a constant treatment with similar average coverage. Finally, figure 2.5b

shows that, for both anti-growth and anti-toxin treatments, increasing p, and thus the average treatment coverage in the population, leads to increased ES virulence, as in the constant case. However, in heterogeneous host populations ($0 < p < 1$), the ES virulence is lower with periodic treatments than with constant treatments. Hence, although, as predicted by Gandon et al (Gandon et al., 2001*b*, 2003), anti-growth and anti-toxin treatments select for higher virulence, flucuations in coverage may actually mitigate the negative evolutionary side-effect of these treatments.

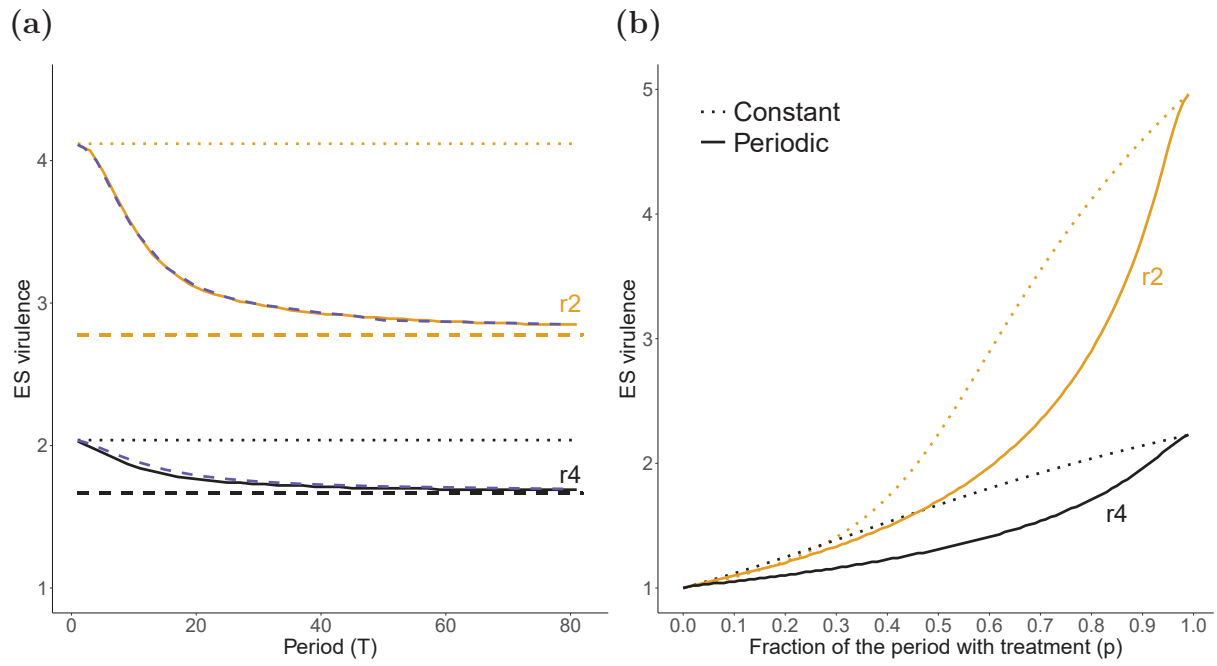

FIGURE 2.5 – Evolutionarily stable virulence according to (a) the period of treatments fluctuations T (with $p = 0.8$), (b) the fraction of time at maximum treatment p (with $T = 50$), for anti-growth (orange) and anti-toxin (black) treatments. Dotted lines show the ESS calculated with a constant average coverage, solid lines show the ESS calculated using the dominant Floquet exponent, compared to the semi-analytical solution of equation (2.10) (dashed purple lines in (a)). The ES virulence is bounded by a lower bound obtained by replacing $\langle c_T \rangle$ with p in equation (2.10) (dashed lines). All with a treatment efficacy of $r_i = 0.8$, and other parameters as in figure 2.2.

2.5 Discussion

Our study sheds light on the potential benefits of periodic treatments, both for short-term epidemiological control of infectious diseases and long-term virulence management. Our model generalises the predictions of Gandon et al. (2001*b*, 2003), who showed for constant treatment coverage that increasing coverage decreases the endemic prevalence, except for anti-toxin treatments. Our results show that this carries over to periodic coverage. For long-term evolution, we show that increasing average treatment coverage has no effect on virulence evolution for anti-infection and anti-transmission treatments but selects for significantly increased virulence with anti-growth and anti-toxin treatments. However, for all treatments, periodic treatments are more beneficial than constant treatments and lead to lower prevalence and virulence.

Our results suggests that periodic treatments over long periods may be a mitigating strategy for virulence management, even for treatments that create selective pressures on pathogen life-history traits. Overall, our model predicts that the best treatment strategy with anti-infection and anti-transmission is a periodic coverage with a high average coverage, to lower the prevalence. Anti-growth treatment strategies require a compromise between high coverage (reduction of prevalence on the short term) and low coverage (to limit the long-term emergence of virulent strains). Anti-toxin treatments are not recommended, but if no alternative exists, periodic strategies of treatment would seem preferable.

At a conceptual level, our modelling approach provides a general method to analyse selective pressures in heterogeneous habitats where habitat quality can vary over time due to environmental fluctuations. Here, the quality of treated hosts for the parasite varies, and we use a dynamical concept of reproductive value (Lion, 2018*a*) to measure this quality and derive the selection gradient. In contrast to previous studies (Ferris and Best, 2018, 2019), which relied on numerical calculations of the invasion fitness, this allows us to derive analytical expressions that can be

readily compared to the selection gradient in constant environments. This is particularly useful as it allows us to capture the effect of periodic coverage on virulence evolution through a single variable, which is the average quality (or reproductive value) of treated hosts over one period.

In our study we focus on periodicity caused by the availability of treatments, which imply seasonality in the susceptible host type and impacts pathogens life-history traits. However, periodic environmental forcing can be caused by other parameters such as seasonality in pathogen transmission rate (Grassly and Fraser, 2006) or in host birth rates (Donnelly et al., 2013), to which our approach could be applied. In particular, considering the effect of seasonal variations of the environment caused by climate change on the evolution of pathogens life-history traits is of particular interest Koelle et al. (2005). Many epidemiological studies have addressed the issue of periodic environments in epidemiology, in particular on the expression of R_0 and the probability of emergence (Grassly and Fraser, 2006; Bacaër and Guernaoui, 2006; Bacaër, 2007; Bacaër, 2011; Carmona and Gandon, 2020). There is however a lack of studies about evolution in fluctuating environments, notably when the population is structured. Partly, this is due to the lack of analytical methods to tackle this question. For instance, Ferris & Best (Ferris and Best, 2018, 2019) have analysed the evolution of host defence in fluctuating environments, but had to resort to numerical calculations of Floquet exponents when selection depends on both susceptible and infected host classes (e.g. when recovery is not negligible). This makes a direct comparison with constant environments difficult. In contrast, the approach we use in this paper allows us to derive an insightful analytical expression for the selection gradient and to capture much of the complexity of environmental fluctuations using the biologically meaningful concept of reproductive value. We think this approach can be more generally applied to analyse other evolutionary scenarios.

In this work, we focus on the evolution of life-history traits and do not consider the possibility that pathogens evolve resistance to treatments. We have shown that increasing the period of treatment leads to a decrease both in the prevalence and the evolutionarily stable virulence,

and seems to be a good treatment strategy. However, large periods means that pathogens are potentially exposed to a treated population during a long time. In principle, this could favour the evolution of pathogen resistance, so that too long a period would probably also have unwanted effects. To sharpen these predictions, our model could be extended to consider other treatements srategies which aim to reduce pathogen resistance, such as combination therapies (patients are treated with several drugs at the same time), mixing (different patients are treated with different drugs) or cycling (each patient is given different drugs in alternace) (Uecker and Bonhoeffer, 2018). For instance, it has been shown that combination therapies are more beneficial than mixing strategies, which are in turn more beneficial than cycling strategies Bonhoeffer et al. (1997). It would be interesting to couple these models with fluctuations in coverage to investigate the robustness of these public health strategies.

There are a number of interesting potential extensions to our study. For instance, the treatment coverage could be a function of disease prevalence, so that the treatment strategy would vary with the spread of the disease. Also, our model assumes that only new individuals (either by birth or migration) are treated, but for some treatments a global coverage over the whole population would be more realistic. Third, it could be interesting to investigate what happens when treated hosts lose their immunity after some time and join the respective susceptible or infected untreated class. Williams and Kamel (2018) have considered a similar heterogeneous model where hosts can switch class over their lifetime. The authors have shown that if an infected host transits from a class with a high reproductive value to a class with a lower reproductive value, selection favours increased host exploitation and therefore increased virulence. These results are consistent with ours, which suggests that the loss of immunity over time would not significantly impact our conclusions.

Our main results were obtained under a number of assumptions. First, we assumed no recovery of infected hosts. This hypothesis is relaxed in appendix B.5 where we explore the effect of non-zero recovery rates. We show that recovery reduces prevalence regardless of the treatment, and decreases

the eradication threshold for all treatments but the anti-toxin. It does not significantly affect the evolutionarily stable virulence. Second, we used a step function for the coverage, which is relaxed in appendix B.6, where we use a sinusoidal function to capture a softer change from no coverage to full coverage. Qualitatively, our results and the associated public health recommendations do not depend of the shape on the periodic coverage function. Third, as commonly assumed in the literature (Gandon et al., 2001*b*; Keeling and Rohani, 2011), we used a density-independent birth rate for simplicity. However, the potential feedback between environmental fluctuations and density-dependent reproduction could be biologically relevant and worth a detailed investigation. Fourth, in contrast with the original model of Gandon et al.(Gandon et al., 2001*b*, 2003), we neglect here the possibility of multiple infections. With superinfection, anti-infection and anti-transmission treatments actually select for lower virulence with constant coverage (Gandon et al., 2001*b*). Although it is beyond the scope of this study, it would be interesting to see how the interplay between within-host selection and population-level environmental fluctuations could alter the selective pressures on virulence.

Importantly, our evolutionary analysis is based on an adaptive dynamics approach, which uncouples epidemiological and evolutionary time-scales. Evolution is supposed to be much slower than epidemiological processes, due to rare mutations. However, many pathogens have high mutation rates and the dominant strain during an epidemic can differ from the strain that is selected in the long run. As experimentally demonstrated in Berngruber et al. (2013), during an epidemic susceptible hosts are abundant and virulent strains investing in transmission are mostly selected, while less virulent strains are favoured at endemic equilibrium, where the proportion of susceptible is lower. It would be interesting to extend our model to take into account potential short-term evolutionary dynamics. Using quantitative genetics methods could help to shed light on these processes (Day and Proulx, 2004; Day and Gandon, 2007).

Finally, it would be interesting to test our theoretical predictions using field or experimental

data. Unfortunately, the kind of field data needed to test our predictions require long-term studies of joint epidemiological and evolutionary dynamics, which are only beginning to appear. Nevertheless, our conclusions could be tested experimentally in microbial, or agricultural systems. Bacteria-phage interactions are well suited to explore the interplay between ecology and evolution in heterogeneous host-parasite interactions (Berngruber et al., 2013; Chabas et al., 2018). By periodically varying the influx of naive or treated susceptible bacteria and monitoring the effects on parasite prevalence and the evolution of phage virulence, it would be possible to test our predictions. We think our theoretical results provide an interesting foundation to guide experimental and empirical studies, which can potentially lead to useful recommendations to control and reduce the damages caused by infectious diseases.

Chapitre 3

Evolutionary implications of spatial heterogeneity in treatment distribution

Alicia Walter, Sylvain Gandon & Sébastien Lion

In preparation

September 2021 version

Abstract

In this chapter, we have developed a spatial metapopulation model, with two subpopulations characterised by different treatment coverages and connected by pathogen migration. In this chapter we study the effects of migration and of the differences in coverage on the long-term virulence evolution. We have shown that the spatial structure of the host population and the selective pressure of treatments on pathogens may yield bistability or evolutionary branching points, which can lead to the coexistence of different pathogenic strains.

3.1 Introduction

Treatment distribution in infectious disease management is of major interest to study pathogens evolution. Because of geography and landscapes, culture and economics, treatment distribution vary between populations. The spatial heterogeneity in treatment distribution creates variations in hosts type with regard to their immunity (treated or naive). These differences in host create strong selective pressure on pathogens, that can have long-term evolutionarily consequences, notably on virulence evolution.

The use of treatments structures the populations into treated and untreated hosts. For the pathogen, they represent different habitats of different qualities. Pathogens are expected to have a better invasion fitness in naive hosts than in treated, which may impact the evolution of pathogens life history traits. Studies have demonstrated the effects of such host-heterogeneity on long-term virulence evolution, with different treatment strategies, either under a constant vaccine coverage (Gandon et al., 2001*b*, 2003), a periodic coverage (Walter and Lion, 2021), by treating the susceptible most at risks (Williams and Day, 2008), or in presence of a spatial structure (Zurita-Gutiérrez and Lion, 2015).

Moreover, populations are often connected to each other which creates metapopulations. Pathogens can move from a population to another by biotic factors, as contact between hosts, or abiotic as for airborne or water-borne diseases. Local adaptation models suggest that a metapopulation with migration between subpopulations leads either to the emergence of specialist or generalist strains (Meszéna et al., 1997; Day, 2000; Ronce and Kirkpatrick, 2001; Débarre et al., 2013; Mirrahimi and Gandon, 2020).

The long-term evolution of pathogens is of major of interest in infectious disease management. Being aware of the long-term effects of treatments on virulence evolution can guide decisions on short-term epidemic management, and the compromise which are required (Dieckmann et al.,

2005). Some treatments that affect pathogens transmission are particularly interesting for their short and long term benefits, as anti-infection and anti-transmission. Indeed, they lower hosts susceptibility or pathogens transmissibility and yields a decrease in pathogens prevalence and the evolutionarily selected virulence (Gandon et al., 2001*b*).

In this study we aim to understand the combined effects of migration and treatment distribution on the long term evolution of virulence in a metapopulation. We study a metapopulation of two subpopulations compounded of naive and treated hosts in different proportions, that are connected by parasite migration. Indeed, we consider the treatment distribution to be heterogeneous among the populations, and that the treatments are imperfect. We explore different treatment distribution from homogeneous (i.e. equal distribution between the two subpopulations) to fully heterogeneous (i.e. one population is completely treated and the other completely naive), and analyse the long-term effects on pathogen virulence evolution. First, the metapopulation is treated with one treatment at a time out of the four studied and second, we explore a combination of different treatments.

3.2 Model

We have developed a SI epidemiological model that characterises a metapopulation composed of two subpopulations A and B, coupled by parasite migration (life cycle depicted in figure 3.1, see table 3.1 for notations). Susceptible hosts are equally produced in both subpopulations at rate b and die at rate d. The metapopulation is infected by a pathogen that can migrate between the two subpopulations at rate m, which varies between 0 and 0.5. For $m = 0$, there is only local transmission of pathogens and susceptible hosts of population A (respectively B) are only infected by infected hosts from population A (respectively B). For $m = 0.5$, susceptible hosts can be equally infected by hosts from A or B. We consider that scenarios where m is greater than

0.5 (i.e. susceptible would be more infected by hosts from the other subpopulation) would not be realistic (Park et al., 2015). Susceptible hosts can be infected at rate h_A or h_B (forces of infections, eq. (3.2)). Infected hosts have an additional disease induced mortality rate which differs for naive (α_A^N and α_B^N) and treated hosts (α_A^T and α_B^T). Subpopulations have a specific treatment coverage respectively noted ν_A and ν_B. We then have the following ODE system for the subpopulation A :

$$\begin{aligned}
\frac{\mathrm{d}S_A^N}{\mathrm{d}t} &= (1-\nu_A)b - S_A^N(d + mh_A + (1-m)h_B)\,, \\
\frac{\mathrm{d}S_A^T}{\mathrm{d}t} &= \nu_A b - S_A^T(d + \sigma(mh_A + (1-m)h_B))\,, \\
\frac{\mathrm{d}I_A^N}{\mathrm{d}t} &= S_A^N(mh_A + (1-m)h_B) - (d + \alpha_A^N)I_A^N\,, \\
\frac{\mathrm{d}I_A^T}{\mathrm{d}t} &= \sigma S_A^T(mh_A + (1-m)h_B) - (d + \alpha_A^T)I_A^T\,,
\end{aligned} \tag{3.1}$$

with the forces of infections, as

$$h^A = \beta_A^N I_A^N + \beta_A^T I_A^T \tag{3.2}$$

and β_A^k the transmission rate in class k. Analogous expressions can be derived for population B.

Inspired by Gandon et al. (2001*b*, 2003), we consider four imperfect treatments that either reduce the susceptibility of hosts (anti-infection, noted r_1 with $\sigma = 1 - r_1$), the within host growth rate of pathogens (anti-growth, noted r_2), pathogen transmission (anti-transmission, noted r_3) or infected hosts death (anti-toxin, noted r_4. Biological examples of each type of treatments are presented in Walter and Lion (2021)). Each treatment varies in efficacy, from ineffectiveness ($r_j = 0$) to perfect treatment ($r_j = 1$). Both transmission and virulence are functions of a trait z that can be considered as the pathogens intra-host reproduction rate, which affects its life history traits. Moreover, we consider an increasing and saturating transmission-virulence trade off (Alizon et al., 2009). We have used $\beta[z] = 5z/(1+z)$ in simulations. In accordance with the properties of

the four treatments, we have :

$$\beta_A^T[z] = (1-r_3)\beta_A^N[(1-r_2)z]\,, \quad \alpha_A^T[z] = (1-r_2)(1-r_4)\alpha_A^N[z]\,.$$

$$\beta_A^N[z] = \beta[z]\,, \quad \alpha_A^N[z] = \alpha[z]\,.$$

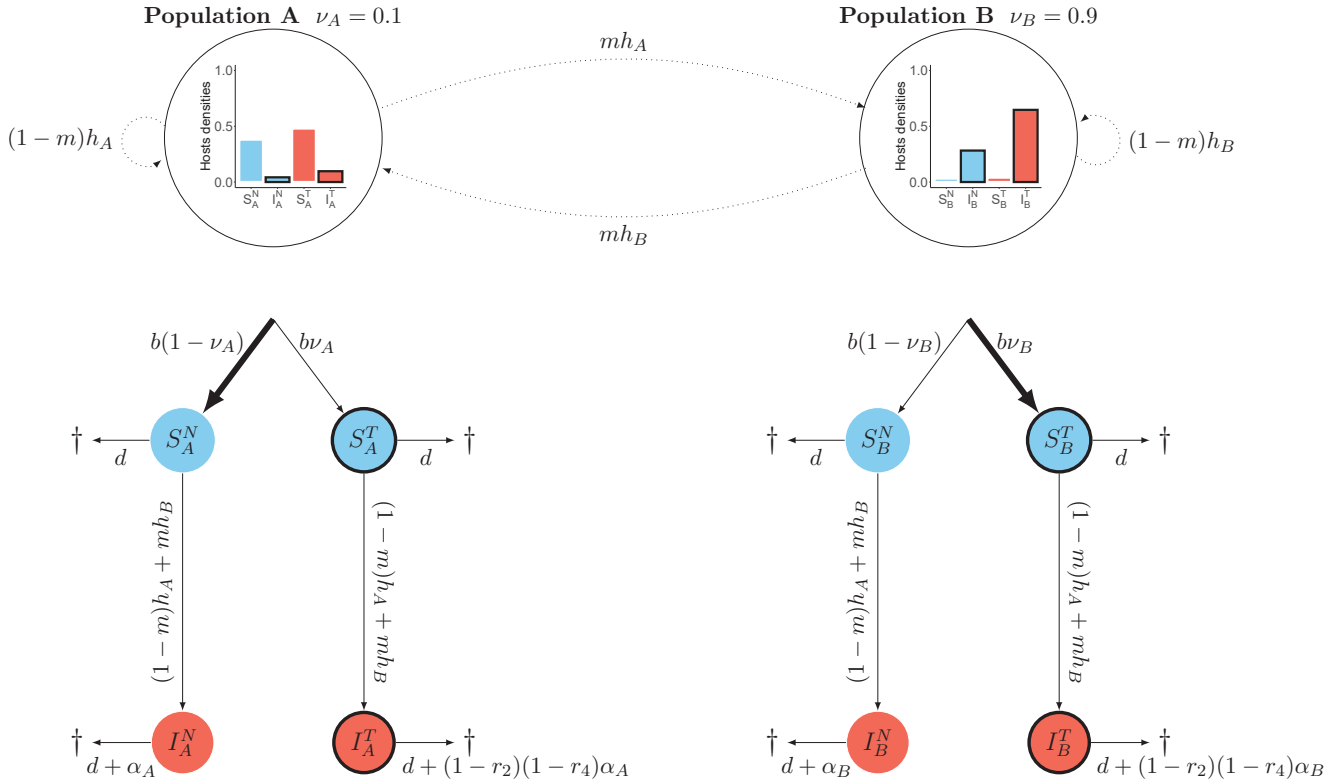

FIGURE 3.1 – Life cycle of the host-pathogen interaction, showing transition rates between classes in the metapopulation. Susceptible hosts are represented in blue and infected hosts in red. Treated hosts are in thick circle and naive hosts in thin. Barplots of hosts densities are shown as examples of populations structure, with $\nu_A = 0.1$, $\nu_B = 0.9$, $r_4 = 0.8$, $b = 2$ and $d = 1$.

In this study we assume that half of the new entrants in the metapopulation (by birth or migration) are treated, so $(\nu_A + \nu_B)/2 = 0.5$. We aim to compare a homogeneous distribution of treatments among the two subpopulations ($\nu_A = \nu_B$), to a heterogeneous distribution ($\nu_A \neq \nu_B$). We consider that population B always receives as much or more treatments than population A.

TABLE 3.1 – Table of parameters and variables.

Parameter	Definition
Life history traits	
α_i^k ($\alpha_i^{k'}$)	disease induced death rate of the resident (mutant) strain in population i and class k
β_i^k ($\beta_i^{k'}$)	transmission of the disease of the resident (mutant) strain in population i and class k
h_i	force of infection in population i
Reproductive values	
c_k	Class reproductive value in population k
Metapopulation dynamics	
b	influx of susceptible
d	natural death rate
m	parasite migration rate
Treatments	
δ	difference in treatment coverage between the subpopulations
ν_i	treatment coverage in population i
r_j	efficacy of the j treatment

i stands for population A or B
j stands for anti-transmission (1), anti-growth (2), anti-transmission (3) or anti-toxin (4) treatments
k stands for naive (N) or treated (T) hosts

Then we have $\nu_B \geq \nu_A$, with $\nu_A \in [0, 0.5]$ and $\nu_B \in [0.5, 1]$. To quantify the difference between the coverage in the subpopulations, we set $\delta = \nu_B - \nu_A$ that varies between 0 (homogeneous distribution) and 1 (maximal heterogeneous distribution).

In appendix C.1 we explore the epidemiological implications of different migrations and coverage on the prevalence and the basic reproductive number.

3.3 Long-term virulence evolution using adaptive dynamics

3.3.1 Mutant invasion fitness

We suppose that our steady host-pathogen metapopulation has reached an endemic equilibrium with a resident pathogen of trait z. A rare small-effect mutation occurs and a mutant strain appears in the metapopulation with a slightly different trait value, noted z'. As we do not consider co-infection, the mutant can either die out or invade and replace the resident strain. Mutant invasiveness depends on its invasion fitness, $R(z, z')$, that represent the number of surviving mutant offspring per mutant parent when the mutant allele is rare (Hurford et al., 2009; Otto and Day, 2011). In our model it is of the form (appendix C.2) :

$$R(z, z') = \frac{1}{2}\left((1-m)(R'_A + R'_B) + \sqrt{4(2m-1)R'_A R'_B + (1-m)^2(R'_A + R'_B)^2}\right), \qquad (3.3)$$

with $R'_A = R'^N_A \hat{S}^N_A + \sigma R'^T_A \hat{S}^T_A$ (analogous expression in population B). Then, the invasion of the mutant depends both on the resident strain in place, through susceptible densities at equilibrium (included in R'_A and R'_B), and on the mutant strain through R'^N_A and R'^T_A, where $R'^N_A = \beta'^N_A/(d + \alpha'^N_A)$ and $R'^T_A = \beta'^T_A/(d + \alpha'^T_A)$ are the mutant fitness in naive or treated hosts in population A.

3.3.2 Selection gradient

To predict the long term evolution of the trait of interest, z (i.e. virulence), we calculate the selection gradient, $\mathcal{S}$. This amounts to evaluating the partial derivative of the mutants invasion fitness at $z = z'$. The zeros of the selection gradient yield evolutionary singularities, noted z^*. In our model, it is expressed as (see appendix. C.2 for calculation details) :

$$\mathcal{S} = c_A \frac{\partial R'_A}{R_A} + c_B \frac{\partial R'_B}{R_B} \tag{3.4}$$

where $\partial R'_k$ are the derivative of the mutant invasion fitness (see appendix C.3 for a full expression), and

$$c_A = \frac{1}{R_A} \frac{R_B(2m-1) + (1-m)}{2 + (m-1)(R_A + R_B)}\,, \quad c_B = \frac{1}{R_B} \frac{R_A(2m-1) + (1-m)}{2 + (m-1)(R_A + R_B)}\,. \tag{3.5}$$

Then, c_A (respectively c_B) can be interpreted as the class reproductive value in population A (respectively B), and can be used to evaluate the quality of hosts A (respectively B) for the pathogen (Lion, 2018*a*; Lion and Gandon, 2021). We can use the class reproductive values properties, and we have $c_A + c_B = 1$ (see appendix C.2).

3.3.3 Second-order derivative

The second order derivative of the invasion fitness, $\mathcal{D}$, provide the stability of the singularities. If $\mathcal{D} < 0$ the evolutionary singularity is stable and pathogen traits converges towards this value. If $\mathcal{D} > 0$, the singularity is unstable and pathogen traits diverge from this value. In our model, it is expressed as

$$\mathcal{D} = c_A \frac{\partial^2 R'_A}{R_A} + c_B \frac{\partial^2 R'_B}{R_B} + \kappa\,, \tag{3.6}$$

TABLE 3.2 – Summary of the epidemiological and evolutionary effects of each treatment.

Treatment	Epidemiology	Evolution
Anti-infection (r_1)	Lower pathogens prevalence	No effect on the evolution
Anti-growth (r_2)	Mitigating effects on pathogens prevalence	ES virulence, branching points or bistability
Anti-transmission (r_3)	Lower pathogens prevalence	No effect on the evolution
Anti-toxin (r_4)	Increase pathogen prevalence	ES virulence or branching points

where $\partial^2 R'_k$ is the second order derivative of the mutant invasion fitness in population k (see appendix C.3 for a full expression), and

$$\kappa = 2(c_A c_B)^{3/2}\sqrt{R_A R_B}\left(\frac{\partial R'_A}{R_A} - \frac{\partial R'_B}{R_B}\right)^2 \frac{1-2m}{m}, \tag{3.7}$$

where $c_A c_B = d\frac{m^2}{(2-(1-m)(R_A+R_B))^2}$.

3.4 Numerical applications

Considering each treatment separately, we distinguish two cases, on the one hand, anti-infection and anti-transmission (r_1 and r_3), and on the other hand, anti-growth and anti-toxin (r_2 and r_4). On table 3.2, we have summarized the major effects of every treatment. In our spatial model anti-infection and anti-transmission treatments have no effect on the long-term evolutionarily state nor on the ES virulence value (see appendix C.4). First, we study the impact of the different treatments on habitats quality for pathogens. Second, we study anti-growth or anti-toxin treatments separately. Third, we extend our study to a combination of treatments.

3.4.1 Habitats quality according to treatments

In figure 3.2 we present the class reproductive value in population A (c_A) according to m and δ for the different treatments. We note the boundary $c_A = 0.5$ reached in a homogenous population

($\delta = 0$), meaning that no population is better for pathogens. We can distinguish three patterns based on the treatments type.

First, anti-infection and anti-transmission treatments decrease pathogens transmission and thus pathogens prevalence (see appendix C.1). Without migration ($m = 0$) and with a heterogeneous distribution of treatments ($\delta > 0$), we have $c_A > 0.5$. It is then more suitable for pathogens to be in the less treated population. Increasing m homogenizes populations, pathogens are more exposed to treated hosts and the quality of habitat A decreases. However, it remains more beneficial for pathogens to be in the subpopulation A (mostly naive).

Second, anti-toxin treatment reduces hosts death caused by the disease and increases pathogens prevalence in the population (see appendix C.1). Without migration ($m = 0$) and with a heterogeneous distribution of treatments ($\delta > 0$), we have $c_A < 0.5$. It is then more suitable for pathogens to be in the more treated subpopulation. Increasing m imply a decrease of the habitat A quality. However, it remains more beneficial for pathogens to be in the subpopulation B (mostly treated).

Third, anti-growth treatment is a bit trickier. Indeed, this treatment both reduce pathogens transmission and virulence. Its use yields bistability and thus two possible ES virulence. On figure 3.2c, we have calculated c_A for each singularity (ESS and branching points) and we see that, according to the value of the ES virulence, hence by the initial value of virulence, it is more suitable for pathogens to be in the more naive or in the more treated population.

3.4.2 Treatments alone

3.4.2.1 Anti-growth

On figure 3.4a, we show the effects of migration and anti-growth distribution on the long-term stability. Low treatments efficiency decreases the effects of the difference in coverages between the subpopulations. Then, we focus on highly efficient treatments to heighten the results. When the

treatment coverage is equal in the subpopulations ($\delta = 0$), the migration has no effect. When the subpopulations are well mixed ($m = 0.5$), there is no effect of δ. Changing simultaneously δ and m leads to three different long-term evolutionary outcomes, (i) a single ESS, (ii) a branching point (BP) or (iii) two ESS that surround a repellor (see figures 3.3a, 3.3b, 3.3c). ESS are mostly observed in homogenized metapopulations, (very connected subpopulations and/or very similar dose distribution). Bistability occurs in a quite heterogeneous metapopulation (low migration and heterogeneous dose distribution), and branching points at the frontier between single and two ESS.

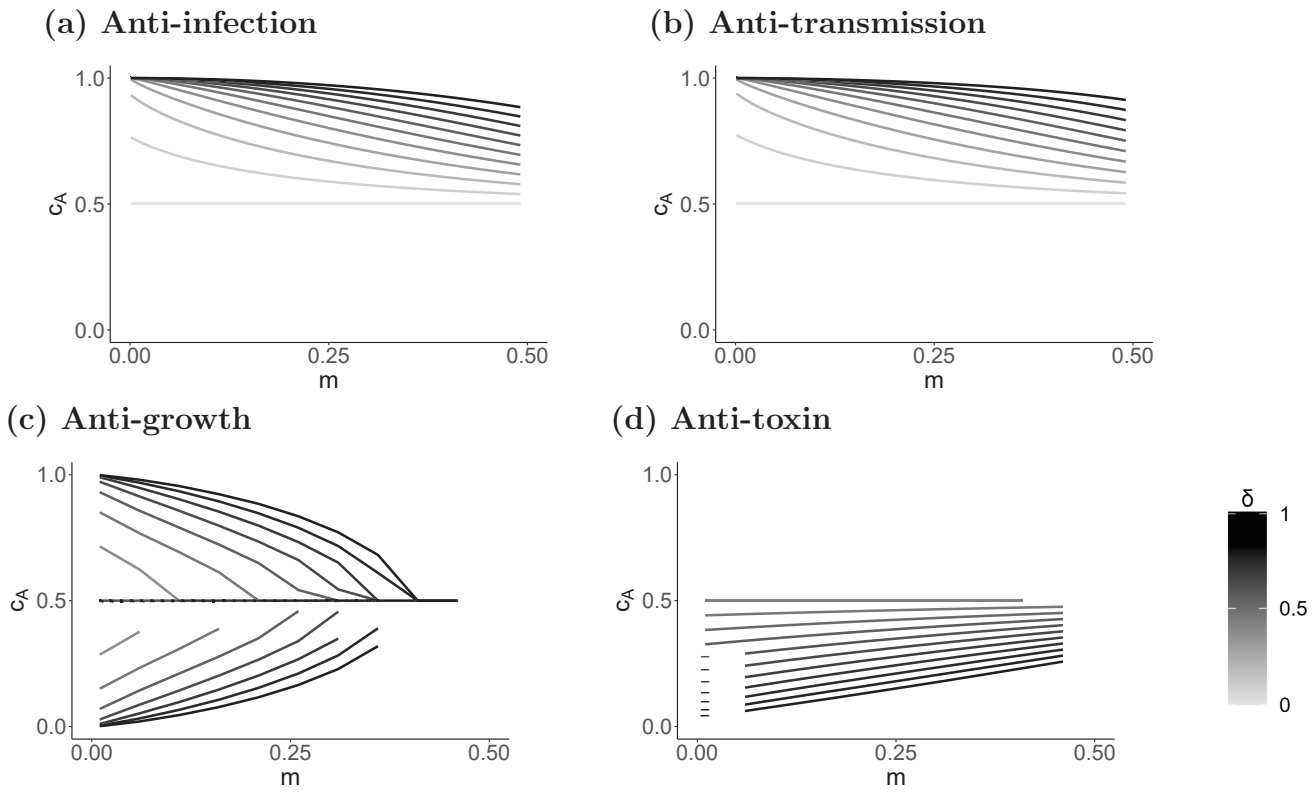

FIGURE 3.2 – Reproductive value in population A (c_A) function of the migration m and different values of δ with (a) anti-infection, (b) anti-transmission, (c) anti-growth and (d) anti-toxin treatments with $r_j = 0.9$. We have calculated c_A's for every singularity, ESS are shown in solid lines and branching points and repellors in dotted. Anti-growth yields bistability, and thus two ESS. The curves above the boundary $c_A = 0.5$ correspond to c_A calculated with the lower value of ES virulence, and curves below, with the higher value. Other parameters as in figure 3.1.

These numerical results can be demonstrated analytically. In equation (3.6), we see that with a concave saturating transmission-virulence trade-off, the left and middle terms (noted $\mathcal{D}_1$) are negative. Then, the sign of the second order derivative depends on κ. The selection is directional and converges towards a stable singularity for $\mathcal{D} < 0$ and is disruptive and diverges from the singularity for $\mathcal{D} > 0$. In our model, we observe stable singularities (ESS) or unstable (BP and repellor). Two ESS are only observed with anti-growth treatment, if κ is sufficiently positive to balance the negativity of $\mathcal{D}_1$. This occurs for small enough m and R'_A different enough from R'_B (e.g. $\nu_A \neq \nu_B$). This is concordent with our numerical results presented in figure 3.4.

Inspired by Débarre et al. (2013), we have added a mutational parameter in order to highlight the value of the virulence reached according to the initial value od the resident strain (model shown in appendix C.5). It appears that branching points leads to the coexistence of pathogen strains with different trait values close to the optimums in A or in B. Then, increasing the heterogeneity in treatments distribution results in the persistence of highly virulent strains in the population.

3.4.2.2 Anti-toxin treatments

On figure 3.4b, we show the long-term state according to m and δ. It appears that an anti-toxin treatment mostly yields single evolutionarily stable states except for low migration and high efficacy, where we observe branching points. Again, balancing populations with high m or low δ stabilizes the long-term states and yields single evolutionary stable virulence. On the contrary, differentiating populations yields branching points and the coexistence of pathogens.

3.4.3 Combination of treatments

Anti-infection and anti-transmission treatments have a similar action on pathogens by reducing their transmissibility. In appendix C.6, we have combined anti-growth or anti-toxin treatments with anti-infection or anti-transmission.

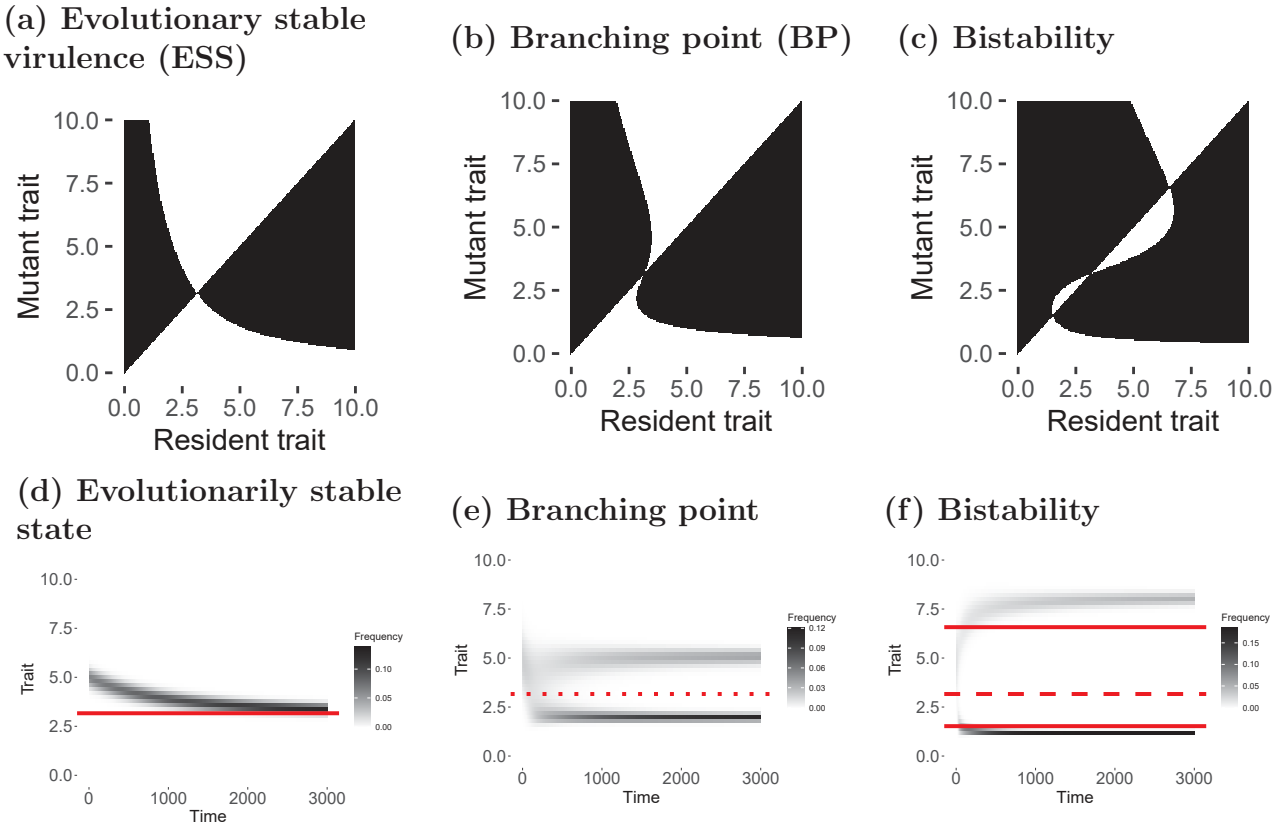

FIGURE 3.3 – (a, b, c) Pairwise Invasibility Plots for anti-growth treatment, corresponding to black dots on figure 3.4a, with $m = 0.2$ and (a) $\delta = 0.15$, (b) $\delta = 0.42$ or (c) $\delta = 0.75$. The mutant strain wins the competition in white areas and the resident strain wins in black areas. (d, e, f) The corresponding simulated evolutionary tree starting with a monomorphic population of trait $z = 5$, with $m = 0.2$ and (d) $\delta = 0.15$, (e) $\delta = 0.42$ or (f) $\delta = 0.75$. In red solid lines, the expected ES virulence, in red dotted lines, the expected branching point, and in dashed red line, the expected repellor, all calculated by adaptive dynamics. Other parameters as in figure 3.1. In appendix C.5 we show the corresponding frequencies dynamics.

3.4.3.1 Combination with anti-growth treatment

Anti-growth treatments aims to reduce pathogens transmission and virulence. This type of treatments have been demonstrated as negative for hosts, by increasing pathogen prevalence and evolutionarily selected virulence. On the contrary, the use of anti-infection treatments reduce pathogen prevalence and have no evolutionary effects (Gandon et al., 2001*b*, 2003; Walter and Lion, 2021).

A combination of a beneficial with a detrimental treatment might neutralize the negative evolutionary effects of treatments. Indeed, we have shown that the use anti-growth treatment affects the long-term evolutionary state, and highly virulent strains can emerge according to the migration, the heterogeneity in distribution and the initial resident strain. As we can see on figure C.12, the addition of an anti-infection or anti-transmission treatment to a population treated with anti-growth treatments, changes the long term stability. Indeed, anti-infection treatment cancels out the branching points and the bistability caused by anti-growth treatment, and so on, reduces the possible emergence and/or coexistence of highly virulent strains.

3.4.3.2 Combination with anti-toxin treatments

On figure C.13, we present the effect of anti-infection or anti-transmission treatment combined with an anti-toxin, on the long-term evolutionary state. Unlike anti-growth, the addition of anti-infection favour branching points for moderately effective treatments (until $r_1 = 0.7$). It means that this particular combination might increase the harmfulness of the epidemic by the coexistence of virulent strains in the metapopulation.

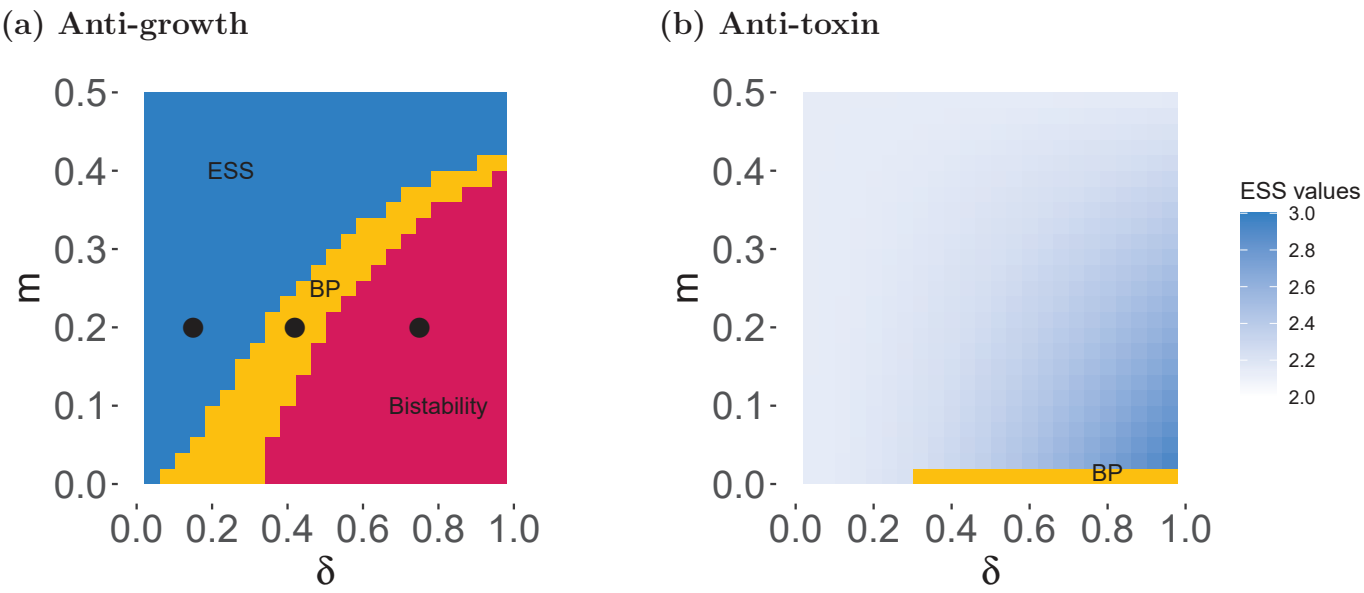

FIGURE 3.4 – Long term evolutionary state calculated using adaptive dynamics, for (a) anti-growth and (b) anti-toxin, with $r_i = 0.9$. On (a) we have represented the evolutionarily state on the long-term, ESS in blue, branching point (BP) in yellow and bistability in pink. On (b) ESS values are represented in a gradient of blue, in addition to the evolutionarily state.

3.5 Discussion

We present here the long-term evolution of pathogens life-history traits in a metapopulation, in response to the selective pressure caused by four different imperfect treatments. We have shown that, as in Walter and Lion (2021), anti-infection and anti-transmission treatments does not affect pathogens evolution. However, it appears that migration and treatment distribution significantly impact the evolutionary outcomes with anti-growth and anti-toxin treatments. In a single structured homogeneous population, selection leads to a single ES virulence, which in our case, corresponds to $m = 0.5$ or $\delta = 0$. These two parameters affect the balance in susceptible between the subpopulations. Balanced populations (homogeneous) have small effects on the long-term evolution of pathogens. Changing the balance imply several potentially dangerous evolutionary outcomes. Indeed, a variation in pathogens migration between the two subpopulation

or a variation in treatments distribution yields branching points or bistability. This is particularly inconvenient because branching points imply the coexistence of multiple potentially virulent strains and bistability might yields virulent strains to emerge according to life-history traits of the initial strain.

We have focused here on pathogen evolution on the long-term, which might seem superfluous when facing an epidemic. However, beneficial treatments in the short-term may turn out to be deleterious in the long-term because of the selection of potentially dangerous strains. For instance, the vaccine against Marek's disease reduces chickens death in the short term, yields the apparition of highly virulent strains in the long-term (Read et al., 2015). Being aware of the long-term effects of treatments on virulence evolution can guide decisions on short-term epidemic management, and the compromise which are required (Dieckmann et al., 2005). Moreover, different techniques of adaptive dynamics would be required for a better understanding of the bistability that occurs in our model.

Some treatments are particularly interesting for their short and long term benefits. Indeed, anti-infection and anti-transmission that lower pathogens transmissibility, also reduce pathogens prevalence and the evolutionarily selected virulence (Gandon et al., 2001*b*). Adding these type of treatments to anti-growth and anti-toxin is a good solution to reduce the negative long-term effects on the virulence. Indeed, from the host point of view we can refer to source-sink ecological models (Rousset, 1999). Anti-infection and anti-transmission treatments that lower pathogens prevalence can be interpreted as source of uninfected hosts. Moreover, populations under these treatments represent unsuitable habitats and pathogens have a better fitness in the naive population. On the contrary, anti-toxin treatment and anti-growth under some circumstances, can be interpreted as sink because pathogens are highly prevalent in these populations and the proportion of susceptible is low. We have seen that in these populations, it might be more suitable to be in the treated habitat. Consequently, a source-sink combination of treatments allows for the beneficial effects of

the source to offset the detrimental effects of the sink, to the point of cancelling them out. Then, a combinations of treatments seems to be a nice method to reduce the negativity of in infectious disease.

Many spatial models focus on local and global dispersion of pathogens. At the local level, the selection favours more "prudent" pathogens strains (i.e. less transmissible and less virulent) (Haraguchi and Sasaki, 2000; Van Baalen, 2002; Lion and Baalen, 2008). Indeed, virulent strains that would spread locally would be too harmful for the hosts and reduce the chances of the pathogen to spread globally, which would be detrimental for it. On the contrary, a global dispersal yields more virulent strains to be selected (Boots and Sasaki, 1999; Boots et al., 2000). In that perspective, Berngruber et al. (2015) have experimentally shown that more structured populations (i.e. that disperse both locally and globally) favours less virulent strains. Our model can be closely compared to Zurita-Gutiérrez and Lion (2015), where the authors have studied the same four imperfect treatments in a spatially structured hosts population in a lattice model. They have shown that an increased dispersal selects for highly virulent strains with anti-infection, anti-transmission and anti-toxin treatments, while it may selects for lower virulence with anti-growth treatment. Setting a local transmission as a low m and global transmission as a high m, the conclusions of Zurita-Gutiérrez and Lion (2015) are not concordant with ours, and more work should be done to link the different type of spatial models (lattice and metapopulation for instance).

In our metapopulation, the only difference between the subpopulations is their proportion of naive and treated susceptible hosts. The host-heterogeneity is established at the host entrance in a subpopulation and permeates in the other class when susceptible hosts get infected. Baker et al. (2020) have shown that the proportion of susceptible in a population is a key-driver in the spread of pandemics, even over climate change, in the context of the SARS CoV-2 pandemic. In our study, the fraction of uninfected hosts greatly impacts the pathogen evolution and in the long term outcome of epidemics. Indeed, the high proportion of susceptible favours more transmissible

strains (Berngruber et al., 2015), and because of the transmission-virulence trade-off that we have implemented, the selection of more transmissible strains imply an increase in virulence. Consequently, the worse evolutionary outcome (coexistence of strains and increased virulence) occurs when the fraction of susceptible is at is highest.

We have focused on the particular case of $\nu_B + \nu_A = 1$ because it maximises the long-term bistability with highly efficient anti-growth treatment. In appendix C.7 we expand our results to all the possible combinations of coverage in subpopulations. Lower or higher values, or a high migration, mostly lead to ESS, but are still worthy of investigations.

Our numerical results were obtained under the assumption that the pathogen life history traits (transmission and virulence) are equivalent in the subpopulations. However, in expressions we have maintained the different notations to include the cases where pathogens would have different life history traits according to the subpopulation in which it is. As a matter of fact, we could imagine that each subpopulation is compounded of hosts from different species. They would be infected by the same pathogen but which would have different transmission and virulence according to the hosts physiology. In the same perspective, the different expressions include the four treatments, to consider all treatments combinations possible, and they can be simplified to consider a single treatment or specific combinations.

This study can be extended to the concept of mozaic in agriculture. This spatial arrangement of fields consists in the fragmentation of landscapes in different patches that communicates with each other (Martín et al., 2006) in order to increase plants heterogeneity. Not only mosaic structure increases biodiversity (Sirami et al., 2019), but it can also be used in epidemic management to slow pathogens adaptation (Djidjou-Demasse et al., 2017). In addition, landscape structure is of major of interest in plant epidemiology that affect pathogens dispersal, emergence and evolution (Plantegenest et al., 2007). In that end, it would be worthwhile to increase the number of patches in our model (i.e. the number of subpopulations) to increase the structure complexity thought

several treatment coverages. Pathogens would face several habitats with different fractions of treated-naive hosts, and the negative evolutionary effects could eventually be reduced. It could provide an interesting theoretical base to understand the effect of complex spatial structure on pathogens life cycle.

Chapitre 4

Vaccine escape in metapopulations, the example of SARS-CoV-2 pandemic

Alicia Walter, Sylvain Gandon & Sébastien Lion

In preparation

September 2021 version

Abstract

In this chapter we have extended our previous metapopulation model, broadly inspired by the Covid-19 pandemic. However, in contrast to the chapter 3, we focus on short-term pathogen evolution and study the speed of emergence of a vaccine escape mutant in a two-population model connected by pathogen migration. This model allows for the study of several scenarios inspired by the management of the pandemic. For instance, different vaccination strategies between connected countries, or the impact of border opening and closure on the speed of emergence of a vaccine escape mutant can be explored.

4.1 Introduction

During an epidemic, the rapid deployment of treatments is necessary to minimize the damaging consequences on the hosts. Unfortunately, treatments might not be available everywhere at the same time. For instance, the vaccine deployment against the SARS-CoV-2 is unequal and we observe important differences in its coverage between close countries (Mathieu et al., 2021). Because of the short generation time of pathogens, the probability that a vaccine escape mutant appears is high. Differences in treatment deployment induce heterogeneities within hosts populations by separating the hosts in classes (treated or naive). This phenomenon may affect the speed of vaccine escape mutant emergence (Gandon and Lion, 2021).

Globalization has connected countries geographically far from each other, easing the travel of pathogens and the spread of infectious diseases. Hence, populations subjected to different vaccine deployment strategies become connected. To slow the spread of the SARS-CoV-2, many countries have closed their borders and restricted the flights to sort the entrance. The effect of border closure on the spread of the pandemic is well documented (Chinazzi et al., 2020; Linka et al., 2020; Wells et al., 2020). However its effect on the evolution of the virus and the speed of adaptation remains to be investigated. Indeed, several variants of the SARS-CoV-2 have appeared with increased transmissibility, virulence or that escape the vaccine (Alizon and Sofonea, 2021).

In Gandon and Lion (2021), the authors have studied vaccine escape mutations, first, in a population where hosts are differentiated by their contact rate, and second, in a population where hosts can receive one or two vaccine doses (the second dose is delayed). They have shown that targeting low contact rates between hosts both reduces hosts death and the spread of vaccine-escape variant. On the contrary, delaying the second dose allows for a larger part of the population to be vaccinated with a single dose, which reduces the global number of host deaths, but also yields an increase in the speed of adaptation.

During a pandemic, close countries may adopt different strategies to fight the disease. To take into account these heterogeneous approaches, we have extended Gandon and Lion (2021) model into a metapopulation model organized in two subpopulations, A and B, that are connected by migration. It allows for the study of different scenarios broadly inspired by the Covid-19 pandemic.

In this chapter we aim to understand the levers that affect the emergence of a vaccine escape mutant strain in all the different layers of the metapopulation. First we track the frequency of the mutant in each class of host of the metapopulation, second in each subpopulation, and third in the global metapopulation. Finally, we present the example of a scenario that could be analysed with our model, and open on several trails interesting to follow.

4.2 Model

We consider an epidemiological model of two subpopulations, A and B, connected by parasite migration. The susceptible hosts, noted S, are born or immigrate at rate b and have a natural death rate d. A proportion ν_k of the susceptible hosts newly arrived in population k are vaccinated and enter the "hat" class, $\widehat{S}^k$. In contrast, a proportion $1-\nu_k$ remain naive (i.e. unvaccinated) and enter the S^k class. Susceptible hosts that get infected enter the I^k or $\widehat{I}^k$ class depending on whether they were previously vaccinated or not. Then, an infected host, I^k or $\widehat{I}^k$, may transmit the pathogen respectively at rate β^k or $\widehat{\beta}^k$ to susceptible hosts, which in turn become infected.

We consider that our population is infected by two pathogen strains, the wild-type and the mutant, respectively noted w and m, and both referred to as i. The difference between the wild-type and the mutant strain is their ability to escape the vaccine, noted e_i. The wild-type can not bypass the vaccine and thus $e_w = 0$. On the contrary the mutant escape ability e_m is ranging from 0 (no vaccine escape) to 1 (full vaccine escape).

Moreover, in our study we consider two different vaccine that either reduce host susceptibility

(noted V_σ) or pathogens transmissiblity, affecting the β's (noted V_τ). The V_σ vaccine gives protection to the susceptible hosts by reducing their odds to be infected, which is expressed in our model as $\rho_\sigma(e_i) = 1 - r_\sigma(1 - e_i)$. The V_τ vaccine reduces the odds of an infected host to transmit the disease, which is expressed in our model as $\rho_\tau(e_i) = 1 - r_\tau(1 - e_i)$. Thus, these two vaccines functions depend on of the vaccine efficacy, r_σ and r_τ and of the vaccine escape, e_i.

Then, the force of infection of a strain i in the population k, noted h_i^k, is function of the transmission rates, the infected hosts densities, the vaccine escape and the vaccine efficacy and expressed as $h_i^k = \beta^k I_i^k + \rho_\tau(e_i)\widehat{\beta}^k \widehat{I}_i^k$.

Lastly, infected hosts leave the infected class at rate δ_i^k, and they can either die at rate c_i^k and reach the dead hosts class (D) or recover at rate $1 - c_i^k$ and reach the recovered hosts class (R). Here c_i^k (respectively $\widehat{c}_i^k$) represent the probability that hosts die after leaving the class I_i^k (respectively $\widehat{I}_i^k$). This leads to the following ODE system in the subpopulation A, which is analogous in population B (see appendix D.1)

$$\begin{aligned}
\dot{S}^A &= b(1-\nu^A(t)) - dS^A - \left((1-m)\sum_i I_i^A h_i^A + m\sum_i I_i^B h_i^B\right) S^A \\
\dot{\widehat{S}}^A &= b\nu^A(t) - d\widehat{S}^A - \left((1-m)\sum_i I_i^A h_i^A + m\sum_i I_i^B h_i^B\right) \rho_\sigma(e_i)\widehat{S}^A \\
\dot{I}_i^A &= \left((1-m)h_i^A + mh_i^B\right) S^A - \delta_i I_i^A \\
\dot{\widehat{I}}_i^A &= \left((1-m)h_i^A + mh_i^B\right) \rho_\sigma(e_i)\widehat{S}^A - \widehat{\delta}_i \widehat{I}_i^A \\
\dot{D} &= \sum_i \left(c_i^A \delta_i^A I_i^A + \widehat{c}_i^A \widehat{\delta}_i^A \widehat{I}_i^A + c_i^B \delta_i^B I_i^B + \widehat{c}_i^B \widehat{\delta}_i^B \widehat{I}_i^B\right)
\end{aligned} \tag{4.1}$$

With this model, we are able to follow the hosts densities dynamics, and we are particularly interested in following the frequency of infected hosts by the mutant strains dynamics and the speed of mutant emergence in all the classes of the metapopulation (see table 4.1 for notations).

4.2.1 Vaccine escape mutant dynamics in each class of the metapopulation

Our metapopulation contains four classes of hosts infected by the mutant strain and four by the wild type strain. On the one hand we have the naive A and the vaccinated $\widehat{A}$ hosts from population A, and on the other hand, the naive B and the vaccinated $\widehat{B}$ hosts from population B. We aim to track the vaccine escape mutant frequency to quantify the speed of its apparition. The mutant frequency might differ in all of these classes because the hosts are vaccinated or not, and the proportion of vaccinated can also differ.

So, we first track the frequency of the vaccine escape mutant in each of these four classes. In Lion (2018*a*), the author derives an expression to track the dynamics of a specific strain in a multi-class population. We have adapted the expression to our model (see appendix D.2) to follow the dynamics of the mutant frequency in the naive and treated classes of populations A and B. In the subpopulation A it is expressed as (analogous expression in B)

$$\begin{aligned}\frac{\mathrm{d}f_m^A}{\mathrm{d}t} =&\beta S^A \Delta\rho_\tau \left[m\omega^{\widehat{B}}\frac{f^{\widehat{B}}}{f^A} + (1-m)\omega^{\widehat{A}}\frac{f^{\widehat{A}}}{f^A}\right] + \\ &\beta S^A \left[(1-m)\overline{\rho_\tau}^{\widehat{A}}(f_m^{\widehat{A}} - f_m^A)\frac{f^{\widehat{A}}}{f^A} + m\left((f_m^B - f_m^A)\frac{f^B}{f^A} + \overline{\rho_\tau}^{\widehat{B}}(f_m^{\widehat{B}} - f_m^A)\frac{f^{\widehat{B}}}{f^A}\right)\right]\end{aligned} \tag{4.2}$$

and

$$\begin{aligned}\frac{\mathrm{d}f_m^{\widehat{A}}}{\mathrm{d}t} =& \beta S^{\widehat{A}}\Delta\rho_\sigma\left(m\omega^B\frac{f^B}{f^{\widehat{A}}} + (1-m)\omega^A\frac{f^A}{f^{\widehat{A}}}\right) + \beta S^{\widehat{A}}\Delta\rho_{\tau\sigma}\left(m\omega^{\widehat{B}}\frac{f^{\widehat{B}}}{f^{\widehat{A}}} + (1-m)\omega^{\widehat{A}}\frac{f^{\widehat{A}}}{f^{\widehat{A}}}\right) + \\ &\beta S^{\widehat{A}}\left[m\left(\overline{\rho_\sigma}^B(f_m^B - f_m^{\widehat{A}})\frac{f^B}{f^{\widehat{A}}} + \overline{\rho_\sigma\rho_\tau}^{\widehat{B}}(f_m^{\widehat{B}} - f_m^{\widehat{A}})\frac{f^{\widehat{B}}}{f^{\widehat{A}}}\right) + \right. \\ &\left.(1-m)\left(\overline{\rho_\sigma}^A(f_m^A - f_m^{\widehat{A}})\frac{f^A}{f^{\widehat{A}}} + \overline{\rho_\sigma\rho_\tau}^{\widehat{A}}(f_m^{\widehat{A}} - f_m^{\widehat{A}})\frac{f^{\widehat{A}}}{f^{\widehat{A}}}\right)\right]\end{aligned} \tag{4.3}$$

where the variance of the mutant strain in class k is $\omega^k = (1-f_m^k)f_m^k$ and the frequency of naive

infected hosts by the mutant strain is given by $f_m^A = I_m^A/(I_w^A + I_m^A)$ (respectively $f_m^{\widehat{A}}$ for the treated hosts). The $\Delta\rho_x$'s terms express the difference between the mutant and the wild type strains with the different vaccines ($x \in \{\tau, \sigma, \tau\sigma\}$), with the special case of $\Delta\rho_{\tau\sigma}$ that express the difference between the mutant and the wild type strains of the vaccines product. Moreover, the frequencies are all positive or zero, thus, the ω's terms are all positives. Then, the first line can be interpreted as the effect of the natural selection on the frequency of the mutant strain and its sign only depends on the sign of the $\Delta\rho$'s terms. If $\Delta\rho_x > 0$, the mutant frequency increases in the population. On the contrary if $\Delta\rho_x < 0$, the frequency of the mutant decreases. Note that if the mutant strain has the same phenotype as the wild type strain ($e_m = e_w$), all the terms in $\Delta\rho_x$ disappear and only remains the effect of the frequencies of the mutant in the different class of the population.

Moreover, the frequency of the mutant in one class is related to its frequency in all the classes of the population through their differences. It implies that if the mutant frequency is the same in all the classes of the populations, all the $f_m^k - f_m^A$ (or $f_m^k - f_m^{\widehat{A}}$) terms in equation (4.2) disappear, and it only remains the effect of the natural selection.

Without migration ($m = 0$), the expressions (4.2) and (4.3) become

$$\frac{\mathrm{d}f_m^A}{\mathrm{d}t} = \beta S^A \left(\Delta\rho_\tau \omega^{\widehat{A}} \frac{f^{\widehat{A}}}{f^A} + \overline{\rho_\tau}^{\widehat{A}} (f_m^{\widehat{A}} - f_m^A) \frac{f^{\widehat{A}}}{f^A} \right) , \tag{4.4}$$

and

$$\frac{\mathrm{d}f_m^{\widehat{A}}}{\mathrm{d}t} = \beta S^{\widehat{A}} \left(\Delta\rho_\sigma \omega^A \frac{f^A}{f^{\widehat{A}}} + \Delta\rho_{\tau\sigma} \omega^{\widehat{A}} \frac{f^{\widehat{A}}}{f^{\widehat{A}}} \right) + \beta S^{\widehat{A}} \left(\overline{\rho_\sigma}^A (f_m^A - f_m^{\widehat{A}}) \frac{f^A}{f^{\widehat{A}}} + \overline{\rho_\sigma \rho_\tau}^{\widehat{A}} (f_m^{\widehat{A}} - f_m^{\widehat{A}}) \frac{f^{\widehat{A}}}{f^{\widehat{A}}} \right) . \tag{4.5}$$

In this case, there are no movements between the subpopulations and the mutant frequency only depends on the subpopulation in which it initially was. Moreover, without migration we found that our expressions for the vaccine escape mutant in the naive and the treated class are very similar

TABLE 4.1 – Table of notations

Notation	Definition		
f^k	hosts frequency in class k	I^k/I	$k \in \{A, \widehat{A}, B, \widehat{B}\}$
f_i^k	frequency of the strain i in class k	I_i^k/I^k	$i \in \{w, m\}$
f_i	frequency of the strain i in the global population	$\sum_k \sum_i I_i^k/I$	
$f_i^{\textcircled{k}}$	frequency of the strain i in the population k	$\sum_j f_i^j I^j/I^{\textcircled{k}}$	$k \in \{A, B\}$, $j \in \{k, \widehat{k}\}$

to the expressions found by Gandon and Day (2007) with a difference caused by the mutational parameter that we have not.

4.2.2 Vaccine escape mutant dynamic in each population

Secondly, we are interested in following the mutant frequency in each subpopulation. For this purpose, we gather naive and treated hosts of subpopulation k in $\textcircled{k}$. Thus, $f_m^{\textcircled{A}} = (I_m^A + I_m^{\widehat{A}})/\sum_i (I_i^A + I_i^{\widehat{A}})$, represent the vaccine escape mutant frequency in the population A which dynamics is expressed as

$$\begin{aligned}
\frac{\mathrm{d}f_m^{\textcircled{A}}}{\mathrm{d}t} = \frac{I}{f^{\textcircled{A}}} \Big[& \beta S^A \Delta\rho_\tau \left(m\omega^{\widehat{B}} f^{\widehat{B}} + (1-m)\omega^{\widehat{A}} f^{\widehat{A}} \right) + \\
& \beta S^{\widehat{A}} \Delta\rho_\sigma \left(m\omega^B f^B + (1-m)\omega^A f^A \right) + \\
& \beta S^{\widehat{A}} \Delta\rho_{\tau\sigma} \left(m\omega^{\widehat{B}} f^{\widehat{B}} + (1-m)\omega^{\widehat{A}} f^{\widehat{A}} \right) + \\
& \beta S^A \Big[m \left((f_m^B - f_m^A) f^B + \overline{\rho_\tau}^{\widehat{B}} \left(f_m^{\widehat{B}} - f_m^{\textcircled{A}} \right) f^{\widehat{B}} + \left(f_m^A - f_m^{\textcircled{A}} \right) f^B \right) + \\
& \qquad (1-m) \left(\overline{\rho_\tau}^{\widehat{A}} \left(f_m^{\widehat{A}} - f_m^{\textcircled{A}} \right) f^{\widehat{A}} + \left(f_m^A - f_m^{\textcircled{A}} \right) f^A \right) \Big] \\
& \beta S^{\widehat{A}} \Big[m \left(\overline{\rho_\sigma}^B \left(f_m^B - f_m^{\textcircled{A}} \right) f^B + \overline{\rho_\sigma \rho_\tau}^{\widehat{B}} \left(f_m^{\widehat{B}} - f_m^{\textcircled{A}} \right) f^{\widehat{B}} \right) + \\
& \qquad (1-m) \left(\overline{\rho_\sigma}^A \left(f_m^A - f_m^{\textcircled{A}} \right) f^A + \overline{\rho_\sigma \rho_\tau}^{\widehat{A}} \left(f_m^{\widehat{A}} - f_m^{\textcircled{A}} \right) f^{\widehat{A}} \right) \Big] \Big] ,
\end{aligned} \tag{4.6}$$

where $f^{\textcircled{A}} = \sum_i (I_i^A + I_i^{\widehat{A}})$ is the global infected hosts density of population A (see appendix D.3 for the calculation details).

Again we note the effect of the natural selection and of the mutant frequencies in each class on the mutant frequency dynamics.

We can also note that with the use of the vaccine V_σ alone, the mutant frequency in the subpopulation A depends on the transmission by naive infected hosts of both subpopulations to treated susceptible from A. On the contrary, with the vaccine V_τ alone, the mutant frequency only depends on the transmission by the treated of both subpopulations to the naive susceptible from A. It makes sense because V_σ reduces hosts susceptibility and thus affect the infections of treated hosts and V_τ reduce pathogens transmission by treated hosts. With an equal distribution of mutant strain in the metapopulation, the differences in frequencies are zeros and the variations in the mutant frequency can be well explained by natural selection.

Without migration ($m = 0$), the equation (4.6) becomes

$$\begin{aligned}\frac{\mathrm{d}f_m^{\textcircled{A}}}{\mathrm{d}t} = \frac{I}{f^{\textcircled{A}}}\beta S^A \Big[\Big(\Delta\rho_\tau\omega^{\widehat{A}}f^{\widehat{A}} + \Delta\rho_\sigma\omega^A f^A + \Delta\rho_{\tau\sigma}\omega^{\widehat{A}}f^{\widehat{A}}\Big) + \\ \left(1+\overline{\rho_\sigma}^A\right)\left(f_m^A - f_m^{\textcircled{A}}\right)f^A + \left(\overline{\rho_\tau}^{\widehat{A}} + \overline{\rho_\sigma\rho_\tau}^{\widehat{A}}\right)\left(f_m^{\widehat{A}} - f_m^{\textcircled{A}}\right)f^{\widehat{A}}\Big]\,,\end{aligned} \tag{4.7}$$

where the frequency only depends on the subpopulation in which the mutant has initially been introduced.

4.2.3 Vaccine escape mutant dynamic in the metapopulation

Thirdly, we aim to follow the vaccine escape mutant in the whole metapopulation. Again, we can apply the expression developped by Lion (2018*a*) to our model (see appendix D.4 for the calculation details). We obtain the dynamic of f_m, the mutant frequency in the global metapopulation,

as,

$$\begin{aligned}
\frac{\mathrm{d}f_m}{\mathrm{d}t} &= \beta\Delta\rho_\sigma\left[m\left(\omega^B f^B S^{\widehat{A}}+\omega^A f^A S^{\widehat{B}}\right)+(1-m)\left(\omega^A f^A S^{\widehat{A}}+\omega^B f^B S^{\widehat{B}}\right)\right]+\\
&\quad \beta\Delta\rho_\tau\left[m\left(\omega^{\widehat{A}} f^{\widehat{A}} S^B+\omega^{\widehat{B}} f^{\widehat{B}} S^A\right)+(1-m)\left(\omega^{\widehat{A}} f^{\widehat{A}} S^A+\omega^{\widehat{B}} f^{\widehat{B}} S^B\right)\right]+\\
&\quad \beta\Delta\rho_{\tau\sigma}\left[m\left(\omega^{\widehat{A}} f^{\widehat{A}} S^{\widehat{B}}+\omega^{\widehat{B}} f^{\widehat{B}} S^{\widehat{A}}\right)+(1-m)\left(\omega^{\widehat{A}} f^{\widehat{A}} S^{\widehat{A}}+\omega^{\widehat{B}} f^{\widehat{B}} S^{\widehat{B}}\right)\right]+\\
&\quad \beta\left(f_m^A-f_m\right)f^A\left[m\left(S^B+S^{\widehat{B}}\overline{\rho_\sigma}^A\right)+(1-m)\left(S^A+S^{\widehat{A}}\overline{\rho_\sigma}^A\right)\right]+\\
&\quad \beta\left(f_m^{\widehat{A}}-f_m\right)f^{\widehat{A}}\left[m\left(S^B\overline{\rho_\tau}^{\widehat{A}}+S^{\widehat{B}}\overline{\rho_\sigma\rho_\tau}^{\widehat{A}}\right)+(1-m)\left(S^A\overline{\rho_\tau}^{\widehat{A}}+S^{\widehat{A}}\overline{\rho_\sigma\rho_\tau}^{\widehat{A}}\right)\right]+\\
&\quad \beta\left(f_m^B-f_m\right)f^B\left[m\left(S^A+S^{\widehat{A}}\overline{\rho_\sigma}^B\right)+(1-m)\left(S^B+S^{\widehat{B}}\overline{\rho_\sigma}^B\right)\right]+\\
&\quad \beta\left(f_m^{\widehat{B}}-f_m\right)f^{\widehat{B}}\left[m\left(S^A\overline{\rho_\tau}^{\widehat{B}}+S^{\widehat{A}}\overline{\rho_\sigma\rho_\tau}^{\widehat{B}}\right)+(1-m)\left(S^{\widehat{B}}\overline{\rho_\tau}^{\widehat{B}}+S^{\widehat{B}}\overline{\rho_\sigma\rho_\tau}^{\widehat{B}}\right)\right]
\end{aligned}$$

As in the previous expressions, the mutant frequency in the metapopulation depends on the natural selection terms ($\Delta\rho_x$) and of the differences in mutant frequencies in the different classes of the metapopulation. Moreover, for an equal frequency of the mutant in all classes, the frequency of the mutant in the subpopulation only depends on the natural selection terms.

Using the V_τ vaccine alone, all the terms depending on σ are zeros. The equation (4.8) becomes

$$\begin{aligned}
\frac{\mathrm{d}f_m}{\mathrm{d}t} &= \beta\Delta\rho_\tau\left[m\left(\omega^{\widehat{A}} f^{\widehat{A}} S^B+\omega^{\widehat{B}} f^{\widehat{B}} S^A\right)+(1-m)\left(\omega^{\widehat{A}} f^{\widehat{A}} S^A+\omega^{\widehat{B}} f^{\widehat{B}} S^B\right)\right]+\\
&\quad \beta\left(f_m^A-f_m\right)f^A\left[mS^B+(1-m)S^A\right]+\\
&\quad \beta\left(f_m^{\widehat{A}}-f_m\right)f^{\widehat{A}}\left[mS^B\overline{\rho_\tau}^{\widehat{A}}+(1-m)S^A\overline{\rho_\tau}^{\widehat{A}}\right]+\\
&\quad \beta\left(f_m^B-f_m\right)f^B\left[mS^A+(1-m)S^B\right]+\\
&\quad \beta\left(f_m^{\widehat{B}}-f_m\right)f^{\widehat{B}}\left[mS^A\overline{\rho_\tau}^{\widehat{B}}+(1-m)S^{\widehat{B}}\overline{\rho_\tau}^{\widehat{B}}\right]
\end{aligned} \tag{4.8}$$

where the mutant frequency in the global population only depends the infection of susceptible hosts from the naive class by infected hosts from the treated class.

On the contrary, using the V_σ vaccine alone, all the terms depending on τ are zeros. The

equation (4.8) becomes

$$\begin{aligned}\frac{\mathrm{d}f_m}{\mathrm{d}t} &= \beta\Delta\rho_\sigma\left[m\left(\omega^B f^B S^{\widehat{A}}+\omega^A f^A S^{\widehat{B}}\right)+(1-m)\left(\omega^A f^A S^{\widehat{A}}+\omega^B f^B S^{\widehat{B}}\right)\right]+\\ &\quad \beta\left(f_m^A-f_m\right)f^A\left[m\left(S^B+S^{\widehat{B}}\overline{\rho_\sigma}^A\right)+(1-m)\left(S^A+S^{\widehat{A}}\overline{\rho_\sigma}^A\right)\right]+\\ &\quad \beta\left(f_m^B-f_m\right)f^B\left[m\left(S^A+S^{\widehat{A}}\overline{\rho_\sigma}^B\right)+(1-m)\left(S^B+S^{\widehat{B}}\overline{\rho_\sigma}^B\right)\right]\end{aligned} \tag{4.9}$$

where the mutant frequency in the global metapopulation depends on the infection of susceptible hosts from the treated class by infected hosts from the naive class.

Without migration ($m = 0$), the equation (4.8) becomes

$$\begin{aligned}\frac{\mathrm{d}f_m}{\mathrm{d}t} &= \beta\left(\Delta\rho_\sigma\left(\omega^A f^A S^{\widehat{A}}+\omega^B f^B S^{\widehat{B}}\right)+\Delta\rho_\tau\left(\omega^{\widehat{A}} f^{\widehat{A}} S^A+\omega^{\widehat{B}} f^{\widehat{B}} S^B\right)+\Delta\rho_{\tau\sigma}\left(\omega^{\widehat{A}} f^{\widehat{A}} S^{\widehat{A}}+\omega^{\widehat{B}} f^{\widehat{B}} S^{\widehat{B}}\right)\right)+\\ &\quad \beta\left(f_m^A-f_m\right)f^A\left[\left(S^A+S^{\widehat{A}}\overline{\rho_\sigma}^A\right)\right]+\beta\left(f_m^{\widehat{A}}-f_m\right)f^{\widehat{A}}\left[\left(S^A\overline{\rho_\tau}^{\widehat{A}}+S^{\widehat{A}}\overline{\rho_\sigma\rho_\tau}^{\widehat{A}}\right)\right]+\\ &\quad \beta\left(f_m^B-f_m\right)f^B\left[\left(S^B+S^{\widehat{B}}\overline{\rho_\sigma}^B\right)\right]+\beta\left(f_m^{\widehat{B}}-f_m\right)f^{\widehat{B}}\left[\left(S^{\widehat{B}}\overline{\rho_\tau}^{\widehat{B}}+S^{\widehat{B}}\overline{\rho_\sigma\rho_\tau}^{\widehat{B}}\right)\right].\end{aligned} \tag{4.10}$$

4.3 Application

We explore here a scenario were the subpopulations A and B have different vaccine coverages. We assume that 90% of the subpopulation A is vaccinated at birth while only 10% of the subpopulation B is vaccinated at birth. These two populations are either fully connected ($m = 0.5$) or very poorly connected ($m = 0.01$). The equations of the model are depicted in equation (4.1) and the life cycle presented in figure 4.1.

In figure 4.3 we present the speed of the mutant adaptation in the all the different classes of the population with the V_σ vaccine. Note that the qualitative effects with the V_τ vaccine are the same as with the V_σ, but the vaccine escape emergence is delayed with V_τ (see appendix D.5).

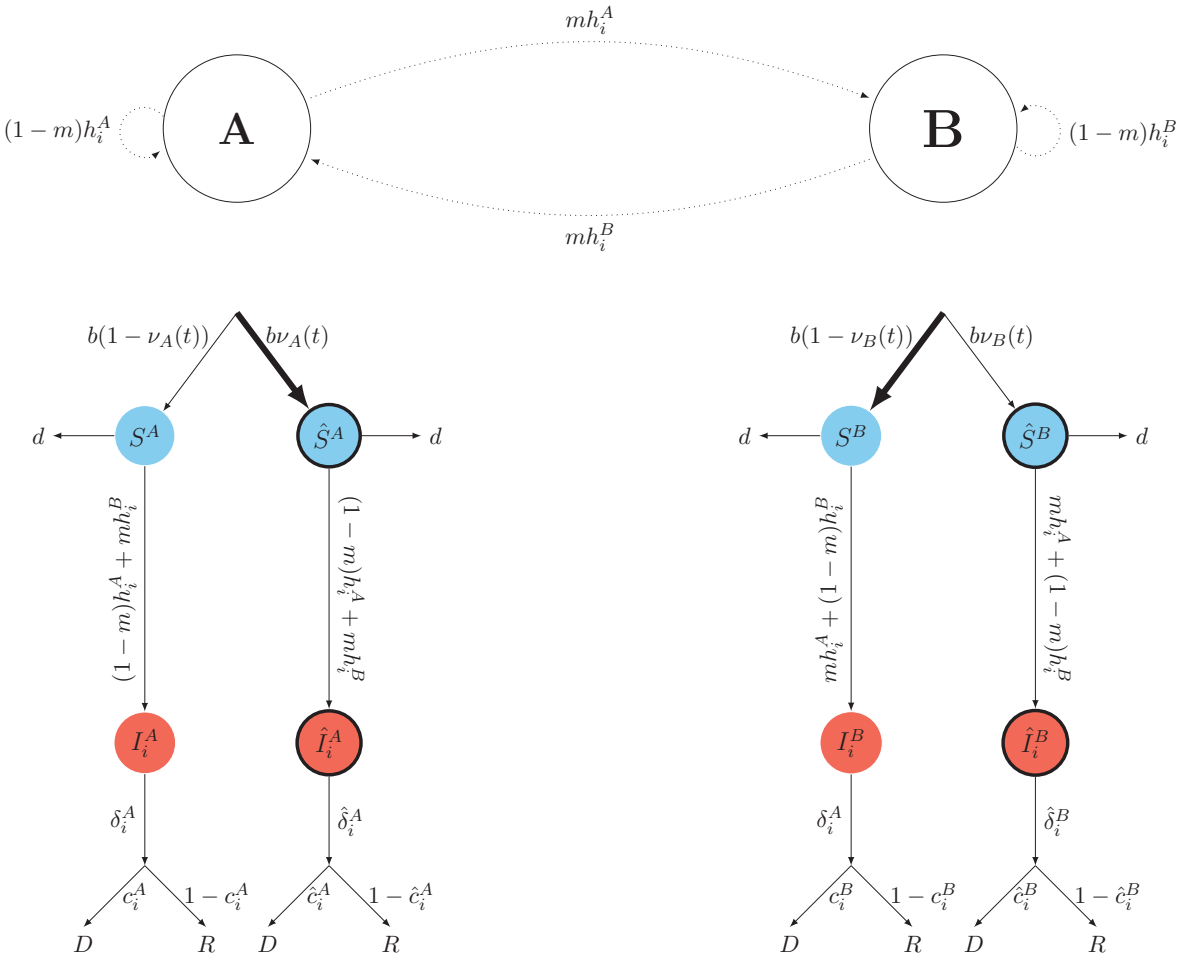

FIGURE 4.1 – Life-cycle of the host-pathogen interaction showing the transition rates between classes in the metapopulation.

First, we note that vaccine coverage affects the speed of adaptation. Indeed, the mutant emerges faster in highly vaccinated population than in poorly vaccinated population (figure 4.2 and 4.3). Second, in a fully connected metapopulation, the mutant frequencies in the different classes tend to be homogenized over the whole population (figure 4.3, right panels). Third, with a low migration, we see that the frequency of the mutant in the global population, f_m, increases in two phases. During a first phase it increases as the mutant becomes predominant in the most treated subpopulation (here A). During a second phase f_m increases with the mutant frequency in the lowly vaccinated population (here B). Fifth and final, it seems that the mutant emergence is delayed in highly connected subpopulations but invade the whole metapopulation faster compared to lowly connected subpopulation where the mutant appears sooner but is longer to invade the whole population (see figure 4.4).

4.4 Discussion and perspectives

In this chapter we have expressed the frequency dynamic of an escape mutant in different layers of a metapopulation. First, among each class of hosts, second, among each subpopulation and finally in the whole metapopulation. Our preliminary simulations highlight the range of possible results we can obtain with our model. We have explored a metapopulation with different coverage between the subpopulations coupled with a high parasite migration or a low parasite migration. We have seen that the frequency of the vaccine escape mutant increases faster in highly vaccinated population than lowly vaccinated. However, this phenomenon can be compensated by the migration that slows down the mutant emergence in the most vaccinated population and speeds it up in the less vaccinated. If we interpret the migration as the opening and border closure between population, it seems that an almost complete closure yields the vaccine escape mutant to emerge faster than a full opening, but would be longer to invade the whole population.

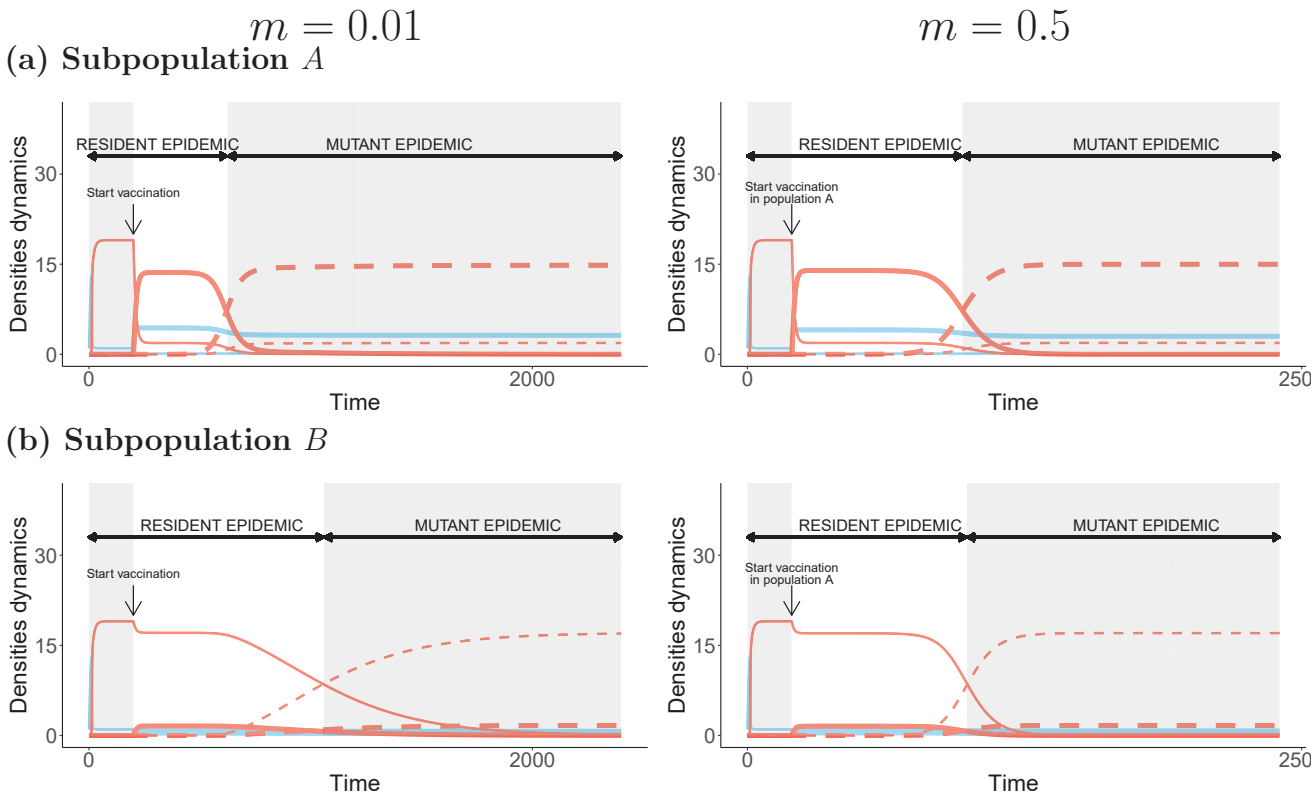

FIGURE 4.2 – Dynamics of the densities with a low migration ($m = 0.01$, left panels) or a full migration ($m = 0.5$, right panels) of hosts. We present in red solid lines, the infected hosts by the resident strain, in red dashed lines the infected hosts by the mutant strain, in blue the susceptible hosts and in thin lines the naive versus the treated in thick lines, with the V_σ vaccine. Here $b = 2$, $d = 1$, $\beta = 0.1$, $\Delta\rho = 0.1$, $c = 0$, $r_\sigma = 0.8$, $e_w = 0$, $e_m = 0.1$ $\nu_A = 0.9$, $\nu_B = 0.1$ and the vaccination starts at $t = 200$

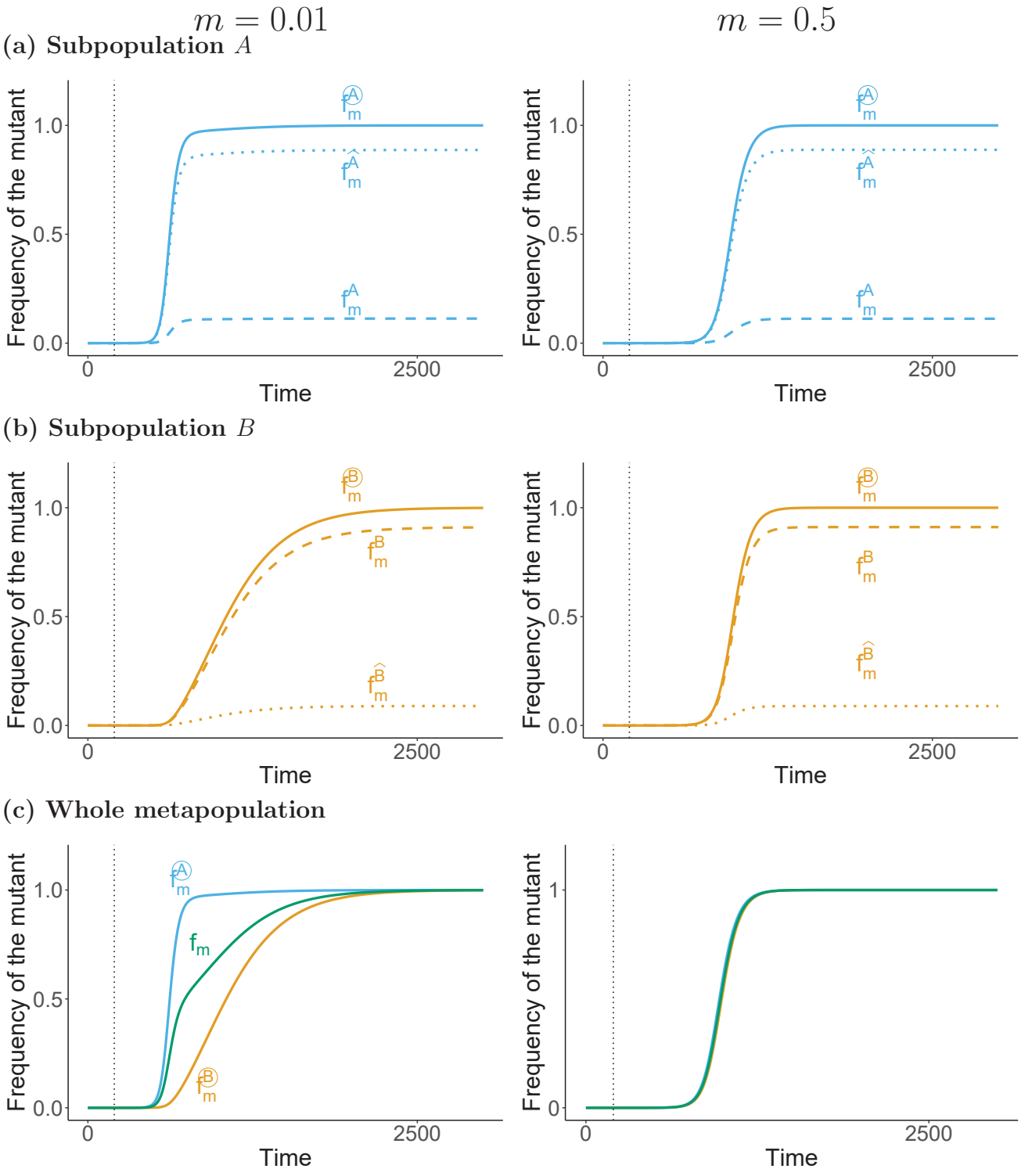

FIGURE 4.3 – Vaccine escape mutant frequency with a low migration ($m = 0.01$, left panels) or a high migration ($m = 0.5$, right panels) in (a) the subpopulation A, (b) the subpopulation B and (c) the whole metapopulation, with the V_σ vaccine. The mutant frequency in the subpopulation A is showed in blue, in the subpopulation B in orange, and the global frequency in green. The dotted lines represent the frequency in the treated hosts, the dashed lines represent the frequency in the naive hosts and the solid lines represent the frequency in the population. Here $m = 0.01$ and the parameter values as in figure 4.2. The vaccination starts at $t = 200$ (dotted black line).

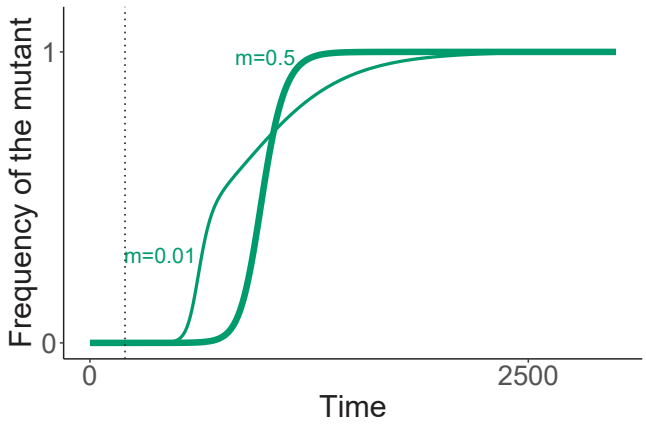

FIGURE 4.4 – Vaccine escape mutant frequency in the global metapopulation (f_m) with a full migration (thick green line, $m = 0.5$) or a low migration (in thin green line, $m = 0.01$), with the V_σ vaccine and the parameter values as in figure 4.2. The vaccination starts at $t = 200$ (dotted black line).

These numerical results are just one sample of all the different situations and of the many scenarios that we could model. For instance, in the SARS-CoV-2 pandemic we have seen differences in the start of vaccination, in the speed of vaccination and in differences in the coverage. Moreover, the successive lock downs or closure and opening of frontiers have affected pathogens transmission and we could use our model to explore how all of these events could affect the speed of emergence of a vaccine escape mutant. In particular, Kortessis et al. (2020) study the spatio temporal variations in pathogens transmission caused by asynchronous measures control. Indeed, different measures to control the pandemic have sometime been taken in different places at a different time, which undoubtedly affect the transmission of the virus. The authors have studied a similar two populations model with asynchronous measures, and have shown that the prevalence increase with the asynchrony. It would be interesting to study the effect of such asynchronous control measures on the speed of a mutant emergence.

Moreover, in our model we consider that there is no cost of being a mutant. Indeed, the mutant invades better the treated hosts than the wild type, but they both invade the naive the same way. One may consider the mutant as a generalist strain while the wild-type would be more

of a specialist. We could imagine scenarios where it would be costly to be a mutant or on the contrary, it would be even more beneficial with a better fitness in naive hosts too.

We have highlighted the effect of the natural selection and of the mutant frequency in the different classes of the metapopulation, on the dynamics of the mutant frequency. However, we note that the mutant frequency dynamic is affected by the different frequencies of the mutant in the different classes of the population. These frequency difference terms could be approximated with reproductive values, that would be a very good approximation in weak selection (Lion, 2018*a*,*b*). These approximations would allow for a better understanding of the effect of the mutant frequencies in the different classes on the global mutant frequency. Moreover, the dynamics of the differentiation $\left(\mathrm{d}f_m^{\textcircled{A}} - f_m^{\textcircled{B}}/\mathrm{d}t \text{ for instance}\right)$ could explain the variations in the speed of adaptation of a vaccine escape mutant among the subpopulations.

To conclude, we have built a theoretical framework to understand the speed of vaccine-escape variant emergence, that can be extended to fit to several situations inspired by the Covid-19 pandemic for instance.

Chapitre 5

Discussion générale

L'hétérogénéité des hôtes affecte la transmission des pathogènes dans les populations (Dwyer et al., 1997) ainsi que leur évolution à court- et long- terme (Regoes et al., 2000). Dans ce travail de thèse, nous avons considéré que l'hétérogénéité des hôtes pouvait varier à la fois dans le temps et dans l'espace. Ces variations spatio-temporelles de l'hétérogénéité des hôtes impliquent une variation périodique de la qualité de l'habitat des pathogènes, ce qui affecte l'épidémiologie et l'évolution. L'objectif de ce travail est de fournir des méthodes théoriques pour étudier et comprendre l'impact de l'hétérogénéité temporelle et spatiale de l'environnement des pathogènes, sur l'évolution des traits d'histoire de vie des pathogènes et de l'échappement aux traitements. Nous discuterons, dans un premier temps, des principaux résultats obtenus dans les différents chapitres, puis nous proposerons des applications concrètes à ces résultats théoriques, et enfin, nous suggérerons quelques perspectives pour poursuivre ce travail.

5.1 Synthèse des résultats

Dans les modèles que nous avons développés, les hôtes diffèrent les uns des autres selon qu'ils aient été traités ou non. En fonction du type de traitement utilisé, les pathogènes subissent une réduction de leur transmission (via la susceptibilité des hôtes ou leur capacité à transmettre le pathogène), de leur virulence ou des deux à la fois, lorsqu'ils exploitent un hôte traité. Du point de vue du pathogène, l'hôte représente son habitat et son environnement, et le problème est d'exploiter de façon optimale cette ressource hétérogène, avec des habitats de qualité variable.

5.1.1 Hétérogénéité d'hôtes

Dans ce travail, nous avons étudié deux manières différentes de créer de l'hétérogénéité chez les hôtes, dont la qualité varie dans le temps ou dans l'espace. Dans les deux cas le pathogène change d'habitat pour passer d'un bon habitat à un mauvais habitat, et inversement. Dans le cas

d'une hétérogénéité temporelle, le pathogène ne se déplace pas, c'est la qualité des habitats qui change dans le temps. Dans le cas d'une hétérogénéité spatiale, le pathogène se déplace entre deux habitats de qualités différentes.

Nous utilisons différents paramètres pour caractériser les hétérogénéité spatio-temporelles des hôtes. L'hétérogénéité temporelle est caractérisée par la période, T, et la proportion de la période qui est traitée, p, ou non traitée, $1-p$. L'hétérogénéité spatiale est caractérisée par la migration entre deux sous-populations, m, et la différence de couverture entre ces deux sous-populations δ. Dans les deux cas, nous nous concentrons sur une couverture moyenne en traitement de 50% des hôtes. Ainsi, les paramètres p et δ impactent la couverture moyenne des traitements dans la population ou métapopulation. Ils permettent donc de quantifier l'habitat moyen que le pathogène exploite. Les paramètres T et m, modifient le temps que le pathogène passe dans les différents habitats. Ils quantifient ainsi le niveau de l'hétérogénéité. Lorsque le pathogène reste longtemps dans le même habitat (période longue ou migration faible), l'hétérogénéité peut être qualifiée de forte. Au contraire, lorsque le pathogène change très rapidement de milieu (période courte ou migration importante), l'hétérogénéité peut être qualifiée de faible. Dans le cas d'une hétérogénéité faible, les différences d'habitats sont homogénéisées.

Ainsi, nous pourrions intuitivement penser que les paramètres T et m, ont des effets similaires sur l'évolution à long-terme des pathogènes. Certains résultats vont en ce sens. Nous observons des valeurs de virulence évolutivement stable plus élevées sur le long-terme avec une période courte plutôt que longue, et avec une migration forte plutôt que faible. A l'inverse, nos résultats montrent aussi que plus la période est grande, plus la virulence sélectionnée sur le long terme est faible, jusqu'à une valeur seuil. En revanche, pour une migration faible, nous observons soit de la bistabilité soit des points de branchements. Dans le cas de la bistabilité, l'évolution peut conduire soit à des valeurs élevées, soit à des valeurs faibles de virulence en fonction de la valeur initiale de virulence. Dans le cas des points de branchements, deux souches spécialistes peuvent

coexister. Ainsi, les paramètres qui caractérisent le niveau de l'hétérogénéité, m et T, ne semblent pas avoir les mêmes effets sur l'évolution à long terme. Cela appelle des études complémentaires pour construire un cadre théorique qui permette de mieux comprendre l'impact de ces différents types d'hétérogénéités sur l'évolution.

5.1.2 Des habitats de bonne ou de mauvaise qualité

La variabilité spatio-temporelle dans la couverture des traitements implique une variation spatio-temporelle de la qualité de l'habitat des pathogènes. Le pathogène se retrouve successivement dans un habitat de bonne ou de mauvaise qualité. Dans cette étude, la qualité de l'habitat du pathogène dépend du statut traité ou non traité de son hôte. En fonction des traitements, le bon habitat peut correspondre à un hôte traité ou non traité. En effet, le traitement anti-toxine augmente la durée de l'infection en diminuant la mortalité des hôtes, c'est donc un bon habitat pour le pathogène. Au contraire, les traitements anti-infection, anti-croissance et anti-transmission diminuent la reproduction du pathogène et représentent donc des mauvais habitats pour le pathogène. Nous avons quantifié la qualité de ces habitats avec les valeurs reproductives de classes, et nous avons comparé ces valeurs dans des habitats constants ou variables. Dans le second chapitre, où la qualité des habitats varie dans le temps, nous avons calculé des valeurs reproductives par classe d'hôtes (naïfs ou traités), qui nous ont permis de pondérer le gradient de sélection. Dans le troisième chapitre, nous avons calculé des valeurs reproductives de classes par sous-population (A ou B), avec chaque sous-population qui contient des hôtes naïfs et traités en différentes proportions (Gandon and Lion, 2021).

Dans le cas d'une variation temporelle de l'hétérogénéité des habitats (chapitre 2), nous avons montré que la valeur reproductive de la classe traitée ($c_T(t)$) suivait les variations de qualité de l'habitat, en oscillant autour de la valeur reproductive de la classe traitée dans le cas constant, sans variations temporelles (c_T^e). Ainsi, plus l'alternance des habitats est rapide, moins le pathogène

ressent les changements de son habitat, et plus la qualité moyenne sur une période de la classe traitée ($\langle c_T(t) \rangle$) est proche de la qualité de l'habitat traité sans variation temporelle, $\langle c_T(t) \rangle \approx c_T^e$. A l'inverse, plus l'alternance est longue entre les deux habitats, plus le pathogène ressent les variations de son environnement, et plus la qualité moyenne sur une période s'éloigne du cas constant pour se rapprocher de la qualité moyenne de son environnement (dans nos résultats, $\langle c_T(t) \rangle \approx \overline{\nu} = 0.5$). De la même manière, sur une période très longue, la qualité de l'habitat naïf se rapproche de la qualité moyenne de l'environnement (dans nos résultats, $\langle c_N(t) \rangle \approx \overline{\nu} = 0.5$) (Lion and Gandon, 2021). Ainsi, si l'habitat des pathogènes change lentement, la qualité du bon habitat diminue et la qualité du mauvais habitat augmente pour converger vers la qualité moyenne de l'environnement. De cette manière, il n'y a plus vraiment de bon ou de mauvais habitat pour le pathogène, et nous pouvons supposer dans ce cas que le pathogène devient généraliste et exploite ses différents habitats de la même manière.

Dans le cas d'une variation spatiale de l'hétérogénéité des habitats (chapitre 3), nous avons sensiblement les mêmes résultats. En effet, plus la migration est faible, plus la qualité de chaque sous-population est proche de la qualité d'une unique population de couverture équivalente. Dans ce cas, nous avons montré que deux souches spécialistes de chaque habitat, peuvent coexister dans la métapopulation. En revanche, plus la migration augmente, plus le pathogène ressent les différences entre les habitats qu'il exploite, et plus les valeurs reproductives de chaque sous-population convergent vers la qualité moyenne de l'habitat (dans nos résultats, $c_A \approx c_B \approx \overline{\nu} = 0.5$).

Ainsi, il semblerait que la vitesse de variation des habitats ait un effet différent dans le cas d'une hétérogénéité temporelle ou spatiale sur l'évolution des pathogènes. D'une part, une alternance temporelle très rapide de l'habitat ou une migration du pathogène faible entre les deux habitats, maintiennent les hétérogénéités de qualité des habitats (un bon et un mauvais). En particulier, dans le cas d'une hétérogénéité spatiale, nous avons montré la coexistence possible de deux souches spécialistes ou d'une seule souche généraliste en fonction du taux de migration entre

les sous-populations (Meszéna et al., 1997; Ronce and Kirkpatrick, 2001; Débarre et al., 2013; Mirrahimi and Gandon, 2020). D'autre part, une alternance temporelle très lente des habitats ou une migration très forte entre les deux habitats aboutissent à homogénéisation des différentes qualités d'habitats, que le pathogène exploite de la même manière. Ces résultats ne sont pas forcément intuitifs, et des recherches supplémentaires sont nécessaires pour mieux comprendre et expliquer l'effet de différents types d'hétérogénéités sur les qualités des habitats pour les pathogènes.

Il serait intéressant d'étendre cette approche par les valeurs reproductives au modèle étudié dans le chapitre 4. Nous pourrions ainsi exprimer la dynamique de la fréquence du mutant dans la métapopulation en fonction des valeurs reproductives de classes (naïfs ou traités) ou de sous-populations (A ou B). Cela nous permettrait de mieux comprendre les effets d'habitats hétérogènes sur l'évolution des pathogènes, et notamment sur la vitesse d'émergence d'un mutant d'échappement.

5.1.3 Évolution à court et long-terme

Dans ce travail nous avons étudié l'évolution des pathogènes à différentes échelles de temps. D'abord, l'évolution de la virulence des pathogènes à long-terme, puis l'évolution d'un trait de résistance (échappement au vaccin) à court-terme. En effet, la pandémie de Covid-19 témoigne que l'étude à court terme des conséquences épidémiologiques et évolutives est nécessaire dans la gestion rapide des épidémies. Cependant les études à long terme sont aussi essentielles afin de choisir des traitements qui auraient des conséquences positives sur le court-terme, en minimisant les conséquences négatives sur le long-terme. Ces deux approches sont donc complémentaires.

De manière générale, dans les modèles que nous avons développés, les traitements réduisant la transmission des pathogènes, semblent plus bénéfiques à la fois sur le court-terme (diminution de la prévalence) et sur le long-terme (pas d'effet évolutif). De plus, les infections multiples peuvent

amplifier l'effet positif en diminuant la virulence, comme montré par Gandon et al. (2001*b*), mais restent à démontrer dans le cas d'habitats hétérogènes dans le temps et dans l'espace. A l'inverse, les traitements diminuant la virulence semblent être néfastes en santé publique sur le court-terme (augmentation de la prévalence) et sur le long-terme (augmentation de la virulence), malgré leurs effets bénéfiques en santé individuelle (diminution de la mortalité).

5.2 Applications des résultats

Les résultats de ce travail théorique ont des implications concrètes, en fournissant des hypothèses sur les différentes stratégies de distribution des traitements à explorer expérimentalement. Afin d'explorer ces implications, nous avons choisi de développer un exemple en agriculture. Cependant ce travail peut aussi être appliqué à la gestion de la santé animale en élevage et à la santé publique.

5.2.1 Un champs de maïs

Imaginons une culture de plantes annuelles, par exemple, un champ de maïs. Dans ce champ, les semences sont traitées chaque année en amont de la plantation pour les protéger des pathogènes. Il existe alors plusieurs stratégies de traitements des semences notamment, (i) traiter toutes les semences tous les ans, (ii) traiter la moitié des semences tous les ans, (iii) traiter la moitié des semences une année sur deux, ou encore (iv) traiter toutes les semences une année sur deux.

Les stratégies (i) de traiter toutes les semences tous les ans ou (ii) de traiter la moitié des semences tous les ans, s'apparentent dans notre étude à une distribution constante ($p = 1$) et maximale ($\nu = 1$) ou moyenne ($\nu = 0.5$) des traitements. Nos résultats ont montré que cette stratégie peut sélectionner des souches plus virulentes en fonction du type de traitement utilisé, mais également qu'un mutant d'échappement peut rapidement apparaître. Cependant, si tous les hôtes de la population sont traités et ne meurent pas des suites de la maladie, la population d'hôtes

se maintient et résiste à l'augmentation graduelle de la virulence. Cette sélection pour des souches plus virulentes peut avoir des graves conséquences sur les champs voisins, qui pourraient avoir adopté une autre stratégie de traitement, et qui ne pourraient pas résister à l'apparition d'une souche très virulente. De plus, la virulence peut évoluer jusqu'à ce que l'immunité conférée aux hôtes traités soit contournée, comme observé pour la maladie de Marek (Read et al., 2015; Miller and Metcalf, 2019).

Les stratégies (iii) de traiter la moitié des semences ou (iv) toutes les semences une année sur deux s'apparentent à une distribution périodique ($p = 0.5$), dont la couverture moyenne serait de $\overline{\nu} = 0.25$ ou $\overline{\nu} = 0.5$. Nos résultats ont montré qu'une distribution périodique des traitements permettait de diminuer à la fois la prévalence du pathogène dans la population, et la virulence sélectionnée sur le long terme. Cette diminution étant maximale lorsque les périodes traitées et non traitées sont équivalentes.

Ainsi, traiter les semences une année sur deux peut permettre de diminuer la virulence et la prévalence des pathogènes. Cependant, dans cet exemple l'hôte n'est présent qu'une partie de l'année, et est ensuite récolté. Dans notre étude nous ne prenons pas en compte ce phénomène qui peut avoir un impact épidémiologique ou évolutif. L'effet de l'absence périodique de l'hôte sur l'évolution est encore discuté dans la littérature. Dans van den Berg et al. (2010) les auteurs ont montré que l'absence de l'hôte n'aboutit pas à un branchement évolutif. A l'inverse, (Hamelin et al., 2011) ont montré que l'absence périodique de l'hôte peut aboutir à la coexistence de deux souches. La coexistence de plusieurs souches peut avoir des conséquences sur les hôtes si une souche est beaucoup plus virulente que l'autre par exemple. La cyclicité dans la présence de l'hôte est une autre manière de caractériser la variation temporelle de l'hétérogénéité des hôtes. Nous pouvons interpréter la présence de l'hôte comme un bon habitat et l'absence de l'hôte comme un mauvais habitat. Cette cyclicité peut être intégrée à nos modèles pour comparer l'impact de ces deux hétérogénéités temporelles d'hôtes différentes sur l'évolution des pathogènes.

5.2.2 Deux champs de maïs

Reprenons l'exemple du champ de maïs, mais en considérant cette fois-ci deux champs de maïs, suffisamment proches pour que des pathogènes puissent migrer d'un champ à l'autre. De nouveau, plusieurs stratégies de traitement peuvent être mises en place, notamment : (i) traiter les semences des deux champs de manière identique, (ii) traiter les semences d'un seul champ ou (iii) traiter plus de semences dans un champ que dans l'autre. Nous pouvons alors nous interroger sur la meilleure stratégie de traitement de ces champs pour la gestion des épidémies.

La stratégie (i) de traiter les semences des deux champs de la même manière s'apparente à la situation où $\delta = 0$. Le pathogène va migrer entre les deux populations qui sont similaires en termes d'hôtes. Ces deux populations n'en formeraient finalement qu'une seule. Dans ce cas, nous pouvons nous référer aux conclusions précédentes, où nous ne considérions qu'un seul champ de maïs.

Les stratégies (ii) de traiter les semences d'un seul champ et pas de l'autre ou (iii) de traiter les semences d'un champ plus que l'autre, s'apparentent à la situation où $\delta \neq 0$. Dans ce cas, il est difficile de prédire l'issue de l'évolution, qui va dépendre du taux de migration du pathogène. Si le pathogène migre beaucoup entre les deux populations, la sélection peut favoriser des souches plus virulentes en fonction du mode d'action du traitement utilisé, et un mutant d'échappement au traitement peut rapidement envahir ces deux champs. A l'inverse, si le pathogène migre peu, la sélection peut favoriser soit une souche très virulente, soit une souche peu virulente soit la coexistence des deux. De plus, nous avons montré qu'un faible taux de migration peut provoquer l'apparition précoce d'un mutant d'échappement dans le champ le plus traité.

Nous pouvons aussi imaginer une situation où un champ serait traité une année et l'autre champ serait traité l'année suivante, et ainsi de suite d'années en années. Tel que nous avons construit notre modèle, les résultats devraient être similaires à ceux obtenus dans une situation

où un champ est complètement traité et l'autre pas du tout, sans alternance entre les deux. Cependant, si nous imaginons que ces deux champs sont de variétés différentes, mais pouvant être infectés par le même pathogène (un champ de maïs et un champ de blé par exemple). Nous pouvons imaginer que la variété du champ affecterait les traits d'histoire de vie du pathogène, qui seraient différents dans un épi de maïs traité ou dans un épi de blé traité. Ainsi, traiter le champ de maïs une année et le champ de blé l'année suivante pourrait, influencer l'issue de l'évolution et de l'épidémie.

5.2.3 n champs de maïs

Imaginons maintenant une surface agricole composée de n champs de maïs où les pathogènes peuvent migrer d'un champ à l'autre. Les mêmes questions de stratégies de distribution de traitements à adopter se posent. Nous pourrions imaginer un modèle de métapopulation à n populations toutes reliées par le taux de migration du pathogène. Toutefois, un tel modèle ne prendrait pas en compte les différences d'échelle de migration du pathogène. En effet, un pathogène peut migrer dans les champs voisins (migration locale) ou migrer pour infecter des champs plus lointains (migration globale). Ces processus d'infections locales et globales sont pris en compte dans des modèles spatiaux plus complexes (en réseau, *lattice*, comme dans Boots and Sasaki (1999); Débarre et al. (2011); Lion and Gandon (2015); Zurita-Gutiérrez and Lion (2015)). Le développement de ce type de modèles peut être intéressant pour étudier l'impact de variations spatio-temporelles dans la qualité des habitats sur l'épidémiologie et l'évolution des pathogènes, quand un grand nombre de populations sont connectées avec un pathogène qui peut migrer à échelle locale ou globale.

5.3 Limites et perspectives

Les phénomènes naturels observés sont complexes et ne peuvent pas être retranscrit à l'identique dans les modèles. Il est donc nécessaire de formuler des hypothèses pour simplifier ces phénomènes et en faciliter l'étude. Ce travail a nécessité des simplifications reposant sur plusieurs hypothèses qu'ils convient de discuter.

5.3.1 Une vaccination plus tardive

Une hypothèse forte de nos trois modèles est que le traitement est uniquement distribué à la naissance ou à l'arrivée dans la population. Cette hypothèse a été faite afin de faciliter la compréhension avec des travaux précédents (Gandon et al., 2001*b*, 2003, 2001*b*; Zurita-Gutiérrez and Lion, 2015). Biologiquement, cela correspond plutôt à des maladies dont la vaccination se fait à la naissance ou quelques mois plus tard, comme par exemple, le pré-traitement de semences en agriculture, les vaccins contre le tétanos chez l'homme ou le vaccin contre la maladie de Marek chez les poules. Cela peut aussi correspondre à une vaccination à l'arrivée dans une population, comme le vaccin contre la fièvre jaune pour se rendre dans certains pays d'Amérique du Sud et d'Afrique. Cependant, les hôtes sont parfois traités à l'âge adulte. Dans le cadre par exemple de la pandémie de Covid-19, ce sont les adultes qui sont principalement vaccinés. C'est également le cas dans les élevages, où les antibiotiques sont parfois distribués dans la nourriture. Il pourrait être intéressant et simple techniquement de modifier nos modèles pour mettre en place une vaccination des adultes, pour se rapprocher au maximum de ces situations, en développant des modèles structurés en âge par exemple.

5.3.2 Mutant d'échappement et fluctuation temporelle

Le modèle développé dans le chapitre 4 caractérise la vitesse d'émergence d'un mutant d'échappement au vaccin dans une métapopulation. Ce modèle pourrait être étendu et adapté pour s'appliquer à plusieurs scénarios inspirés de la pandémie de Covid-19 et de sa gestion dans les différents pays. Dans Kortessis et al. (2020), les auteurs ont par exemple développé un modèle pour quantifier l'impact de mesures de contrôles asynchrone (tels que les confinements), qui affectent la transmission du SARS-CoV-2, sur la prévalence du virus. Il pourrait être intéressant de quantifier l'effet de cette asynchronie sur la vitesse d'apparition d'un mutant d'échappement grâce à notre modèle. De plus, ce scénario permettrait de prendre en compte une fluctuation temporelle de l'épidémie, et viendrait compléter le cadre théorique de l'évolution de la virulence et de mutants d'échappements, dans des environnements qui varient dans le temps et dans l'espace.

5.3.3 Application expérimentales

Enfin, certaines des hypothèses de nos modèles pourraient être testées expérimentalement. Les interactions bactéries-phages représentent une interaction hôte-pathogène bien adaptées à l'étude en environnement hétérogène (Berngruber et al., 2013; Chabas et al., 2018). La plante *Arabidopsis thaliana* est également un hôte adapté aux études expérimentales du fait de son cycle de vie court et de la facilité technique de mesures de la production de graines pour la plante ou spores pour le champignon pathogène (Tian et al., 2003; Brown and Tellier, 2011). Nous pourrions imaginer des expérimentations d'une ou deux populations, plus ou moins connectées, où les proportions d'hôtes traités et non traités varient au cours du temps et/ou dans l'espace, pour mettre en évidence les effets de l'hétérogénéité spatio-temporelles des traitements sur l'évolution des pathogènes à court- et long-terme.

Annexes

Annexe A: Version du Chapitre 2 publiée dans *Proceedings of The Royal Society B*

PROCEEDINGS B

royalsocietypublishing.org/journal/rspb

Research

Cite this article: Walter A, Lion S. 2021 Epidemiological and evolutionary consequences of periodicity in treatment coverage. *Proc. R. Soc. B* **288**: 20203007.
https://doi.org/10.1098/rspb.2020.3007

Received: 2 December 2020
Accepted: 15 February 2021

Subject Category:
Evolution

Subject Areas:
evolution, theoretical biology, health and disease and epidemiology

Keywords:
evolution of virulence, host heterogeneity, periodicity, treatments, vaccines, reproductive value

Author for correspondence:
Alicia Walter
e-mail: alicia.walter@cefe.cnrs.fr

Electronic supplementary material is available online at https://doi.org/10.6084/m9.figshare.c.5320318.

THE ROYAL SOCIETY PUBLISHING

Epidemiological and evolutionary consequences of periodicity in treatment coverage

Alicia Walter and Sébastien Lion

CEFE, CNRS, Univ Montpellier, EPHE, IRD, Univ Paul Valéry Montpellier 3. 1919, route de Mende, Montpellier, France

AW, 0000-0002-7334-0247; SL, 0000-0002-4081-0038

Host heterogeneity is a key driver of host–pathogen dynamics. In particular, the use of treatments against infectious diseases creates variation in quality among hosts, which can have both epidemiological and evolutionary consequences. We present a general theoretical model to highlight the consequences of different imperfect treatments on pathogen prevalence and evolution. These treatments differ in their action on host and pathogen traits. In contrast with previous studies, we assume that treatment coverage can vary in time, as in seasonal or pulsed treatment strategies. We show that periodic treatment strategies can limit both disease spread and virulence evolution, depending on the type of treatment. We also introduce a new method to analytically calculate the selection gradient in periodic environments, which allows our predictions to be interpreted using the concept of reproductive value, and can be applied more generally to analyse eco-evolutionary dynamics in class-structured populations and fluctuating environments.

1. Introduction

Parasites are an ubiquitous threat to plant, animal and human populations. This has led to the development of numerous pre- and post-infection treatments, which play a central role in the fight against infectious diseases. At a fundamental level, this has also motivated a long line of research in epidemiology to devise control measures that can limit the potentially dramatic effects of epidemics for animal and plant species [1,2]. A key driver of this theoretical work is to find the optimal strategy to deploy treatments in order to maximize the short-term (epidemiological) benefits of treatments while mitigating their potential long-term (evolutionary) negative consequences.

Indeed, it is increasingly acknowledged that pathogens may evolve in response to treatments, as exemplified by the evolution of antibiotic resistance or vaccine escape. Pathogen evolution is fuelled by the high reproduction rate of pathogens and the increasing use of treatments. In particular, both empirical evidence [3–5] and theoretical predictions [6–8] support the idea that imperfect treatments may cause selection on pathogen life-history traits, such as transmission and virulence.

In practice, treatments are rarely perfect, either because of partial efficacy, or limited coverage. From an ecological perspective, this introduces heterogeneity in the host population. Indeed, naive and treated hosts can be viewed as two habitats with different qualities for the pathogen. We expect pathogens to have higher fitness in good habitats (e.g. untreated hosts), and lower fitness in bad habitats (e.g. treated hosts). However, if the pathogen adapts to the bad habitat by increasing its virulence, this can negatively impact untreated hosts in the population. The potential negative effects of such imperfect treatments have been theoretically studied, showing in particular that some types of treatments (notably those reducing host susceptibility or pathogen transmissibility) can be viewed as evolution-proof, while others (such as those that

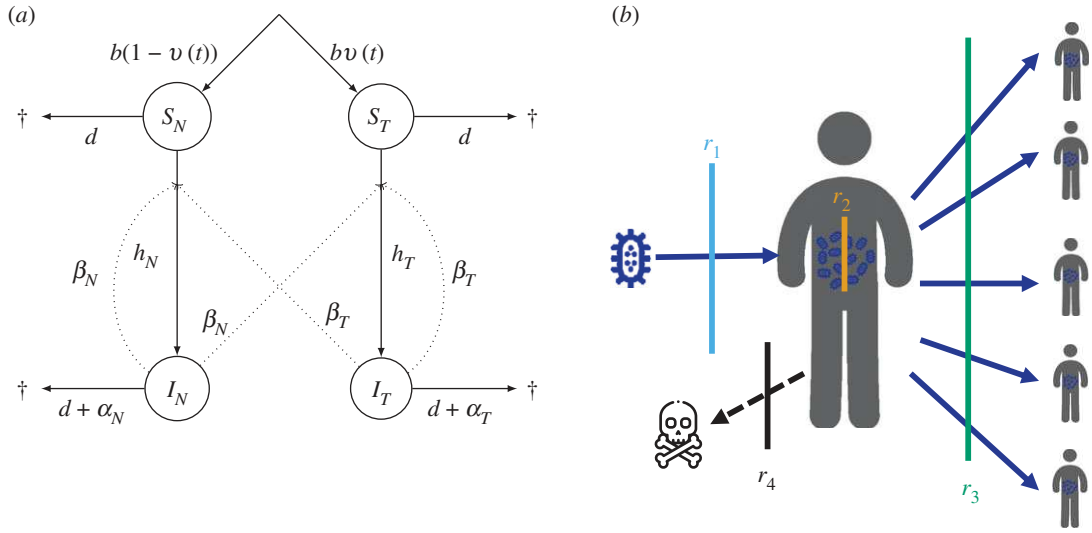

Figure 1. (*a*) Life cycle of the host–pathogen interaction, showing transition rates between classes. (*b*) Infection process and the different treatment mechanisms: anti-infection (r_1, blue), anti-growth (r_2, orange), anti-transmission (r_3, green) and anti-toxin (r_4, black), with a human as illustration of hosts. (Online version in colour.)

mainly increase the tolerance of hosts to the disease) can lead to the long-term evolution of virulence [7–9].

A central assumption of these earlier studies is that treatment coverage is constant in time. In practice, however, treatment coverage fluctuates in time, either because of social or economical constraints (vaccine scares, shortage in drugs, vaccination campaigns linked to time-limited humanitarian or scientific missions), or because of specific treatment strategies. For instance, pulse vaccination has been the main strategy deployed to eradicate polio and significantly decreased its incidence [10]. In addition, many crop diseases are seasonally treated, either directly in fields, or by pre-treatment at the seed stage. Periodic treatments may also be implemented through rotation between naive and treated plants, which has been shown to reduce pathogen prevalence [11]. In this context, it is of major interest to study the consequences of periodic treatment strategies through theoretical studies to guide future experimentations or applications. In particular, an important question is whether temporal variations in treatment may increase or decrease selection on pathogen virulence or transmission. At a conceptual level, fluctuations in treatment coverage will cause temporal variation in host quality for the pathogen, and it is not clear that the optimal strategy in a constant environment will also maximize pathogen fitness in this context.

Our purpose here is to analyse the epidemiological and evolutionary effects of periodic imperfect prophylactic treatments that create heterogeneity among hosts. Building on previous theoretical studies of imperfect treatments with constant coverage [7–9], we first present the consequences of periodic treatment coverage on the prevalence of the disease and the pathogen's basic reproduction number. We then assume that a rare mutation occurs in the pathogen, modifying the life-history traits, and we analyse how the selective pressures on the mutant pathogen depend on (i) the mode of action, and (ii) the temporal distribution of treatments. Part of our analysis is based on a new approach to analyse selection in fluctuating environments, which allows us to measure host quality using a dynamical concept of reproductive value [12]. We discuss the practical and conceptual implications of our work.

2. Model

We consider a host–pathogen interaction with the life cycle depicted in figure 1*a* (see table 1 for notations). The host population is structured in two classes corresponding to the host's immune state, naive (N) or treated (T). Hosts can be either susceptible (S) or infected by a pathogen responsible for an infectious disease (I). This leads to four different types of hosts, S_N, S_T, I_N and I_T. Host reproduction occurs at rate b. Upon birth, offspring have a probability ν of being treated, in which case they enter the S_T class, and a probability $(1-\nu)$ of remaining untreated, in which case they enter the S_N class. All hosts (susceptible and infected) have a background mortality rate, d, with an additional disease-induced mortality (i.e. virulence), which we note α_N and α_T, respectively, for naive or treated infected hosts. A susceptible naive (respectively, treated) host can be infected by naive and treated infected hosts, I_N and I_T, at rate h_N (respectively, h_T). The forces of infections, h_N and h_T, directly depend on the horizontal transmission of the pathogen, such that $h_N = \beta_N I_N + \beta_T I_T$ and $h_T = \sigma h_N$, where β_N and β_T are the transmissibilities of naive and treated hosts, respectively, and σ represents the relative susceptibility of treated hosts. With these assumptions, the epidemiological dynamics can be described by the following ODE system

$$\frac{dS_N}{dt} = (1-\nu(t))b - (d+h_N)S_N, \tag{2.1a}$$

$$\frac{dS_T}{dt} = \nu(t)b - (d+h_T)S_T, \tag{2.1b}$$

$$\frac{dI_N}{dt} = h_N S_N - (d+\alpha_N)I_N \tag{2.1c}$$

and

$$\frac{dI_T}{dt} = h_T S_T - (d+\alpha_T)I_T, \tag{2.1d}$$

The model is based on a previously analysed model of imperfect vaccines [7,8], but instead of a constant treatment coverage, we consider that ν is a function of time. In most simulations, we use a T-periodic square function (figure 2*a*) that varies between $\nu_{\min}$ and $\nu_{\max}$. The treatment coverage takes the value $\nu_{\max}$ during pT and $\nu_{\min}$ during $(1-p)T$, with p the fraction of the period with a maximum coverage.

Table 1. Table of parameters and variables.

parameter	definition
life-history traits	
α_k	disease-induced death rate (virulence) of the resident strain in class k
α_k'	disease-induced death rate (virulence) of the mutant strain in class k
α^*	evolutionarily stable virulence
β_k	transmission rate of the resident strain in class k
β_k'	transmission rate of the mutant strain in class k
b	birth rate
d	natural death rate
h_k	force of infection in class k
σ	susceptibility of hosts
treatments	
$\nu(t)$	periodic treatment coverage function
T	period of the treatment function
p	fraction of T with treatment
r_i	efficacy of the i treatment (see §2)
reproductive values	
c_k^e	pathogen class reproductive value in class k under a constant coverage
c_k	pathogen class reproductive value in class k under a periodic coverage
	k stands for naive (N) or treated (T) hosts

The average coverage is thus $\bar{\nu} = p\,\nu_{\max} + (1-p)\,\nu_{\min}$. For the sake of simplicity, we choose $\nu_{\max} = 1$ and $\nu_{\min} = 0$ in our simulations, so that the average coverage is $\bar{\nu} = p$.

As typical in the literature, we assume a trade-off between transmission and virulence, so that a pathogen cannot see its transmission increase without paying a cost through an increase of the host's death [13,14]. Following this hypothesis, we assume an increasing saturating trade-off between transmission, β and virulence, α. In figures, we typically use the function $\beta[\alpha] = 5\alpha/(1+\alpha)$.

As in [7–9], we assume that treatments are imperfect: being treated does not guarantee a full and lifelong protection against pathogens. Several imperfect vaccines against cholera for instance have been reported, with various efficacies [15,16]. Following [7], we consider four different types of treatments showed in figure 1*b*. First, we consider an anti-infection treatment that prevents the primary infection of the host by the pathogen. Potential examples include the human papillomavirus (HPV) vaccine, which aims to reduce the penetration of the HP virus into cells [17], or the copper in Bordeaux mixture, which lowers the risk of infection by preventing the germination of fungal spores on leaves [18]. Second, we consider an anti-growth treatment which aims to decrease the intra-host growth rate of the pathogen, and has an action on its life-history traits (virulence α and transmission β). This is reminiscent of the mode of action of the ABT-538 drug, which reduces the within-host replication of HIV [19,20]. The third treatment acts by reducing the transmission of pathogens to other hosts. For instance, it has been shown that an effect of the feline calcivirus vaccine is to reduce virus shedding [21,22]. Fourth, we consider a leaky anti-toxin treatment that only reduces pathogen's virulence, as documented for instance for the vaccine against Marek's disease [4], or the toxoid vaccine against diphteria [3].

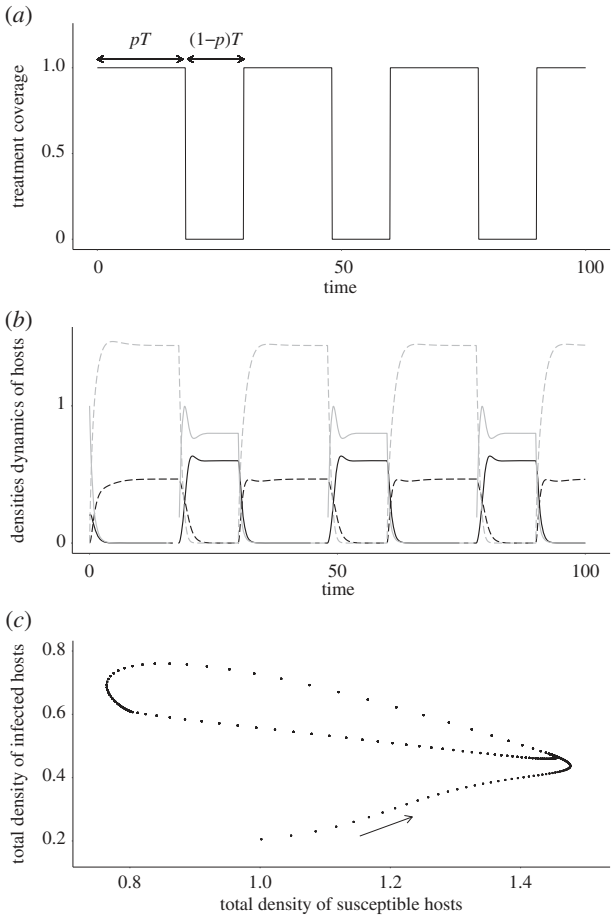

Figure 2. Typical behaviour of the model, for an anti-growth treatment. (*a*) Square function for treatment coverage: ν takes the value 1 during pT (all newborns are treated), and the value 0 during $(1-p)T$ (no newborn is treated). (*b*) Density dynamics for susceptible naive (plain grey), susceptible treated (plain black), infected naive (dashed grey) and infected treated (dashed black). (*c*) Phase portrait for the total densities of susceptible ($S_N + S_T$) and infected ($I_N + I_T$) hosts, showing convergence to a periodic attractor. Parameter values: $r_2 = 0.8$, $p = 0.6$, $T = 30$, $\alpha = 1$, $b = 2$, $d = 1$. Typical behaviours of the model with anti-infection, anti-transmission and anti-toxin treatments are shown in electronic supplementary material, appendix S.1.

In naive hosts, the virulence and transmission rates are simply $\alpha_N = \alpha$ and $\beta_N = \beta(\alpha)$, where α is the virulence trait. Treatments cause a reduction in virulence, transmission or susceptibility of hosts, depending on the treatment type i, with an efficacy r_i that takes values between 0 (no effect) and 1 (perfect treatment). With our definitions for the different types of treatments, we have

$$\sigma = 1 - r_1, \quad \alpha_T = (1-r_2)(1-r_4)\alpha, \quad \beta_T = (1-r_3)\beta[(1-r_2)\alpha]. \tag{2.2}$$

3. Epidemiology

In this section, we investigate how the periodicity of treatment coverage affects the ability of a pathogen to spread in an uninfected host population and the endemic prevalence of the disease. The invasion success of a pathogen can be quantified by its basic reproduction number, R_0, which represents the average number of hosts to which a single infected host in a disease-free population can transmit the

pathogen over its lifetime. In a deterministic model, the pathogen can create an epidemic if $R_0 > 1$, or die out if $R_0 < 1$ [23–25]. R_0 is calculated in the stable population in the absence of the disease, typically an equilibrium in most studies. In our model, however, the disease-free population settles on a periodic attractor, due to the periodic forcing $\nu(t)$.

(a) Constant treatment coverage

When the treatment coverage is constant ($\nu(t) = \bar{\nu}$), the population settles on an equilibrium in the absence of the disease. We can therefore calculate R_0 using the next-generation theorem (see electronic supplementary material, appendix S.2.1, [24,26]), which leads to

$$R_0 = R_N S_N^0 + \sigma R_T S_T^0 \tag{3.1}$$

with

$$R_N = \frac{\beta_N}{d + \alpha_N} \quad \text{and} \quad R_T = \frac{\beta_T}{d + \alpha_T}, \tag{3.2}$$

the basic reproductive numbers in a fully naive ($\bar{\nu} = 0$) or fully treated ($\bar{\nu} = 1$) population respectively, and S_N^0 and S_T^0 the densities of susceptible hosts at the disease-free equilibrium, which are given by $S_N^0 = (1 - \bar{\nu})b/d$ and $S_T^0 = \bar{\nu}b/d$ (electronic supplementary material, appendix S.3). Thus, the basic reproductive number in a heterogeneous population corresponds to the sum of R_0's in a fully naive and a fully treated population, weighted by the densities of susceptible hosts in each class.

(b) Periodic treatment coverage

When host dynamics are periodic (figure 2*a*,*b*), the next-generation theorem cannot be applied to calculate the basic reproductive number. However, the concept of Floquet multipliers can be used to extend the definition of R_0 [24] to periodic environments [27,28]. Floquet theory allows for the study of the stability of continuous-time periodical systems ([29]; e.g. [30] for an ecologically oriented treatment). In our study, we can distinguish two cases: anti-infection and anti-transmission treatments, for which an analytical study is possible, and anti-growth and anti-toxin treatments for which R_0 can only be calculated numerically.

(i) Anti-infection and anti-transmission treatments

For these treatments, we show in electronic supplementary material, appendix S.2.2 that, following [27], we can calculate the basic reproduction number as:

$$R_0 = \frac{\beta}{d + \alpha}\left(\langle S_N^0 \rangle + (1 - r_1)(1 - r_3)\langle S_T^0 \rangle\right), \tag{3.3}$$

where $\langle S_k^0 \rangle = \int_t^{t+T} S_k^0(\tau)\,\mathrm{d}\tau$ gives the average density of susceptible hosts in class k during one period. In particular, we show in electronic supplementary material, appendix S.3 that, for our model

$$\langle S_N^0 \rangle = \frac{(1 - \bar{\nu})b}{d} \quad \text{and} \quad \langle S_T^0 \rangle = \frac{\bar{\nu}b}{d}. \tag{3.4}$$

We can see that the average susceptible densities, $\langle S_N^0 \rangle$ and $\langle S_T^0 \rangle$ have the same expressions as the equilibrium densities in the constant case, and only depend on b, d, and the average treatment coverage, $\bar{\nu}$ (equation (3.4)). As a result, the invasion threshold is independent of the period, and only depends on the average coverage $\bar{\nu}$. Hence, any periodic treatment with average coverage $\bar{\nu}$ leads to the same condition for pathogen invasion as a constant treatment with coverage $\bar{\nu}$.

After pathogen invasion, the population settles on a periodic endemic attractor (figure 2*c*), and the average prevalence is then the fraction of infected hosts in the population integrated over one period. Increasing the average coverage ($\bar{\nu} = p$) decreases the average prevalence for these treatments (figure 3*a*, blue and green lines), until extinction above a critical value of p. Moreover, an increase of the period T also reduces the average prevalence (figure 3*b*). Note that periodicity in treatment coverage always leads to a lower prevalence compared to the corresponding constant coverage.

(ii) Anti-growth and anti-toxin treatments

For these treatments, the basic reproduction number cannot be expressed in a closed analytical form, but can be calculated numerically using Floquet's theory [30,31]. We show in electronic supplementary material, appendix S.2.3 that the effect of periodicity on R_0 is weak, but tends to slightly lower the extinction threshold for both types of treatments.

As the average coverage ($\bar{\nu} = p$) increases, the average prevalence decreases with an anti-growth treatment and increases with an anti-toxin. This can be intuitively explained by the fact that anti-toxin treatments merely reduce the survival cost of pathogens and cause infected hosts to transmit for a longer time. By contrast, anti-growth treatment directly impacts the transmission-virulence trade-off. It causes a reduction of pathogen spread for treated hosts, counterbalanced by a reduction of host mortality. This explains the lower decrease of the prevalence compared to anti-infection or anti-transmission treatments (figure 3*a*). As for previous treatments, the average prevalence decreases when the period increases and the periodic treatment is beneficial compared to the constant coverage in terms of average prevalence reduction (figure 3*b*).

To understand why, note that the prevalence for short periods can be approximated by the prevalence with the corresponding constant average coverage. Indeed, the dynamics are characterized by small oscillations around the equilibrium solution. Hence, for short periods, pathogens are exposed, at any given time, to a heterogeneous population of naive and treated hosts. For large periods, however, the environment experienced by the pathogen alternates between temporary equilibria corresponding to either fully naive or fully treated populations. The average prevalence then tends to the arithmetic mean between the equilibrium prevalences in fully naive and fully treated poulations, which is always lower than the prevalence in a heterogeneous population at equilibrium (figure 3*b*). Note that, due to the epidemiological feedbacks, the endemic attractor is more sensitive to the forcing period than the disease-free state of the population, which explains why periodicity has a weaker impact on the invasion threshold compared to the average prevalence.

4. Evolution

Assuming the population has reached an endemic attractor, we now aim to understand how imperfect treatments and periodicity may jointly affect the evolution of pathogen life-history traits, such as virulence. In this section, we consider that a pathogen strain is characterized by a trait z (for instance the pathogen's within-host growth rate) and that the virulence and transmission traits are all functions of this trait. For

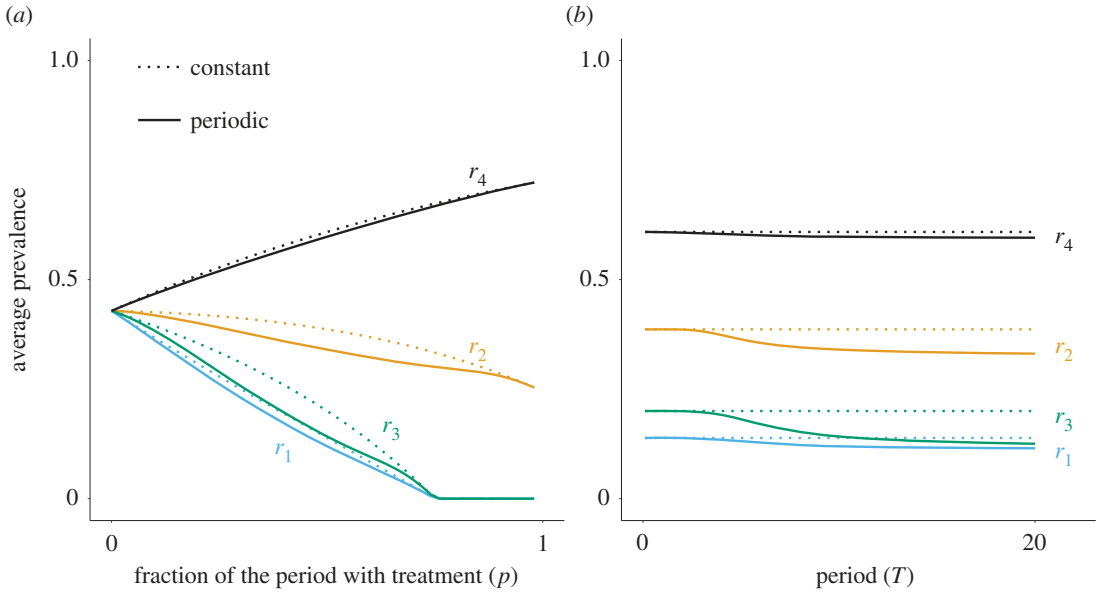

Figure 3. Disease prevalence as a function of (*a*) the fraction of time at maximum treatment p ($T = 10$), or (*b*) the period T ($p = 0.5$), for anti-infection (blue), anti-growth (orange), anti-transmission (green) and anti-toxin (black) treatments, all with efficacy $r_i = 0.8$. (Solid lines: periodic treatment, dotted lines: constant treatment.) Other parameters as in figure 2. (Online version in colour.)

simplicity, we assume $\alpha_N = z$, so that z represents virulence in naive hosts. Eventually, a host population infected by the resident strain settles on its endemic attractor ($\hat{S}_N(t)$, $\hat{S}_T(t)$, $\hat{I}_N(t)$, $\hat{I}_T(t)$). Extensive numerical simulations show that the period of the attractor is always equal to the period of $\nu(t)$. Now let us assume that a mutant with a trait z' which is slightly different from the resident's appears (the full model including the infected hosts by the mutant strain is shown in electronic supplementary material, appendix S.4.1). Whether the mutant can invade the population or not is determined by the sign of its invasion fitness [32–35]. We use this conceptual tool to investigate the direction of selection on pathogen traits, and potential evolutionary endpoints.

(a) Anti-infection and anti-transmission treatments

For these treatments, the invasion fitness of a rare mutant pathogen can be calculated analytically from the mutant pathogen's basic reproduction number $R(z', z)$, which acts as a proxy for invasion fitness [25]. Using the same approach used to derive equation (3.3), we find that a rare mutant can invade the resident population on its periodic attractor if $R(z', z) > 1$, where

$$R(z', z) = \frac{\beta(z')}{d + \alpha(z')}\left(\left\langle \hat{S}_N \right\rangle + (1 - r_1)(1 - r_3)\left\langle \hat{S}_T \right\rangle\right). \tag{4.1}$$

Because for the resident pathogen, we have $\left\langle \hat{S}_N \right\rangle + (1 - r_1)(1 - r_3)\left\langle \hat{S}_T \right\rangle = (d + \alpha(z))/\beta(z) = 1/R_0(z)$, it follows that

$$R(z', z) = \frac{R_0(z')}{R_0(z)}. \tag{4.2}$$

Equation (4.2) shows that selection favours the strain that maximizes the epidemiological R_0, as in the case with constant coverage [7–9]. As a result, periodicity in treatment coverage does not impact the evolutionarily stable virulence for these two treatments. This can be numerically confirmed using Floquet's theory (electronic supplementary material, figure S.5). For completeness, we note that, in the original models by Gandon *et al.* [7,8], the prediction that higher efficacy selects for lower virulence was due to the possibility of superinfection, which we ignore here, as a full analysis of the interplay between multiple infections and environmental fluctuations is beyond the scope of this paper.

(b) Anti-growth and anti-toxin treatments

For anti-growth and anti-toxin treatments, an analytical expression of the invasion fitness $s(z', z)$ (or its proxy $R(z', z)$) is beyond our reach. However, we use a new approach to derive an analytical expression of the selection gradient, $\mathcal{S}(z) = \partial s/\partial z'|_{z'=z}$. The zeros of the selection gradient give the evolutionarily singular points [36].

As a useful baseline scenario, we first examine the case of a constant coverage analysed in [7,8]. We then have

$$\mathcal{S}_e = c_N^e\left(\beta_N'(z)\frac{d + \alpha_N}{\beta_N} - \alpha_N'(z)\right) + c_T^e\left(\beta_T'(z)\frac{d + \alpha_T}{\beta_T} - \alpha_T'(z)\right). \tag{4.3}$$

The selection gradient then takes the form of a weighted sum, where the weights c_N^e and $c_T^e = 1 - c_N^e$ are the pathogen's class reproductive values in naive and treated hosts, in a resident population at equilibrium [9,12,37,38]. Thus, the ES virulence is intermediate between the value which maximizes the basic reproduction number in a fully naive population (i.e. when $c_N^e = 1$) and the value which that maximizes the basic reproduction number in a fully treated population (i.e. when $c_T^e = 1$). The class reproductive value c_T^e is a measure of the quality of treated hosts from the point of view of the parasite.

With periodic treatment coverage, we show in electronic supplementary material, appendix S.4.2 that the average change in mean trait over one period on the resident periodic attractor, is approximately proportional to

$$\mathcal{S} = \langle c_N \rangle\left(\beta_N'(z)\frac{d + \alpha_N}{\beta_N} - \alpha_N'(z)\right) + \langle c_T \rangle\left(\beta_T'(z)\frac{d + \alpha_T}{\beta_T} - \alpha_T'(z)\right), \tag{4.4}$$

where $c_T(t)$ is the class reproductive value of resident pathogens infecting treated hosts at time t, and $c_N(t) = 1 - c_T(t)$ is the class reproductive value on naive hosts. Note that equation (4.4) is directly comparable to equation (4.3), but, in contrast with the classical definition, reproductive values are here time-dependent quantities [12]. This reflects the fact that the relative qualities of the different classes of hosts for the pathogen change as the population moves along the periodic attractor.

Equation (4.4) shows that, as in the constant treatment model, the ES virulence in a heterogeneous host population is intermediate between the value which maximizes the basic reproduction number in a fully naive population and that maximizes the basic reproduction number in a fully treated population. Interestingly, the potentially complex effects of fluctuations on the exact value of the ESS are captured by a single variable, which is the average class reproductive value over one period, $\langle c_T \rangle$. In general, $\langle c_T \rangle$ will deviate from the class reproductive value c_T^e in the constant treatment model (figure 4*a–c*), and as a result the ESS will be different in periodic versus constant environments.

For anti-toxin treatments, where $\beta_N = \beta_T = \beta(\alpha)$ and $\alpha_T = \alpha(1 - r_4)$, a useful graphical representation can be obtained from equation (4.4) by noting that the ES virulence must satisfy

$$\beta'(\alpha) = \frac{\beta(\alpha)}{d + \alpha} \frac{1 - r_4 \langle c_T \rangle}{1 - r_4 \langle c_T \rangle \frac{\alpha}{d + \alpha}} \tag{4.5}$$

which is a form of marginal value theorem [39]. As shown graphically in figure 4*d*, the ES virulence for periodic anti-toxin treatment is lower than in a constant treatment. This effect is mediated by the average class reproductive value which decreases as the period T increases (figure 4*c*). For large T, $\langle c_T \rangle$ converges towards $\bar{\nu} = p$ (electronic supplementary material, appendix S.4.2), which provides a lower bound for the reduction in virulence that can be achieved by using periodic treatments. For our trade-off function $\beta(\alpha) = 5\alpha/(1 + \alpha)$, this lower bound can be calculated as

$$\alpha^* = \frac{1}{\sqrt{1 - pr_4}}, \tag{4.6}$$

which implies that, for a fixed efficacy r_4, the ES virulence should be lower for low values of p (e.g. short bouts of treatment).

While the average value $\langle c_T \rangle$ is sufficient to determine the ES virulence, the impact of periodicity on the full dynamics of $c_T(t)$ sheds light on the process by which higher periods select for lower virulence. Figure 4*a* shows that, for short periods, the class reproductive value rapidly fluctuates around its mean value, which is close to the equilibrium value c_T^e but overestimates the average state of the environment, $\bar{\nu}$. As the period increases, the environmental change becomes slower and easier to track by the pathogen, and the class reproductive value more closely matches the environmental signal $\nu(t)$ (figure 4*b*). Because the pathogen is now better able to perceive the true alternance of good and bad epochs, its optimal strategy is less biased towards treated hosts. Note that equation (4.4) also allows us to understand why anti-infection and anti-transmission treatments are insensitive to periodicity, since, for these treatments, the class-specific selection gradients (the terms between brackets) are equal, so that both classes have the same optimum.

These analytical predictions can be checked using a numerical calculation of the invasion fitness $s(z', z)$, which is the Floquet exponent associated with the mutant dynamics on the resident periodic attractor (see electronic supplementary material, appendix S.4.3). Figure 5*a* shows that the predictions of equation (4.4) closely match the Floquet analysis and confirms that the ES virulence decreases as the period increases, with a stronger effect for anti-growth than for anti-toxin treatments. There is however a lower bound to the reduction in virulence that can be achieved using periodic treatments, as the ES virulence saturates as T becomes large. Nonetheless, a tentative conclusion of our work is that selection for virulence is weaker with treatments with periodic coverage such as pulse vaccination, compared to a constant treatment with similar average coverage. Finally, figure 5*b* shows that, for both anti-growth and anti-toxin treatments, increasing p, and thus the average treatment coverage in the population, leads to increased ES virulence, as in the constant case. However, in heterogeneous host populations ($0 < p < 1$), the ES virulence is lower with periodic treatments than with constant treatments. Hence, although, as predicted by Gandon *et al.* [7,8], anti-growth and anti-toxin treatments select for higher virulence, fluctuations in coverage may actually mitigate the negative evolutionary side-effect of these treatments.

5. Discussion

Our study sheds light on the potential benefits of periodic treatments, both for short-term epidemiological control of infectious diseases and long-term virulence management. Our model generalizes the predictions of [7,8], who showed for constant treatment coverage that increasing coverage decreases the endemic prevalence, except for anti-toxin treatments. Our results show that this carries over to periodic coverage. For long-term evolution, we show that increasing average treatment coverage has no effect on virulence evolution for anti-infection and anti-transmission treatments but selects for significantly increased virulence with anti-growth and anti-toxin treatments. However, for all treatments, periodic treatments are more beneficial than constant treatments and lead to lower prevalence and virulence.

Our results suggests that periodic treatments over long periods may be a mitigating strategy for virulence management, even for treatments that create selective pressures on pathogen life-history traits. Overall, our model predicts that the best treatment strategy with anti-infection and anti-transmission is a periodic coverage with a high average coverage, to lower the prevalence. Anti-growth treatment strategies require a compromise between high coverage (reduction of prevalence on the short term) and low coverage (to limit the long-term emergence of virulent strains). Anti-toxin treatments are not recommended, but if no alternative exists, periodic strategies of treatment would seem preferable.

At a conceptual level, our modelling approach provides a general method to analyse selective pressures in heterogeneous habitats where habitat quality can vary over time due to environmental fluctuations. Here, the quality of treated hosts for the parasite varies, and we use a dynamical concept of reproductive value [12] to measure this quality and derive the selection gradient. In contrast to previous studies [40,41], which relied on numerical calculations of the invasion fitness, this allows us to derive analytical expressions that can be

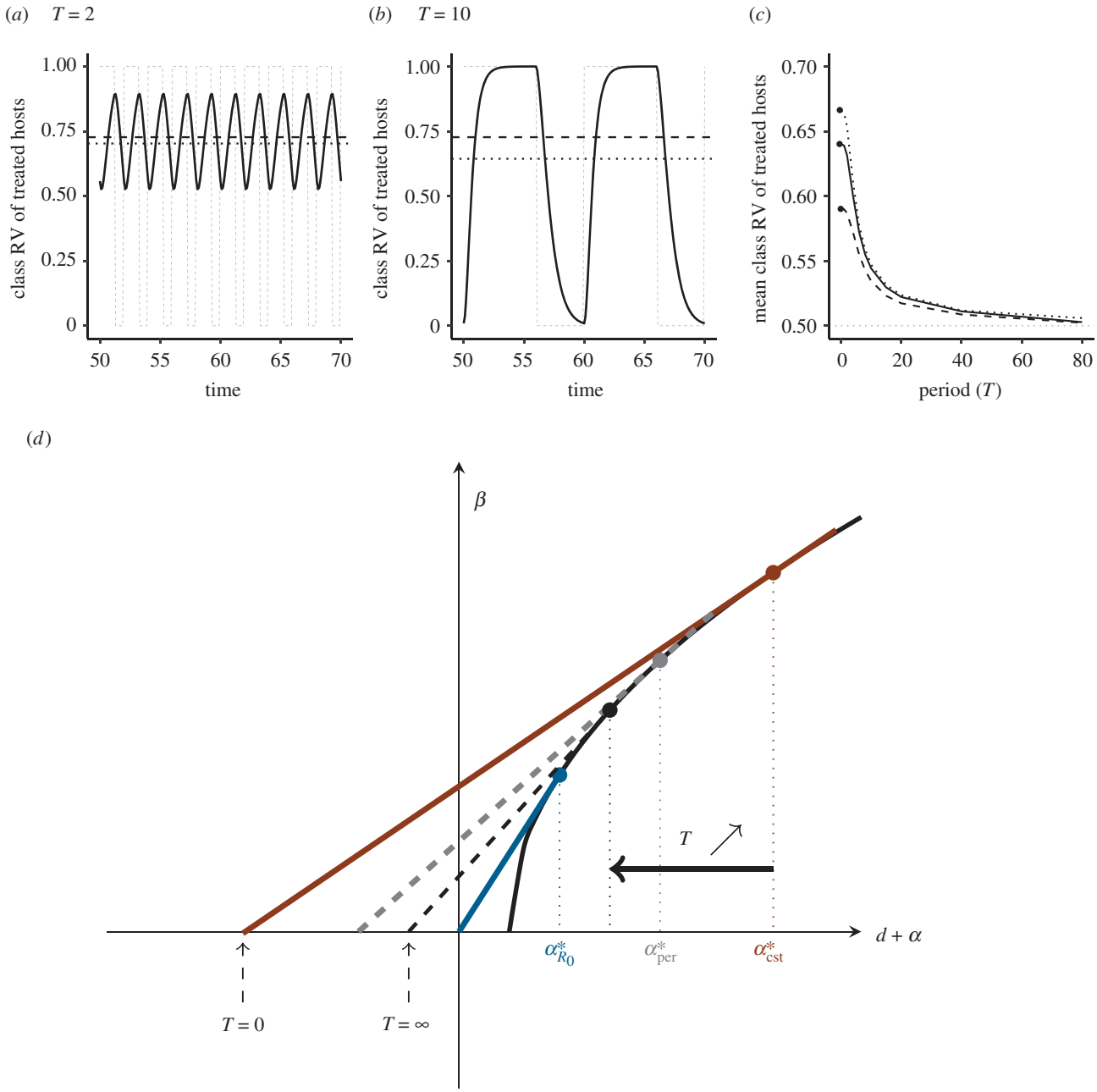

Figure 4. (*a*,*b*) Dynamics of the class reproductive value of treated hosts, $c_T(t)$ for short (*a*, $T = 2$) and longer (*b*, $T = 10$) period of an anti-toxin treatment coverage. Also shown are the periodic treatment function $\nu(t)$ (dashed grey lines), the mean value $\langle c_T(t)\rangle$ (dotted lines) and the value in the constant model c_T^e (dashed line). Parameters: $r_4 = 0.5$, $p = 0.6$, $z = 1$. (*c*) Mean class reproductive value $\langle c_T(t)\rangle$ as a function of the period. Parameters: $r_4 = 0.5$, $\bar{\nu} = p = 0.5$, $z = 0.5$ (dashed), 1 (solid), 1.4 (dotted). Other parameters as in figure 2. (*d*) Graphical representation of the effect of periodicity on the ES virulence for an anti-toxin treatment. In a homogeneous population, the ES virulence $\alpha^*_{R_0}$ is obtained by maximizing the epidemiological R_0. Graphically, this implies that the slope at the ESS goes through the origin (blue line). For a constant treatment ($T = 0$), the slope at the ESS is smaller (red line), resulting in a higher ES virulence α^*_{cst}. As the period increases, so does the slope at the ESS, given by equation (4.5), resulting in a lower ES virulence. The slope at the ES virulence (grey line) then goes through the point $(-d\, r_4\langle c_T\rangle)/(1 - r_4\langle c_T\rangle, 0)$, where $\langle c_T\rangle$ is the average class reproductive value of treated hosts over one period. Because, as the period T goes to infinity, $\langle c_T\rangle$ converges to its lower bound p (figure 4*c*), the ES virulence under periodic anti-growth treatment coverage also has a lower bound, which is always greater than $\alpha^*_{R_0}$ (which would be the solution for $\langle c_T\rangle = 0$). (*a*) $T = 2$, (*b*) $T = 10$. (Online version in colour.)

readily compared to the selection gradient in constant environments. This is particularly useful as it allows us to capture the effect of periodic coverage on virulence evolution through a single variable, which is the average quality (or reproductive value) of treated hosts over one period.

In our study, we focus on periodicity caused by the availability of treatments, which implies seasonality in the susceptible host type and impacts pathogens life-history traits. However, periodic environmental forcing can be caused by other parameters such as seasonality in pathogen transmission rate [42] or in host birth rates [43], to which our approach could be applied. In particular, considering the effect of seasonal variations of the environment caused by climate change on the evolution of pathogens life-history traits is of particular interest [44]. Many epidemiological studies have addressed the issue of periodic environments in epidemiology, in particular on the expression of R_0 and the probability of emergence [27,28,31,42,45]. There is however a lack of studies about evolution in fluctuating environments, notably when the population is structured. Partly, this is due to the lack of

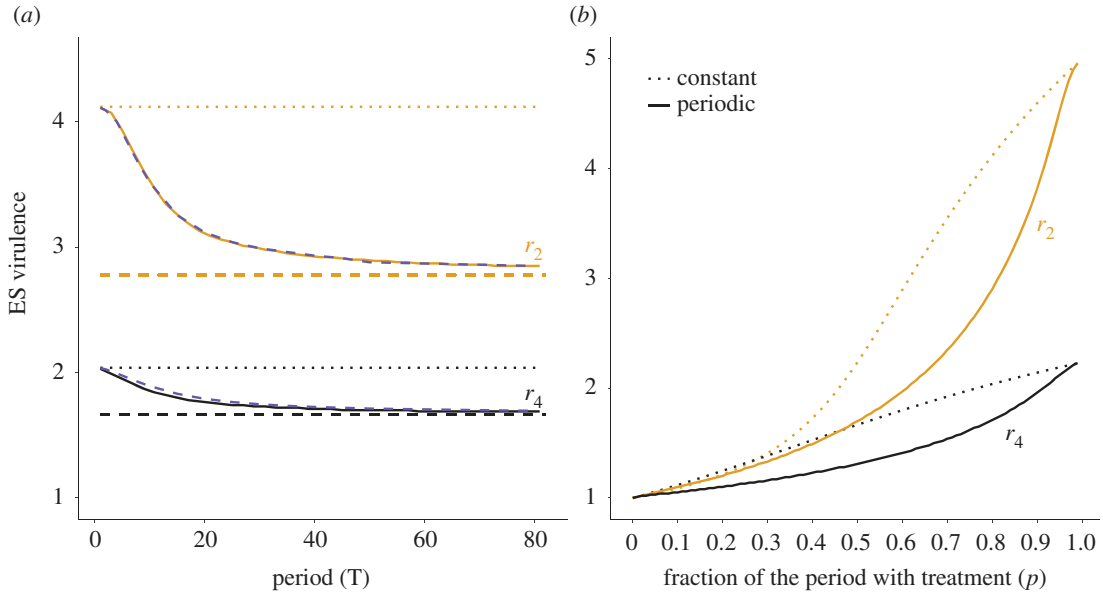

Figure 5. Evolutionarily stable virulence according to (*a*) the period of treatments fluctuations T (with $p = 0.8$), (*b*) the fraction of time at maximum treatment p (with $T = 50$), for anti-growth (orange) and anti-toxin (black) treatments. Dotted lines show the ESS calculated with a constant average coverage, solid lines show the ESS calculated using the dominant Floquet exponent, compared to the semi-analytical solution of equation (4.4) (dashed purple lines in (a)). The ES virulence is bounded by a lower bound obtained by replacing $\langle c_T \rangle$ with p in equation (4.4) (dashed lines). All with a treatment efficacy of $r_i = 0.8$, and other parameters as in figure 2. (Online version in colour.)

analytical methods to tackle this question. For instance, Ferris & Best [40,41] have analysed the evolution of host defence in fluctuating environments, but had to resort to numerical calculations of Floquet exponents when selection depends on both susceptible and infected host classes (e.g. when recovery is not negligible). This makes a direct comparison with constant environments difficult. By contrast, the approach we use in this paper allows us to derive an insightful analytical expression for the selection gradient and to capture much of the complexity of environmental fluctuations using the biologically meaningful concept of reproductive value. We think this approach can be more generally applied to analyse other evolutionary scenarios.

In this work, we focus on the evolution of life-history traits and do not consider the possibility that pathogens evolve resistance to treatments. We have shown that increasing the period of treatment leads to a decrease both in the prevalence and the evolutionarily stable virulence, and seems to be a good treatment strategy. However, large periods means that pathogens are potentially exposed to a treated population during a long time. In principle, this could favour the evolution of pathogen resistance, so that too long a period would probably also have unwanted effects. To sharpen these predictions, our model could be extended to consider other treatements strategies which aim to reduce pathogen resistance, such as combination therapies (patients are treated with several drugs at the same time), mixing (different patients are treated with different drugs) or cycling (each patient is given different drugs in alternace) [46]. For instance, it has been shown that combination therapies are more beneficial than mixing strategies, which are in turn more beneficial than cycling strategies [47]. It would be interesting to couple these models with fluctuations in coverage to investigate the robustness of these public health strategies.

There are a number of interesting potential extensions to our study. For instance, the treatment coverage could be a function of disease prevalence, so that the treatment strategy would vary with the spread of the disease. Also, our model assumes that only new individuals (either by birth or migration) are treated, but for some treatments a global coverage over the whole population would be more realistic. Third, it could be interesting to investigate what happens when treated hosts lose their immunity after some time and join the respective susceptible or infected untreated class. Williams & Kamel [48] have considered a similar heterogeneous model where hosts can switch class over their lifetime. The authors have shown that if an infected host transits from a class with a high reproductive value to a class with a lower reproductive value, selection favours increased host exploitation and therefore increased virulence. These results are consistent with ours, which suggests that the loss of immunity over time would not significantly impact our conclusions.

Our main results were obtained under a number of assumptions. First, we assumed no recovery of infected hosts. This hypothesis is relaxed in electronic supplementary material, appendix S.5 where we explore the effect of non-zero recovery rates. We show that recovery reduces prevalence regardless of the treatment, and decreases the eradication threshold for all treatments but the anti-toxin. It does not significantly affect the evolutionarily stable virulence. Second, we used a step function for the coverage, which is relaxed in electronic supplementary material, appendix S.6, where we use a sinusoidal function to capture a softer change from no coverage to full coverage. Qualitatively, our results and the associated public health recommendations do not depend of the shape on the periodic coverage function. Third, as commonly assumed in the literature [2,7], we used a density-independent birth rate for simplicity. However, the potential feedback between environmental fluctuations and density-dependent reproduction could be biologically relevant and worth a detailed investigation. Fourth, in contrast with the original model of Gandon *et al.* [7,8], we neglect here the possibility of multiple infections. With superinfection, anti-infection and anti-transmission

treatments actually select for lower virulence with constant coverage [7]. Although it is beyond the scope of this study, it would be interesting to see how the interplay between within-host selection and population-level environmental fluctuations could alter the selective pressures on virulence.

Importantly, our evolutionary analysis is based on an adaptive dynamics approach, which uncouples epidemiological and evolutionary timescales. Evolution is supposed to be much slower than epidemiological processes, due to rare mutations. However, many pathogens have high mutation rates and the dominant strain during an epidemic can differ from the strain that is selected in the long run. As experimentally demonstrated in [49], during an epidemic susceptible hosts are abundant and virulent strains investing in transmission are mostly selected, while less virulent strains are favoured at endemic equilibrium, where the proportion of susceptible is lower. It would be interesting to extend our model to take into account potential short-term evolutionary dynamics. Using quantitative genetics methods could help to shed light on these processes [50,51].

Finally, it would be interesting to test our theoretical predictions using field or experimental data. Unfortunately, the kind of field data needed to test our predictions require long-term studies of joint epidemiological and evolutionary dynamics, which are only beginning to appear. Nevertheless, our conclusions could be tested experimentally in microbial, or agricultural systems. Bacteria–phage interactions are well suited to explore the interplay between ecology and evolution in heterogeneous host–parasite interactions [49,52]. By periodically varying the influx of naive or treated susceptible bacteria and monitoring the effects on parasite prevalence and the evolution of phage virulence, it would be possible to test our predictions. We think our theoretical results provide an interesting foundation to guide experimental and empirical studies, which can potentially lead to useful recommendations to control and reduce the damages caused by infectious diseases.

Data accessibility. Code and data of numerical simulations are available from the Dryad Digital Repository at https://doi.org/10.5061/dryad.nzs7h44qx [53].

Authors' contributions. A.W. analysed the model, produced numerical analyses and figures and wrote the first draft of the manuscript. Both A.W. and S.L. contributed to subsequent versions of the manuscript. S.L. derived the analysis in electronic supplementary material, appendix S.4.3.

Competing interests. We declare we have no competing interests.

Funding. This work was funded by Agence Nationale de la Recherche grant ANR-16-CE35-0012-01 "STEEP" to S.L.

Acknowledgements. We thank Philippe Carmona and Sylvain Gandon for very useful discussions and suggestions. We are grateful to three anonymous reviewers for helpful comments.

References

1. Anderson RM. May RM 1991. *Infectious diseases of humans: dynamics and control*. Oxford, UK: Oxford University Press.
2. Keeling MJ, Rohani P. 2011 *Modeling infectious diseases in humans and animals*. Princeton, NJ: Princeton University Press.
3. Gandon S, Day T. 2008 Evidences of parasite evolution after vaccination. *Vaccine* **26**, C4–C7. (doi:10.1016/j.vaccine.2008.02.007)
4. Read AF, Baigent SJ, Powers C, Kgosana LB, Blackwell L, Smith LP, Kennedy DA, Walkden-Brown SW, Nair VK. 2015 Imperfect vaccination can enhance the transmission of highly virulent pathogens. *PLoS Biol.* **13**, e1002198. (doi:10.1371/journal.pbio.1002198)
5. World Health Organization. Antimicrobial resistance: global report on surveillance. Geneva, Switzerland: World Health Organization; 2014.
6. Dieckmann U, Metz JAJ, Sabelis MW, Sigmund K (eds). 2002 Adaptive dynamics of infectious diseases. In pursuit of virulence management. Cambridge studies in adaptive dynamics. Cambridge, UK: Cambridge University Press.
7. Gandon S, Mackinnon MJ, Nee S, Read AF. 2001 Imperfect vaccines and the evolution of pathogen virulence. *Nature* **414**, 751. (doi:10.1038/414751a)
8. Gandon S, Mackinnon M, Nee S, Read A. 2003 Imperfect vaccination: some epidemiological and evolutionary consequences. *Proc. R. Soc. Lond. B* **270**, 1129–1136. (doi:10.1098/rspb.2003.2370)
9. Zurita-Gutiérrez YH, Lion S. 2015 Spatial structure, host heterogeneity and parasite virulence: implications for vaccine-driven evolution. *Ecol. Lett.* **18**, 779–789. (doi:10.1111/ele.12455)
10. John TJ, Pandian R, Gadomski A, Steinhoff M, John M, Ray M. 1983 Control of poliomyelitis by pulse immunisation in Vellore, India. *Br. Med. J. (Clin Res Ed)* **286**, 31–32. (doi:10.1136/bmj.286.6358.31)
11. Nilusmas S, Mercat M, Perrot T, Djian-Caporalino C, Castagnone-Sereno P, Touzeau S, Calcagno V, Mailleret L. 2020 Multiseasonal modelling of plant-nematode interactions reveals efficient plant resistance deployment strategies. *Evol. Appl.* **13**, 2206–2221. (doi:10.1111/eva.12989)
12. Lion S. 2018 Class structure, demography, and selection: reproductive-value weighting in nonequilibrium, polymorphic populations. *Am. Nat.* **191**, 620–637. (doi:10.1086/696976)
13. Anderson RM, May RM. 1982 Coevolution of hosts and parasites. *Parasitology* **85**, 411–426. (doi:10.1017/S0031182000055360)
14. Alizon S, Hurford A, Mideo N, Van Baalen M. 2009 Virulence evolution and the trade-off hypothesis: history, current state of affairs and the future. *J. Evol. Biol.* **22**, 245–259. (doi:10.1111/j.1420-9101.2008.01658.x)
15. Richie E *et al.* 2000 Efficacy trial of single-dose live oral cholera vaccine CVD 103-HgR in North Jakarta, Indonesia, a cholera-endemic area. *Vaccine* **18**, 2399–2410. (doi:10.1016/S0264-410X(00)00006-2)
16. Sur D *et al.* 2009 Efficacy and safety of a modified killed-whole-cell oral cholera vaccine in India: an interim analysis of a cluster-randomised, double-blind, placebo-controlled trial. *Lancet* **374**, 1694–1702. (doi:10.1016/S0140-6736(09)61297-6)
17. Giuliano AR *et al.* 2011 Efficacy of quadrivalent HPV vaccine against HPV Infection and disease in males. *N. Engl. J. Med.* **364**, 401–411. (doi:10.1056/NEJMoa0909537)
18. Barker B, Gimingham C. 1911 The fungicidal action of bordeaux mixtures. *J. Agric. Sci.* **4**, 76–94. (doi:10.1017/S0021859600001489)
19. Ho DD, Neumann AU, Perelson AS, Chen W, Leonard JM, Markowitz M. 1995 Rapid turnover of plasma virions and CD4 lymphocytes in HIV-1 infection. *Nature* **373**, 123–126. (doi:10.1038/373123a0)
20. Otto SP, Day T 2011 *A biologist's guide to mathematical modeling in ecology and evolution*. Princeton, NJ: Princeton University Press.
21. Lappin MR, Sebring RW, Porter M, Radecki SJ, Veir J. 2006 Effects of a single dose of an intranasal feline herpesvirus 1, calicivirus, and panleukopenia vaccine on clinical signs and virus shedding after challenge with virulent feline herpesvirus 1. *J. Feline Med. Surg.* **8**, 158–163. (doi:10.1016/j.jfms.2005.12.001)
22. Radford AD, Coyne KP, Dawson S, Porter CJ, Gaskell RM. 2007 Feline calicivirus. *Vet. Res.* **38**, 319–335. (doi:10.1051/vetres:2006056)
23. Anderson RM, May RM. 1986 The invasion, persistence and spread of infectious diseases within animal and plant communities. *Phil. Trans. R. Soc. Lond. B* **314**, 533–570. (doi:10.1098/rstb.1986.0072)
24. Diekmann O, Heesterbeek JAP, Metz JAJ. 1990 On the definition and the computation of the basic reproduction ratio R0 in models for infectious

diseases in heterogeneous populations. *J. Math. Biol.* **28**, 365–382. (doi:10.1007/BF00178324)

25. Lion S, Metz JAJ. 2018 Beyond R0 maximisation: on pathogen evolution and environmental dimensions. *Trends Ecol. Evol.* **33**, 458–473. (doi:10.1016/j.tree.2018.02.004)
26. Hurford A, Cownden D, Day T. 2009 Next-generation tools for evolutionary invasion analyses. *J. R. Soc. Interface* **7**, 561–571. (doi:10.1098/rsif.2009.0448)
27. Bacaër N, Guernaoui S. 2006 The epidemic threshold of vector-borne diseases with seasonality. *J. Math. Biol.* **53**, 421–436. (doi:10.1007/s00285-006-0015-0)
28. Bacaër N. 2011 Le paramètre R0 pour la dynamique des populations dans un environnement périodique. Université Pierre et Marie Curie (Paris 6). HDR. See https://hal.archives-ouvertes.fr/tel-01540200.
29. Drazin PG, Drazin PD 1992 *Nonlinear systems*, vol. 10. Cambridge, UK: Cambridge University Press.
30. Klausmeier CA. 2008 Floquet theory: a useful tool for understanding nonequilibrium dynamics. *Theor. Ecol.* **1**, 153–161. (doi:10.1007/s12080-008-0016-2)
31. Bacaër N. 2007 Approximation of the basic reproduction number R0 for vector-borne diseases with a periodic vector population. *Bull. Math. Biol.* **69**, 1067–1091. (doi:10.1007/s11538-006-9166-9)
32. Metz JAJ, Nisbet RM, Geritz SA. 1992 How should we define 'fitness' for general ecological scenarios? *Trends Ecol. Evol.* **7**, 198–202. (doi:10.1016/0169-5347(92)90073-K)
33. Metz JAJ, Geritz SA, Meszéna G, Jacobs FJ, Van Heerwaarden JS. 1995 Adaptive dynamics: a geometrical study of the consequences of nearly faithful reproduction. IIASA Working Paper, WP-95-099. Laxenburg, Austria: IIASA.
34. Geritz SA, Meszéna G, Metz JAJ. 1998 Evolutionarily singular strategies and the adaptive growth and branching of the evolutionary tree. *Evol. Ecol.* **12**, 35–57. (doi:10.1023/A:1006554906681)
35. Lion S. 2018 Theoretical approaches in evolutionary ecology: environmental feedback as a unifying perspective. *Am. Nat.* **191**, 21–44. (doi:10.1086/694865)
36. Geritz SA, Metz JAJ. 1997 Dynamics of adaptation and evolutionary branching. *Phys. Rev. Lett.* **78**, 2024. (doi:10.1103/PhysRevLett.78.2024)
37. Taylor PD. 1990 Allele-frequency change in a class-structured population. *Am. Nat.* **135**, 95–106. (doi:10.1086/285034)
38. Rousset F 2004 *Genetic structure and selection in subdivided populations (MPB-40)*, vol. 40. Princeton, NJ: Princeton University Press.
39. Charnov EL. 1976 Optimal foraging, the marginal value theorem. *Theor. Popul. Biol.* **9**, 129–136.
40. Ferris C, Best A. 2018 The evolution of host defence to parasitism in fluctuating environments. *J. Theor. Biol.* **440**, 58–65. (doi:10.1016/j.jtbi.2017.12.006)
41. Ferris C, Best A. 2019 The effect of temporal fluctuations on the evolution of host tolerance to parasitism. *Theor. Popul. Biol.* **130**, 182–190. (doi:10.1016/j.tpb.2019.07.015)
42. Grassly NC, Fraser C. 2006 Seasonal infectious disease epidemiology. *Proc. R. Soc. B* **273**, 2541–2550. (doi:10.1098/rspb.2006.3604)
43. Donnelly R, Best A, White A, Boots M. 2013 Seasonality selects for more acutely virulent parasites when virulence is density dependent. *Proc. R. Soc. B* **280**, 20122464. (doi:10.1098/rspb.2012.2464)
44. Koelle K, Pascual M, Yunus M. 2005 Pathogen adaptation to seasonal forcing and climate change. *Proc. R. Soc. B* **272**, 971–977. (doi:10.1098/rspb.2004.3043)
45. Carmona P, Gandon S. 2020 Winter is coming: pathogen emergence in seasonal environments. *PLoS Comput. Biol.* **16**, e1007954. (doi:10.1371/journal.pcbi.1007954)
46. Uecker H, Bonhoeffer S. 2018 Antibiotic treatment protocols revisited: the challenges of a conclusive assessment by mathematical modeling. *bioRxiv* 372938.
47. Bonhoeffer S, Lipsitch M, Levin BR. 1997 Evaluating treatment protocols to prevent antibiotic resistance. *Proc. Natl Acad. Sci. USA* **94**, 12 106–12 111. (doi:10.1073/pnas.94.22.12106)
48. Williams PD, Kamel SJ. 2018 The evolution of pathogen virulence: effects of transitions between host types. *J. Theor. Biol.* **438**, 1–8. (doi:10.1016/j.jtbi.2017.11.008)
49. Berngruber TW, Froissart R, Choisy M, Gandon S. 2013 Evolution of virulence in emerging epidemics. *PLoS Pathog* **9**, e1003209. (doi:10.1371/journal.ppat.1003209)
50. Day T, Proulx SR. 2004 A general theory for the evolutionary dynamics of virulence. *Am. Nat.* **163**, E40–E63. (doi:10.1086/382548)
51. Day T, Gandon S. 2007 Applying population-genetic models in theoretical evolutionary epidemiology. *Ecol. Lett.* **10**, 876–888. (doi:10.1111/j.1461-0248.2007.01091.x)
52. Chabas H, Lion S, Nicot A, Meaden S, van Houte S, Moineau S, Wahl LM, Westra ER, Gandon S. 2018 Evolutionary emergence of infectious diseases in heterogeneous host populations. *PLoS Biol.* **16**, e2006738. (doi:10.1371/journal.pbio.2006738)
53. Walter A, Lion S. 2021 Data from: Epidemiological and evolutionary consequences of periodicity in treatment coverage. Dryad Digital Repository. (https://doi.org/10.5061/dryad.nzs7h44q).

Annexe B: Supplementary Information : Epidemiological and evolutionary consequences of periodicity in treatment coverage

B.1 Typical behaviour of the heterogeneous model for various types of treatments

(a) Anti-infection (r_1)

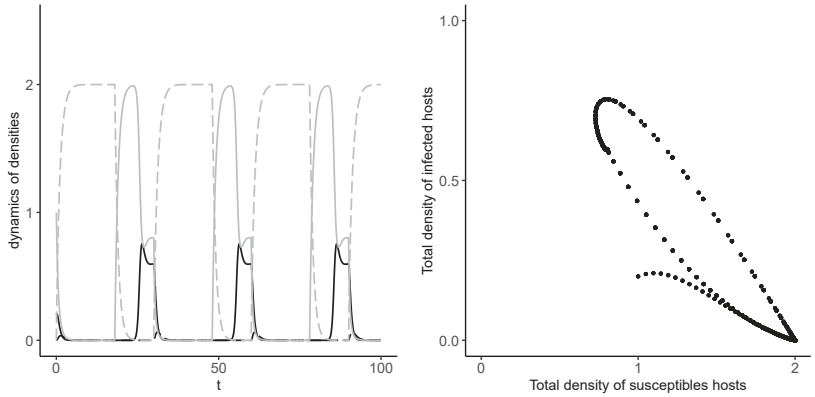

(b) Anti-transmission (r_3)

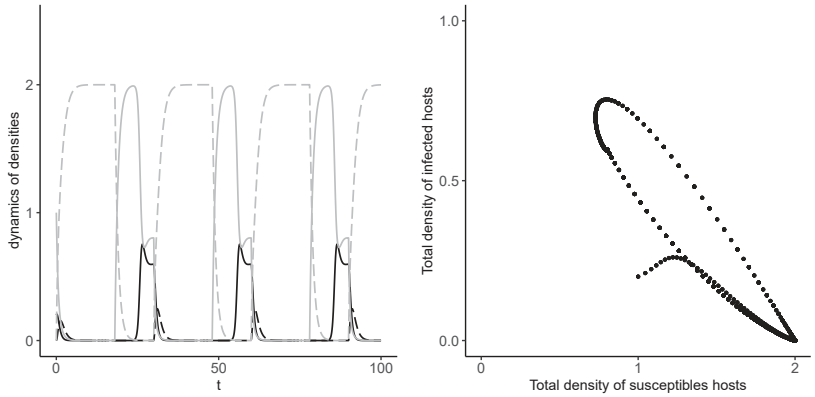

(c) Anti-toxin (r_4)

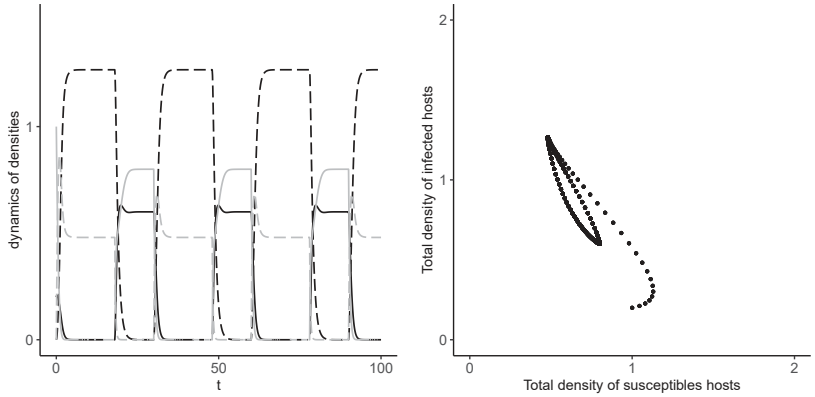

FIGURE B.1 – Dynamics of the model with anti-infection (a), anti-transmission (b) and anti-infection (c) treatments. ν takes the value 1 during pT (all newborns are treated), and the value 0 during $(1-p)T$ (no newborn is vaccinated). Left panels : Dynamics for the densities of susceptible naive (plain grey), susceptible treated (plain black), infected naive (dotted grey) and infected treated hosts (dotted black). Right panels : Corresponding periodic attractors. Parameters : $r_i = 0.8$, $p = 0.6$, $T = 30$, $\alpha = 1$, $b = 2$, $d = 1$.

B.2 Basic reproduction number R_0

2.1 Basic reproduction number in a constant environment

Omitting time dependency, we have the following equations for the densities of infected :

$$\begin{aligned} \dot{I}_N &= (\beta_N(z)I_N + \beta_T(z)I_T)S_N - (d + \alpha_N + \gamma_N(z))I_N\,, \\ \dot{I}_T &= (\beta_N(z)I_N + \beta_T(z)I_T)\sigma S_T - (d + \alpha_T + \gamma_T(z))I_T. \end{aligned}$$

In matrix form, the densities of infected hosts are associated to the Jacobian matrix $\mathbf{A}(t)$ at equilibrium, like :

$$\mathbf{A}(t) = \begin{pmatrix} S_N^0(t)\beta_N + (d + \alpha_N + \gamma_N) & S_N^0(t)\beta_T \\ \sigma S_T^0(t)\beta_N & \sigma S_T^0(t)\beta_T(\alpha) + (d + \alpha_T + \gamma_T) \end{pmatrix}. \tag{B.1}$$

The Jacobian matrix $\mathbf{A}$ can be written as $\mathbf{F}-\mathbf{V}$, with $\mathbf{F}$ the birth matrix and $\mathbf{V}$ the death matrix :

$$\begin{aligned} \mathbf{F}(t) &= \begin{pmatrix} S_N^0(t)\beta_N & S_N^0(t)\beta_T \\ \sigma S_T^0(t)\beta_N & \sigma S_T^0(t)\beta_T \end{pmatrix} \\ \mathbf{V} &= \begin{pmatrix} d + \alpha_N + \gamma_N & 0 \\ 0 & d + \alpha_T + \gamma_T \end{pmatrix} \end{aligned}$$

Since the elements of $\mathbf{V}^{-1}$ and $\mathbf{F}$ are positive and $-\mathbf{V}$ has strictly negative eigenvalues, we can apply the Next Generation Theorem, which states that the basic reproduction number in a constant environment correspond to the dominant eigenvalue of $F.V^{-1}$. Straightforward algebra then leads to :

$$R_0 = \frac{\beta_N(z)}{d + \alpha_N + \gamma_N(z)}\hat{S}_N + \frac{\beta_T(z)}{d + \alpha_T + \gamma_T(z)}\sigma\hat{S}_T\,.$$

2.2 Basic reproduction number in a periodic environment for anti-infection (r_1) and anti-transmission (r_3) treatments

Omitting time dependency, we have the following equations for densities of infected for anti-infection (r_1) and anti-transmission (r_3) treatments :

$$\begin{aligned} \dot{I}_N &= (\beta(z)I_N + (1-r_3)\beta(z)I_T)S_N - (d+\alpha+\gamma(z))I_N\,, \\ \dot{I}_T &= (\beta(z)I_N + (1-r_3)\beta(z)I_T)(1-r_1)S_T - (d+\alpha+\gamma(z))I_T\,, \end{aligned} \tag{B.2}$$

Setting $Z = I_N + (1-r_3)I_T$ the weighted total density of infected hosts, we obtain from system B.2 the scalar equation :

$$\dot{Z} = B(t)Z - D(t)Z \tag{B.3}$$

with $B(t) = \beta(\alpha)(S_N(t) + (1-r_1)(1-r_3)S_T(t))$ and $D(t) = (d+\alpha+\gamma(z))$. In this case, Bacaër & Guernaoui Bacaër and Guernaoui (2006) have shown that in a periodic environment R_0 can be calculated as :

$$R_0 = \frac{\int_0^T B(t)\,\mathrm{d}t}{\int_0^T D(t)\mathrm{d}t} \tag{B.4}$$

Gathering eq. (B.3) and eq. (B.4), we obtain the expression of the basic reproduction number for anti-infection and anti-transmission treatments, which corresponds to eq. (3.3) in the main text :

$$R_0 = \frac{\beta(z)}{d+\alpha+\gamma(z)}\left(\left\langle S_N^0\right\rangle + (1-r_1)(1-r_3)\left\langle S_T^0\right\rangle\right)\,,$$

where $\langle S_N^0\rangle$ and $\langle S_T^0\rangle$ are calculated in Appendix B.3. For anti-infection (r_1) and anti-transmission (r_3) treatments, the basic reproduction number in a periodic environment with average coverage $\bar{\nu}$

is equal to the basic reproduction number in an environment with constant coverage $\bar{\nu}$, as verified in figure B.2. Note also that r_1 and r_3 play the same role in the expression, hence the pathogen has the same R_0 in both cases, for a fixed treatment efficacy.

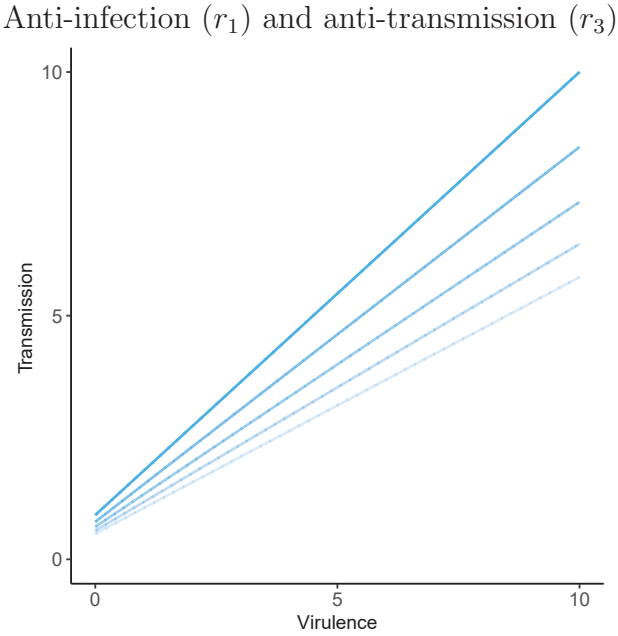

FIGURE B.2 – Invasion boundaries (lines $R_0 = 1$) calculated with Floquet's exponent as a function of the transmission rate β and the virulence α, for the anti-infection and anti-transmission treatments (the results are identical for both treatments), with $T = 2$ and $p = 0.5$. Efficacies are represented as a gradient of transparency where $r_i = 0.1$ (lighter), $r_i = 0.3$ $r_i = 0.5$, $r_i = 0.7$ and $r_i = 0.9$ (darker). Here there is no difference between the periodic treatment coverage (solid line) and the constant treatment coverage (dotted line).

2.3 Basic reproduction number in a periodic environment for anti-growth (r_2) and anti-toxin (r_4) treatments

The densities of infected hosts can be written in matrix form :

$$\frac{\mathrm{d}}{\mathrm{d}t}\begin{pmatrix} I_N \\ I_T \end{pmatrix} = \mathbf{A}(t).\begin{pmatrix} I_N \\ I_T \end{pmatrix},$$

with

$$\mathbf{A}(t) = \begin{pmatrix} S_N^0(t)\beta_N(z) - (d + \alpha_N + \gamma_N(z)) & S_N^0(t)\beta_T(z) \\ \sigma S_T^0(t)\beta_N(z) & \sigma S_T^0(t)\beta_T(z) - (d + \alpha_T + \gamma_T(z)) \end{pmatrix}$$

The Jacobian matrix $\mathbf{A}(t)$ can be written as $\mathbf{A}(t) = \mathbf{F}(t) - \mathbf{V}$, with $\mathbf{F}(t)$ the periodic fecundity matrix and $\mathbf{V}$ the mortality matrix :

$$\mathbf{F}(t) = \begin{pmatrix} S_N^0(t)\beta_N(z) & S_N^0(t)\beta_T(z) \\ \sigma S_T^0(t)\beta_N(z) & \sigma S_T^0(t)\beta_T(z) \end{pmatrix}$$

$$\mathbf{V} = \begin{pmatrix} d + \alpha_N + \gamma_N & 0 \\ 0 & d + \alpha_T + \gamma_T \end{pmatrix}$$

To compute R_0, we follow Bacaër Bacaër (2011) and we solve the following matrix ODE over one period of the disease-free attractor :

$$\frac{\mathrm{d}\mathbf{X}}{\mathrm{d}t} = \frac{\mathbf{F}(t)}{R_0}.\mathbf{X} - \mathbf{V}.\mathbf{X}\,, \tag{B.5}$$

with initial condition $\mathbf{X}(0) = \begin{pmatrix} 1 & 0 \\ 0 & 1 \end{pmatrix}$. We numerically calculate the dominant eigenvalue of $\mathbf{X}(T)$, ρ, which is the Floquet multiplier, for values of R_0 varying by dichotomy. The value of R_0 that corresponds to $\rho = 1$ is the value of the basic reproduction number of the population (Bacaër, 2011). This gives the invasion threshold on figure B.3.

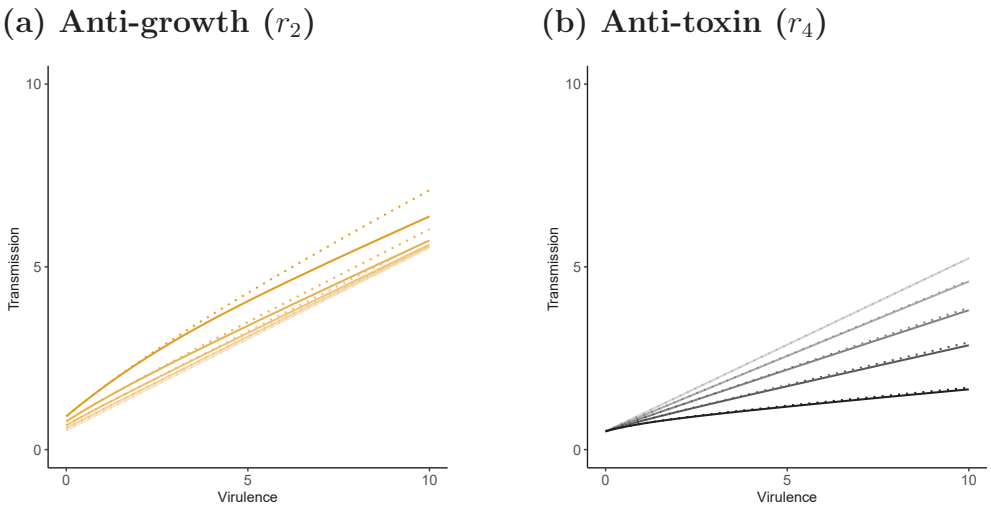

FIGURE B.3 – Invasion boundaries ($R_0 = 1$ lines) as a function of the transmission rate β and the virulence α, for (a) anti-growth (r_2) and (b) anti-toxin (r_4) treatments, with $T = 2$ and $p = 0.5$. The efficacy of treatments are shown in different colours : in shades of orange for anti-growth (r_2) and in shades of black for anti-toxin (r_4). The efficacy takes the values $r_i = 0.1, 0.3, 0.5, 0.7,, 0.9$, represented in a gradient of transparency, from light to dark. The periodic treatment coverage (solid line) is compared to the constant treatment coverage (dotted line).

2.4 Invasion threshold as a function of r and p

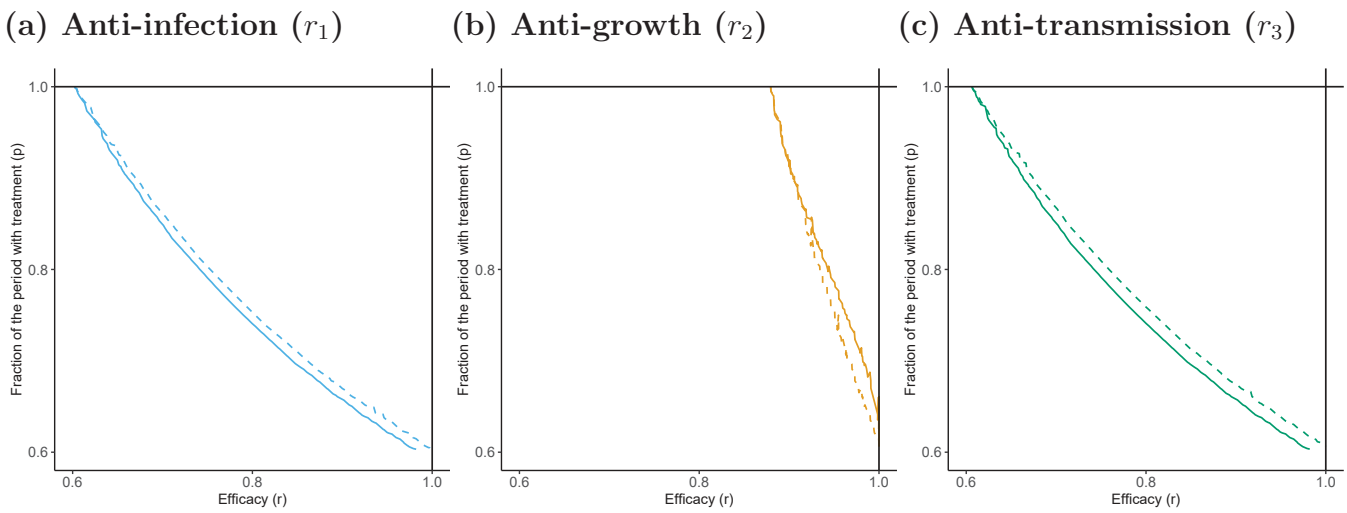

FIGURE B.4 – Conditions of persistence of the pathogen in hosts populations according to the efficacy of the treatment (r), and the proportion of maximal treatments (p), for (a) anti-infection, (b) anti-growth and (c) anti-transmission treatments, with a periodic coverage (solid lines) or a constant coverage (dotted lines) The pathogen goes extinct above the curves (top right corner) and persist under. Anti-toxin is not shown because in this case, the pathogen persist in the population. Here $b = 2$, $d = 1$, $T = 10$, $\alpha = 1$.

B.3 Disease-free dynamics

The dynamics of susceptible hosts in the absence of disease are such that :

$$\begin{aligned} \dot{S}_N(t) &= (1-\nu(t))b - dS_N(t)\,, \\ \dot{S}_T(t) &= \nu(t)b - dS_T(t)\,. \end{aligned} \tag{B.6}$$

Let $S_N^0(t)$ and $S_T^0(t)$ be the (periodic) solutions of the system on the disease-free attractor. For a function f on the attractor, we define $\langle f \rangle = \int_0^T f(t)\,\mathrm{d}t$. On the attractor, we have $\left\langle \dot{S}_N \right\rangle =$

$\left\langle \dot{S}_T \right\rangle = 0$, which leads to :

$$\begin{aligned} \left\langle S_N^0 \right\rangle &= \frac{b\int_0^T (1-\nu(t))\mathrm{d}t}{d} = \frac{(1-\bar{\nu})b}{d}\,, \\ \left\langle S_T^0 \right\rangle &= \frac{b\int_0^T \nu(t)\mathrm{d}t}{d} = \frac{\bar{\nu}b}{d} \end{aligned} \tag{B.7}$$

Equations (C.1) can be written as $\dot{\mathbf{X}}(t) = \mathbf{A}(t).\mathbf{X} + \mathbf{b}(t).\mathbf{X}$, where

$$\mathbf{X} = \begin{pmatrix} S_N(t) \\ S_T(t) \end{pmatrix}, \qquad \mathbf{A}(t) = \begin{pmatrix} -d & 0 \\ 0 & -d \end{pmatrix} \qquad \text{and} \qquad \mathbf{b}(t) = \begin{pmatrix} (1-\nu(t)) \\ \nu(t) \end{pmatrix}.$$

As shown by Perko Perko (2013), for $\mathbf{A}(t)$ a $(n\times n)$ matrix and $\mathbf{b}(t)$ a vector of continuous functions, the solutions of the nonhomogeneous linear system has the form $\mathbf{X}(t) = e^{\mathbf{A}.t} + \left(\mathbf{X}(0) + \int_0^t e^{-\mathbf{A}.s}.\mathbf{b}(s)\mathrm{d}s\right)$. Applied to our system, the periodical solution of our system on the disease free periodic attractor is :

$$\begin{aligned} S_N^0(t) &= e^{-dt}\left(S_N(0) + \int_0^t e^{ds}(1-\nu(s))b\,\mathrm{d}s\right), \\ S_T^0(t) &= e^{-dt}\left(S_T(0) + \int_0^t e^{ds}\nu(s)b\,\mathrm{d}s\right). \end{aligned} \tag{B.8}$$

B.4 Evolutionary dynamics

4.5 Resident-mutant dynamics

The full model including the mutant dynamics is

$$\begin{aligned}
\frac{\mathrm{d}S_N}{\mathrm{d}t} &= (1-\nu(t))b - (d + h_N + h'_N)S_N + (\gamma_N + \gamma'_N)S_N\,,\\
\frac{\mathrm{d}S_T}{\mathrm{d}t} &= \nu(t)b - (d + h_T + h'_T)S_T + (\gamma_T + \gamma'_T)S_T\,,\\
\frac{\mathrm{d}I_N}{\mathrm{d}t} &= (\beta_N(z)I_N + \beta_T(z)I_T)S_N - (d + \alpha_N + \gamma_N(z))I_N\,,\\
\frac{\mathrm{d}I_T}{\mathrm{d}t} &= (\beta_N(z)I_N + \beta_T(z)I_T)\sigma S_T - (d + \alpha_T + \gamma_T(z))I_T\,,\\
\frac{\mathrm{d}I'_N}{\mathrm{d}t} &= (\beta_N(z')I'_N + \beta_T(z')I'_T)S_N - (d + \alpha'_N + \gamma_N(z'))I'_N\,,\\
\frac{\mathrm{d}I'_T}{\mathrm{d}t} &= (\beta_N(z')I'_N + \beta_T(z')I'_T)\sigma S_T - (d + \alpha'_T + \gamma_T(z'))I'_T\,.
\end{aligned} \tag{B.9}$$

with

$$\alpha'_T = (1-r_2)(1-r_4)z'\,, \qquad \alpha'_N = z'$$

4.6 Analytical derivation for the selection gradient using time-dependent reproductive values

We start with equation (23) in Lion (2018*a*), which gives the selection gradient for a class-structured population on a periodic attractor. For our model, this gives

$$\mathcal{S} = \left\langle \mathbf{v}^\top \left.\frac{\mathrm{d}\mathbf{A}'}{\mathrm{d}z'}\right|_{z'=z} \mathbf{f}^\top \right\rangle \tag{B.10}$$

where $\mathbf{v}(t)$ is the vector of reproductive values at time t, $\mathbf{f}(t)$ is the vector of class frequencies at time t, and $\mathbf{A}'(t)$ is the matrix given by (B.22). Equation (23) in Lion (2018*a*) can be derived by computing the dynamics of the reproductive-value weighted mean trait, then assuming that

the trait distribution is tightly clustered around its mean (weak selection), so that the dynamics of the mean trait is approximately proportional to the neutral variance times $\mathbf{v}^\top \frac{\mathrm{d}\mathbf{A}'}{\mathrm{d}z'}\big|_{z'=z} \mathbf{f}^\top$. Since the neutral variance is constant on the periodic attractor, the sign of $\mathcal{S}$ is sufficient to predict the direction of selection. w Expanding the right-hand side of eq. (B.10) yields after some rearragements

$$\mathcal{S} = \left\langle c_N \left(\beta'_N(z) \frac{v_N \hat{S}_N(t) + v_T \sigma \hat{S}_T(t)}{v_N} - \alpha'_N(z) \right) + c_T \left(\beta'_T(z) \frac{v_N \hat{S}_N(t) + v_T \sigma \hat{S}_T(t)}{v_T} - \alpha'_T(z) \right) \right\rangle \tag{B.11}$$

where $c_N(t) = v_N(t) f_N(t)$ is the class reproductive value of parasites in naive hosts, and $c_T(t) = v_T(t) f_T(t)$ is the class reproductive values in treated hosts. Note that the class reproductive values are normalised so that $c_N(t) + c_T(t) = 1$.

In eq. (B.11), the reproductive values and class frequencies are computed in a neutral (or monomorphic) populatio. In matrix form, the dynamics of the densities of infected hosts in the resident population can be written as

$$\frac{\mathrm{d}}{\mathrm{d}t} \begin{pmatrix} I_N \\ I_T \end{pmatrix} = \mathbf{A}(t) \begin{pmatrix} I_N \\ I_T \end{pmatrix} \tag{B.12}$$

with

$$\mathbf{A}(t) = \begin{pmatrix} \beta_N S_N(t) - (d + \alpha_N) & \beta_T S_N(t) \\ \beta_N \sigma_T S_T(t) & \beta_T \sigma_T S_T(t) - (d + \alpha_T) \end{pmatrix}. \tag{B.13}$$

Following Lion (2018*a*), the vector of class frequencies $\mathbf{f} = \begin{pmatrix} f_N & f_T \end{pmatrix}^\top$ has dynamics

$$\frac{\mathrm{d}\mathbf{f}}{\mathrm{d}t} = \mathbf{A}(t)\mathbf{f} - r(t)\mathbf{f} \tag{B.14}$$

where $r(t) = \mathbf{1}^\top \mathbf{A}(t)\mathbf{f}$ is the total growth rate of the population, while the dynamics of the vector

of reproductive values, $\mathbf{v}$, is given by the adjoint equation

$$\frac{\mathrm{d}\mathbf{v}^\top}{\mathrm{d}t} = -\mathbf{v}^\top \mathbf{A}(t) + r(t)\mathbf{v}^\top \tag{B.15}$$

(note that $\mathbf{v}^\top$ is a row vector). The reproductive values $v_N(t)$ and $v_T(t)$ give the "value" of a parasite in class N and T respectively, at time t, i.e. how much future descendance this parasite can expect at time t.

In general, the reproductive values on the periodic attractor can only be calculated numerically, but even without calculating the reproductive values, we can make some analytical progress by noting that

$$\frac{1}{v_N}\frac{\mathrm{d}v_N}{\mathrm{d}t} = -\beta_N \omega_N + (d + \alpha_N + r(t)) \tag{B.16}$$

where, for $k = N$ or T,

$$\omega_k = \frac{v_N \hat{S}_N(t) + v_T \sigma \hat{S}_T(t)}{v_k}. \tag{B.17}$$

Integrating eq. (B.16) over one period, we obtain

$$\langle \omega_N \rangle = \frac{d + \alpha_N}{\beta_N}. \tag{B.18}$$

From the dynamics of $v_T(t)$, we similarly obtain

$$\langle \omega_T \rangle = \frac{d + \alpha_T}{\beta_T}. \tag{B.19}$$

Hence ω_N and ω_T fluctuate around $(d + \alpha_N)/\beta_N$ and $(d + \alpha_T)/\beta_T$ respectively. An interpretation of ω_k is as follows : the numerator indicates the average value of an "offspring", i.e. a parasite propagule landing on a new host (either a naive host, with "probability" S_N, in which case the propagule has value v_N, or a treated host, with "probability" S_T, in which case the propagule has value v_T), and the denominator gives the value of the "adult" parasite in class k. So ω_k gives the

relative value of an offspring relative to the value of an adult in class k.

We can use this result and the definition of a covariance to simplify eq. (B.11) as

$$\begin{aligned}\mathcal{S} = \langle c_N \rangle \left(\beta'_N(z) \frac{d + \alpha_N}{\beta_N} - \alpha'_N(z) \right) + \langle c_T \rangle \left(\beta'_T(z) \frac{d + \alpha_T}{\beta_T} - \alpha'_T(z) \right) \\ + \beta'_N(z) \mathrm{Cov}\left(c_N, \omega_N\right) + \beta'_T(z) \mathrm{Cov}\left(c_T, \omega_T\right).\end{aligned} \tag{B.20}$$

The second line depends on the temporal covariances between the class reproductive values $c_k(t)$ and the relative offspring values $\omega_k(t)$. To obtain our final approximation, we simply neglect these terms, which can be expected to be of second order for small fluctuations, so that the selection gradient can be written as

$$\mathcal{S} = \langle c_N \rangle \left(\beta'_N(z) \frac{d + \alpha_N}{\beta_N} - \alpha'_N(z) \right) + \langle c_T \rangle \left(\beta'_T(z) \frac{d + \alpha_T}{\beta_T} - \alpha'_T(z) \right) \tag{B.21}$$

as in the main text. Note that $\langle c_N \rangle + \langle c_T \rangle = 1$, so that $\mathcal{S}$ takes the form of a weighted sum of the class-specific selection gradients (the terms between brackets).

For the anti-toxin treatment, straightforward simplifications leads to eq. (4.5) in the main text.

Note that, with our periodic step function $\nu(t)$, it is easy to see that, in the limit of large periods, $c_T(t)$ tends towards $\nu(t)$, and therefore $\langle c_T \rangle = \bar{\nu} = p$. Indeed, when T is large, the system essentially behaves as a succession of homogeneous equilibrium populations with either $\nu = 0$ or $\nu = 1$. When $\nu = 1$ (i.e during a fraction p of the period), only treated hosts are present, so that $c_T = 1$. When $\nu = 0$, only untreated hosts are present, so that $c_T = 0$. Hence, $\langle c_T \rangle = p$. This can be confirmed numerically (results not shown).

4.7 Numerical calculation of invasion fitness using Floquet's theory

Invasion fitness can be numerically calculated as the dominant Floquet exponent associated with the matrix

$$\mathbf{A}'(t) = \begin{pmatrix} \hat{S}_N(t)\beta_N(z') - (d + \alpha_N(z') + \gamma_N(z')) & \hat{S}_N(t)\beta_T(z') \\ \sigma\hat{S}_T(t)\beta_N(z') & \sigma\hat{S}_T(t)\beta_T(z') - (d + \alpha_T(z') + \gamma_T(z')) \end{pmatrix} \quad \text{(B.22)}$$

where $\hat{S}_N(t)$ and $\hat{S}_T(t)$ are the densities of susceptible hosts on the endemic attractor. That is, we use the same method as in Appendix B.2, but evaluate the invasion matrix on the endemic attractor instead of the disease-free attractor. As for the epidemiological R_0 in appendix B.2, the Floquet multiplier ρ is related to the invasion fitness R', through the relationship $\rho > 1 \Leftrightarrow R' > 1$. For anti-infection ($r_1$) and anti-transmission (r_3) treatments, this allows us to check that periodicity has no effect on the ES virulence (figure B.5), as predicted by our direct analytical calculation of the mutant's basic reproduction number (equation (4.1) in the main text). The numerical calculations using Floquet's theory for anti-growth and anti-toxin treatments are shown in figures B.6 and B.7, respectively according to the period T and the fraction of the period with treatment p.

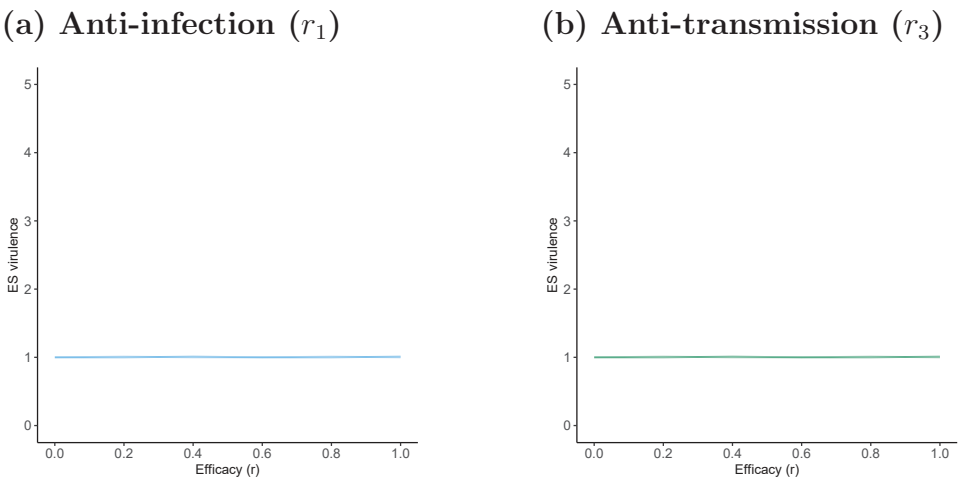

FIGURE B.5 – Numerical calculation of the evolutionarily stable virulence for anti-infection (r_1) and anti-transmission (r_3) treatments.

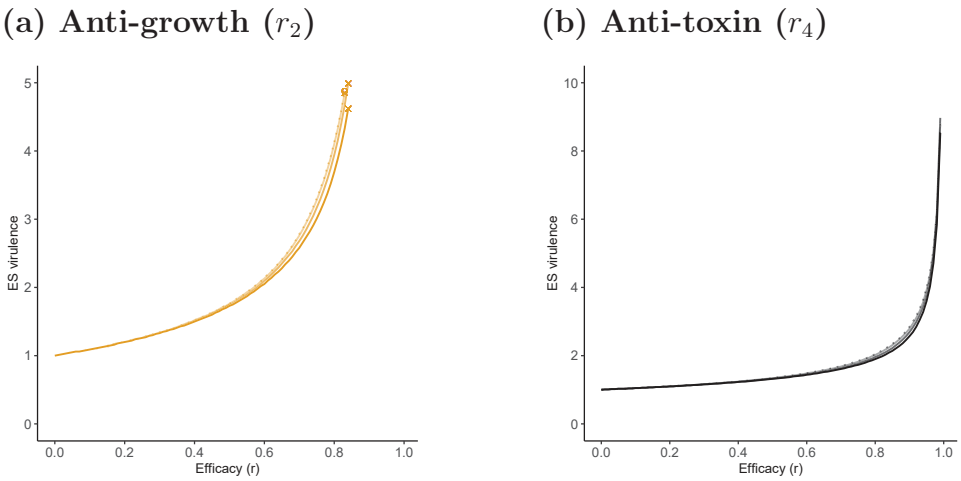

FIGURE B.6 – Numerical calculation of the evolutionarily stable virulence for (a) anti-growth treatment in shape of orange and (b) anti-toxin treatment in shape of black, with a periodic treatment coverage (solid lines) and different periods : $T = 2$ (lighter), $T = 5$, $T = 8$ (darker). Compared to a constant treatment coverage with $p = \bar{\nu} = 0.8$ (dotted line), with the extinction thresholds for anti-growth treatment with a periodic coverage (orange crosses) or constant coverage (orange circle).

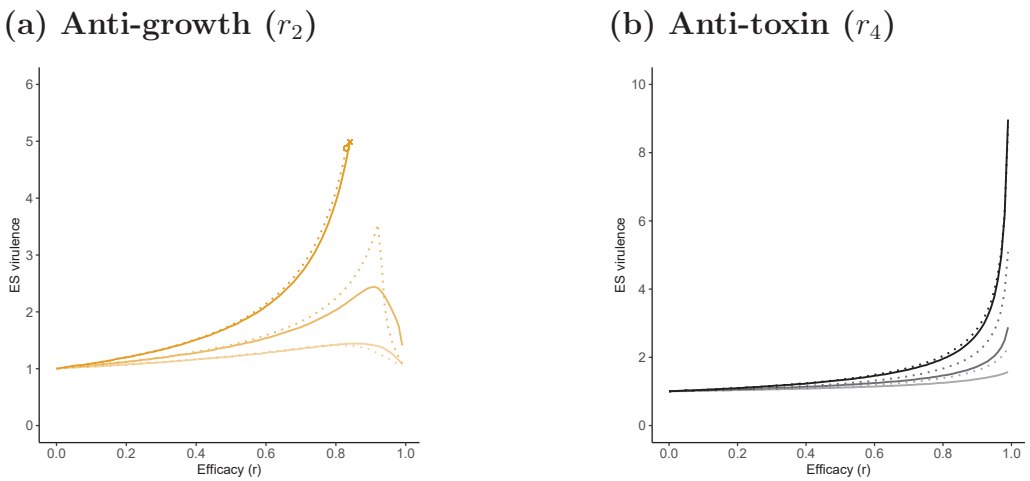

FIGURE B.7 – Numerical calculation of the evolutionarily stable virulence for (a) anti-growth treatment (orange) and (b) anti-toxin treatment (black), with a periodic treatment coverage (solid lines) and different values of $p : p = 0.3$ (lighter), $p = 0.5$ or $p = 0.8$ (darker), for $T = 5$. Compared to a constant treatment coverage with $\bar{\nu} = p$ (dotted line), with the extinction thresholds for anti-growth treatment with a periodic coverage (orange crosses) or constant coverage (orange circle).

B.5 Impact of recovery

To highlight the effect of a non-zero recovery on our study, we set $\gamma = \gamma_N = \gamma_T$, and we perform numerical simulations for different values of γ. On figure B.8 we see that a non-zero recovery affects the prevalence of the disease. For anti-infection, anti-growth and anti-transmission treatments we observe a lower extinction threshold, while for anti-toxin treatments, recovery increases the prevalence. The quantitative effect on virulence evolution appears small, except for near-perfect anti-growth treatments.

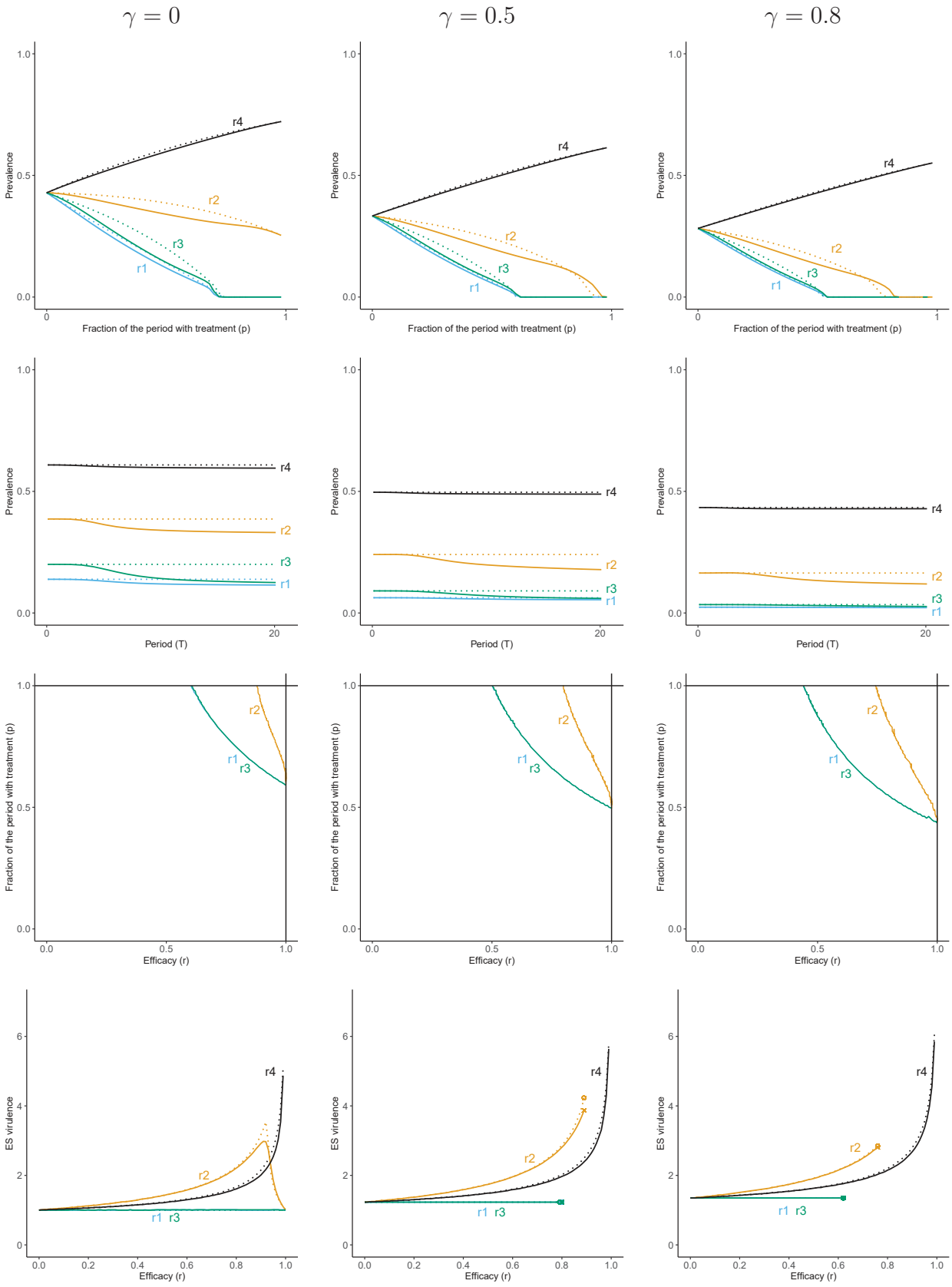

FIGURE B.8 – Effect of a non-zero recovery on the prevalence and p (first line), on the prevalence and T (second line), the extinction threshold (third line) and the evolution of virulence (fourth line), for anti-infection (blue), anti-growth (orange), anti-transmission (green) and anti-toxin (black). Left panels : $\gamma = 0$ (as in the main text). Middle panels : $\gamma = 0.5$. Right panels : $\gamma = 0.8$.

B.6 Impact of the shape of the coverage functions

To check the robustness of our results, we performed simulations with a different function for treatment coverage : $\nu(t) = \frac{1}{2}\left(1 + \frac{\arctan(\sin(2\pi\omega t)/\delta)}{\arctan(1/\delta)}\right)$, which approximates a square wave for $\delta \approx 0$, and a sine wave when δ becomes large. For all values of δ, $\bar{\nu} = 1/2$.

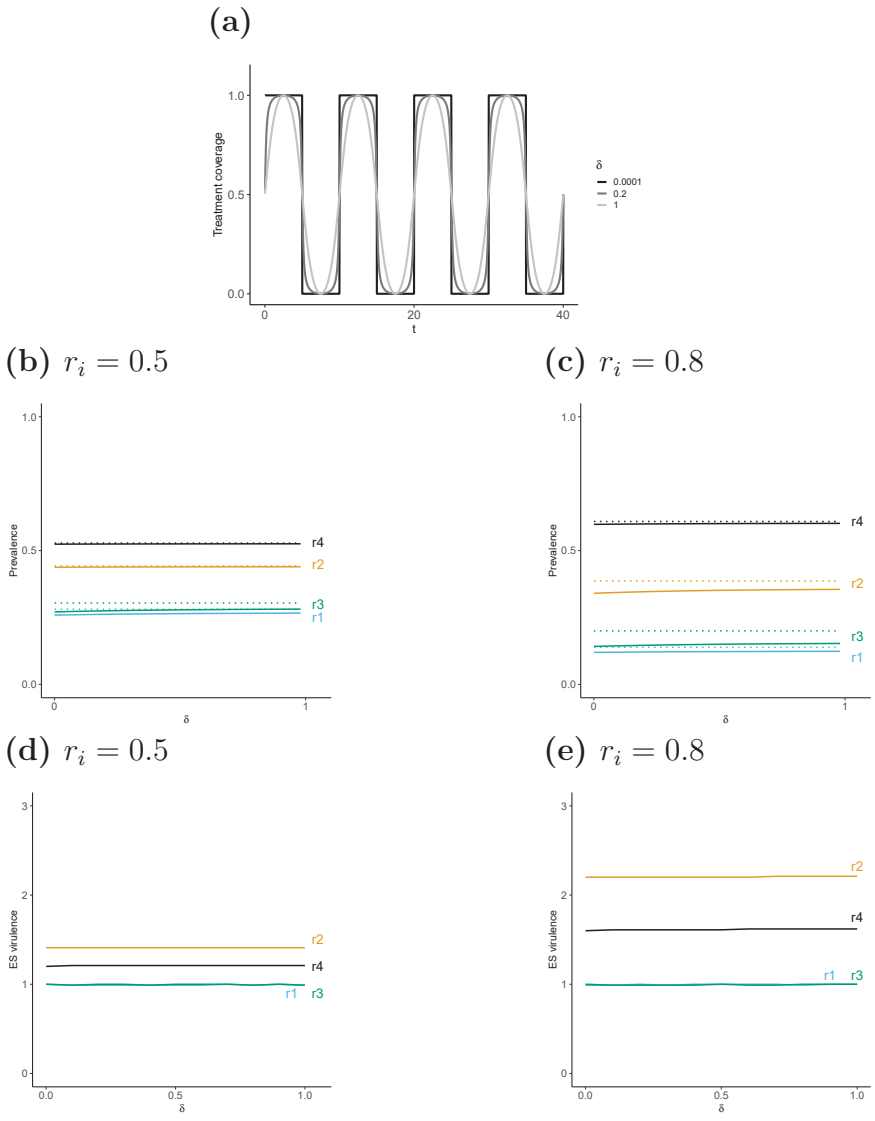

FIGURE B.9 – Effect of (a) different shapes treatment coverage functions defined by δ, on (b,c) the prevalence and (d,e) the evolutionarily stable virulence, for anti-infection (blue), anti-growth (orange), anti-transmission (green) and anti-toxin (black) treatments, associated to the periodic coverage (solid lines) or the respective average coverage (dotted lines). Here $p = 0.5$, $T = 10$.

Annexe C: Annexes du chapitre 2

C.1 Epidemiology

1.1 Equilibrium

In a disease free environment, we have an equilibrium of susceptible hosts (S^N_{0A}, S^T_{0A}, S^N_{0B}, S^T_{0B}), that can be calculated as :

$$\left(\frac{(1-\nu_A)b}{d}, \frac{\nu_A b}{d}, \frac{(1-\nu_B)b}{d}, \frac{\nu_B b}{d}\right), \tag{C.1}$$

We do not have explicit expression for the endemic equilibrium.

1.2 Basic reproduction number

Using Next Generation theorem, whose conditions are fulfilled, pathogen basic reproduction number in the metapopulation is given by the dominant eigen value of matrix $\mathbf{F}.\mathbf{V}^{-1}$ (Hurford et al., 2009) :

$$\mathbf{F}.\mathbf{V}^{-1} = \begin{pmatrix} (1-m)S^N_{A0}R^N_A & (1-m)S^N_{A0}R^T_A & mS^N_{A0}R^N_B & m\beta^T_B S^N_{A0}R^T_B \\ \sigma(1-m)S^T_{A0}R^N_A & \sigma(1-m)S^T_{A0}R^T_A & \sigma mS^T_{A0}R^N_B & \sigma mS^T_{A0}R^T_B \\ mS^N_{B0}R^N_A & mS^N_{B0}R^T_A & (1-m)S^N_{B0}R^N_B & (1-m)S^N_{B0}R^T_B \\ \sigma mS^T_{B0}R^N_A & mS^T_{B0}R^T_A & \sigma(1-m)S^T_{B0}R^N_B & \sigma(1-m)S^T_{B0}R^T_B \end{pmatrix}. \tag{C.2}$$

It leads to the expression of the R_0 as

$$R_0 = \frac{1}{2}\left((1-m)(R_{0A}+R_{0B}) + \sqrt{4(2m-1)R_{0A}R_{0B} + (1-m)^2(R_{0A}+R_{0A})^2}\right). \tag{C.3}$$

with, $R_{0k} = R^N_k S^N_{0k} + \sigma R^T_k S^T_{0k}$, the basic reproduction number in population k, where $R^N_k = \beta^N_k/(d+\alpha^N_k)$, and $R^T_k = \beta^T_k/(d+\alpha^T_k)$. S^N_{0k} and S^T_{0k} are the susceptible hosts densities in population

k in the absence of disease and are expressed as eq. C.1.

1.3 Prevalence

On figure C.10, it show the prevalence calulated as

$$prev = \frac{\hat{I}_A^N + \hat{I}_A^T + \hat{I}_B^N + \hat{I}_B^T}{\hat{S}_A^N + \hat{S}_A^T + \hat{S}_B^N + \hat{S}_B^T + \hat{I}_A^N + \hat{I}_A^T + \hat{I}_B^N + \hat{I}_B^T}$$

function of the migration for different values of δ. It appears that an equal distribution of doses between population A and B leads lower prevalence than a heterogeneous distribution of doses for anti-infection and anti-transmission treatments. For anti-toxin treatment there is very low effect of different doses distributions. For anti-growth treatment, a highly heterogeneous distribution of doses lower the prevalence for low migration rates.

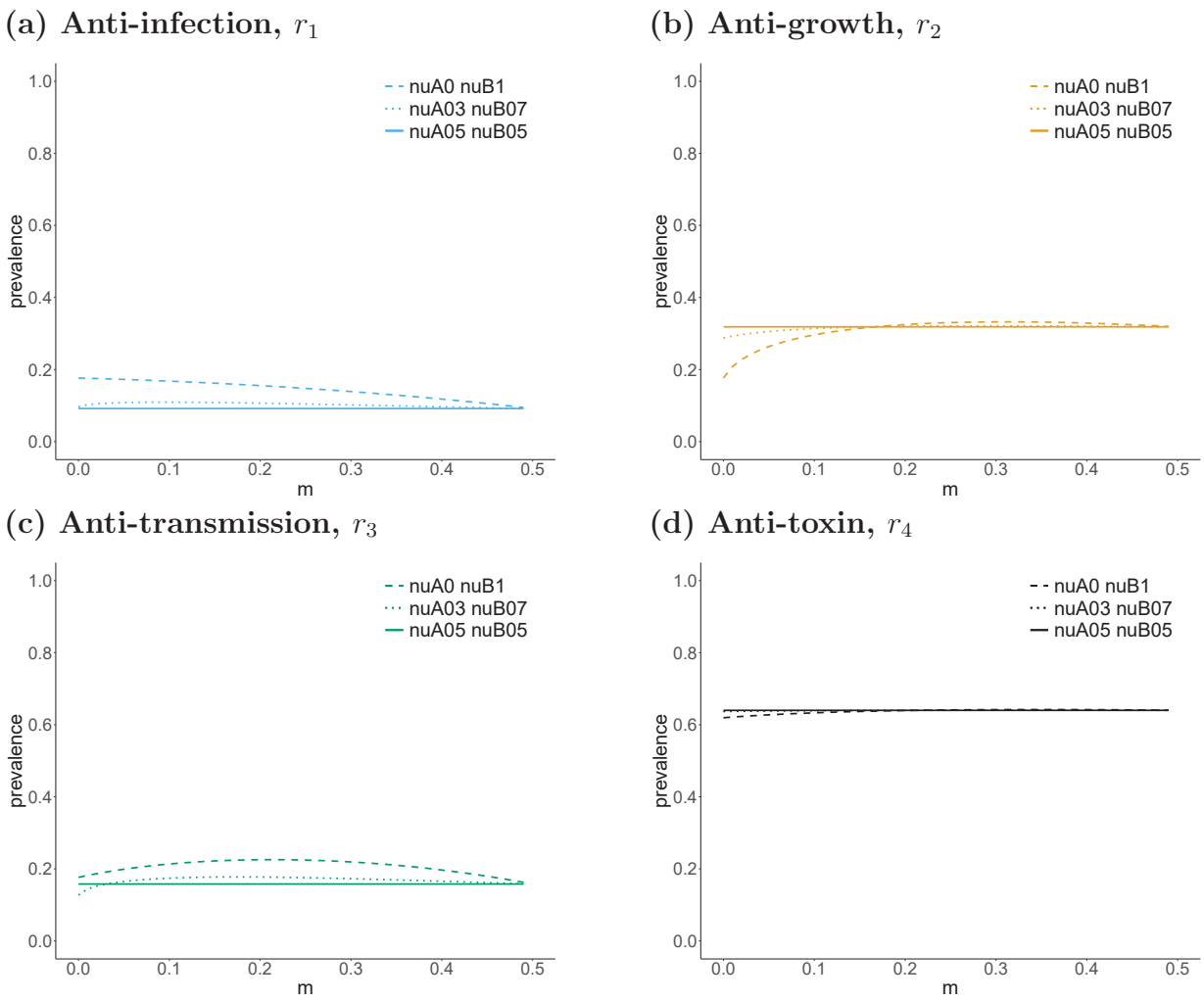

FIGURE C.10 – Prevalence according to the migration rate m for (a) anti-infection, (b) anti-growth, (c) anti-transmission and (d) anti-toxin treatments. Linetype correspond to different distribution of doses, with $\nu_A = 0$, $\nu_B = 1$ in dashed lines, $\nu_A = 0.3$, $\nu_B = 0.7$ in dotted lines, $\nu_A = \nu_B = 0.5$ in solid lines, and $r_i = 0.9$.

C.2 Evolution

2.4 Mutant invasion fitness

The mutant invasion fitness correspond to the dominant eigenvalue if the matrix $\mathbf{F}'.\mathbf{V}'^{-1}$ (analogous to $\mathbf{F}.\mathbf{V}^{-1}$ shown in eq. (C.2). It leads to :

$$R(z,z') = \frac{1}{2}\left((1-m)(R'_A+R'_B) + \sqrt{4(2m-1)R'_AR'_B + (1-m)^2(R'_A+R'_B)^2}\right), \qquad \text{(C.4)}$$

2.5 Selection gradient expression

The selection gradient corresponds to the derivative of the mutant invasion fitness when $z = z'$,

$$\mathcal{S} = \left.\frac{\partial R(z,z')}{\partial z'}\right|_{z'=z}.$$

With $R(z,z') = 1$, we have the following equality :

$$\sqrt{4(2m-1)(R_AR_B) + (1-m)^2(R_A+R_B)^2} \;=\; 2-(1-m)(R_A+R_B) \qquad \text{(C.5)}$$

that can be used to express the selection gradient as

$$\mathcal{S} = \left(\frac{1-m}{2}\right)(\partial R'_A + \partial R'_B) + \frac{1}{4}\frac{4(2m-1)(\partial R'_AR_B + R_A\partial R'_B) + 2(1-m)^2(R_A+R_B)(\partial R'_A+\partial R'_B)}{2-(1-m)(R_A+R_B)}. \qquad \text{(C.6)}$$

From eq.C.5, we can go further in simplifying the expression as

$$\begin{aligned}
\Leftrightarrow 4(2m-1)(R_A R_B) + (1-m)^2(R_A+R_B)^2 &= (2-(1-m)(R_A+R_B))^2 \\
\Leftrightarrow 4(2m-1)(R_A R_B) + (1-m)^2(R_A+R_B)^2 &= 4+(1-m)^2(R_A+R_B)^2 - 4(1-m)(R_A+R_B) \\
\Leftrightarrow (1-m)(R_A+R_B) + (2m-1)R_A R_B &= 1 \qquad \text{(C.7)}
\end{aligned}$$

Note that

$$\begin{aligned}
X_A R_A + X_B R_B &= \frac{2(2m-1)R_A R_B + (1-m)(R_A+R_B)}{2-(1-m)(R_A+R_B)} \\
&= \frac{2\left(1-(1-m)(R_A+R_B)\right) + (1-m)(R_A+R_B)}{2-(1-m)(R_A+R_B)}
\end{aligned}$$

Coupled with (C.7), we have $X_A R_A + X_B R_B = 1$.

2.6 Second order derivative calculation

The second order derivative informs about the stability of singularities and is given by

$$\mathcal{D} = \left.\frac{\partial^2 R(z,z')}{\partial z'^2}\right|_{z'=z=z^*}. \qquad \text{(C.8)}$$

If $\mathcal{D} < 0$ the evolutionary singularity is stable and pathogen traits converges towards this value. If $\mathcal{D} > 0$, the singularity is unstable and diverge from this value. In our model, the second derivation of eq (3.3) leads to :

$$\begin{aligned}
\mathcal{D} = \frac{1}{2}\Big(&(1-m)(\partial^2 R'_A + \partial^2 R'_B) \qquad \text{(C.9)} \\
&+ \frac{4(2m-1)(\partial^2 R'_A R_B + \partial^2 R'_B R_A + 2\partial R'_A \partial R'_B) + 2(1-m)^2\left((\partial R'_A + \partial R'_B)^2 + (R_A+R_B)(\partial^2 R'_A + \partial^2 R'_B)\right)}{2\sqrt{4(2m-1)R_A R_B + (1-m)^2(R_A+R_B)^2}} \\
&- \frac{\left(4(2m-1)(\partial R'_A R_B + R_A \partial R'_B) + 2(1-m)^2(R_A+R_B)(\partial R'_A + \partial R'_B)\right)^2}{4\left(4(2m-1)R_A R_B + (1-m)^2(R_A+R_B)^2\right)^{3/2}}\Big).
\end{aligned}$$

Expression (C.9) can be dissociated in : $X_A\partial^2 R'_A + X_B\partial^2 R'_B + \kappa$, with :

$$\begin{aligned} X_A &= \frac{(2m-1)R_B + (1-m)}{2-(1-m)(R_A+R_B)} \\ X_B &= \frac{(2m-1)R_A + (1-m)}{2-(1-m)(R_A+R_B)} \\ \kappa &= -\frac{2m^2(2m-1)(\partial R'_A - \partial R'_B)^2}{(2-(1-m)(R_A+R_B))^3}\,. \end{aligned} \tag{C.10}$$

We have

$$\begin{aligned} X_A X_B &= \frac{(1-m)^2 + (1-2m)^2 R_A R_B - (1-2m)(1-m)(R_A+R_B)}{\left(2-(1-m)(R_A+R_B)\right)^2}\,, \\ &= \frac{(1-m)^2 - (1-2m)}{\left(2-(1-m)(R_A+R_B)\right)^2}\,, \\ &= \frac{m^2}{\left(2-(1-m)(R_A+R_B)\right)^2} \end{aligned} \tag{C.11}$$

We can then rewrite κ as :

$$\kappa = -2(X_A X_B)^{3/2}\frac{2m-1}{m}\left(\partial R'_A R_B - \partial R'_B R_A\right)^2\,. \tag{C.12}$$

Using $c_A = X_A R_A = 1 - c_B = 1 - X_B R_B$, we can express the second order derivative as

$$\mathcal{D} = c_A\frac{\partial^2 R'_A}{R_A} + c_B\frac{\partial^2 R'_B}{R_B} + 2(c_A c_B)^{3/2}\sqrt{R_A R_B}\left(\frac{\partial R'_A}{R_A} - \frac{\partial R'_B}{R_B}\right)^2\frac{1-2m}{m} \tag{C.13}$$

which correspond to the equation (3.6) in the main text.

C.3 R_A and R_B and their derivatives

$$
\begin{aligned}
R'_A &= \hat{S}^N_A R^N_A + \sigma \hat{S}^T_A R^T_A = \hat{S}^N_A \frac{\beta^N_A[z']}{d+\alpha^N_A[z']} + \sigma \hat{S}^T_A \frac{\beta^T_A[z']}{d+\alpha^T_A[z']}\,, \\
R'_B &= \hat{S}^N_B R^N_B + \sigma \hat{S}^T_B R^T_B = \hat{S}^N_B \frac{\beta^N_B[z']}{d+\alpha^N_B[z']} + \sigma \hat{S}^T_B \frac{\beta^T_B[z']}{d+\alpha^T_B[z']}\,,
\end{aligned}
\tag{C.14}
$$

First-order derivatives

$$
\begin{aligned}
\partial R'_A &= \hat{S}^N_A \left(\frac{(d+\alpha^N_A)\partial\beta^N_A - \beta^N_A \partial\alpha^N_A}{(d+\alpha^N_A)^2} \right) + \sigma \hat{S}^T_A \left(\frac{(d+\alpha^T_A)\partial\beta^T_A - \beta^T_A \partial\alpha^T_A}{(d+\alpha^T_A)^2} \right)\,, \\
\partial R'_B &= \hat{S}^N_B \left(\frac{(d+\alpha^N_B)\partial\beta^N_B - \beta^N_B \partial\alpha^N_B}{(d+\alpha^N_B)^2} \right) + \sigma \hat{S}^T_B \left(\frac{(d+\alpha^T_B)\partial\beta^T_B - \beta^T_B \partial\alpha^T_B}{(d+\alpha^T_B)^2} \right)\,,
\end{aligned}
\tag{C.15}
$$

Second-order derivatives

$$
\begin{aligned}
\partial^2 R'_A &= \hat{S}^N_A \left(\frac{2\beta^N_A(\partial\alpha^N_A)^2 - (d+\alpha^N_A)\partial^2\alpha^N_A}{(d+\alpha^N_A)^3} - \frac{2\partial\alpha^N_A\partial\beta^N_A}{(d+\alpha^N_A)^2} + \frac{\partial^2\beta^N_A}{d+\alpha^N_A} \right) + \\
&\quad \sigma \hat{S}^T_A \left(-\frac{\beta^T_A((d+\alpha^T_A)\partial^2\alpha^T_A - 2(\partial\alpha^T_A)^2)}{(d+\alpha^T_A)^3} - \frac{2\partial\alpha^T_A\partial\beta^T_A}{(d+\alpha^T_A)^2} + \frac{\partial^2\beta^T_A}{d+\alpha^T_A} \right)\,, \\
\partial^2 R'_B &= \hat{S}^N_B \left(\frac{2\beta^N_B(\partial\alpha^N_B)^2 - (d+\alpha^N_B)\partial^2\alpha^N_B}{(d+\alpha^N_B)^3} - \frac{2\partial\alpha^N_B\partial\beta^N_B}{(d+\alpha^N_B)^2} + \frac{\partial^2\beta^N_B}{d+\alpha^N_B} \right) + \\
&\quad \sigma \hat{S}^T_B \left(-\frac{\beta^T_B((d+\alpha^T_B)\partial^2\alpha^T_B - 2(\partial\alpha^T_B)^2)}{(d+\alpha^T_B)^3} - \frac{2\partial\alpha^T_B\partial\beta^T_B}{(d+\alpha^T_B)^2} + \frac{\partial^2\beta^T_B}{d+\alpha^T_B} \right)\,,
\end{aligned}
\tag{C.16}
$$

C.4 Anti-infection and anti-transmission treatments

Anti-infection aims to reduce host susceptibility to pathogens and anti-transmission treatments reduce the transmission of infected to susceptible hosts. With these treatments, we have the following measure of pathogen fitness in population A :

$$R'_A = \frac{\beta'^N_A}{d + \alpha'^N_A} \left(\hat{S}^N_A + (1 - r_1)(1 - r_3)\hat{S}^T_A \right) .$$

Setting $Z_A = \hat{S}^N_A + (1 - r_1)(1 - r_3)\hat{S}^T_A$, it simplifies to $R'_A = R'^N_A Z_A$.

The only difference between subpopulations A and B is their treatment coverage, included in susceptible densities. Then we have $R'^N_A = R'^N_B = R'^N$ and the selection gradient eq.(3.4) can be expressed as :

$$\mathcal{S} = \frac{\partial R'^N}{R^N}(Z_A c_A + Z_B c_B) \tag{C.17}$$

Knowing the susceptible densities (Z_k) and class reproductive values (c_k) are positive, then $\mathcal{S} = 0$ is equivalent to $\partial R'^N = 0$. It comes down to maximizing $\beta'^N/(d+\alpha'^N)$ to calculate the singularities z^*. As z^*'s do not depend on r_1 nor r_3, these treatments does not affect the evolutionary outcome in the long-term.

C.5 Evolution in a monomorphic population

The model eq. (3.1) then becomes :

$$\begin{aligned}
\frac{\mathrm{d}S_A^N}{\mathrm{d}t} &= (1-\nu_A)b - S_A^N(d + mh_{A,x} + (1-m)h_{B,x})\,, \\
\frac{\mathrm{d}S_A^T}{\mathrm{d}t} &= \nu_A b - S_A^T(d + \sigma(mh_{A,x} + (1-m)h_{B,x}))\,, \\
\frac{\mathrm{d}I_{A,x}^N}{\mathrm{d}t} &= S_A^N(mh_{A,x} + (1-m)h_{B,x}) - (d+\alpha_A^N)I_{A,x}^T + \frac{\mathrm{Vm}}{2}\frac{\partial^2 I_{A,x}^N}{\partial z^2}\,, \\
\frac{\mathrm{d}I_{A,x}^T}{\mathrm{d}t} &= \sigma S_A^T(mh_A^x + (1-m)h_B^x) - (d+\alpha_A^T)I_{A,x}^T + \frac{\mathrm{Vm}}{2}\frac{\partial^2 I_{A,x}^T +}{\partial z^2}\,,
\end{aligned} \tag{C.18}$$

where x characterises the value of the trait that varies from 1 to n, and Vm the variance of the mutation times the probability of the mutation (Débarre et al., 2013). In numerical simulations, the diffusion parameter is discretised in class k as,

$$\frac{\partial^2 I_{A,x}^k}{\partial z^2} = \begin{cases} x \neq 1,\, x \neq n\,, & \frac{1}{\mathrm{d}z}\left(I_{A,x-1}^k - 2I_{A,x}^k + I_{A,x+1}^k\right) \\ x = 1\,, & \frac{1}{\mathrm{d}z}\left(I_{A,2}^k - I_{A,1}^k\right) \\ x = n\,, & \frac{1}{\mathrm{d}z}\left(I_{A,n-1}^k - I_{A,n}^k\right) \end{cases}$$

with $\mathrm{d}z$ the mutational step. Forces of infection becomes :

$$h_{A,x} = \sum_{x}^{x=n}\left(\beta_A^N I_{A,x}^N + \beta_A^T I_{A,x}^T\right) \tag{C.19}$$

(a) Evolutionarily stable state

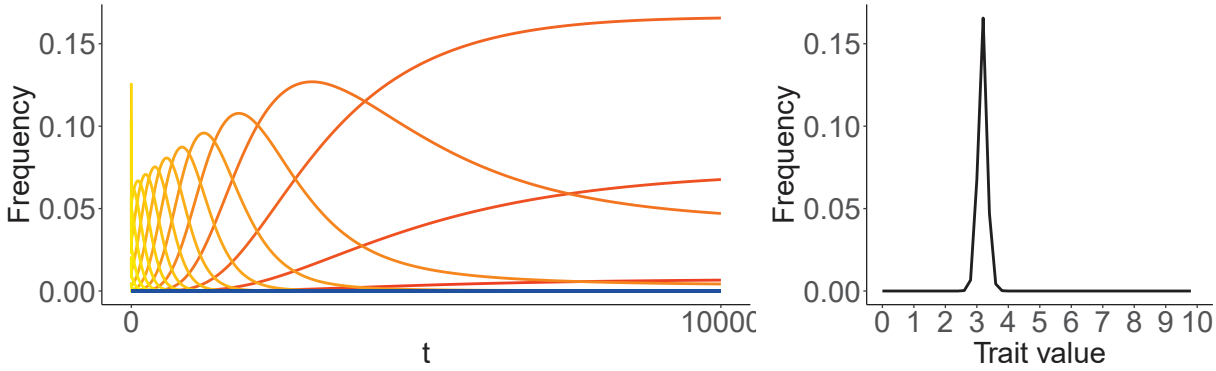

(b) Branching point

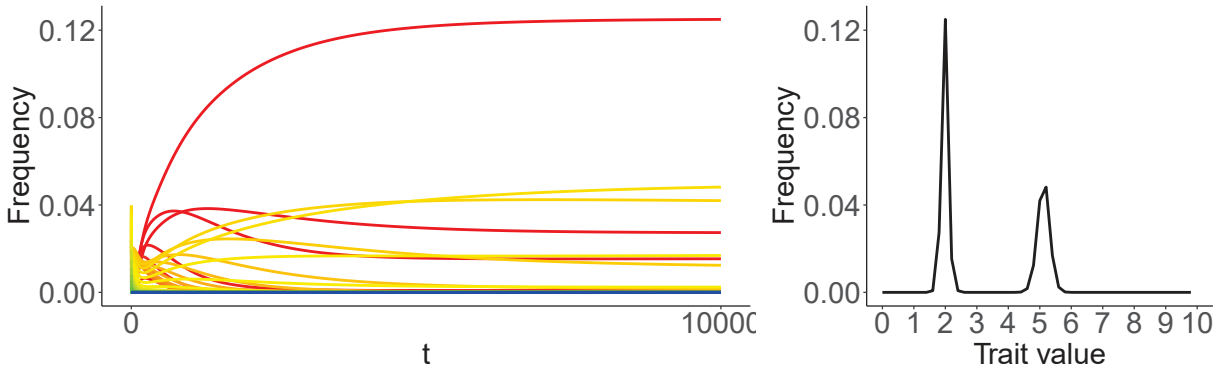

(c) Bistability

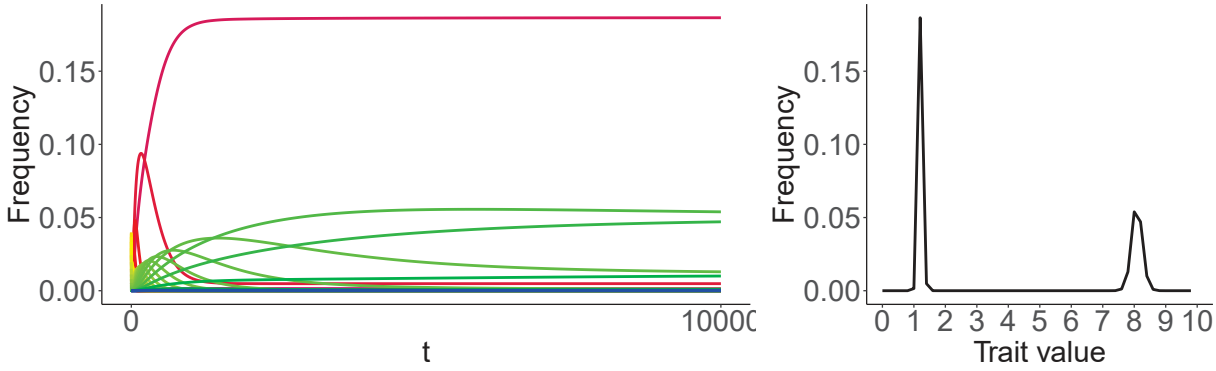

FIGURE C.11 – Long term strains selected represented by infected hosts densities dynamics versus time (left panels) and strains densities in the population (right panels) : (a) an ESS with $m = 0.2$ and $\delta = 0.15$, (b) a branching point with $m = 0.2$ and $\delta = 0.42$ and (c) a bistability with $m = 0.2$ and $\delta = 0.75$. The value of the evolving trait varies in a gradient of colors from blue ($z = 0$) to red ($z = 5$), to purple ($z = 10$).

C.6 Combination of treatments

(a) Anti-growth with anti-infection

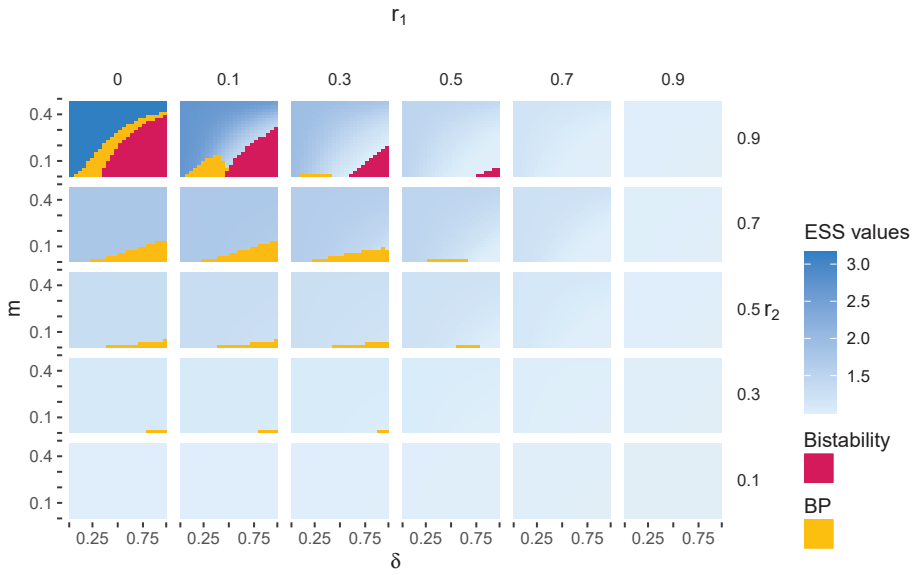

(b) Anti-growth with anti-transmission

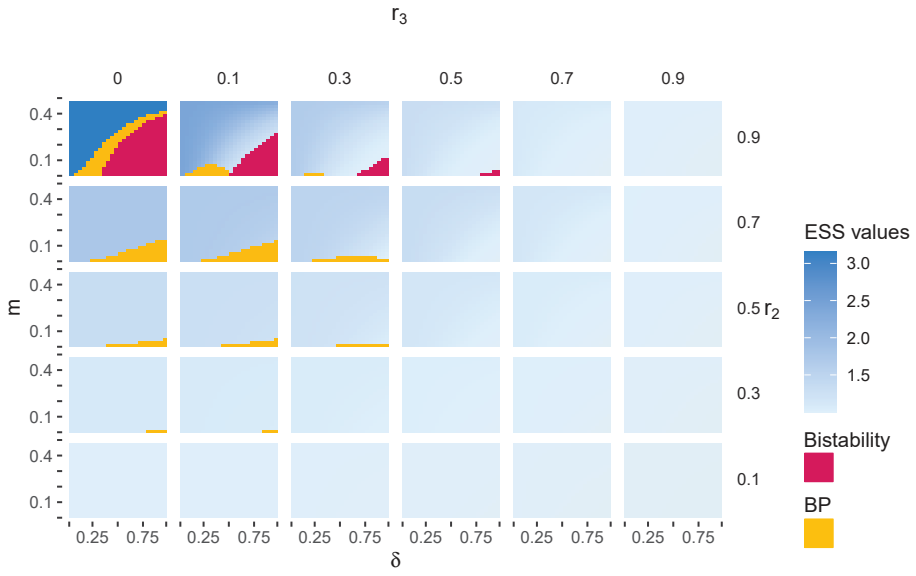

FIGURE C.12 – Long term evolutionary state calculated using adaptive dynamics, for anti-growth treatment combined with (anti-infection and (b) anti-transmission, according to m and δ. Branching point (BP) are represented in yellow, bistability in pink, and ESS values in a gradient of blue. Other parameters as in figure 3.1.

(a) Anti-toxin with anti-infection

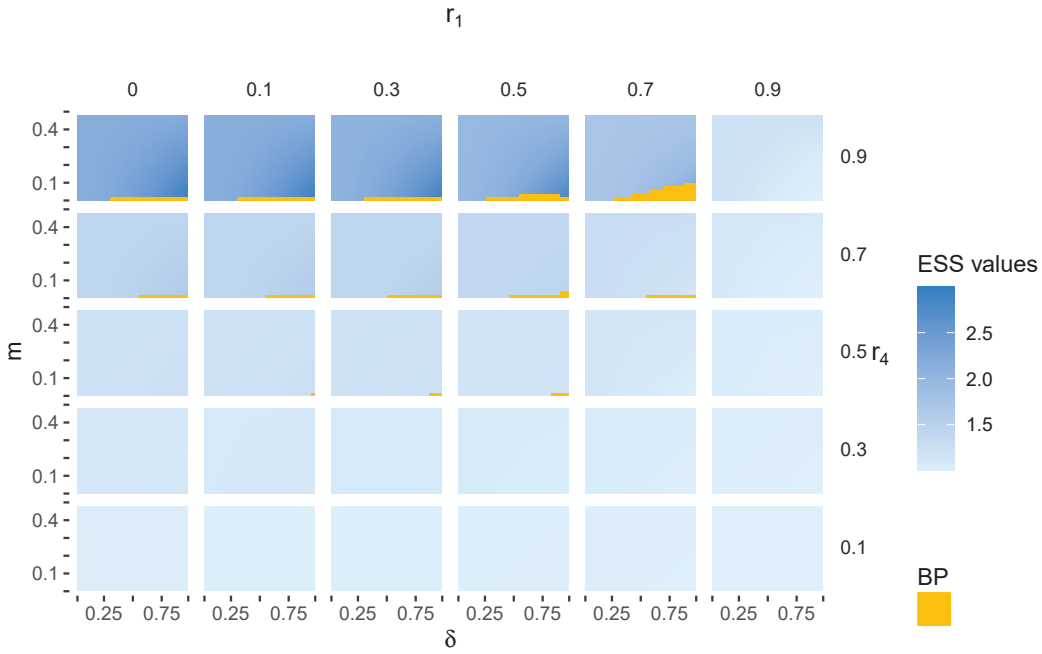

(b) Anti-toxin with anti-transmission

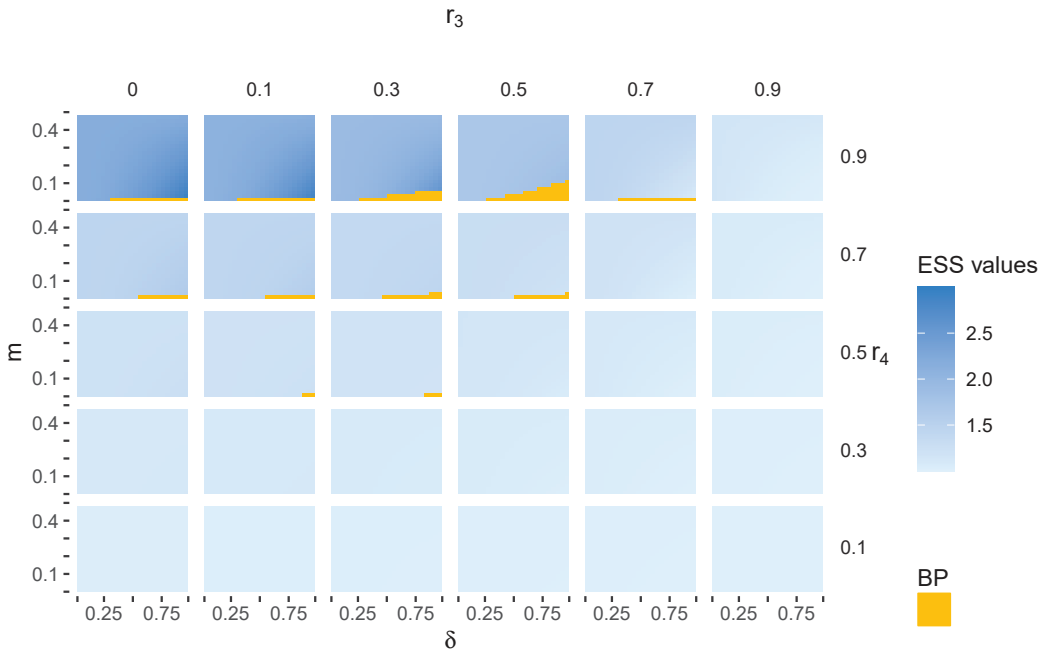

FIGURE C.13 – Long term evolutionary state calculated using adaptive dynamics, for anti-toxin treatment combined with (anti-infection and (b) anti-transmission, according to m and δ. Branching point (BP) are represented in yellow, bistability in pink, and ESS values in a gradient of blue. Other parameters as in figure 3.1.

C.7 Numerical exploration of all combinations of ν_A and ν_B, with different migration rates or efficacy, for anti-growth and anti-toxin treatments

(a) $r_4 = 0.7$

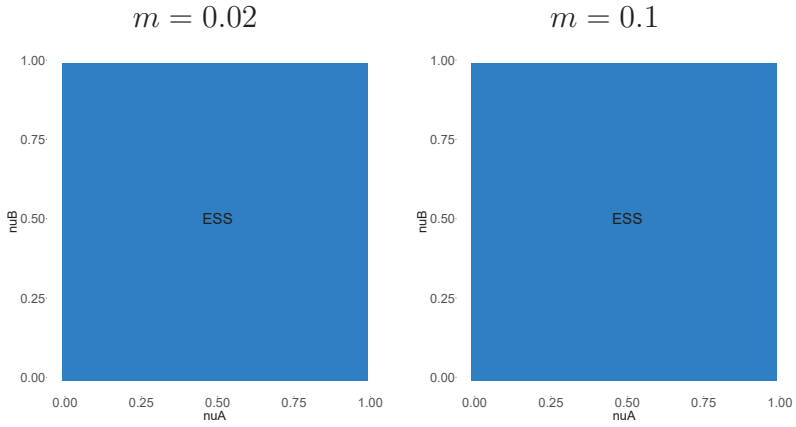

(b) $r_4 = 0.9$

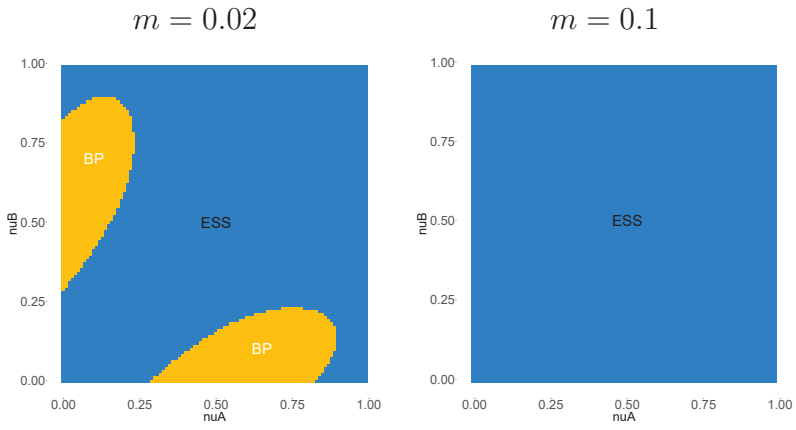

FIGURE C.14 – Long term evolutionary state calculated using adaptive dynamics, for anti-toxin treatments, with (a) $r_4 = 0.7$ and (b) $r_4 = 0.9$ with $m = 0.02$ or $m = 0.1$. ESS are represented in blue, branching point (BP) in yellow and bistability in pink.

(a) $r_2 = 0.7$

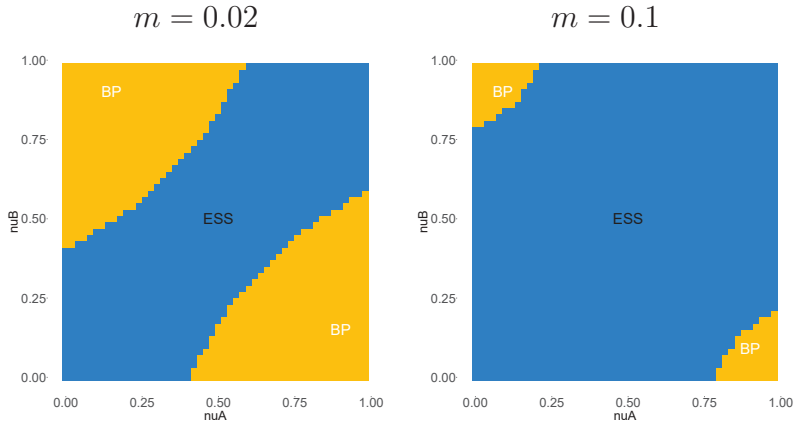

(b) $r_2 = 0.9$

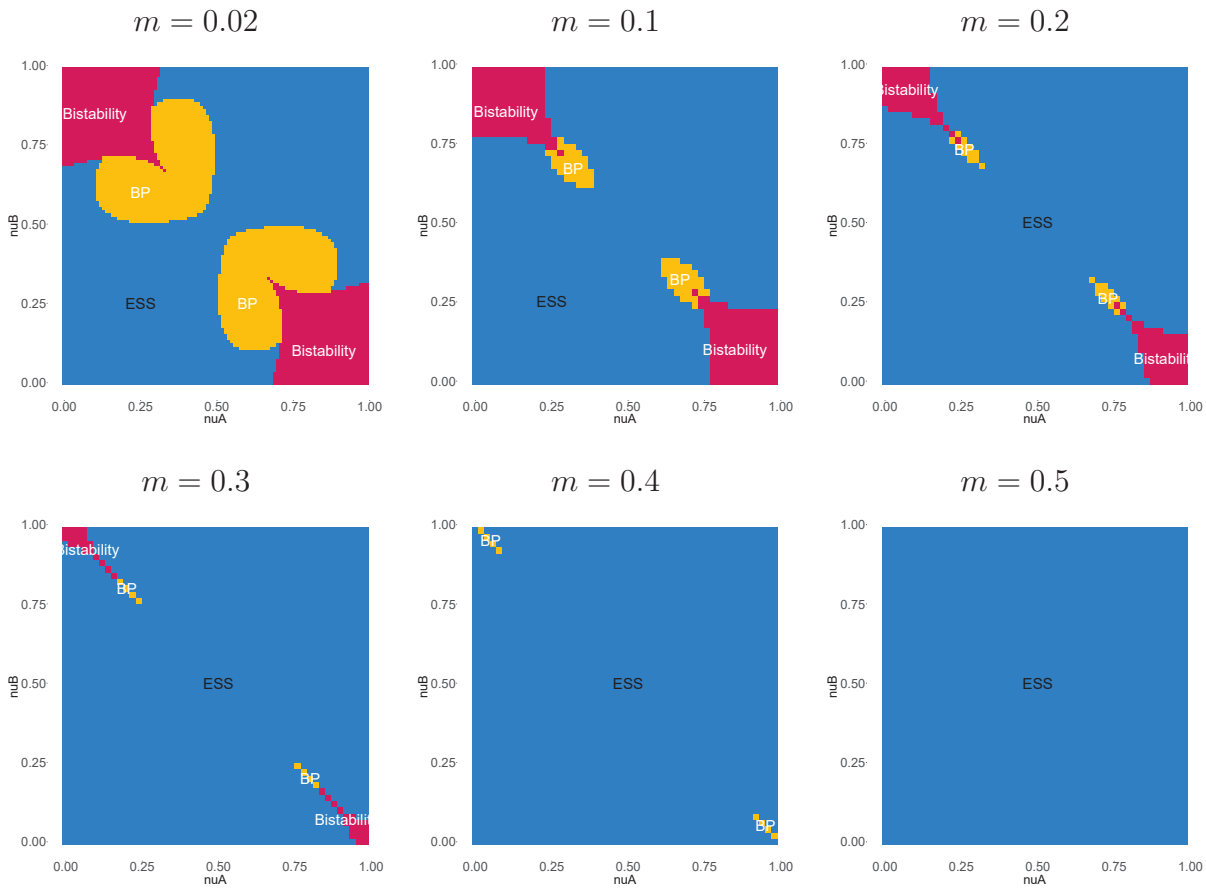

FIGURE C.15 – Long term evolutionary state calculated using adaptive dynamics, for anti-growth treatments, with (a) $r_2 = 0.7$ and $m = 0.02$ or $m = 0.1$ and (b) $r_2 = 0.9$ $m = 0.02\,, 0.1\,, 0.2\,, 0.3\,, 0.4\,, 0.5$. ESS are represented in blue, branching point (BP) in yellow and bistability in pink.

Annexe D: Annexes du chapitre 3

D.1 Full ODE system

$$
\begin{aligned}
\dot{S}^A &= b(1-\nu^A(t)) - dS^A - \left((1-m)h_i^A + mh_i^B\right) S^A \\
\dot{\widehat{S}}^A &= b\nu^A(t)\widehat{S}^A - d\widehat{S}^A - \left((1-m)h_i^A + mh_i^B\right) \rho_\sigma(e_i)\widehat{S}^A \\
\dot{S}^B &= b(1-\nu^B(t)) - dS^B - \left((1-m)h_i^B + mh_i^A\right) S^B \\
\dot{\widehat{S}}^B &= b\nu^B(t)\widehat{S}^B - d\widehat{S}^B - \left((1-m)h_i^B + mh_i^A\right) \rho_\sigma(e_i)\widehat{S}^B \\
\dot{I}_i^A &= \left((1-m)h_i^A + mh_i^B\right) S^A - \delta_i I_i^A \\
\dot{\widehat{I}}_i^A &= \left((1-m)h_i^A + mh_i^B\right) \rho_\sigma(e_i)\widehat{S}^A - \widehat{\delta}_i \widehat{I}_i^A \\
\dot{I}_i^B &= \left((1-m)h_i^B + mh_i^A\right) S^B - \delta_i I_i^B \\
\dot{\widehat{I}}_i^B &= \left((1-m)h_i^B + mh_i^A\right) \rho_\sigma(e_i)\widehat{S}^B - \widehat{\delta}_i \widehat{I}_i^B \\
\dot{D} &= \sum_i \left(c_i^A \delta_i^A I_i^A + \widehat{c}_i^A \widehat{\delta}_i^A \widehat{I}_i^A + c_i^B \delta_i^B I_i^B + \widehat{c}_i^B \widehat{\delta}_i^B \widehat{I}_i^B \right)
\end{aligned}
\tag{D.1}
$$

Transition between class

The 4 x 4 transition matrix, $\mathbf{R}_i$ of the metapopulation is

$$
\begin{pmatrix}
(1-m)\beta^A S^A - \delta^A & (1-m)\widehat{\beta}^A \rho_\tau(e_i) S^A & m\beta^B S^A & m\widehat{\beta}^B \rho_\tau(e_i) S^A \\
(1-m)\beta^A \rho_\sigma(e_i)\widehat{S}^A & (1-m)\widehat{\beta}^A \rho_\tau(e_i)\rho_\sigma(e_i)\widehat{S}^A - \widehat{\delta}^A & m\beta^B \rho_\sigma(e_i)\widehat{S}^A & m\widehat{\beta}^B \rho_\tau(e_i)\rho_\sigma(e_i)\widehat{S}^A \\
m\beta^A S^B & m\widehat{\beta}^A \rho_\tau(e_i) S^B & (1-m)\beta^B S^B - \delta^B & (1-m)\widehat{\beta}^B \rho_\tau(e_i) S^B \\
m\beta^A \rho_\sigma(e_i)\widehat{S}^B & m\widehat{\beta}^A \rho_\tau(e_i)\rho_\sigma(e_i)\widehat{S}^B & (1-m)\beta^B \rho_\sigma(e_i)\widehat{S}^B & (1-m)\widehat{\beta}^B \rho_\tau(e_i)\rho_\sigma(e_i)\widehat{S}^B - \widehat{\delta}^B
\end{pmatrix}
\tag{D.2}
$$

In expressions we use the notation r^{kj} with k and j being different class of hosts, to refer to the

transition matrix as

$$\mathbf{R}_i = \begin{pmatrix} r_i^{AA} & r_i^{A\widehat{A}} & r_i^{AB} & r_i^{A\widehat{B}} \\ r_i^{\widehat{A}A} & r_i^{\widehat{A}\widehat{A}} & r_i^{\widehat{A}B} & r_i^{\widehat{A}\widehat{B}} \\ r_i^{BA} & r_i^{B\widehat{A}} & r_i^{BB} & r_i^{B\widehat{B}} \\ r_i^{\widehat{B}A} & r_i^{\widehat{B}\widehat{A}} & r_i^{\widehat{B}B} & r_i^{\widehat{B}\widehat{B}} \end{pmatrix} \tag{D.3}$$

D.2 Rate of change of the vaccine escape mutant in each class

In Lion (2018*a*), the authors derive an expression to track the dynamic of infected hosts by a strain i in class k as :

$$\frac{\mathrm{d}f_i^k}{\mathrm{d}t} = f_i^k(r_i^k - \overline{r}^k) \tag{D.4}$$

with the per capita growth rate of strain i in class k,

$$r_i^k = \sum_j r_i^{kj} \frac{f_i^j}{f_i^k} \frac{f^j}{f^k}$$

and the average per capita growth rate of individuals in class k,

$$\overline{r}^k = \sum_j \overline{r}^{kj} \frac{f^j}{f^k} .$$

The frequency of the strain i in class k is noted $f_i^k = I_i^k/I^k$, the frequency of infected hosts in class k is noted $f^k = I^k/I$, the transition rates from class j to k are noted r^{kj} (see matrix (D.3) for the equivalence in the transition matrix (D.2)) and the average transition rates from class j to k noted $\overline{r}^{kj} = \sum_i r_i^{kj} f_i^j$.

Then, we have

$$\begin{aligned}
\frac{\mathrm{d}f_i^k}{\mathrm{d}t} &= f_i^k \sum_j r_i^{kj} \frac{f_i^j}{f_i^k} \frac{f^j}{f^k} - f_i^k \sum_j \overline{r}^{kj} \frac{f^j}{f^k} \\
&= \sum_j \frac{f^j}{f^k} \left(r_i^{kj} f_i^j - \overline{r}^{kj} f_i^k \right) \\
&= \sum_j \frac{f^j}{f^k} \left((r_i^{kj} - \overline{r}^{kj}) f_i^j + (f_i^j - f_i^k) \overline{r}^{kj} \right) \\
&= \sum_j (r_i^{kj} - \overline{r}^{kj}) f_m^j \frac{f^j}{f^k} + \sum_j \overline{r}^{kj} (f_i^j - f_i^k) \frac{f^j}{f^k}
\end{aligned} \tag{D.5}$$

Then, equation (D.5) allows us to track the dynamic of the frequency of the vaccine escape mutant strain in all class. Let us develop the equation (D.5) in the class A, which corresponds to the untreated infected hosts by the mutant in class A. With $k = A$ and $j \in \{A\,, \widehat{A}\,, B\,, \widehat{B}\}$, we have,

$$\begin{aligned}
\frac{\mathrm{d}f_m^A}{\mathrm{d}t} = \; & (r_m^{AA} - \overline{r}^{AA}) f_m^A \frac{f^A}{f^A} + \overline{r}^{AA} (f_m^A - f_m^A) \frac{f^A}{f^A} + (r_m^{A\widehat{A}} - \overline{r}^{A\widehat{A}}) f_m^{\widehat{A}} \frac{f^{\widehat{A}}}{f^A} + \overline{r}^{A\widehat{A}} (f_m^{\widehat{A}} - f_m^A) \frac{f^{\widehat{A}}}{f^A} + \\
& (r_m^{AB} - \overline{r}^{AB}) f_m^B \frac{f^B}{f^A} + \overline{r}^{AB} (f_m^B - f_m^A) \frac{f^B}{f^A} + (r_m^{A\widehat{B}} - \overline{r}^{A\widehat{B}}) f_m^{\widehat{B}} \frac{f^{\widehat{B}}}{f^A} + \overline{r}^{A\widehat{B}} (f_m^{\widehat{B}} - f_m^A) \frac{f^{\widehat{B}}}{f^A}
\end{aligned} \tag{D.6}$$

Assuming that $\beta = \beta^A = \beta^{\widehat{A}} = \beta^B = \beta^{\widehat{B}}$,the $\overline{r}^{kj}$'s take the form

$$\begin{aligned}
r_m^{AA} - \overline{r}^{AA} &= r_m^{AA} - r_m^{AA} f_m^A - r_w^{AA} f_w^A = r_m^{AA}(1 - f_m^A) - r_w^{AA}(1 - f_m^A) = (r_m^{AA} - r_w^{AA})(1 - f_m^A) \\
&= ((1-m)\beta S^A - (1-m)\beta S^A)(1 - f_m^A) = 0 \\
r_m^{A\widehat{A}} - \overline{r}^{A\widehat{A}} &= (1-m)\beta S^A(\rho_\tau(e_m) - \rho_\tau(e_w)))(1 - f_m^{\widehat{A}}) \\
r_m^{AB} - \overline{r}^{AB} &= (m\beta S^A - m\beta S^A)(1 - f_m^B) = 0 \\
r_m^{A\widehat{B}} - \overline{r}^{A\widehat{B}} &= m\beta S^A(\rho_\tau(e_m) - \rho_\tau(e_w)))(1 - f_m^{\widehat{B}})
\end{aligned} \tag{D.7}$$

With $k \neq j$ we have (with $k = j$, m is replaced by $(1-m)$),

$$\begin{aligned}
\overline{r}^{\widehat{k}\widehat{j}} &= m\beta S^{\widehat{k}}\left(\rho_\sigma(e_m)\rho_\tau(e_m)f_m^{\widehat{j}} + \rho_\sigma(e_w)\rho_\tau(e_w)f_w^{\widehat{j}}\right) = m\beta S^{\widehat{k}}\overline{\rho_\sigma\rho_\tau}^{j} \\
\overline{r}^{k\widehat{j}} &= m\beta S^{k}\left(\rho_\tau(e_m)f_m^{\widehat{j}} + \rho_\tau(e_w)f_w^{\widehat{j}}\right) = m\beta S^{k}\overline{\rho_\tau}^{j} \\
\overline{r}^{\widehat{k}j} &= m\beta S^{\widehat{k}}\left(\rho_\sigma(e_m)f_m^{j} + \rho_\sigma(e_w)f_w^{j}\right) = m\beta S^{\widehat{k}}\overline{\rho_\sigma}^{j} \\
\overline{r}^{kj} &= m\beta S^{k}\left(f_m^{j} + f_w^{j}\right) = m\beta S^{k}
\end{aligned} \tag{D.8}$$

where $\overline{\rho_x}^j = \overline{\rho_x}^j$ and $\overline{\rho_\sigma\rho_\tau}^j = \rho_\sigma(e_m)\rho_\tau(e_m)f_m^j + \rho_\sigma(e_w)\rho_\tau(e_w)f_w^j$, with $x \in \{\sigma\ \tau\}$ and $j \in \{A\ \widehat{A},\ B\ \widehat{B}\}$.

Then (D.6) can be written as

$$\begin{aligned}
\frac{\mathrm{d}f_m^A}{\mathrm{d}t} &= \beta S^A\left(m\left((f_m^B - f_m^A)\frac{f^B}{f^A} + (\rho_\tau(e_m) - \rho_\tau(e_w))(1-f_m^{\widehat{B}})f_m^{\widehat{B}}\frac{f^{\widehat{B}}}{f^A} + \overline{\rho_\tau}^{\widehat{B}}(f_m^{\widehat{B}} - f_m^A)\frac{f^{\widehat{B}}}{f^A}\right) + \right. \\
&\left. (1-m)\left((\rho_\tau(e_m) - \rho_\tau(e_w))(1-f_m^{\widehat{A}})f_m^{\widehat{A}}\frac{f^{\widehat{A}}}{f^A} + \overline{\rho_\tau}^{\widehat{A}}(f_m^{\widehat{A}} - f_m^A)\frac{f^{\widehat{A}}}{f^A}\right)\right)
\end{aligned} \tag{D.9}$$

In the same manner we obtain the expressions of the vaccine escape mutant dynamic in class $\widehat{A}$, B and $\widehat{B}$ as

$$\begin{aligned}
\frac{\mathrm{d}f_m^B}{\mathrm{d}t} &= \beta S^B\left(m\left((f_m^A - f_m^B)\frac{f_m^A}{f_m^B} + (\rho_\tau(e_m) - \rho_\tau(e_w))(1-f_m^{\widehat{A}})f_m^{\widehat{A}}\frac{f^{\widehat{A}}}{f^B} + \overline{\rho_\tau}^{\widehat{A}}(f_m^{\widehat{A}} - f_m^B)\frac{f^{\widehat{A}}}{f^B}\right) + \right. \\
&\left. (1-m)\left((\rho_\tau(e_m) - \rho_\tau(e_w))(1-f_m^{\widehat{B}})f_m^{\widehat{B}}\frac{f^{\widehat{B}}}{f^B} + \overline{\rho_\tau}^{\widehat{B}}(f_m^{\widehat{B}} - f_m^B)\frac{f^{\widehat{B}}}{f^B}\right)\right)
\end{aligned} \tag{D.10}$$

$$\begin{aligned}\frac{\mathrm{d}f_m^{\widehat{A}}}{\mathrm{d}t} &= \beta S^A \Bigg(m \Bigg((\rho_\sigma(e_m) - \rho_\sigma(e_w))(1 - f_m^B) f_m^B \frac{f^B}{f^{\widehat{A}}} + \overline{\rho_\sigma}^B (f_m^B - f_m^{\widehat{A}}) \frac{f^B}{f^{\widehat{A}}} + \\ &\quad (\rho_\sigma(e_m)\rho_\tau(e_m) - \rho_\sigma(e_w)\rho_\tau(e_w))(1 - f_m^{\widehat{B}}) f_m^{\widehat{B}} \frac{f^{\widehat{B}}}{f^{\widehat{A}}} + \overline{\rho_\sigma\rho_\tau}^{\widehat{B}} (f_m^{\widehat{B}} - f_m^{\widehat{A}}) \frac{f^{\widehat{B}}}{f^{\widehat{A}}} \Bigg) + \\ &\quad (1-m) \Bigg((\rho_\sigma(e_m) - \rho_\sigma(e_w))(1 - f_m^A) f_m^A \frac{f^A}{f^{\widehat{A}}} + \overline{\rho_\sigma}^A (f_m^A - f_m^{\widehat{A}}) \frac{f^A}{f^{\widehat{A}}} + \\ &\quad (\rho_\sigma(e_m)\rho_\tau(e_m) - \rho_\sigma(e_w)\rho_\tau(e_w))(1 - f_m^{\widehat{A}}) f_m^{\widehat{A}} \frac{f^{\widehat{A}}}{f^{\widehat{A}}} + \overline{\rho_\sigma\rho_\tau}^{\widehat{A}} (f_m^{\widehat{A}} - f_m^{\widehat{A}}) \frac{f^{\widehat{A}}}{f^{\widehat{A}}} \Bigg) \Bigg) \end{aligned} \quad \text{(D.11)}$$

$$\begin{aligned}\frac{\mathrm{d}f_m^{\widehat{B}}}{\mathrm{d}t} &= \beta S^B \Bigg(m \Bigg((\rho_\sigma(e_m) - \rho_\sigma(e_w))(1 - f_m^A) f_m^A \frac{f^A}{f^{\widehat{B}}} + \overline{\rho_\sigma}^A (f_m^A - f_m^{\widehat{B}}) \frac{f^A}{f^{\widehat{B}}} + \\ &\quad (\rho_\sigma(e_m)\rho_\tau(e_m) - \rho_\sigma(e_w)\rho_\tau(e_w))(1 - f_m^{\widehat{A}}) f_m^{\widehat{A}} \frac{f^{\widehat{A}}}{f^{\widehat{B}}} + \overline{\rho_\sigma\rho_\tau}^{\widehat{A}} (f_m^{\widehat{A}} - f_m^{\widehat{B}}) \frac{f^{\widehat{A}}}{f^{\widehat{B}}} \Bigg) + \\ &\quad (1-m) \Bigg((\rho_\sigma(e_m) - \rho_\sigma(e_w))(1 - f_m^B) f_m^B \frac{f^B}{f^{\widehat{B}}} + \overline{\rho_\sigma}^B (f_m^B - f_m^{\widehat{B}}) \frac{f^B}{f^{\widehat{B}}} + \\ &\quad (\rho_\sigma(e_m)\rho_\tau(e_m) - \rho_\sigma(e_w)\rho_\tau(e_w))(1 - f_m^{\widehat{B}}) f_m^{\widehat{B}} \frac{f^{\widehat{B}}}{f^{\widehat{B}}} + \overline{\rho_\sigma\rho_\tau}^{\widehat{B}} (f_m^{\widehat{B}} - f_m^{\widehat{B}}) \frac{f^{\widehat{B}}}{f^{\widehat{B}}} \Bigg) \Bigg) \end{aligned} \quad \text{(D.12)}$$

D.3 Vaccine escape mutant dynamics in each subpopulation

We have developed the expression of the mutant strain in a specific class of our metapopulation. Now we would like to follow the frequency of the mutant in each subpopulation. Hence, we introduce new notations, $f_m^{\textcircled{A}}$ and $f_m^{\textcircled{B}}$ that characterise the mutant frequency in the population A or B such as

$$f_m^{\textcircled{k}} = \frac{I_m^k + I_m^{\widehat{k}}}{f^{\textcircled{k}}} = \frac{I_m^k}{I^k}\frac{I^k}{f^{\textcircled{k}}} + \frac{I_m^{\widehat{k}}}{I^{\widehat{k}}}\frac{I^{\widehat{k}}}{f^{\textcircled{k}}} = f_m^k \frac{I^k}{f^{\textcircled{k}}} + f_m^{\widehat{k}} \frac{I^{\widehat{k}}}{f^{\textcircled{k}}} \quad \text{(D.13)}$$

here $f^{\textcircled{k}} = I^k + I^{\widehat{k}} = I_m^k + I_w^k + I_m^{\widehat{k}} + I_w^{\widehat{k}}$ is the total density of infected hosts in the population k, with $\dot{f^{\textcircled{k}}} = \overline{r}^k I^k + \overline{r}^{\widehat{k}} I^{\widehat{k}}$.

Differentiating eq. (D.13) yields

$$\begin{aligned}
\frac{\mathrm{d}f_m^{\textcircled{k}}}{\mathrm{d}t} &= \dot{f}_m^K \frac{I^k}{f^{\textcircled{k}}} + f_m^k \frac{\dot{I}^k f^{\textcircled{k}} - I^k \dot{f^{\textcircled{k}}}}{f^{\textcircled{k}2}} + \dot{f}_m^{\widehat{k}} \frac{I^{\widehat{k}}}{f^{\textcircled{k}}} + f_m^{\widehat{k}} \frac{\dot{I^{\widehat{k}}} f^{\textcircled{k}} - I^{\widehat{k}} \dot{f^{\textcircled{k}}}}{f^{\textcircled{k}2}} \\
&= \dot{f}_m^k \frac{I^k}{f^{\textcircled{k}}} + \dot{f}_m^{\widehat{k}} \frac{I^{\widehat{k}}}{f^{\textcircled{k}}} + f_m^K \frac{\dot{I}^K f^{\textcircled{k}}}{f^{\textcircled{k}2}} - f_m^k \frac{I^k}{f^{\textcircled{k}}} \frac{\dot{f^{\textcircled{k}}}}{f^{\textcircled{k}}} + f_m^{\widehat{k}} \frac{\dot{I^{\widehat{k}}} f^{\textcircled{k}}}{f^{\textcircled{k}2}} - f_m^{\widehat{k}} \frac{I^{\widehat{k}}}{f^{\textcircled{k}}} \frac{\dot{f^{\textcircled{k}}}}{f^{\textcircled{k}}} \\
&= \dot{f}_m^k \frac{I^k}{f^{\textcircled{k}}} + \dot{f}_m^{\widehat{k}} \frac{I^{\widehat{k}}}{f^{\textcircled{k}}} + f_m^k \frac{\dot{I}^k}{f^{\textcircled{k}}} + f_m^{\widehat{k}} \frac{\dot{I^{\widehat{k}}}}{f^{\textcircled{k}}} - f_m^{\textcircled{k}} \frac{\dot{f^{\textcircled{k}}}}{f^{\textcircled{k}}} \\
&= \frac{1}{f^{\textcircled{k}}} \left(\dot{f}_m^k I^k + \dot{f}_m^{\widehat{k}} I^{\widehat{k}} + f_m^k \dot{I}^k + f_m^{\widehat{k}} \dot{I}^{\widehat{k}} - f_m^{\textcircled{k}} \dot{f^{\textcircled{k}}} \right)
\end{aligned} \tag{D.14}$$

Using $\dot{f^{\textcircled{k}}} = \dot{I}^k + \dot{I}^{\widehat{k}}$ and $\dot{I}^k = \overline{r}^k I^k$ we have

$$\begin{aligned}
\frac{\mathrm{d}f_m^{\textcircled{k}}}{\mathrm{d}t} &= \frac{1}{f^{\textcircled{k}}} \left(\dot{f}_m^k I^k + \dot{f}_m^{\widehat{k}} I^{\widehat{k}} + (f_m^k - f_m^{\textcircled{k}}) \dot{I}^k + (f_m^{\widehat{k}} - f_m^{\textcircled{k}}) \dot{I}^{\widehat{k}} \right) \\
&= \frac{1}{f^{\textcircled{k}}} \left(\dot{f}_m^k I^k + \dot{f}_m^{\widehat{k}} I^{\widehat{k}} + (f_m^k - f_m^{\textcircled{k}}) \overline{r}^k I^k + (f_m^{\widehat{k}} - f_m^{\textcircled{k}}) \overline{r}^{\widehat{k}} I^{\widehat{k}} \right)
\end{aligned} \tag{D.15}$$

Moreover, we have $f^k = I^k / I$ with $I = \sum_k I^k$, and $k \in A\,, \widehat{A}\,, B\,, \widehat{B}$, then

$$\begin{aligned}
\frac{\mathrm{d}f_m^{\textcircled{k}}}{\mathrm{d}t} &= \frac{I}{f^{\textcircled{k}}} \left(\dot{f}_m^k f^k + \dot{f}_m^{\widehat{k}} f^{\widehat{k}} + (f_m^k - f_m^{\textcircled{k}}) \overline{r}^k f^k + (f_m^{\widehat{k}} - f_m^{\textcircled{k}}) \overline{r}^k f^{\widehat{k}} \right) \\
&= \frac{I}{f^{\textcircled{k}}} f^k \left(\overline{r}^k (f_m^k - f_m^{\textcircled{k}}) + \dot{f}_m^k \right) + \frac{I}{f^{\textcircled{k}}} f^{\widehat{k}} \left(\overline{r}^{\widehat{k}} (f_m^{\widehat{k}} - f_m^{\textcircled{k}} f_m^{\textcircled{k}}) + \dot{f}_m^{\widehat{k}} \right)
\end{aligned} \tag{D.16}$$

Knowing $\overline{r}^k = \sum_j \overline{r}^{kj} f^j / f^k$, we can develop $\dot{q}_m^A$ as

$$
\begin{aligned}
\frac{\mathrm{d}f_m^{\textcircled{A}}}{\mathrm{d}t} &= \frac{I}{f^{\textcircled{k}}}\left(f^A\dot{f}_m^A + \left(\overline{r}^{AA}f^A + \overline{r}^{A\widehat{A}}f^{\widehat{A}} + \overline{r}^{AB}f^B + \overline{r}^{A\widehat{B}}f^{\widehat{B}}\right)(f_m^A - f_m^{\textcircled{A}})\right) + \\
&\quad \frac{I}{f^{\textcircled{k}}}\left(f^{\widehat{A}}\dot{f}_m^{\widehat{A}} + \left(\overline{r}^{\widehat{A}A}f^A + \overline{r}^{\widehat{A}\widehat{A}}f^{\widehat{A}} + \overline{r}^{\widehat{A}B}f^B + \overline{r}^{\widehat{A}\widehat{B}}f^{\widehat{B}}\right)(f_m^{\widehat{A}} - f_m^{\textcircled{A}})\right) \\
&= \frac{I}{f^{\textcircled{k}}}\left(f^A\dot{f}_m^A + \beta S^A\left((1-m)(f^A + \overline{\rho_\tau}^{\widehat{A}}f^{\widehat{A}}) + m(f^B + \overline{\rho_\tau}^{\widehat{B}}f^{\widehat{B}}\right)(f_m^A - f_m^{\textcircled{A}})\right) + \qquad \text{(D.17)} \\
&\quad \frac{I}{f^{\textcircled{k}}f^{\textcircled{k}}}\left(f^{\widehat{A}}\dot{f}_m^{\widehat{A}} + \beta S^{\widehat{A}}\left((1-m)(\overline{\rho_\sigma}^A f^A + \overline{\rho_\sigma\rho_\tau}^{\widehat{A}}f^{\widehat{A}}) + m(\overline{\rho_\sigma}^B f^B + \overline{\rho_\sigma\rho_\tau}^{\widehat{B}}f^{\widehat{B}}\right)(f_m^{\widehat{A}} - f_m^{\textcircled{A}})\right)
\end{aligned}
$$

With the expression of $\dot{f}_m^A$ and $\dot{f}_m^{\widehat{A}}$ from equations (D.9) and (D.11), we have

$$
\begin{aligned}
\frac{\mathrm{d}f_m^{\textcircled{A}}}{\mathrm{d}t} &= \frac{I}{f^{\textcircled{A}}}\beta S^A\left(m\left((f_m^B - f_m^A)f^B + \Delta\rho_\tau\omega^{\widehat{B}}f^{\widehat{B}} + \overline{\rho_\tau}(f_m^{\widehat{B}} - f_m^A)f^{\widehat{B}}\right) + \right. \\
&\quad \left.(1-m)\left(\Delta\rho_\tau\omega^{\widehat{A}}f^{\widehat{A}} + \overline{\rho_\tau}(f_m^{\widehat{A}} - f_m^A)f^{\widehat{A}}\right)\right) + \\
&\quad \frac{I}{f^{\textcircled{A}}}\beta S^A\left((1-m)(f^A + \overline{\rho_\tau}f^{\widehat{A}}) + m(f^B + \overline{\rho_\tau}f^{\widehat{B}}\right)(f_m^A - f_m^{\textcircled{A}}) + \\
&\quad \frac{I}{f^{\textcircled{A}}}\beta S^{\widehat{A}}\left(m\left(\Delta\rho_\sigma\omega^B f^B + \overline{\rho_\sigma}(f_m^B - f_m^{\widehat{A}})f^B + \Delta\rho_{\tau\sigma}\omega^{\widehat{B}}f^{\widehat{B}} + \overline{\rho_\sigma\rho_\tau}(f_m^{\widehat{B}} - f_m^{\widehat{A}})f^{\widehat{B}}\right) + \right. \qquad \text{(D.18)} \\
&\quad \left.(1-m)\left(\Delta\rho_\sigma\omega^A f^A + \overline{\rho_\sigma}(f_m^A - f_m^{\widehat{A}})f^A + \Delta\rho_{\tau\sigma}\omega^{\widehat{A}}f^{\widehat{A}} + \overline{\rho_\sigma\rho_\tau}(f_m^{\widehat{A}} - f_m^{\widehat{A}})f^{\widehat{A}}\right)\right) + \\
&\quad \frac{I}{f^{\textcircled{A}}}\beta S^{\widehat{A}}\left((1-m)(\overline{\rho_\sigma}f^A + \overline{\rho_\sigma\rho_\tau}f^{\widehat{A}}) + m(\overline{\rho_\sigma}f^B + \overline{\rho_\sigma\rho_\tau}f^{\widehat{B}}\right)(f_m^{\widehat{A}} - f_m^{\textcircled{A}}) \\
&= \frac{I}{f^{\textcircled{A}}}\beta S^A\left(m\left((f_m^B - f_m^A)f^B + \Delta\rho_\tau\omega^{\widehat{B}}f^{\widehat{B}} + \overline{\rho_\tau}(f_m^{\widehat{B}} - f_m^A)f^{\widehat{B}} + (f^B + \overline{\rho_\tau}f^{\widehat{B}})(f_m^A - f_m^{\textcircled{A}})\right) + \right. \\
&\quad \left.(1-m)\left(\Delta\rho_\tau\omega^{\widehat{A}}f^{\widehat{A}} + \overline{\rho_\tau}(f_m^{\widehat{A}} - f_m^A)f^{\widehat{A}}\right) + (f^A + \overline{\rho_\tau}f^{\widehat{A}})(f_m^A - f_m^{\textcircled{A}})\right) + \\
&\quad \frac{I}{f^{\textcircled{A}}}\beta S^{\widehat{A}}\left(m\left(\Delta\rho_\sigma\omega^B f^B + \overline{\rho_\sigma}(f_m^B - f_m^{\widehat{A}})f^B + \Delta\rho_{\tau\sigma}\omega^{\widehat{B}}f^{\widehat{B}} + \overline{\rho_\sigma\rho_\tau}(f_m^{\widehat{B}} - f_m^{\widehat{A}})f^{\widehat{B}} + (\overline{\rho_\sigma}f^B + \overline{\rho_\sigma\rho_\tau}f^{\widehat{B}})(f_m^{\widehat{A}} - f_m^{\textcircled{A}})\right)\right. \\
&\quad \left.(1-m)\left(\Delta\rho_\sigma\omega^A f^A + \overline{\rho_\sigma}(f_m^A - f_m^{\widehat{A}})f^A + \Delta\rho_{\tau\sigma}\omega^{\widehat{A}}f^{\widehat{A}} + \overline{\rho_\sigma\rho_\tau}(f_m^{\widehat{A}} - f_m^{\widehat{A}})f^{\widehat{A}} + (\overline{\rho_\sigma}f^A + \overline{\rho_\sigma\rho_\tau}f^{\widehat{A}})(f_m^{\widehat{A}} - f_m^{\textcircled{A}})\right)
\end{aligned}
$$

$$\begin{aligned}\frac{\mathrm{d}f_m^{\textcircled{A}}}{\mathrm{d}t} &= \frac{I}{f^{\textcircled{A}}}\beta S^A\left(m\left((f_m^B-f_m^A)f^B+\Delta\rho_\tau\omega^{\widehat{B}}f^{\widehat{B}}+\overline{\rho_\tau}^{\widehat{B}}(f_m^{\widehat{B}}-f_m^{\textcircled{A}})f^{\widehat{B}}+f^B(f_m^A-f_m^{\textcircled{A}})\right)+\right.\\ &\quad (1-m)\left(\Delta\rho_\tau\omega^{\widehat{A}}f^{\widehat{A}}+\overline{\rho_\tau}^{\widehat{A}}(f_m^{\widehat{A}}-f_m^{\textcircled{A}})f^{\widehat{A}}+f^A(f_m^A-f_m^{\textcircled{A}})\right)+\\ &\quad \frac{I}{f^{\textcircled{A}}}\beta S^{\widehat{A}}\left(m\left(\Delta\rho_\sigma\omega^B f^B+\overline{\rho_\sigma}^B(f_m^B-f_m^{\textcircled{A}})f^B+\Delta\rho_{\tau\sigma}\omega^{\widehat{B}}f^{\widehat{B}}+\overline{\rho_\sigma\rho_\tau}^{\widehat{B}}(f_m^{\widehat{B}}-f_m^{\textcircled{A}})f^{\widehat{B}}\right)+\right.\\ &\quad \left.(1-m)\left(\Delta\rho_\sigma\omega^A f^A+\overline{\rho_\sigma}^A(f_m^A-f_m^{\textcircled{A}})f^A+\Delta\rho_{\tau\sigma}\omega^{\widehat{A}}f^{\widehat{A}}+\overline{\rho_\sigma\rho_\tau}^{\widehat{A}}(f_m^{\widehat{A}}-f_m^{\textcircled{A}}f_m^{\textcircled{A}})f^{\widehat{A}}\right)\right.\end{aligned} \tag{D.19}$$

and

$$\begin{aligned}\frac{\mathrm{d}f_m^{\textcircled{B}}}{\mathrm{d}t} &= \frac{I}{f^{\textcircled{B}}}\beta S^B\left(m\left((f_m^A-f_m^B)f^A+\Delta\rho_\tau\omega^{\widehat{A}}f^{\widehat{A}}+\overline{\rho_\tau}^{\widehat{A}}(f_m^{\widehat{A}}-f_m^{\textcircled{B}})f^{\widehat{A}}+f^A(f_m^B-f_m^{\textcircled{B}})\right)+\right.\\ &\quad (1-m)\left(\Delta\rho_\tau\omega^{\widehat{B}}f^{\widehat{B}}+\overline{\rho_\tau}^{\widehat{B}}(f_m^{\widehat{B}}-f_m^{\textcircled{B}})f^{\widehat{B}}+f^B(f_m^B-f_m^{\textcircled{B}})\right)+\\ &\quad \frac{I}{f^{\textcircled{B}}}\beta S^{\widehat{B}}\left(m\left(\Delta\rho_\sigma\omega^A f^A+\overline{\rho_\sigma}^A(f_m^A-f_m^{\textcircled{B}})f^A+\Delta\rho_{\tau\sigma}\omega^{\widehat{A}}f^{\widehat{A}}+\overline{\rho_\sigma\rho_\tau}^{\widehat{B}}(f_m^{\widehat{B}}-f_m^{\textcircled{B}})f^{\widehat{A}}\right)+\right.\\ &\quad \left.(1-m)\left(\Delta\rho_\sigma\omega^B f^B+\overline{\rho_\sigma}^B(f_m^B-f_m^{\textcircled{B}})f^B+\Delta\rho_{\tau\sigma}\omega^{\widehat{B}}f^{\widehat{B}}+\overline{\rho_\sigma\rho_\tau}^{\widehat{B}}(f_m^{\widehat{B}}-f_m^{\textcircled{B}})f^{\widehat{B}}\right)\right.\end{aligned} \tag{D.20}$$

D.4 Vaccine escape mutant dynamics in the global population

In Lion (2018*a*), the authors also derive an expression to calculate the dynamic of infected hosts by a strain i as :

$$\frac{\mathrm{d}f_i}{\mathrm{d}t} = \sum_k\sum_j\left(r_i^{kj}-\overline{r}^{kj}\right)f_i^j f^j+\sum_k\sum_j\left(f_i^j-f_i\right)\overline{r}^{kj}f^j \tag{D.21}$$

where k and j are the hosts class, f_i^j, the frequency of the strain i in class j, f_i the frequency of the strain i, r^{kj} is the transition rate from class j to k and the $\overline{r}^{kj}$ the average transition rate from class j to k. Applied to our model, j and $k \in \{A\,,\widehat{A}\,,B\,,\widehat{B}\}$, and we can follow the dynamic of

the frequency escape mutant in the global population, $\mathrm{d}f_m/\mathrm{d}t$ as

$$\begin{aligned}
\frac{\mathrm{d}f_m}{\mathrm{d}t} &= \sum_k \sum_j \left(r_m^{kj} - \overline{r}^{kj}\right) f_m^j f^j + \sum_k \sum_j \left(f_m^j - f_m\right) \overline{r}^{kj} f^j \\
&= f_m^A f^A \left(r_m^{AA} - \overline{r}^{AA} + r_m^{\widehat{A}A} - \overline{r}^{\widehat{A}A} + r_m^{BA} - \overline{r}^{BA} + r_m^{\widehat{B}A} - \overline{r}^{\widehat{B}A}\right) + \\
&\quad f_m^{\widehat{A}} f^{\widehat{A}} \left(r_m^{A\widehat{A}} - \overline{r}^{A\widehat{A}} + r_m^{\widehat{A}\widehat{A}} - \overline{r}^{\widehat{A}\widehat{A}} + r_m^{B\widehat{A}} - \overline{r}^{B\widehat{A}} + r_m^{\widehat{B}\widehat{A}} - \overline{r}^{\widehat{B}\widehat{A}}\right) + \\
&\quad f_m^B f^B \left(r_m^{AB} - \overline{r}^{AB} + r_m^{\widehat{A}B} - \overline{r}^{\widehat{A}B} + r_m^{BB} - \overline{r}^{BB} + r_m^{\widehat{B}B} - \overline{r}^{\widehat{B}B}\right) + \\
&\quad f_m^{\widehat{B}} f^{\widehat{B}} \left(r_m^{A\widehat{B}} - \overline{r}^{A\widehat{B}} + r_m^{\widehat{A}\widehat{B}} - \overline{r}^{\widehat{A}\widehat{B}} + r_m^{B\widehat{B}} - \overline{r}^{B\widehat{B}} + r_m^{\widehat{B}\widehat{B}} - \overline{r}^{\widehat{B}\widehat{B}}\right) + \\
&\quad \left(f_m^A - f_m\right) f^A \left(\overline{r}^{AA} + \overline{r}^{\widehat{A}A} + \overline{r}^{BA} + \overline{r}^{\widehat{B}A}\right) + \\
&\quad \left(f_m^{\widehat{A}} - f_m\right) f^{\widehat{A}} \left(\overline{r}^{A\widehat{A}} + \overline{r}^{\widehat{A}\widehat{A}} + \overline{r}^{B\widehat{A}} + \overline{r}^{\widehat{B}\widehat{A}}\right) + \\
&\quad \left(f_m^B - f_m\right) f^B \left(\overline{r}^{AB} + \overline{r}^{\widehat{A}B} + \overline{r}^{BB} + \overline{r}^{\widehat{B}B}\right) + \\
&\quad \left(f_m^{\widehat{B}} - f_m\right) f^{\widehat{B}} \left(\overline{r}^{A\widehat{B}} + \overline{r}^{\widehat{A}\widehat{B}} + \overline{r}^{B\widehat{B}} + \overline{r}^{\widehat{B}\widehat{B}}\right)
\end{aligned} \tag{D.22}$$

Replacing the per capita and average growth rates by their expressions given by eq. (D.2) and with $\Delta\rho_x = \rho_x(e_m) - \rho_x(e_w)$ with $x \in \{\sigma,\, \tau,\, \tau\sigma\}$, we have

$$\begin{aligned}
\frac{\mathrm{d}f_m}{\mathrm{d}t} &= (1 - f_m^A) f_m^A f^A \left((1-m)\beta S^{\widehat{A}} \Delta\rho_\sigma + m\beta S^{\widehat{B}} \Delta\rho_\sigma\right) + \\
&\quad (1 - f_m^{\widehat{A}}) f_m^{\widehat{A}} f^{\widehat{A}} \left((1-m)\beta S^A \Delta\rho_\tau + (1-m)\beta S^{\widehat{A}} \Delta\rho_{\tau\sigma} + m S^B \Delta\rho_\tau + m\beta S^{\widehat{B}} \Delta\rho_{\tau\sigma}\right) + \\
&\quad (1 - f_m^B) f_m^B f^B \left(m\beta S^{\widehat{A}} \Delta\rho_\sigma + (1-m)\beta S^{\widehat{B}} \Delta\rho_\sigma\right) + \\
&\quad (1 - f_m^{\widehat{B}}) f_m^{\widehat{B}} f^{\widehat{B}} \left(m\beta S^A \Delta\rho_\tau + m\beta S^{\widehat{A}} \Delta\rho_{\tau\sigma} + (1-m)\beta S^B \Delta\rho_\tau + (1-m)\beta S^{\widehat{B}} \Delta\rho_{\tau\sigma}\right) + \\
&\quad \left(f_m^A - f_m\right) f^A \left((1-m)\beta S^A + (1-m)\beta S^{\widehat{A}} \overline{\rho_\sigma}^A + m\beta S^B + m\beta S^{\widehat{B}} \overline{\rho_\sigma}^A\right) + \\
&\quad \left(f_m^{\widehat{A}} - f_m\right) f^{\widehat{A}} \left((1-m)\beta S^A \overline{\rho_\tau}^{\widehat{A}} + (1-m)\beta S^{\widehat{A}} \overline{\rho_\sigma \rho_\tau}^{\widehat{A}} + m\beta S^B \overline{\rho_\tau}^{\widehat{A}} + m\beta S^{\widehat{B}} \overline{\rho_\sigma \rho_\tau}^{\widehat{A}}\right) + \\
&\quad \left(f_m^B - f_m\right) f^B \left(m\beta S^A + m\beta S^{\widehat{A}} \overline{\rho_\sigma}^B + (1-m)\beta S^B + (1-m)\beta S^{\widehat{B}} \overline{\rho_\sigma}^B\right) + \\
&\quad \left(f_m^{\widehat{B}} - f_m\right) f^{\widehat{B}} \left(m\beta S^A \overline{\rho_\tau}^{\widehat{B}} + m\beta S^{\widehat{A}} \overline{\rho_\sigma \rho_\tau}^{\widehat{B}} + (1-m)\beta S^{\widehat{B}} \overline{\rho_\tau}^{\widehat{B}} + (1-m)\beta S^{\widehat{B}} \overline{\rho_\sigma \rho_\tau}^{\widehat{B}}\right)
\end{aligned} \tag{D.23}$$

Finally, with $\omega^k = (1 - f_m^k) f^k$ we have

$$\begin{aligned}
\frac{\mathrm{d}f_m}{\mathrm{d}t} &= \beta\Delta\rho_\sigma \left[m \left(\omega^B f^B S^{\widehat{A}} + \omega^A f^A S^{\widehat{B}} \right) + (1-m) \left(\omega^A f^A S^{\widehat{A}} + \omega^B f^B S^{\widehat{B}} \right) \right] + \\
&\quad \beta\Delta\rho_\tau \left[m \left(\omega^{\widehat{A}} f^{\widehat{A}} S^B + \omega^{\widehat{B}} f^{\widehat{B}} S^A \right) + (1-m) \left(\omega^{\widehat{A}} f^{\widehat{A}} S^A + \omega^{\widehat{B}} f^{\widehat{B}} S^B \right) \right] + \\
&\quad \beta\Delta\rho_{\tau\sigma} \left[m \left(\omega^{\widehat{A}} f^{\widehat{A}} S^{\widehat{B}} + \omega^{\widehat{B}} f^{\widehat{B}} S^{\widehat{A}} \right) + (1-m) \left(\omega^{\widehat{A}} f^{\widehat{A}} S^{\widehat{A}} + \omega^{\widehat{B}} f^{\widehat{B}} S^{\widehat{B}} \right) \right] + \\
&\quad \beta \left(f_m^A - f_m \right) f^A \left[m \left(S^B + S^{\widehat{B}} \overline{\rho_\sigma}^A \right) + (1-m) \left(S^A + S^{\widehat{A}} \overline{\rho_\sigma}^A \right) \right] + \\
&\quad \beta \left(f_m^{\widehat{A}} - f_m \right) f^{\widehat{A}} \left[m \left(S^B \overline{\rho_\tau}^{\widehat{A}} + S^{\widehat{B}} \overline{\rho_\sigma \rho_\tau}^{\widehat{A}} \right) + (1-m) \left(S^A \overline{\rho_\tau}^{\widehat{A}} + S^{\widehat{A}} \overline{\rho_\sigma \rho_\tau}^{\widehat{A}} \right) \right] + \\
&\quad \beta \left(f_m^B - f_m \right) f^B \left[m \left(S^A + S^{\widehat{A}} \overline{\rho_\sigma}^B \right) + (1-m) \left(S^B + S^{\widehat{B}} \overline{\rho_\sigma}^B \right) \right] + \\
&\quad \beta \left(f_m^{\widehat{B}} - f_m \right) f^{\widehat{B}} \left[m \left(S^A \overline{\rho_\tau}^{\widehat{B}} + \beta S^{\widehat{A}} \overline{\rho_\sigma \rho_\tau}^{\widehat{B}} \right) + (1-m) \left(S^{\widehat{B}} \overline{\rho_\tau}^{\widehat{B}} + S^{\widehat{B}} \overline{\rho_\sigma \rho_\tau}^{\widehat{B}} \right) \right]
\end{aligned} \tag{D.24}$$

D.5 Vaccine escape frequency with the V_τ vaccine

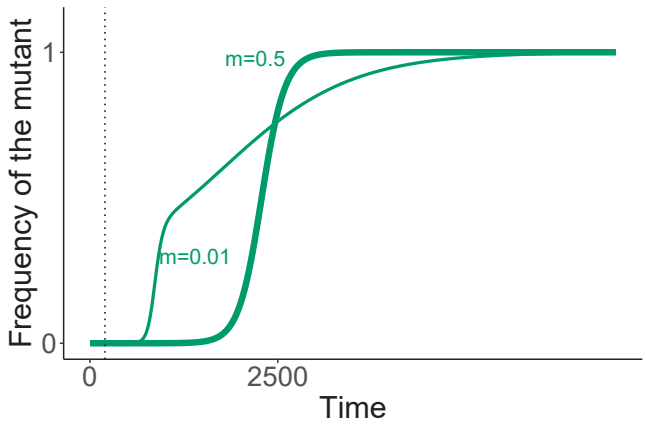

FIGURE D.17 – Vaccine escape mutant frequency in the global metapopulation (f_m) with a full migration (thick green line, $m = 0.5$) or a low migration (in thin green line, $m = 0.01$), with the V_σ vaccine, $r_\sigma = 0$, $r_tau = 0.8$ and the parameter values as in figure 4.2. The vaccination starts at $t = 200$ (dotted black line).

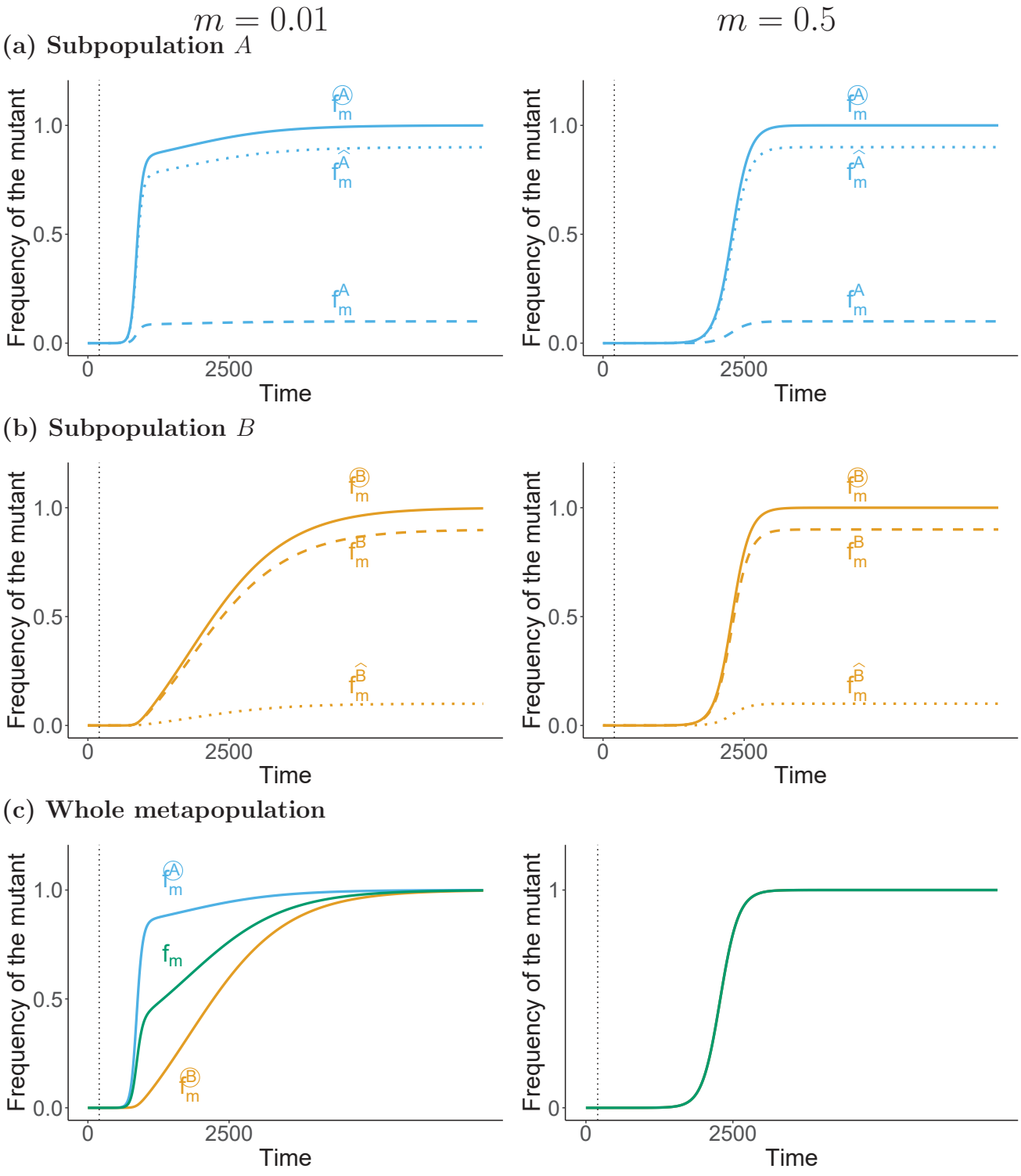

FIGURE D.16 – Vaccine escape mutant frequency with a low migration ($m = 0.01$, left panels) or a high migration ($m = 0.5$, right panels) in (a) the subpopulation A, (b) the subpopulation B and (c) the whole metapopulation, with the V_τ vaccine. The mutant frequency in the subpopulation A is showed in blue, in the subpopulation B in orange, and the global frequency in green. The dotted lines represent the frequency in the treated hosts, the dashed lines represent the frequency in the naive hosts and the solid lines represent the frequency in the population. Here $m = 0.01$ and the parameter values as in figure 4.2. The vaccination starts at $t = 200$ (dotted black line).

Bibliographie

Alizon, S., A. Hurford, N. Mideo, and M. Van Baalen. 2009. Virulence evolution and the trade-off hypothesis : history, current state of affairs and the future. Journal of evolutionary biology 22 :245–259.

Alizon, S., and M. T. Sofonea. 2021. Sars-cov-2 virulence evolution : Avirulence theory, immunity and trade-offs. Journal of Evolutionary Biology .

Alizon, S., and M. van Baalen. 2005. Emergence of a convex trade-off between transmission and virulence. The American Naturalist 165 :E155–E167.

Anderson, R. M., and R. M. May. 1982. Coevolution of hosts and parasites. Parasitology 85 :411–426.

———. 1986. The invasion, persistence and spread of infectious diseases within animal and plant communities. Philosophical Transactions of the Royal Society of London. B, Biological Sciences 314 :533–570.

———. 1991. Infectious diseases of humans : dynamics and control. Oxford University Press, Oxford.

Bacaër, N. 2007. Approximation of the basic reproduction number r0 for vector-borne diseases with a periodic vector population. Bulletin of mathematical biology 69 :1067–1091.

———. 2011. A short history of mathematical population dynamics. Springer Science & Business Media.

Bacaër, N., and S. Guernaoui. 2006. The epidemic threshold of vector-borne diseases with seasonality. Journal of mathematical biology 53 :421–436.

Bacaër, N. 2011. Le paramètre R0 pour la dynamique des populations dans un environnement périodique. Université Pierre et Marie Curie (Paris 6). HDR.

Baker, R. E., W. Yang, G. A. Vecchi, C. J. E. Metcalf, and B. T. Grenfell. 2020. Susceptible supply limits the role of climate in the early sars-cov-2 pandemic. Science 369 :315–319.

Barker, B., and C. Gimingham. 1911. The fungicidal action of bordeaux mixtures. The Journal of Agricultural Science 4 :76–94.

Berche, P. 2012. Louis pasteur, from crystals of life to vaccination. Clinical microbiology and infection 18 :1–6.

Berngruber, T. W., R. Froissart, M. Choisy, and S. Gandon. 2013. Evolution of virulence in emerging epidemics. PLoS pathogens 9 :e1003209.

Berngruber, T. W., S. Lion, and S. Gandon. 2015. Spatial structure, transmission modes and the evolution of viral exploitation strategies. PLoS pathogens 11 :e1004810.

Bollet, A. J., and A. B. Jay. 2004. Plagues & poxes : the impact of human history on epidemic disease. Demos Medical Publishing.

Bonhoeffer, S., M. Lipsitch, and B. R. Levin. 1997. Evaluating treatment protocols to prevent antibiotic resistance. Proceedings of the National Academy of Sciences 94 :12106–12111.

Boots, M., and A. Sasaki. 1999. ‘small worlds’ and the evolution of virulence : infection occurs

locally and at a distance. Proceedings of the Royal Society of London B : Biological Sciences 266 :1933–1938.

Boots, M., A. Sasaki, et al. 2000. The evolutionary dynamics of local infection and global reproduction in host-parasite interactions. Ecology Letters 3 :181–185.

Breman, J. G., and I. Arita. 1980. The confirmation and maintenance of smallpox eradication. New England Journal of Medicine 303 :1263–1273.

Brent, K. J., and D. W. Hollomon. 1998. Fungicide resistance : the assessment of risk, vol. 2. Global Crop Protection Federation Brussels.

Brown, J. K., and A. Tellier. 2011. Plant-parasite coevolution : bridging the gap between genetics and ecology. Annual review of phytopathology 49 :345–367.

Carman, W. F., P. Karayiannis, J. Waters, H. Thomas, A. Zanetti, G. Manzillo, and A. t. Zuckerman. 1990. Vaccine-induced escape mutant of hepatitis b virus. The lancet 336 :325–329.

Carmona, P., and S. Gandon. 2020. Winter is coming : Pathogen emergence in seasonal environments. PLoS computational biology 16 :e1007954.

Chabas, H., S. Lion, A. Nicot, S. Meaden, S. van Houte, S. Moineau, L. M. Wahl, E. R. Westra, and S. Gandon. 2018. Evolutionary emergence of infectious diseases in heterogeneous host populations. PLoS biology 16 :e2006738.

Charnov, E. L., et al. 1976. Optimal foraging, the marginal value theorem .

Chinazzi, M., J. T. Davis, M. Ajelli, C. Gioannini, M. Litvinova, S. Merler, A. P. y Piontti, K. Mu, L. Rossi, K. Sun, et al. 2020. The effect of travel restrictions on the spread of the 2019 novel coronavirus (covid-19) outbreak. Science 368 :395–400.

Cortez, M. H., and J. S. Weitz. 2013. Distinguishing between indirect and direct modes of transmission using epidemiological time series. The American Naturalist 181 :E43–E52.

Darwin, C. 1964. On the origin of species : A facsimile of the first edition. Harvard University Press.

Day, T. 2000. Competition and the effect of spatial resource heterogeneity on evolutionary diversification. The American Naturalist 155 :790–803.

———. 2001. Parasite transmission modes and the evolution of virulence. Evolution 55 :2389–2400.

———. 2002. On the evolution of virulence and the relationship between various measures of mortality. Proceedings of the Royal Society of London. Series B : Biological Sciences 269 :1317–1323.

Day, T., and S. Gandon. 2006. Insights from price's equation into evolutionary epidemiology. Disease evolution : models, concepts, and data analyses 71 :23–44.

———. 2007. Applying population-genetic models in theoretical evolutionary epidemiology. Ecology Letters 10 :876–888.

Day, T., and S. R. Proulx. 2004. A general theory for the evolutionary dynamics of virulence. The American Naturalist 163 :E40–E63.

De Roode, J. C., A. J. Yates, and S. Altizer. 2008. Virulence-transmission trade-offs and population divergence in virulence in a naturally occurring butterfly parasite. Proceedings of the national academy of sciences 105 :7489–7494.

Débarre, F., S. Lion, M. Van Baalen, and S. Gandon. 2011. Evolution of host life-history traits in a spatially structured host-parasite system. The American Naturalist 179 :52–63.

Débarre, F., O. Ronce, and S. Gandon. 2013. Quantifying the effects of migration and mutation on adaptation and demography in spatially heterogeneous environments. Journal of Evolutionary Biology 26 :1185–1202.

Dieckmann, U. 2002. Adaptive dynamics of pathogen-host interactions .

Dieckmann, U., J. A. Metz, and M. W. Sabelis. 2005. Adaptive dynamics of infectious diseases : in pursuit of virulence management. 2. Cambridge University Press.

Diekmann, O., J. A. P. Heesterbeek, and J. A. Metz. 1990. On the definition and the computation of the basic reproduction ratio r 0 in models for infectious diseases in heterogeneous populations. Journal of mathematical biology 28 :365–382.

Djidjou-Demasse, R., B. Moury, and F. Fabre. 2017. Mosaics often outperform pyramids : insights from a model comparing strategies for the deployment of plant resistance genes against viruses in agricultural landscapes. New Phytologist 216 :239–253.

Domingo, E., C. Escarmis, E. Baranowski, C. M. Ruiz-Jarabo, E. Carrillo, J. I. Nunez, and F. Sobrino. 2003. Evolution of foot-and-mouth disease virus. Virus research 91 :47–63.

Donnelly, R., A. Best, A. White, and M. Boots. 2013. Seasonality selects for more acutely virulent parasites when virulence is density dependent. Proceedings of the Royal Society of London B : Biological Sciences 280 :20122464.

Doumayrou, J., A. Avellan, R. Froissart, and Y. Michalakis. 2013. An experimental test of the transmission-virulence trade-off hypothesis in a plant virus. Evolution : International Journal of Organic Evolution 67 :477–486.

Dowell, S. F. 2001. Seasonal variation in host susceptibility and cycles of certain infectious diseases. Emerging infectious diseases 7 :369.

Drazin, P. G., and P. D. Drazin. 1992. Nonlinear systems, vol. 10. Cambridge University Press.

Dwyer, G., J. S. Elkinton, and J. P. Buonaccorsi. 1997. Host heterogeneity in susceptibility and disease dynamics : tests of a mathematical model. The American Naturalist 150 :685–707.

Dwyer, G., S. A. Levin, and L. Buttel. 1990. A simulation model of the population dynamics and evolution of myxomatosis. Ecological monographs 60 :423–447.

Ewald, P. W. 1983. Host-parasite relations, vectors, and the evolution of disease severity. Annual Review of Ecology and Systematics 14 :465–485.

Fenner, F., D. Henderson, I. Arita, Z. Jezek, and I. Ladnyi. 1988. The history of smallpox and its spread around the world. Smallpox and its Eradication pages 209–244.

Ferris, C., and A. Best. 2018. The evolution of host defence to parasitism in fluctuating environments. Journal of theoretical biology 440 :58–65.

———. 2019. The effect of temporal fluctuations on the evolution of host tolerance to parasitism. Theoretical population biology 130 :182–190.

Fine, P. E. 1993. Herd immunity : history, theory, practice. Epidemiologic reviews 15 :265–302.

Fisher, R. A. 1930. The genetical theory of natural selection. The Clarendon Press.

Fleming-Davies, A. E., P. D. Williams, A. A. Dhondt, A. P. Dobson, W. M. Hochachka, A. E. Leon, D. H. Ley, E. E. Osnas, and D. M. Hawley. 2018. Incomplete host immunity favors the evolution of virulence in an emergent pathogen. Science 359 :1030–1033.

Frank, S. A. 1996. Models of parasite virulence. The Quarterly review of biology 71 :37–78.

Fraser, C., T. D. Hollingsworth, R. Chapman, F. de Wolf, and W. P. Hanage. 2007. Variation in hiv-1 set-point viral load : epidemiological analysis and an evolutionary hypothesis. Proceedings of the National Academy of Sciences 104 :17441–17446.

Galvani, A. P. 2003. Epidemiology meets evolutionary ecology. Trends in Ecology & Evolution 18 :132–139.

Gandon, S., and T. Day. 2007. The evolutionary epidemiology of vaccination. Journal of the Royal Society Interface 4 :803–817.

———. 2008. Evidences of parasite evolution after vaccination. Vaccine 26 :C4–C7.

Gandon, S., V. A. Jansen, and M. Van Baalen. 2001*a*. Host life history and the evolution of parasite virulence. Evolution 55 :1056–1062.

Gandon, S., and S. Lion. 2021. Targeted vaccination and the speed of sars-cov-2 adaptation. medRxiv .

Gandon, S., M. Mackinnon, S. Nee, and A. Read. 2003. Imperfect vaccination : some epidemiological and evolutionary consequences. Proceedings of the Royal Society of London B : Biological Sciences 270 :1129–1136.

Gandon, S., M. J. Mackinnon, S. Nee, and A. F. Read. 2001*b*. Imperfect vaccines and the evolution of pathogen virulence. Nature 414 :751.

Geritz, S. A., G. Mesze, J. A. Metz, et al. 1998. Evolutionarily singular strategies and the adaptive growth and branching of the evolutionary tree. Evolutionary ecology 12 :35–57.

Geritz, S. A., J. A. Metz, É. Kisdi, and G. Meszéna. 1997. Dynamics of adaptation and evolutionary branching. Physical Review Letters 78 :2024.

Gimeno, I. M. 2008. Marek's disease vaccines : a solution for today but a worry for tomorrow ? Vaccine 26 :C31–C41.

Giuliano, A. R., J. M. Palefsky, S. Goldstone, E. D. Moreira Jr, M. E. Penny, C. Aranda, E. Vardas,

H. Moi, H. Jessen, R. Hillman, et al. 2011. Efficacy of quadrivalent hpv vaccine against hpv infection and disease in males. New England Journal of Medicine 364 :401–411.

Goldstein, R. E. 2018. Point of view : Are theoretical results 'results' ? Elife 7 :e40018.

Grassly, N. C., and C. Fraser. 2006. Seasonal infectious disease epidemiology. Proceedings of the Royal Society of London B : Biological Sciences 273 :2541–2550.

Habicht, M. E., F. D. Pate, E. Varotto, and F. M. Galassi. 2020. Epidemics and pandemics in the history of humankind and how governments dealt with them a review from the bronze age to the early modern age. Riv. Trimest. Sci. Dell Amministrazione 30.

Hamelin, F. M., M. Castel, S. Poggi, D. Andrivon, and L. Mailleret. 2011. Seasonality and the evolutionary divergence of plant parasites. Ecology 92 :2159–2166.

Haraguchi, Y., and A. Sasaki. 2000. The evolution of parasite virulence and transmission rate in a spatially structured population. Journal of Theoretical Biology 203 :85–96.

Harper, K. 2019. Comment l'Empire romain s' est effondré : le climat, les maladies et la chute de Rome. La Découverte.

Hays, J. N. 2005. Epidemics and pandemics : their impacts on human history. Abc-clio.

Henderson, D. A. 2009. Smallpox : the death of a disease : the inside story of eradicating a worldwide killer. Prometheus Books.

Ho, D. D., A. U. Neumann, A. S. Perelson, W. Chen, J. M. Leonard, and M. Markowitz. 1995. Rapid turnover of plasma virions and cd4 lymphocytes in hiv-1 infection. Nature 373 :123–126.

Hurford, A., D. Cownden, and T. Day. 2009. Next-generation tools for evolutionary invasion analyses. Journal of the Royal Society Interface 7 :561–571.

John, T. J., R. Pandian, A. Gadomski, M. Steinhoff, M. John, and M. Ray. 1983. Control of poliomyelitis by pulse immunisation in vellore, india. Br Med J (Clin Res Ed) 286 :31–32.

Keeling, M. J., and P. Rohani. 2011. Modeling infectious diseases in humans and animals. Princeton University Press.

Kennedy, D. A., and A. F. Read. 2017. Why does drug resistance readily evolve but vaccine resistance does not ? Proc. R. Soc. B 284 :20162562.

Kerr, P. J. 2012. Myxomatosis in australia and europe : a model for emerging infectious diseases. Antiviral research 93 :387–415.

Klausmeier, C. A. 2008. Floquet theory : a useful tool for understanding nonequilibrium dynamics. Theoretical Ecology 1 :153–161.

Koelle, K., M. Pascual, and M. Yunus. 2005. Pathogen adaptation to seasonal forcing and climate change. Proceedings of the Royal Society of London B : Biological Sciences 272 :971–977.

Kokayeff, N. 2012. Dying to be discovered : Miasma vs germ theory. ESSAI 10 :24.

Kortessis, N., M. W. Simon, M. Barfield, G. E. Glass, B. H. Singer, and R. D. Holt. 2020. The interplay of movement and spatiotemporal variation in transmission degrades pandemic control. Proceedings of the National Academy of Sciences 117 :30104–30106.

Lappin, M. R., R. W. Sebring, M. Porter, S. J. Radecki, and J. Veir. 2006. Effects of a single dose of an intranasal feline herpesvirus 1, calicivirus, and panleukopenia vaccine on clinical signs and virus shedding after challenge with virulent feline herpesvirus 1. Journal of Feline Medicine and Surgery 8 :158–163.

Linka, K., M. Peirlinck, F. Sahli Costabal, and E. Kuhl. 2020. Outbreak dynamics of covid-19 in europe and the effect of travel restrictions. Computer Methods in Biomechanics and Biomedical Engineering 23 :710–717.

Lion, S. 2018*a*. Class structure, demography, and selection : reproductive-value weighting in nonequilibrium, polymorphic populations. The American Naturalist 191 :620–637.

———. 2018*b*. From the price equation to the selection gradient in class-structured populations : a quasi-equilibrium route. Journal of theoretical biology 447 :178–189.

———. 2018*c*. Theoretical approaches in evolutionary ecology : environmental feedback as a unifying perspective. The American Naturalist 191 :21–44.

Lion, S., and M. v. Baalen. 2008. Self-structuring in spatial evolutionary ecology. Ecology letters 11 :277–295.

Lion, S., and S. Gandon. 2015. Evolution of spatially structured host–parasite interactions. Journal of evolutionary biology 28 :10–28.

———. 2021. Life-history evolution of class-structured populations in fluctuating environments. bioRxiv .

Lion, S., and J. A. Metz. 2018. Beyond r0 maximisation : on pathogen evolution and environmental dimensions. Trends in ecology & evolution 33 :458–473.

Mackinnon, M. J., and A. F. Read. 1999. Genetic relationships between parasite virulence and transmission in the rodent malaria plasmodium chabaudi. Evolution 53 :689–703.

Martín, M. J. J., C. L. De Pablo, and P. M. De Agar. 2006. Landscape changes over time : comparison of land uses, boundaries and mosaics. Landscape Ecology 21 :1075–1088.

Mathieu, E., H. Ritchie, E. Ortiz-Ospina, M. Roser, J. Hasell, C. Appel, C. Giattino, and L. Rodés-Guirao. 2021. A global database of covid-19 vaccinations. Nature human behaviour pages 1–7.

Messenger, S. L., I. J. Molineux, and J. Bull. 1999. Virulence evolution in a virus obeys a trade off. Proceedings of the Royal Society of London. Series B : Biological Sciences 266 :397–404.

Meszéna, G., I. Czibula, and S. Geritz. 1997. Adaptive dynamics in a 2-patch environment : a toy model for allopatric and parapatric speciation. Journal of Biological Systems 5 :265–284.

Metz, J. A., S. A. Geritz, G. Meszéna, F. J. Jacobs, and J. S. Van Heerwaarden. 1995. Adaptive dynamics : a geometrical study of the consequences of nearly faithful reproduction .

Metz, J. A., R. M. Nisbet, and S. A. Geritz. 1992. How should we define 'fitness' for general ecological scenarios ? Trends in Ecology & Evolution 7 :198–202.

Michalakis, Y., F. Thomas, and J. Guégan. 2009. Parasitism and the evolution of life-history traits. Ecology and evolution of parasitism. Oxford University Press, Oxford pages 19–30.

Miller, I. F., and C. J. Metcalf. 2019. Vaccine-driven virulence evolution : consequences of unbalanced reductions in mortality and transmission and implications for pertussis vaccines. Journal of The Royal Society Interface 16 :20190642.

Mirrahimi, S., and S. Gandon. 2020. Evolution of specialization in heterogeneous environments : equilibrium between selection, mutation and migration. Genetics 214 :479–491.

Nilusmas, S., M. Mercat, T. Perrot, C. Djian-Caporalino, P. Castagnone-Sereno, S. Touzeau, V. Calcagno, and L. Mailleret. 2020. Multiseasonal modelling of plant-nematode interactions reveals efficient plant resistance deployment strategies. Evolutionary Applications .

Otto, S. P., and T. Day. 2011. A biologist's guide to mathematical modeling in ecology and evolution. Princeton University Press.

Park, A. W., J. Haven, R. Kaplan, and S. Gandon. 2015. Refugia and the evolutionary epidemiology of drug resistance. Biology letters 11 :20150783.

Pastoret, P.-P., K. Yamanouchi, U. Mueller-Doblies, M. M. Rweyemamu, M. Horzinek, and T. Barrett. 2006. Rinderpest—an old and worldwide story : history to c. 1902. Pages 86–VI *in* Rinderpest and peste des petits ruminants. Elsevier.

Perko, L. 2013. Differential equations and dynamical systems, vol. 7. Springer Science & Business Media.

Plantegenest, M., C. Le May, and F. Fabre. 2007. Landscape epidemiology of plant diseases. Journal of the Royal Society Interface 4 :963–972.

Radford, A. D., K. P. Coyne, S. Dawson, C. J. Porter, and R. M. Gaskell. 2007. Feline calicivirus. Veterinary research 38 :319–335.

Read, A. F. 1994. The evolution of virulence. Trends in microbiology 2 :73–76.

Read, A. F., S. J. Baigent, C. Powers, L. B. Kgosana, L. Blackwell, L. P. Smith, D. A. Kennedy, S. W. Walkden-Brown, and V. K. Nair. 2015. Imperfect vaccination can enhance the transmission of highly virulent pathogens. PLoS Biology 13 :e1002198.

Regoes, R. R., M. A. Nowak, and S. Bonhoeffer. 2000. Evolution of virulence in a heterogeneous host population. Evolution 54 :64–71.

Richie, E., N. H. Punjabi, Y. Sidharta, K. Peetosutan, M. Sukandar, S. S. Wasserman, M. Lesmana, F. Wangsasaputra, S. Pandam, M. M. Levine, et al. 2000. Efficacy trial of single-dose live oral cholera vaccine cvd 103-hgr in north jakarta, indonesia, a cholera-endemic area. Vaccine 18 :2399–2410.

Riedel, S. 2005. Edward jenner and the history of smallpox and vaccination. Pages 21–25 *in* Baylor University Medical Center Proceedings. Vol. 18. Taylor & Francis.

Roche, B., J. M. Drake, and P. Rohani. 2011. The curse of the pharaoh revisited : evolutionary bi-stability in environmentally transmitted pathogens. Ecology letters 14 :569–575.

Roeder, P. L. 2011. Rinderpest : the end of cattle plague. Preventive veterinary medicine 102 :98–106.

Ronce, O., and M. Kirkpatrick. 2001. When sources become sinks : migrational meltdown in heterogeneous habitats. Evolution 55 :1520–1531.

Roush Sandra, W., and V. Murphy Trudy. 2007. Historical comparisons of morbidity and mortality for vaccine-preventable diseases in the united states. JAMA 298.

Rousset, F. 1999. Reproductive value vs sources and sinks. Oikos 86 :591–596.

———. 2004. Genetic structure and selection in subdivided populations (MPB-40), vol. 40. Princeton University Press.

Saunders, D. G., Z. A. Pretorius, and M. S. Hovmøller. 2019. Tackling the re-emergence of wheat stem rust in western europe. Communications biology 2 :1–3.

Schmidt-Hempel, P. 2011. Evolutionary parasitology.

Sirami, C., N. Gross, A. B. Baillod, C. Bertrand, R. Carrié, A. Hass, L. Henckel, P. Miguet, C. Vuillot, A. Alignier, et al. 2019. Increasing crop heterogeneity enhances multitrophic diversity across agricultural regions. Proceedings of the National Academy of Sciences 116 :16442–16447.

Sur, D., A. L. Lopez, S. Kanungo, A. Paisley, B. Manna, M. Ali, S. K. Niyogi, J. K. Park, B. Sarkar, M. K. Puri, et al. 2009. Efficacy and safety of a modified killed-whole-cell oral cholera vaccine in india : an interim analysis of a cluster-randomised, double-blind, placebo-controlled trial. The Lancet 374 :1694–1702.

Taylor, P. D. 1990. Allele-frequency change in a class-structured population. The American Naturalist 135 :95–106.

Thompson, R. N., E. M. Hill, and J. R. Gog. 2021. Sars-cov-2 incidence and vaccine escape. The Lancet Infectious Diseases .

Tian, D., M. Traw, J. Chen, M. Kreitman, and J. Bergelson. 2003. Fitness costs of r-gene-mediated resistance in arabidopsis thaliana. Nature 423 :74–77.

Uecker, H., and S. Bonhoeffer. 2018. Antibiotic treatment protocols revisited : The challenges of a conclusive assessment by mathematical modeling. bioRxiv page 372938.

Van Baalen, M. 2002. Contact networks and the evolution of virulence. Adaptive dynamics of infectious diseases : in pursuit of virulence management. Cambridge Univ. Press, Cambridge, UK pages 85–103.

van den Berg, F., C. Gilligan, D. J. Bailey, and F. Van Den Bosch. 2010. Periodicity in host availability does not account for evolutionary branching as observed in many plant pathogens : an application to gaeumannomyces graminis var. tritici. Phytopathology 100 :1169–1175.

Walter, A., and S. Lion. 2021. Epidemiological and evolutionary consequences of periodicity in treatment coverage. Proceedings of the Royal Society B 288 :20203007.

Wells, C. R., P. Sah, S. M. Moghadas, A. Pandey, A. Shoukat, Y. Wang, Z. Wang, L. A. Meyers, B. H. Singer, and A. P. Galvani. 2020. Impact of international travel and border control measures on the global spread of the novel 2019 coronavirus outbreak. Proceedings of the National Academy of Sciences 117 :7504–7509.

WHO. 2019. Polio endgame strategy 2019-2023 : eradication, integration, certification and containment. Tech. rep.

WHO, et al. 2014. Antimicrobial resistance : global report on surveillance. World Health Organization.

Williams, P. D., and T. Day. 2008. Epidemiological and evolutionary consequences of targeted vaccination. Molecular ecology 17 :485–499.

Williams, P. D., and S. J. Kamel. 2018. The evolution of pathogen virulence : Effects of transitions between host types. Journal of theoretical biology 438 :1–8.

Witte, W. 2000. Selective pressure by antibiotic use in livestock. International journal of antimicrobial agents 16 :19–24.

Zurita-Gutiérrez, Y. H., and S. Lion. 2015. Spatial structure, host heterogeneity and parasite virulence : implications for vaccine-driven evolution. Ecology letters 18 :779–789.

Résumé

Évolution des pathogènes en réponse à l'hétérogénéité spatio-temporelle des traitements

mot clés : Interaction hôte-parasite, évolution des pathogènes, traitements, structure spatiale, fluctuations temporelles, hétérogénéité d'hôtes

Les parasites constituent une menace sévère pour les populations humaines, animales et végétales. Dans une perspective de gestion des maladies infectieuses, il est nécessaire de prédire l'évolution de certains traits critiques des parasites, comme la transmission et la virulence. Parmi les facteurs environnementaux qui peuvent affecter l'issue de l'évolution, l'utilisation de traitements prophylactiques, qui peuvent exercer des pressions de sélection fortes sur les pathogènes, doit être considérée. En outre, les variations spatio-temporelles dans la distribution des traitements, couplées à la mobilité accrue des parasites et des hôtes, sont des facteurs-clés à considérer dans l'épidémiologie évolutive des interactions hôte-parasite. Le but de cette thèse a été de développer une approche théorique pour étudier l'épidémiologie évolutive à court et long terme des interactions hôte-parasite structurées, en considérant différents types de traitements qui fluctuent dans le temps et l'espace. Cette approche théorique peut être appliquée à l'évolution des traits d'histoire de vie des pathogènes (comme la virulence dans les deux premières parties), ou à celle de traits de résistance (comme l'échappement aux vaccins dans la troisième partie).

Dans une première partie, nous avons développé un modèle théorique d'une population d'hôte hétérogène, sous une distribution périodique de traitements. Grâce au cadre de la dynamique adaptative et au concept des valeurs reproductives, nous avons mis en évidence l'impact de la périodicité dans la distribution des traitements sur l'épidémiologie à court terme et sur l'évolution des traits d'histoire de vie des pathogènes à long terme. Nos résultats suggèrent qu'une utilisation

périodique des traitements peut limiter à la fois la propagation de la maladie et l'évolution de la virulence, en fonction du type de traitement.

Dans une seconde partie, nous avons développé un modèle spatial de metapopulation, avec deux sous populations caractérisées par des couvertures en traitements différentes, et connectées par la migration du pathogène. Dans cette partie nous avons étudié les effets de la migration et des différences de couvertures sur l'évolution de la virulence à long terme. Nous montrons que la structuration spatiale des populations d'hôtes ainsi que la pression de sélection exercée par les traitements sur les pathogènes peuvent mener à de la bistabilité ou à des points de branchements évolutifs, entrainant potentiellement la coexistence de souches de pathogènes différentes.

Finalement, la troisième partie est une extension du précédent modèle de métapopulation, inspirée par les problèmes posés par la pandémie de Covid-19. Cependant, à l'inverse de la partie précédente, nous nous concentrons sur l'évolution des pathogènes à court-terme. En effet, nous avons étudié la vitesse d'émergence d'un mutant d'échappement au vaccin dans un modèle à deux populations connectées par la migration du pathogène. Ce modèle permet d'étudier plusieurs scénarios inspirés par la gestion de la pandémie. Par exemple, différentes stratégies de vaccination entre des pays connectés, ou l'impact des fermetures et ouvertures successives des frontières peuvent être explorées.

Nos modèles se veulent généraux et les conclusions peuvent être adaptées à des interactions hôtes-pathogènes spécifiques. Ainsi, nos résultats ont des implications dans la gestion des épidémies en agriculture et en santé animale et publique.

Abstract

Pathogen evolution in response to spatio-temporal heterogeneity in treatments

key words : Host-parasite interaction, pathogen evolution, treatments, spatial structure, temporal fluctuations, host heterogeneity

Parasites are an acute threat to plant, animal and human populations. To effectively manage infectious diseases, we need to predict the evolution of critical parasite traits, such as transmission and virulence. Among the environmental factors that may affect pathogens evolution, the use of prophylactic treatments, which may exert strong selective pressures on pathogens, must be considered. In addition, spatio-temporal variations in treatment distribution, coupled with the increased mobility of parasites and hosts, are key factors affecting the evolutionary epidemiology of host-parasite interactions. The goal of this thesis was to develop theory to study the short- and long-term evolutionary epidemiology of structured host-parasite interactions in the presence of treatments, taking into account different types of treatments that fluctuate in both time and space. This theory can be applied to pathogens life-history traits evolution (such as virulence in the first two parts), or to resistance traits evolution (such as vaccine escape in the third part).

In a first part, we have developed a theoretical model of a heterogeneous population of hosts, under a periodic treatment coverage. Using the adaptive dynamics framework and the concept of reproductive values, we have highlighted the impact of periodicity in treatment coverage on the short-term epidemiology and on the long-term evolution of pathogens life-history traits. Our results suggest that periodic treatment strategies can limit both disease spread and virulence evolution, depending on the type of treatment.

In a second part, we have developed a spatial metapopulation model, with two subpopulations

characterised by different treatment coverages and connected by pathogen migration. In this part we study the effects of migration and of the differences in coverage on the long-term virulence evolution. We have shown that the spatial structure of the host population and the selective pressure of treatments on pathogens may yield bistability or evolutionary branching points, which can lead to the coexistence of different pathogenic strains.

Finally, the third part is an extension of the previous metapopulation model, broadly inspired by the Covid-19 pandemic. However, in contrast to the previous part, we focus on short-term pathogen evolution and study the speed of emergence of a vaccine escape mutant in a two-population model connected by pathogen migration. This model allows for the study of several scenarios inspired by the management of the pandemic. For instance, different vaccination strategies between connected countries, or the impact of border opening and closure on the speed of emergence of a vaccine escape mutant can be explored.

Our models aim to remain general and conclusions could be adapted to specific host-pathogen interactions. Thus, our results have interesting implications for the management of infectious disease in animal and public health, and in agriculture.